Generation, recycling and release of inflammatory peptidoglycan fragments by pathogenic and nonpathogenic *Neisseria*

By

Jia Mun Chan

A dissertation submitted in partial fulfillment of the requirements for the degree of

Doctor of Philosophy

(Microbiology)

at the

UNIVERSITY OF WISCONSIN-MADISON

2018

Date of final oral examination: May 14, 2018

This dissertation is approved by the following members of the Final Oral Committee:

Joseph P. Dillard, Professor, Medical Microbiology & Immunology
Heidi Goodrich-Blair, Honorary Associate, Bacteriology
Federico Rey, Assistant Professor, Bacteriology
John-Demian (JD) Sauer, Assistant Professor, Medical Microbiology & Immunology
Douglas B. Weibel, Professor, Chemistry, Biochemistry and Biomedical Engineering
Jon P. Woods, Professor, Medical Microbiology & Immunology.

ABSTRACT

Peptidoglycan (PG) is a mesh-like polymeric structure made of amino sugars and amino acids that determines cell shape and protects against osmotic shock. Breakdown of existing strands of PG and insertion of newly synthesized strands of PG are important processes necessary for cell enlargement and cell separation. Small PG fragments are generated in the periplasm as a consequence of routine PG remodeling and are typically efficiently imported back into the cytoplasm for recycling in Gram-negative bacteria. However, a subset of Gram-negative bacteria release immunologically relevant amounts of PG fragments into the extracellular milieu. *Neisseria gonorrhoeae* is an obligate human pathogen that infects mucosal surfaces in the genitourinary tract, pharyngeal, rectal and conjunctival tissues. The release of PG fragments by this bacterial species causes death of ciliated cells and damage to the Fallopian tube epithelium during ascending infection of the upper female reproductive tract. As such, mechanisms of PG fragment generation and release in *N. gonorrhoeae* have been a major focus of study.

The closely related species *N. meningitidis* was recently discovered to also release PG fragments, albeit at different amounts compared to *N. gonorrhoeae*. *N. meningitidis* is most frequently found as an asymptomatic colonizer of the human nasal and oral cavities, although it is most infamous for causing fatal invasive meningococcal diseases. *N. meningitidis* releases less tripeptide PG monomers, which are known human NOD1 agonists, and more PG peptides and anhydro-*N*-acetylmuramic acid compared to *N. gonorrhoeae*. Human NOD1 is a pattern recognition receptor that induces an inflammatory response upon detection of intracellular PG fragments such as tripeptide PG monomer and L-Ala-D-Glu-*meso*DAP tripeptide.

My thesis work explores the molecular explanations for the differences in PG monomer release by *N. gonorrhoeae* and *N. meningitidis*, the identification of PG peptides released by *N.*

meningitidis and the proteins that generated such peptides, and the characterization of PG fragment release by nonpathogenic *Neisseria* that colonizes human, macaque and mice nasopharyngeal and oropharyngeal spaces. I determined that natural polymorphisms at specific sites of AmpG, an inner membrane permease responsible for importing PG fragments into the cytoplasm, alter the amount of PG monomers released by *N. gonorrhoeae*, *N. meningitidis* and *N. lactamica*. I found that PG-derived peptides released by *N. meningitidis* include the NOD1 agonist L-Ala-D-Glu-*meso*DAP tripeptide, which are generated by the action of the cell separation amidase AmiC and its activator protein NlpD, and that the release of PG peptides is necessary to activate human NOD1 in a HEK293-Blue reporter cell line. I also provide first evidence that like their pathogenic counterpart, nonpathogenic *Neisseria* release PG fragments. However, different *Neisseria* isolates show variation in the amounts of PG fragments released, and some species do not release PG dimers at all. Cumulatively, my work expands the scope of PG fragment release studies in the genus *Neisseria* beyond examination of *N. gonorrhoeae*, and suggests that comparative studies between different *Neisseria* species could provide insight into the mechanisms that *N. gonorrhoeae* utilize to release more inflammatory PG fragments compared to other bacteria.

ACKNOWLEDGEMENTS

This thesis work would not have been possible without Joe, who provided me with mentorship, inspiration and opportunities to develop as a scientist throughout the years. Thank you for being a great mentor! I would also like to thank current and past members of the Dillard lab – Katie, Melanie, Amy, Ryan, Jon, Ami, Emma, Krizia, Tiffany, Lyons, Meghan, Fisher, Macy, Miriam, and the many undergrads - for the highly supportive and collaborative environment in the lab. Thanks to Katie, Lyons and Meghan for their mentorship, with special thanks to Katie for being the best lab manager ever, and to Melanie and Ami for starting the initial window drawing of moral support. I couldn't have asked for better colleagues and friends.

There has been a decent amount of flux in my committee, so thanks to Heidi, Jon and Doug for being around from the beginning, to Federico and JD for agreeing to join much later in the game, and to Margaret for her stay. Thank you for all the advices throughout the years! I would also like to thank my undergrad mentors Dan and Sarah for encouraging my curiosity and introducing me to research. Additionally, many thanks to Cathy for running the program seemingly effortlessly, and for making sure we have our paperwork and enroll for classes and get paid. Along the same lines, thank you to John, Tracy, Renee, Brenda, Theng and other members of the MMI and BacT staff for all their help. Thanks to the core facility staffs Elle, Ben and Greg for providing experimental support, and to Jae-Hyuk for being a great MTF mentor.

Last but not least, I would like to thank my family and friends for all the love and support they have given me, without which I wouldn't be here today. Finally, thank you to my SO, CJ, for always taking care of me even as he navigates his own PhD.

TABLE OF CONTENTS

Appendices

LIST OF TABLES

LIST OF FIGURES

CHAPTER 1

Introduction

Jia Mun Chan and Joseph P. Dillard

JM Chan and JP Dillard wrote the manuscript.

Portions have been previously published as

Chan JM, Dillard JP. 2017. Attention seeker: Production, modification, and release of inflammatory peptidoglycan fragments in *Neisseria*. J Bacteriol **199**:e00354-17.

Republished with the permission of the American Society for Microbiology and *Journal of Bacteriology* with modifications.

Human restricted pathogenic *Neisseria*

The genus *Neisseria* consists of multiple species of Gram-negative bacteria, most of which are found associated with a host organism (1, 2). The two most famous species in this genus are *Neisseria gonorrhoeae* and *Neisseria meningitidis*. *N. gonorrhoeae*, also known as gonococcus (GC), is a human restricted mucosal pathogen that can infect the reproductive tract, pharynx, rectum and conjunctiva of humans (3). Gonococcus causes the sexually transmitted infection gonorrhea, which predominantly manifests as uncomplicated cervicitis in women and urethritis in men. Gonococcal infections are frequently asymptomatic and thus remain undetected and untreated, which increases the risk of complications such as pelvic inflammatory disease, ectopic pregnancies and disseminated gonococcal disease (4). An infected mother can also transmit *N. gonorrhoeae* to an infant during delivery, resulting in neonatal ophthalmia that could cause blindness if left untreated (5). There were 468,514 reported cases of gonorrhea in the United States in 2016, and it is estimated that the actual number of new gonococcal infections worldwide in 2012 is around 78 million (6, 7). A major public health concern is the emergence of multidrug resistant *N. gonorrhoeae*, including an isolate resistant to both ceftriaxone and azithromycin, which are currently used as a last-line antibiotic treatment (8–12). There is an urgent need to find new ways to prevent and treat gonococcal infections.

N. meningitidis, also known as meningococcus (MC), is also a human specific pathogen and is best known for causing the acute invasive diseases meningococcal meningitis and septicemia, which have a mortality rate of 10-15% even with rapid treatment (13–15). Approximately 11-19% of survivors suffer from lifelong sequelae such as hearing loss or amputation (16). Meningococcus can also cause pneumonia and urethritis (17–19). Despite the devastating consequences of invasive meningococcal disease, *N. meningitidis* is actually more

commonly found as an asymptomatic colonizer of the human nasopharyngeal space, and colonizes 8-25% of population at any time without causing disease (14). Meningococcal carriage rates can be as high as 70% in areas of high human density, such as at college dormitories, military barracks and during the Hajj pilgrimage (14, 15, 20, 21). There are twelve serogroups of *N. meningitidis*, which are characterized based on the type of polysaccharide capsule encoded. However, only six serogroups, A, B, C, W, X and Y, cause almost all of the diseases seen worldwide (22). Epidemics of meningococcal disease are more likely to occur in dry conditions (23, 24). Persons with defects in the complement pathway are also more susceptible to meningococcal disease (14). A combination of bacterial, host and environmental factors likely determine whether a strain of meningococcus colonizes humans asymptomatically or causes invasive disease.

Human-associated nonpathogenic *Neisseria*

In addition to *N. meningitidis*, there are multiple species of human-associated nonpathogenic *Neisseria* that asymptomatically colonize the human nasopharyngeal space and oral cavity without causing disease (25, 26). *Neisseria* is one of the more dominant genera in the human oropharyngeal space, and is considered part of core oral microbiome in healthy humans (27, 28). Despite the name, nonpathogenic *Neisseria* do encode some virulence factors and can very infrequently cause disease in immunocompromised persons or post-trauma, which are reviewed in (1, 2, 29). However, unlike *N. meningitidis*, nonpathogenic *Neisseria* have not been reported to cause disease in otherwise healthy individuals with no underlying conditions or extenuating circumstances. Different species of nonpathogenic *Neisseria* preferentially colonize different sites within the oral cavity (30, 31). *N. sicca, N. mucosa* and *N. elongata* are

predominantly found in the gingival plaque. On the other hand, *N, flavescens* and *N. subflava* are enriched at the tongue dorsum, and *N. meningitidis* is usually found in the throat. Colonization with *N. lactamica* also confers some protection against meningococcal carriage and may protect against meningococcal disease, especially in children (21, 32, 33).

Animal-associated nonpathogenic *Neisseria*

Multiple strains of *Neisseria* have been isolated from a variety of animals and insects, including but not limited to mosquitoes, geese, iguana lizards, cows, cats, dogs and macaques (2). A fraction of these strains cause disease in their host animals; for example, a neisserial species infects and causes embryo mortality in Artic-nesting goose eggs (34). Like human-associated *Neisseria*, most of the non-human mammal-associated strains are found as asymptomatic colonizers in the naso- and oropharyngeal cavities of their natural host organisms (2). One exception is a species of *Neisseria* that makes up 25% of the foregut microbiota in three-toed sloths (35). Avian-associated *Neisseria* are also frequently found in the gastrointestinal tract (2, 34). Due to the host-specificity of different *Neisseria* species, it is difficult to study human-restricted pathogenic *Neisseria* in an animal model. This is partly because *N. gonorrhoeae* and *N. meningitidis* evolved multiple strategies to evade the human immune response, but are very susceptible to killing by complement protein from other animals (36). While there is significant work done to generated humanized mice for infection studies, such animal models are not yet perfect and do not recapitulate the symptoms and tissue damage associated with infections in humans (37–39). Recent efforts to identify and characterize natural colonizers of macaques and mice have led to the establishment of animal-associated *Neisseria* as a model for studying neisserial colonization, infection and transmission in a natural host. Such

model organisms include macaque isolates and a newly described species, *N. musculi*, that was isolated from wild mice (40–42).

A limited number of Gram-negative bacteria release peptidoglycan fragments during growth

Peptidoglycan (PG) forms a mesh-like sacculus surrounding the cell membrane of a bacterial cell, providing cell shape and protection against turgor pressure. Expansion and reshaping of the sacculus during cell growth and cell separation is a dynamic process requiring spatiotemporally coordinated degradation and synthesis of PG. Small PG fragments are generated as cross-links are broken and PG strands are degraded, and these PG fragments are either taken up into the cytoplasm for recycling or are released from the cell. *Neisseria gonorrhoeae* is unusual among Gram-negative bacteria in that it releases significant amounts of soluble PG fragments during growth (43).

The release of PG fragments by *N. gonorrhoeae* has been of particular interest due to the effects of these molecules in gonococcal infections. Host tissue damage during gonococcal infections is partly facilitated by host inflammation and cytokine production upon recognition of certain PG fragments (44, 45). It was demonstrated that PG fragments from *N. gonorrhoeae* induce the death and sloughing of ciliated cells in human Fallopian tube (FT) organ culture, reproducing the tissue damage seen in patients with gonococcal pelvic inflammatory disease (43, 46). The PG fragments that damage FT tissue are monomeric subunits of PG comprised of disaccharides with either a three or four amino acid chain attached to the *N*-acetylmuramic acid, referred to as PG monomers (Fig 1A, compounds III).

A few other Gram-negative bacterial species have been shown to use PG fragments in a very similar way. *Bordetella pertussis* releases PG monomer with a four amino acid chain, and this molecule induces the death and sloughing of ciliated cells in tracheal tissue (47, 48). *Vibrio fischeri* uses the same PG monomer to induce tissue regression and ciliated cell death in the Hawaiian bobtail squid during the establishment of symbiosis (49, 50). *N. meningitidis* is also known to release PG fragments (51); however, the role of the released fragments in the nonpathogenic or the pathogenic lifestyles of meningococcus is unknown.

Structure and composition of PG in *N. gonorrhoeae* and *N. meningitidis*

Gonococcal and meningococcal PG have the same basic structure as that of most Gram-negative bacteria (52). The glycan backbone is made of repeating subunits of *N*-acetylglucosamine (GlcNAc) and *N*-acetylmuramic acid (MurNAc) linked by β-1,4-glycosidic bonds. The peptide stem consists of two to five amino acids, in the order: L-alanine, D-glutamate, *meso*-diaminopimelic acid (DAP), D-alanine and D-alanine, in which L-alanine forms an amide bond with MurNAc. The composition of gonococcal and meningococcal sacculi are largely similar to each other with small differences. Approximately 70-80% of the peptide stems in the gonococcal sacculus are tetrapeptides, 20-30% are tripeptides and a minimal percentage are pentapeptide or dipeptides (53–55). Most of the free peptide stems in the meningococcal sacculi are tetrapeptides, followed by pentapeptides, tripeptides and dipeptides (56). Both *N. gonorrhoeae* and *N. meningitidis* have high levels (~40%) of PG cross-linking (53, 56). Cross-links in gonococcus are primarily in the form of amide bonds between a DAP moiety of one peptide stem and D-alanine of another, with a lesser amount of DAP-DAP bonds (53). In contrast, DAP-DAP bonds were not seen in the meningococcal sacculi (56). Some Gram-

negative bacteria such as *Escherichia coli* anchor the PG layer and outer membrane via the covalently bound Braun's lipoprotein, however gonococci lack Braun's lipoprotein (57). Instead, *Neisseria* express OmpA-domain outer membrane proteins that bind PG noncovalently, such as gonococcal protein III (known as RmpM in *N. meningitidis*). These proteins act to stabilize the outer membrane and may function to anchor the outer membrane to the PG layer (58, 59). Unlike *E. coli*, but similar to many other Gram-negative bacteria, *N. gonorrhoeae* and *N. meningitidis* acetylates PG at the C-6 position of MurNAc (*O*-acetylation) (60–63). *O*-acetylation of PG confers protection against lysozyme action *in vitro*; however, the absence of *O*-acetylation does not significantly alter *N. gonorrhoeae* survival in the presence of lysozyme (62, 63). Additionally, deacetylation of PG is required for degradation of the PG strands by lytic transglycosylases and the generation of most of the soluble PG fragments (64).

Chemical identities of PG fragments released by *N. gonorrhoeae*

Although *N. gonorrhoeae* releases some large fragments of PG by autolysis, the majority of PG fragments released are small fragments liberated during normal PG turnover and cell growth, without lysis (54, 65). PG fragments released by *N. gonorrhoeae* during growth have 1,6-anhydro bonds on the MurNAc sugar due to the action of lytic transglycosylases (54). This is in contrast to PG fragments liberated by lysozyme treatment, which produces reducing ends. Release of these PG fragments can be tracked by metabolic labeling of PG, and the types and amounts of PG fragments released can be analyzed using size-exclusion chromatography (66). Gonococci release PG monomers, PG dimers, tetrasaccharide peptides, disaccharide, anhydro-MurNAc and free peptide stems (Fig 1A-B). PG dimers are two monomeric units linked by a

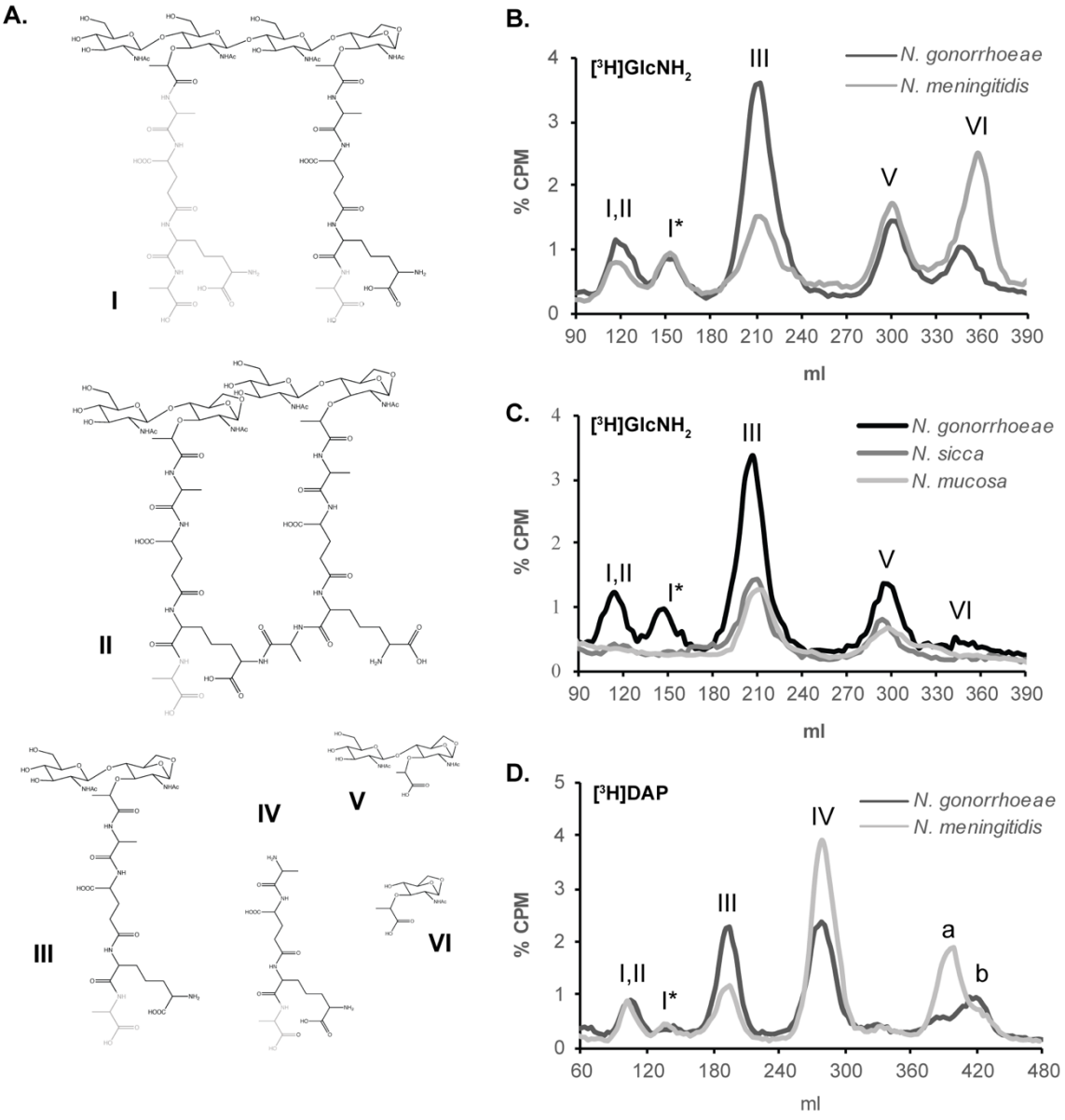

Figure 1. Small PG fragments released by *Neisseria*. A) Chemical structures of PG fragments released by *Neisseria*, which include (I) glycosidically linked PG dimers, (I*) tetrasaccharide peptide, (II) cross-linked PG dimers, (III) PG monomers, (IV) free peptide, (V) free disaccharide, and (VI) free anhydro-MurNAc. Lighter shading indicates portions of peptides present in some, but not in all PG fragments. Note that all muropeptides have anhydro-ends on the MurNAc sugar. B-D) PG fragments labeled with [^{3}H] glucosamine ($GlcNH_2$) (B,C) or [^{3}H] DAP (D)

released by *N. gonorrhoeae* (B-D)*, N. meningitidis* (B, D)*, N. sicca* (C) and *N. mucosa* (C) separated using size-exclusion chromatography. Peaks correspond to the structures in (A). Peaks **a** and **b** have not been identified by mass spectrometry.

glycosidic bond between the two disaccharide units (glycosidically-linked dimer) or by cross-linking of the two peptide stems (peptide-linked dimer). Tetrasaccharide peptides have two glycosidically-linked disaccharide units with only one peptide stem attached to the anhydro-MurNAc sugar (55).

Most of the PG fragments released by *N. gonorrhoeae* are in the form of PG monomers with tripeptide or tetrapeptide stems (Fig 1B). Tetrapeptide monomer is also commonly known as tracheal cytotoxin or TCT (67). Gonococci release about 72-80% tripeptide monomer and 20-28% tetrapeptide monomer (51, 68). This is in contrast to the amount of tripeptide vs. tetrapeptide stems in the sacculi (20-30% vs 70-80% respectively), suggesting that an L,D-carboxypeptidase in the periplasm trims the peptide stem prior to release (53, 54). It is also possible that tetrapeptide monomers are recycled more efficiently than tripeptide monomer in *Neisseria.* By contrast, *B. pertussis* releases exclusively tetrapeptide monomer (47, 67). *Escherichia coli*, which is known not to release much PG monomer, releases 6-8% of free peptides per generation, the majority being DAP-D-alanine dipeptides (69).

Consequences of PG fragment release

PG fragments have known arthropathic, somnogenic, pyrogenic, cytotoxic, and appetite suppression effects (46, 47, 70–73). Gonococcal-derived PG fragments as small as PG monomers stimulate arthritis when injected into rats (70). Treatment of Fallopian tube explants with PG monomers or whole bacteria results in the death and sloughing of ciliated FT cells, mimicking the pathophysiology of pelvic inflammatory disease (Fig 2) (46). The mechanisms involved in the cytotoxic effects of PG monomers are still being worked out. In studies of *B. pertussis*, treatment of hamster tracheal tissue explants with tetrapeptide monomer (TCT)

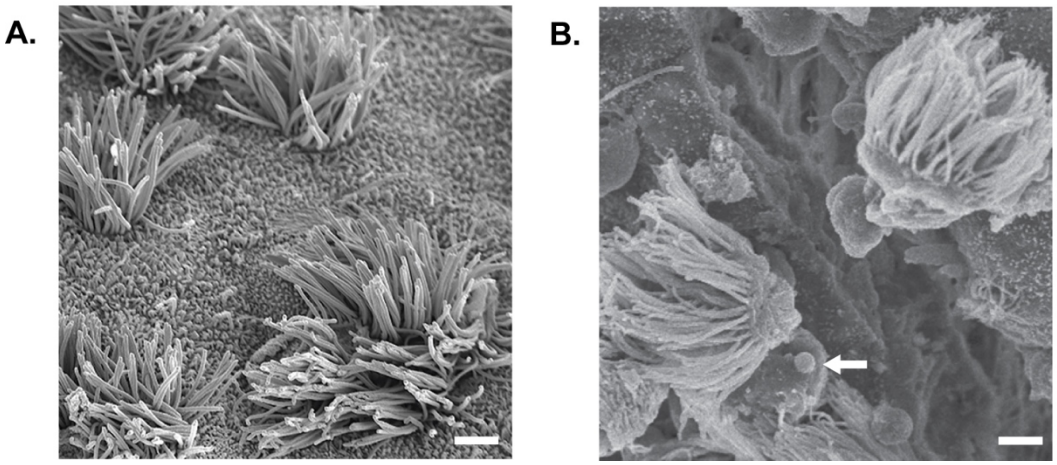

Figure 2. PG released by *N. gonorrhoeae* kills and causes extrusion of ciliated FT cells. SEM micrographs of uninfected (A) and gonococci-infected (B) FT explants. Arrow points to a gonococcal cell. Scale bar = 2 μm.

resulted in IL-1 and nitric oxide production in non-ciliated epithelial cells, and the nitric oxide caused ciliated cell death (47). It is not clear if this model is applicable to death of ciliated FT cells during gonococcal infection as inhibition of nitric oxide synthesis did not reduce cell death in FT during gonococcal infection (74). Furthermore, McGee *et al.* demonstrated a correlation between TNF-α and FT damage (75). Additionally, not all tissue and cell types respond to PG fragments equally due to heterogeneity in PG receptor expression levels (76).

Nevertheless, recognition of small PG fragments by intracellular receptors NOD1 and NOD2 elicits a proinflammatory immune response in humans and other mammals (77). Human NOD1 senses free tripeptide and tripeptide monomer and is expressed by many different cell types in humans (78–80). Human NOD2 binds to muramyl dipeptide (MDP; MurNAc-L-alanine-D-glutamate), responds to PG monomers with a reducing end and is expressed by a limited set of cell types which includes leukocytes and epithelial cells (81–85). Curiously, murine NOD1 recognizes tetrapeptide monomer instead of tripeptide monomer (86). The human receptor that recognizes tetrapeptide monomer has not been definitively identified, although there is some evidence suggesting that NOD1 can recognize tetrapeptide monomer at micromolar concentration (76, 86). As such, studies examining PG-related effects on pathogenesis in mice must be interpreted with caution when considering their relation to human diseases. Regardless, in both mice and humans, recognition of PG fragments by NOD receptors culminates in a local NF-κB dependent proinflammatory innate immune response, typically mediated by the production of cytokines such as TNF-α, IL-6, IL-8, and IL-1β (75, 78, 81, 87, 88).

One consequence of proinflammatory cytokine release is the recruitment of neutrophils to the infection site. While neutrophils are capable of killing *N. gonorrhoeae*, around 50% of *N. gonorrhoeae* cells survive and replicate intracellularly in neutrophils (89–91). Neutrophils do not

appear to express NOD1 (92). Infection of neutrophils with a gonococcal strain that produced no PG monomers but instead produced more PG glycosidically-linked dimers resulted in increased killing by neutrophils, partly due to increased susceptibility of these mutants to lysozyme and elastase action (93). Neutrophils infected with the mutant also showed increased primary and secondary granule exocytosis and increased secondary granule fusion with the phagosome (93). One possible explanation of this result is that the PG dimers produced by the mutant were degraded by neutrophil lysozyme, creating reducing monomers capable of stimulating NOD2 and causing enhanced killing of the bacteria (76, 85). Thus it appears that *N. gonorrhoeae* diminishes a NOD2 response in neutrophils by degrading PG fragments to 1,6-anhydro-containing PG monomers (85).

Generation and release of PG fragments by *N. meningitidis* and human-associated nonpathogenic *Neisseria* species.

N. meningitidis has the same set of peptidoglycan-degrading enzymes and releases different amounts of the same types of PG fragments as released by *N. gonorrhoeae* (Fig 1B, 1D) (Appendix 5). *N. meningitidis* releases 3-fold less of the proinflammatory PG monomers than *N. gonorrhoeae* and a smaller percentage of the tripeptide monomers that are NOD1 agonists (51). *N. meningitidis* shows greatly increased release of broken-down PG fragments including free peptides and anhydro-MurNAc. Comparing overall release of PG by the two pathogenic Neisseria species, *N. meningitidis* releases 4% of PG fragments generated from cell wall breakdown, whereas *N. gonorrhoeae* releases 15%. Thus, it is clear that *N. meningitidis* releases less PG overall and breaks down more fragments into their constituents. It is not clear if PG fragment release adds to the inflammatory response in invasive meningococcal disease, but the

lower amounts of PG fragment release by *N. meningitidis* may allow the bacteria to adopt their usual asymptomatic lifestyle.

I have analyzed PG fragment release in a few species of human associated nonpathogenic *Neisseria*. Detailed results from these experiments are described in Chapter 2 and Chapter 4. These experiments show that PG fragment release is lower in overall amounts and that release of PG monomers is significantly lower than for *N. gonorrhoeae* (94). *N. mucosa* and *N. sicca* were each found to release 5% of the PG monomers removed from their cell walls. The types of fragments released were similar to those released by *N. meningitidis*; however, *N. mucosa* and *N. sicca* do not release PG dimers (Fig 1C). This difference in dimer release by pathogenic and nonpathogenic *Neisseria* may have immunological implications as glycosidically-linked dimers stimulate NOD2 (85). Thus the absence of PG dimer release may help these non-pathogens avoid immune stimulation (85).

Generation of PG dimers and monomers by lytic transglycosylases

There are five characterized and two putative lytic transglycosylases (LTs) encoded on the gonococcal chromosome, of which two LTs, LtgA and LtgD, play a major role in the generation of PG monomers (Fig 3) (37). LtgA and LtgD are homologs of the *E. coli* soluble LT Slt70 and MltB/Slt35, which has a membrane bound and soluble form, respectively (96, 97). In contrast to the *E. coli* proteins, neisserial LtgA and LtgD are both found exclusively as lipid-anchored outer-membrane proteins (64). Deletion of *ltgA* results in a 38% reduction in the amount of PG monomers released while deletion of *ltgD* results in a 62% reduction (95, 98, 99). The *ltgA* and *ltgD* mutants each release less disaccharide and more PG dimers and multimers than wild type (98, 99). Deletion of both *ltgA* and *ltgD* abolishes release of PG monomers and

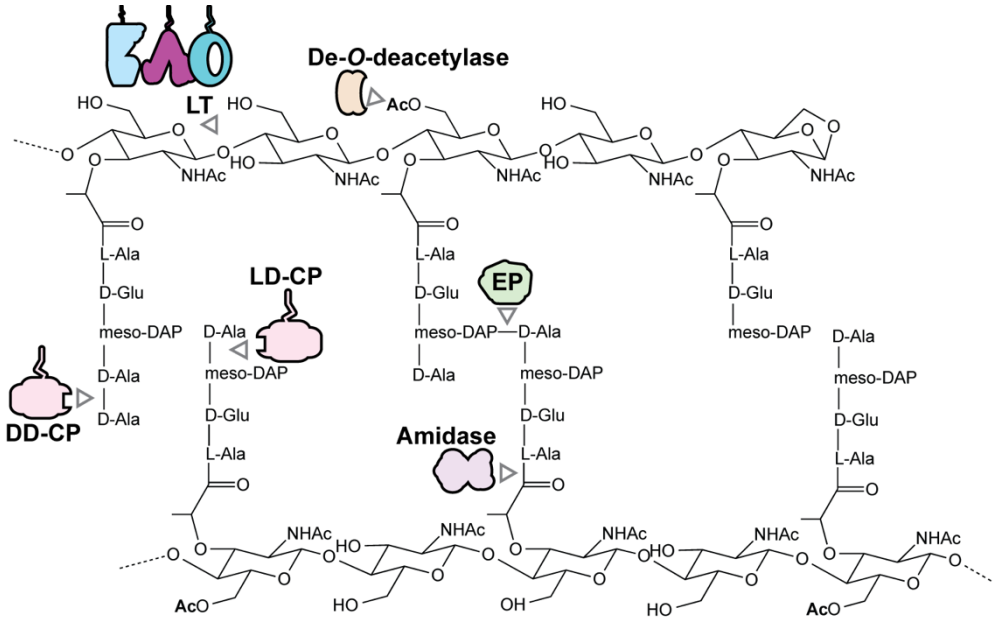

Figure 3. Sites of enzyme activity on PG strands. Lytic transglycosylases (LT) act to digest the bond between *N*-acetylmuramic acid and *N*-acetylglucosamine, while amidases sever the linkage between the peptide chain and the sugar backbone. Endopeptidases (EP) cleave the crosslinks between two peptide chains while D,D- and L,D-carboxypeptidases (DD-CP and LD-CP) trim the peptide stems. PG de-*O*-acetylases (also known as acetyl-PG-esterases) remove the *O*-acetyl group on the C6 hydroxyl of MurNAc.

disaccharide and increases the release of glycosidically-linked dimers and larger PG fragments (99). Interestingly, deletion of *ltgA* in a mutant defective for PG recycling results in more PG monomer released compared to deletion of *ltgD* released in the same background, indicating that LtgA generates more PG fragments in the periplasm compared to LtgD (64)

While both LtgA or LtgD can digest fragments as small as a synthetic PG dimer *in vitro*, LtgA liberates more species of PG fragments from whole sacculi compared to LtgD (64). Sequential digestion of sacculi with LtgA and then LtgD or vice versa liberates larger amounts of PG fragments compared to sequential digestion with the same enzyme (64). In addition, LtgA is found to localize to the septum while LtgD is distributed around the gonococcal cell (Fig 4) (64). Collectively these results indicate that while LtgA and LtgD may largely digest the same substrates, they each also have specificities for substrates not acted on by the other enzyme, with LtgA having a wider substrate range than LtgD. Furthermore, LtgA produces more PG fragments than LtgD, although PG fragments generated by LtgA are more efficiently recycled by AmpG compared to those generated by LtgD. By contrast, a larger amount of LtgD-generated PG fragments is released.

Generation of PG-derived peptides and disaccharide

N. gonorrhoeae has only one periplasmic *N*-acetylmuramyl-L-alanine amidase, AmiC, that cleaves septal PG between two daughter cells and therefore plays an important role in cell separation. By contrast, *E. coli* encodes four periplasmic amidases, in which three of the four have substantially redundant functions (100, 101). Such amidases cleave the bond between MurNAc and L-alanine, thereby severing the peptide stem from the glycan chain (Fig 3). In *E. coli* and in *N. gonorrhoeae*, AmiC activity is enhanced by the regulatory protein NlpD (55, 102–

104). NlpD is proposed to bind to and displace an inhibitory loop to expose the AmiC active site, as has been described for the *E. coli* activator protein EnvC and amidases AmiA and AmiB (55, 103–105). Deletion of gonococcal *amiC* or *nlpD* results in a cell separation defect and increased rate of cell death, potentially due to a loss of outer membrane integrity in large bacterial clumps sharing an outer membrane (55, 65, 104).

In terms of PG fragment release, deletion of *amiC* in *N. gonorrhoeae* results in an increase in PG dimer release and abolishment of tetrasaccharide peptide, disaccharide, and peptide release (55, 65). Purified gonococcal AmiC is able to digest whole sacculi, generating free peptides and cross-linked peptides, indicating that AmiC is able to act on cross-linked, multi-stranded PG, such as the thick septal PG (55). This result is consistent with *E. coli* literature, where amidases have been demonstrated to localize to and cleave peptides at the septum during cell separation (106, 107). Purified gonococcal AmiC is also able to cleave a synthetic dimer to generate tetrasaccharide peptide and a free peptide, consistent with *in vivo* results that tetrasaccharide peptide release is abrogated in an *amiC* mutant, and suggesting that AmiC may bind to at least one muropeptide moiety to cleave the peptide off an adjacent unit (55).

LtgC (*E. coli* homolog MltA) is an LT that plays a minor role in generating PG fragments and is necessary for cell separation. Deletion of *ltgC* results in large clumps of cells with irregular or thickened septa that are more sensitive to autolysis in *N. gonorrhoeae* and the closely related species *N. meningitidis* (108–110). In an *ltgC* mutant, disaccharide release is abolished, suggesting that LtgC may preferentially digest glycan strands that have been acted upon by AmiC (95, 108). Mutants defective in *ltgC* release little to no tetrasaccharide-peptide (108). The *E. coli* LtgC homolog can also digest naked glycan strands to generate free disaccharide (111).

Collectively these results suggest an order of operation for some of the PG degradation reactions in *N. gonorrhoeae*. AmiC removes stem peptides from PG strands, allowing LtgC to degrade the mostly naked glycan strands into disaccharides and tetrasaccharide-peptide. LtgA is also localized to the septum (Fig 4), but since it is not required for cell separation, it is unlikely that it is directly involved with the septum-splitting proteins (64, 99).

Generation of peptide stem variations in PG fragments

Trimming of peptide stems and cleavage of peptide cross-links are done by carboxypeptidases and endopeptidases respectively (Fig 3). *N. gonorrhoeae* encodes several PGases that are able to perform either or both functions. Two low molecular weight penicillin binding proteins, PBP3 and PBP4, have D,D-carboxypeptidase activity and preferentially digest cross-linked peptides (112–114). Gonococcal PBP3 and PBP4 are homologues of *E. coli* PBP4 and PBP7, respectively. PBP3 also has D,D-endopeptidase activity (112). *N. gonorrhoeae* lacking PBP3 releases more PG dimers and more pentapeptide monomer, and has more pentapeptide stems in the sacculi ((115), unpublished observation). *N. gonorrhoeae* lacking both PBP3 and PBP4 releases less disaccharide and PG monomers, more PG multimer, and multiple unidentified PG fragment peaks, nearly all of which are larger than PG monomers (115). The double mutant also exhibits reduced viability and more irregularly sized (smaller or larger) cells (112, 115). Cumulatively, these data suggest that PBP3 and PBP4 perform overlapping but important functions in symmetric cell division and PG fragment release.

Zarantonelli *et al*. examined a penicillin-insensitive strain of *N. meningitidis* and found that it had reduced D,D-carboxypeptidase activity, even though the genetic alteration to make it

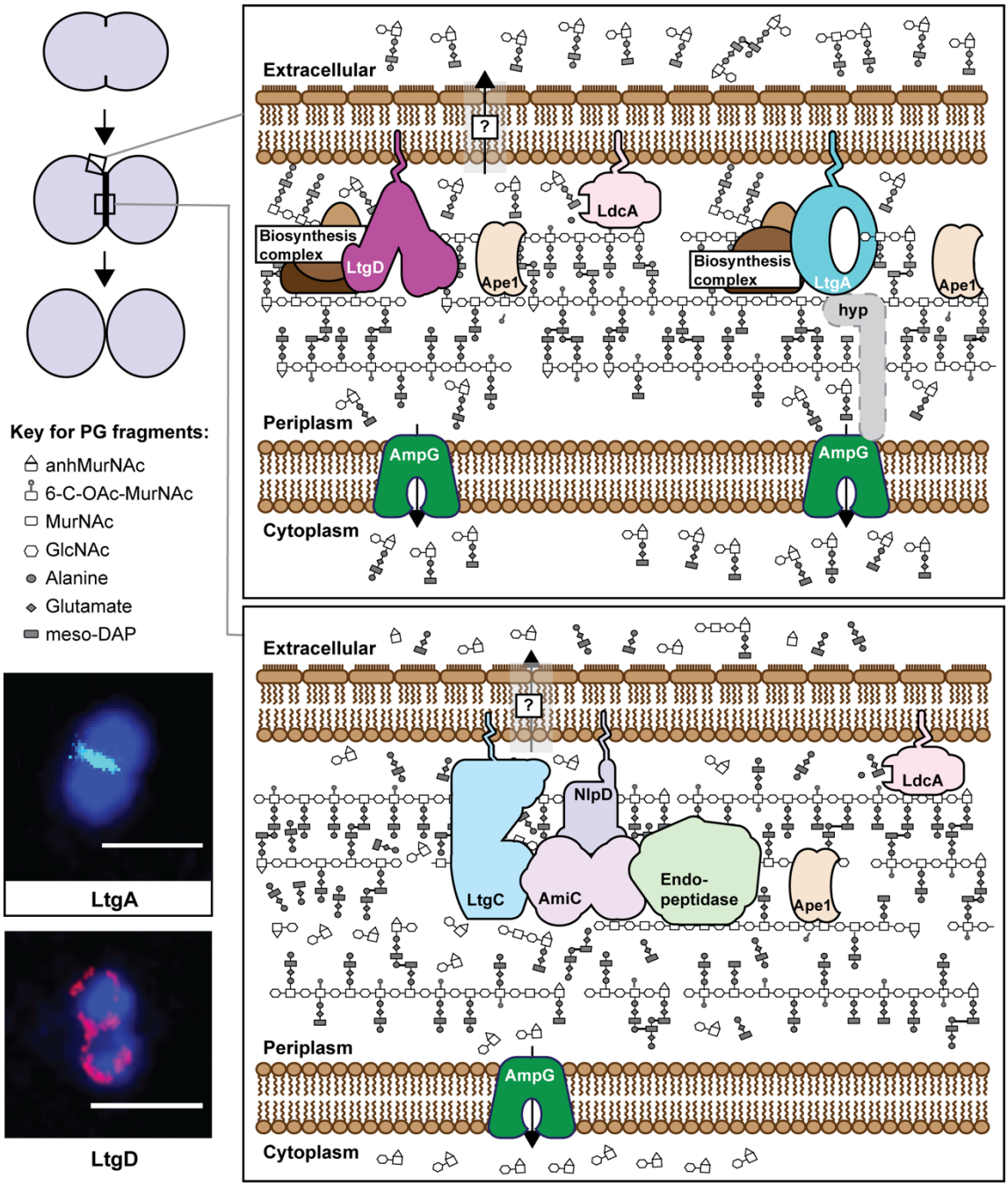

Figure 4. Model of PG fragment generation in *N. gonorrhoeae*. Model for PG fragment generation, release and recycling by LtgA and LtgD (top right inset) and by the septal apparatus during cell separation (bottom right inset). STORM images (bottom left insets) demonstrate subcellular localization of LtgA and LtgD in *N. gonorrhoeae.* Scale bar = 1 μm.

penicillin insensitive was in the gene for the biosynthetic transpeptidase PBP2 (116). The sacculus composition showed decreased amounts of tetrapeptide stems and increased amounts of pentapeptide stems as well as increased tetra-penta and tetra-tetra-penta crosslinks (116). The penicillin insensitive strain stimulated a smaller NOD1 response in human epithelial cells than the wild type strain, suggesting that it released less PG monomers (116). To explain the decreased D,D-carboxypeptidase activity, PBP2 was investigated for a physical interaction with PBP3, and binding was detected (116). Overall, these results suggest that PBP3 activity is necessary for wild type levels of pro-inflammatory PG fragment release.

Generation of tripeptide stems in gonococcal and meningococcal liberated PG fragments occurs through the action of an L,D-carboxypeptidase, LdcA (117, 118). Mutation of *ldcA* in *N. gonorrhoeae* or *N. meningitidis* leads to an increase in the release of PG dimers and multimers (45, 119). PG monomers and free peptides released by an *ldcA* mutant are exclusively comprised of four amino acid versions (119). The increase in PG dimers and multimers released by the *ldcA* mutants compared to wild type demonstrates the endopeptidase activity of LdcA. LdcA encoded by *Neisseria* and closely-related genera contains a Tat signal sequence and a lipidation site and functions as an outer membrane lipoprotein (45, 119). In *E. coli* and most other Gram-negative bacteria, LdcA is a cytoplasmic protein that plays a role in PG recycling by digesting tetrapeptides into tripeptides, which can then be directly attached to UDP-MurNAc to generate the PG precursor UDP-MurNAc-tripeptide (120). The periplasmic localization of LdcA in the *Neisseriaceae* and the loss of tripeptide monomer release in the *ldcA* mutant suggest that *Neisseria* has evolved strategies to ensure release of NOD1 agonists.

Recycling of PG fragments and impact on PG release

In Gram-negative bacteria, PG fragments liberated from the sacculi are usually efficiently transported back into the cytoplasm by the permease AmpG, broken down into smaller constituents and utilized to synthesize new PG strands or for general metabolism (121). Deletion of *ampG* in *N. gonorrhoeae*, *N. meningitidis*, *N. sicca* and *N. mucosa* leads to a large increase in the amount of PG monomers, an increase in the amount of disaccharide but no obvious differences in the amount of PG dimers released compared to wild type (51, 94, 117). It is not known if AmpG can transport PG dimers, although our findings suggest that AmpG does not or is inefficient at transporting PG dimers. The role of AmpG in modulating the amount of PG fragments released is not limited to *Neisseria.* Mutation of *ampG* results in 24- and 100-fold increases in the amount of TCT released by *B. pertussis* and *V. fischeri* (122, 123). In fact, the release of TCT by *B. pertussis* is a direct effect of the presence of an insertion sequence 85bp upstream of the *B. pertussis ampG* coding sequence, reducing *ampG* expression (122). Deletion of *ampG* in *E. coli* results in a large amount of disaccharide released with a small amount of monomer released, suggesting that *E. coli* digests PG fragments extensively into smaller pieces in the periplasm (66). This result is reminiscent of the PG fragment release pattern of *N. meningitidis*, which releases less PG monomers and more anhydro-MurNAc compared to *N. gonorrhoeae* (51, 94).

Different species of *Neisseria* have different PG recycling efficiencies. Despite 97% amino acid identity between the AmpG sequence of *N. gonorrhoeae* and that of *N. meningitidis*, gonococcal AmpG is less efficient at recycling PG fragments compared to meningococcal AmpG (94). Three residues near the C-terminal end of AmpG cooperatively control the difference in recycling efficiency seen in *N. gonorrhoeae* and *N. meningitidis*. Mutations of these three

residues from the gonococcal to the meningococcal variants decrease PG monomer release by *N. gonorrhoeae* by half. The reverse experiment increases the amount of PG monomer released by *N. meningitidis* by 40%. Gonococcal AmpG is also less efficient at recycling compared to the AmpG variants from *N. sicca* and *N. mucosa* (94).

AmpD is a cytoplasmic amidase that cleaves the peptide stem off PG monomers and anhydro-MurNAc-peptide to generate disaccharide or anhydro-MurNAc (124, 125). AmpD does not play a direct role in the generation of free peptides in the periplasm. However, a gonococcal *ampD* mutant releases less PG monomers and minimal amounts of disaccharide (117). In the absence of AmpD, *N. gonorrhoeae* increases uptake and metabolism of disaccharide thereby altering the amounts of PG fragments released (117). This result suggests that *N. gonorrhoeae* is able to regulate PG fragment release in response to different levels of PG recycling intermediates in the cytoplasm. Accumulation of the recycling intermediate anhydro-MurNAc-peptide in an *ampD* mutant led to constitutive expression of the AmpC beta-lactamase in a number of Gram-negative species, including *Pseudomonas aeruginosa*, *Citrobacter freundii*, *Enterobacter cloacae* and *Stenotrophomonas maltophila*, conferring resistance against beta-lactam antibiotics (126–130). Perturbation to the PG biosynthesis and recycling pathway due to beta-lactam antibiotic treatment is thought to lead to the same accumulation of anhydro-MurNAc-peptide and induction of AmpC expression. While *Neisseria* do not have the AmpC beta-lactamase system or a homolog of the PG-binding transcriptional regulator AmpR, perturbations to the recycling pathway can lead to alteration of the amounts of PG fragments released by the bacteria. Given that a gonococcal *ampD* mutant amasses anhydro-MurNAc-peptide in the cytoplasm, it is plausible that PG fragment recycling intermediates may play a role as messenger molecules for

regulating gene expression of one or more PG recycling enzymes in gonococci through an uncharacterized mechanism (117).

Model of PG fragment generation in *N. gonorrhoeae*

The analyses of PG fragment release by different PG-degradation mutants allow us to propose a model for PG fragment generation and release (Fig 4). The PG strands are first deacetylated by the PG de-*O*-acetylase, ApeI. LtgA and LtgD then act to generate PG monomers and PG dimers, by degrading the PG strands from the GlcNAc end and toward the anhydro-MurNAc found at the end of each strand (131). Degradation of strands to PG monomers requires an endopeptidase, likely PBP3 or PBP4, to remove peptide cross-links. Prior to their release from the cell, some of the PG fragments are acted on by LdcA, which converts a majority of PG monomers into the tripeptide monomer form that serves as a NOD1 agonist. LdcA also degrades some of the peptide-linked dimers to PG monomers. LtgA is localized to the septum, and most of the PG fragments it produces are shuttled into the cytoplasm for recycling. It is unclear why PG fragments produced by LtgA are so efficiently recycled, but we hypothesize that the PG fragment permease AmpG might be associated with LtgA via interactions with an unknown protein (Fig 4, hyp protein). The proteins that function in cell separation act to create the free sugars and free peptides that gonococci release. An endopeptidase together with AmiC acts to cut cross-links and remove peptide stems from the PG strands. LtgC degrades the mostly naked PG strands into free anhydro-disaccharide plus tetrasaccharide peptide. Some of the free peptides that are liberated are acted on by LdcA to create free tripeptides before they are released into the milieu. Upon digestion of existing PG strands, the PG biosynthetic machinery acts to build new strands of PG for cellular enlargement (132, 133).

Discussion, current work and future directions

Neisseria may have been particularly well-suited to evolve PG fragment release that is immunostimulatory in the human host. *Neisseria* and closely-related genera localize LdcA to the outer membrane and thus generate NOD1 agonists at the outer membrane rather than in the cytoplasm. Furthermore, the LTs that generate PG monomers and dimers are also localized to the outer membrane, and at least for LtgD, this localization increases PG monomer release (64). With only a few changes to the AmpG sequence, the efficiency of the *N. meningitidis* AmpG permease is decreased to match that of *N. gonorrhoeae* (94). The resulting 3-fold increase in toxic PG monomer release is sufficient to increase NOD1 signaling and inflammatory cytokine production (51). The other changes to PG fragment breakdown that result in *N. gonorrhoeae* releasing mostly PG monomers and *N. meningitidis* or nonpathogenic Neisseria releasing more degraded PG fragments have yet to be determined.

The widely-used model for PG synthesis and degradation in rod shaped bacteria proposes that there are two sets of differentially localized enzymes, referred to as the elongasome and the divisome, that promote cell enlargement and cell division respectively (132, 133). Conversely, cocci have been assumed to only have one, septally-localized machinery. Recent discoveries on PG degradation and release in *Neisseria* suggest that *Neisseria* have septal and dispersed PG apparatuses. A septal apparatus facilitates cell separation. PG fragments generated at the septum, for the most part, are taken up into the cytoplasm for recycling. The dispersed PG apparatus is likely to play a role in cell enlargement and liberates PG fragments that are mostly released rather than recycled. Additional work has to be done to determine the components and functions of these machineries, but with the relatively small number of PG degradation proteins present in *Neisseria*, determining their locations and functions seems possible.

There is still much that we do not understand about the breakdown and release of small PG fragments. It appears that *N. gonorrhoeae* has the ability to sense PG fragments and regulate PG fragment release, but the mechanisms involved are not understood. *N. gonorrhoeae* that reach late-log to stationary phase do not show free disaccharide release, suggesting that this molecule is either consumed or not released as the bacteria experience nutrient deprivation. Similarly, *ltgA ltgD* mutants produce free disaccharide and some PG monomers that are present in the periplasm but not released, and *ampD* mutants make free disaccharide that is not released (93, 117). These results suggest that gonococci can sense the decrease in certain PG fragments in the cytoplasm in these recycling-deficient mutants and respond by increasing PG fragment uptake. This increased uptake was directly demonstrated for the *ampD* mutant (117). *N. gonorrhoeae* does not encode an obvious homolog of the PG-binding transcriptional regulator AmpR, suggesting that a different mechanism exists in these bacteria for regulating PG metabolism (134). Transcription of *ltgA* is positively regulated by the transcriptional regulator MtrR, suggesting that not only PG fragment recycling, but also PG fragment generation, may be controlled (135). If gonococci are able to regulate PG fragment breakdown and release, then changes in PG release might partly explain the differences in inflammatory responses seen in different forms of gonococcal infections.

Study of PG breakdown may lead to new antibiotic strategies. Breakdown of PG strands precedes the incorporation of new PG strands and is thus a necessary process (132). Also, changing the way the PG is broken down makes the bacteria particularly sensitive to host defenses. In studies of PG-acetylation, Veyrier *et al.* studied *N. meningitidis* mutants that cannot remove the acetyl groups from MurNAc and thus cannot degrade PG strands using LTs. They found these mutants were attenuated in a mouse model of infection (136). Similarly, Ragland *et*

al. found that *ltgA ltgD* mutants of *N. gonorrhoeae* are highly susceptible to killing by human neutrophils (93). A recent report demonstrated that the natural product bulgecin A binds and inhibits LtgA (137). Furthermore, bulgecin A treatment was sufficient to make penicillin-insensitive *N. gonorrhoeae* strains susceptible to a number of beta-lactam antibiotics. Therefore, LTs and other PG-breakdown enzymes are attractive targets for further study and future antibiotic therapy.

The overarching goal of my thesis project is to characterize PG fragments released by human- and animal-associated species of *Neisseria*, and to understand the molecular mechanisms underpinning any differences seen. To accomplish this aim, I have analyzed and compared the PG recycling permease AmpG in *N. gonorrhoeae*, *N. meningitidis* and *N. lactamica*, and discovered that polymorphisms at specific AmpG residues lead to differences in the amount of PG monomers released by the three species. These findings are described in Chapter 2, Chapter 4 and Appendix 1. I have also examined PG fragment release by seven isolates of human- and animal-associated nonpathogenic *Neisseria* and built complementation plasmids for use with *N. sicca* and *N. mucosa*. These findings are described in Chapter 4 and Appendix 2. Additionally, my colleagues and I characterized the PG peptides released by *N. meningitidis*, examined enzymes that generate these peptides and determined that the peptides stimulate NOD1 activation in HEK293 reporter cells. Our results are detailed in Chapter 3. Overall, my thesis work revealed that nonpathogenic *Neisseria* also release inflammatory PG fragments, and suggests that different species of *Neisseria* evolved distinct strategies to carefully control the types and amounts of PG fragments released.

Acknowledgements

We thank Kathleen T. Hackett, Ryan E. Schaub and Yolande A. Chan for providing images used in the figures. We also thank R.E.S. and Melanie M. Callaghan for critical reading and discussion of the manuscript.

REFERENCES

1. **Johnson AP**. 1983. The pathogenic potential of commensal species of *Neisseria*. J Clin Pathol **36**:213–23.
2. **Liu G**, **Tang CM**, **Exley RM**. 2015. Non-pathogenic *Neisseria*: members of an abundant, multi-habitat, diverse genus. Microbiology **161**:1297–1312.
3. **Quillin SJ**, **Seifert HS**. 2018. *Neisseria gonorrhoeae* host adaptation and pathogenesis. Nat Publ Gr **16**:226–240.
4. **Pariser H**. 1972. Asymptomatic gonorrhea. Med Clin North Am **56**:1127–1132.
5. **MacDonald N**, **Mailman T**, **Desai S**. 2008. Gonococcal infections in newborns and in adolescents. Adv Exp Med Biol **609**:108–130.
6. **CDC**. 2016 Sexually Transmitted Disease Surveillance: Gonorrhea. Accessed from <https://www.cdc.gov/std/stats16/CDC_2016_STDS_Report-for508WebSep21_2017_1644.pdf>.
7. **Newman L**, **Rowley J**, **Hoorn S Vander**, **Wijesooriya NS**, **Unemo M**, **Low N**, **Stevens G**, **Gottlieb S**, **Kiarie J**, **Temmerman M**. 2015. Global estimates of the prevalence and incidence of four curable sexually transmitted infections in 2012 based on systematic review and global reporting. PLoS One **10**:e0143304.
8. **Centers for Disease Control and Prevention**. 2013. Antibiotic resistance threats in the United States, 2013. US Dep Heal Hum Serv. Accessed from <https://www.cdc.gov/drugresistance/pdf/ar-threats-2013-508.pdf>.
9. **WHO**. 2014. Antimicrobial resistance: global report on surveillance. Accessed from < http://apps.who.int/iris/bitstream/handle/10665/112642/9789241564748_eng.pdf;jsessionid=7535354C2ACACF975EDC7E28A13C9CCA?sequence=1>.
10. **Fifer H**, **Natarajan U**, **Jones L**, **Alexander S**, **Hughes G**, **Golparian D**, **Unemo M**. 2016. Failure of dual antimicrobial therapy in treatment of gonorrhea. N Engl J Med **374**:2504–2506.
11. **Suay-Garcia B**, **Perez-Gracia MT**. 2017. Drug-resistant *Neisseria gonorrhoeae*: latest developments. Eur J Clin Microbiol Infect Dis **36**:1065–1071.
12. **Public Health England**. 2018. UK case of *Neisseria gonorrhoeae* with high-level resistance to azithromycin and resistance to ceftriaxone acquired abroad. Heal Prot Rep **12**.
13. **Swartz MN**. 2004. Bacterial meningitis — A view of the past 90 years. N Engl J Med **351**:1826–1828.
14. **Stephens DS**, **Greenwood B**, **Brandtzaeg P**. 2007. Epidemic meningitis, meningococcaemia, and *Neisseria meningitidis*. Lancet **369**:2196–2210.
15. **Roupheal NG**, **Stephens DS**. 2012. *Neisseria meningitidis*: biology, microbiology and epidemiology. Methods Mol Biol **799**:1–20.
16. **CDC**. 2017. Meningococcal Disease: Clinical Information. Accessed from < https://www.cdc.gov/meningococcal/clinical-info.html>.
17. **Vossen M**, **Mitteregger D**, **Steininger C**. 2016. Meningococcal pneumonia. Vaccine **34**:4364–4370.
18. **Bazan JA**, **Peterson AS**, **Kirkcaldy RD**, **Briere EC**, **Maierhofer C**, **Turner AN**, **Licon DB**, **Parker N**, **Dennison A**, **Ervin M**, **Johnson L**, **Weberman B**, **Hackert P**, **Wang X**, **Kretz CB**, **Abrams AJ**, **Trees DL**, **Del Rio C**, **Stephens DS**, **Tzeng Y-L**, **DiOrio M**, **Roberts MW**. 2016. Notes from the field. Increase in *Neisseria meningitidis*-associated

urethritis among men at two sentinel clinics - Columbus, Ohio, and Oakland County, Michigan, 2015. Morb Mortal Wkly Rep **65**:550–552.
19. **Bazan JA**, **Turner AN**, **Kirkcaldy RD**, **Retchless AC**, **Kretz CB**, **Briere E**, **Tzeng Y-L**, **Stephens DS**, **Maierhofer C**, **Del Rio C**, **Abrams AJ**, **Trees DL**, **Ervin M**, **Licon DB**, **Fields KS**, **Roberts MW**, **Dennison A**, **Wang X**. 2017. Large Cluster of *Neisseria meningitidis* urethritis in Columbus, Ohio, 2015. Clin Infect Dis **65**:92–99.
20. **Yezli S**, **Wilder-Smith A**, **Saeed AA**. 2016. Carriage of *Neisseria meningitidis* in the Hajj and Umrah mass gatherings. Int J Infect Dis **47**:65–70.
21. **Deasy AM**, **Guccione E**, **Dale AP**, **Andrews N**, **Evans CM**, **Bennett JS**, **Bratcher HB**, **Maiden MCJ**, **Gorringe AR**, **Read RC**. 2015. Nasal inoculation of the commensal *Neisseria lactamica* inhibits carriage of *Neisseria meningitidis* by young adults: A controlled human infection study. Clin Infect Dis **60**:1512–1520.
22. **Jafri RZ**, **Ali A**, **Messonnier NE**, **Tevi-Benissan C**, **Durrheim D**, **Eskola J**, **Fermon F**, **Klugman KP**, **Ramsay M**, **Sow S**, **Zhujun S**, **Bhutta ZA**, **Abramson J**. 2013. Global epidemiology of invasive meningococcal disease. Popul Health Metr **11**:17.
23. **Schoen C**, **Blom J**, **Claus H**, **Schramm-Glück A**, **Brandt P**, **Müller T**, **Goesmann A**, **Joseph B**, **Konietzny S**, **Kurzai O**, **Schmitt C**, **Friedrich T**, **Linke B**, **Vogel U**, **Frosch M**. 2008. Whole-genome comparison of disease and carriage strains provides insights into virulence evolution in *Neisseria meningitidis*. Proc Natl Acad Sci U S A **105**:3473–3478.
24. **Harrison LH**, **Trotter CL**, **Ramsay ME**. 2009. Global epidemiology of meningococcal disease. Vaccine **27 Supplem**:B51–B63.
25. **Knapp JS**. 1988. Historical perspectives and identification of *Neisseria* and related species. Clin Microbiol Rev **1**:415–431.
26. **Bennett JS**, **Jolley KA**, **Earle SG**, **Corton C**, **Bentley SD**, **Parkhill J**, **Maiden MCJ**. 2012. A genomic approach to bacterial taxonomy: An examination and proposed reclassification of species within the genus *Neisseria*. Microbiology **158**:1570–1580.
27. **Aas JA**, **Paster BJ**, **Stokes LN**, **Olsen I**, **Dewhirst FE**. 2005. Defining the normal bacterial flora of the oral cavity. J Clin Microbiol **43**:5721–5732.
28. **Zaura E**, **Keijser BJ**, **Huse SM**, **Crielaard W**. 2009. Defining the healthy "core microbiome" of oral microbial communities. BMC Microbiol **9**:259.
29. **Marri PR**, **Paniscus M**, **Weyand NJ**, **Rendon MA**, **Calton CM**, **Hernandez DR**, **Higashi DL**, **Sodergren E**, **Weinstock GM**, **Rounsley SD**, **So M**. 2010. Genome sequencing reveals widespread virulence gene exchange among human *Neisseria* species. PLoS One **5**:e11835.
30. **Eren AM**, **Borisy GG**, **Huse SM**, **Mark Welch JL**. 2014. Oligotyping analysis of the human oral microbiome. Proc Natl Acad Sci United States **111**:E2875–E2884.
31. **Donati C**, **Zolfo M**, **Albanese D**, **Truong DT**, **Asnicar F**, **Iebba V**, **Cavalieri D**, **Jousson O**, **Filippo C De**, **Huttenhower C**, **Segata N**. 2016. Uncovering oral *Neisseria* tropism and persistence using metagenomic sequencing. Nat Microbiol **1**:1–9.
32. **Gold R**, **Goldschneider I**, **Lepow ML**, **Draper TF**, **Randolph M**. 1978. Carriage of *Neisseria meningitidis* and *Neisseria lactamica* in infants and children. J Infect Dis **137**:112–121.
33. **Oliver KJ**, **Reddin KM**, **Bracegirdle P**, **Hudson MJ**, **Borrow R**, **Feavers IM**, **Robinson A**, **Cartwright K**, **Gorringe AR**. 2002. *Neisseria lactamica* protects against experimental meningococcal infection. Infect Immun **70**:3621–3626.
34. **Hansen CM**, **Meixell BW**, **Van Hemert C**, **Hare RF**, **Hueffer K**. 2015. Microbial

infections are associated with embryo mortality in Arctic-nesting geese. Appl Environ Microbiol **81**:5583–5592.
35. **Dill-McFarland KA**, **Weimer PJ**, **Pauli JN**, **Peery MZ**, **Suen G**. 2016. Diet specialization selects for an unusual and simplified gut microbiota in two- and three-toed sloths. Environ Microbiol **18**:1391–1402.
36. **Welsch JA**, **Ram S**. 2009. Factor H and Neisserial pathogenesis. Vaccine **26**:140–145.
37. **Zarantonelli M-L**, **Szatanik M**, **Giorgini D**, **Hong E**, **Huerre M**, **Guillou F**, **Alonso J-M**, **Taha M**. 2007. Transgenic mice expressing human transferrin as a model for meningococcal infection. Infect Immun **75**:5609–5614.
38. **Johswich KO**, **McCaw SE**, **Islam E**, **Sintsova A**, **Gu A**, **Shively JE**, **Gray-Owen SD**. 2013. *In vivo* adaptation and persistence of *Neisseria meningitidis* within the nasopharyngeal mucosa. PLoS Pathog **9**:e1003509.
39. **Melican K**, **Aubey F**, **Duménil G**. 2014. Humanized mouse model to study bacterial infections targeting the microvasculature. J Vis Exp **85**:e51134.
40. **Weyand NJ**, **Wertheimer AM**, **Hobbs TR**, **Sisko JL**, **Taku N a**, **Gregston LD**, **Clary S**, **Higashi DL**, **Biais N**, **Brown LM**, **Planer SL**, **Legasse AW**, **Axthelm MK**, **Wong SW**, **So M**. 2013. *Neisseria* infection of rhesus macaques as a model to study colonization, transmission, persistence, and horizontal gene transfer. Proc Natl Acad Sci U S A **110**:3059–64.
41. **Weyand NJ**, **Ma M**, **Phifer-Rixey M**, **Taku NA**, **Rendón MA**, **Hockenberry AM**, **Kim WJ**, **Agellon AB**, **Biais N**, **Suzuki TA**, **Goodyer-Sait L**, **Harrison OB**, **Bratcher HB**, **Nachman MW**, **Maiden MCJ**, **So M**. 2016. Isolation and characterization of *Neisseria musculi* sp. nov., from the wild house mouse. Int J Syst Evol Microbiol **66**:3585–3593.
42. **Ma M**, **Powell DA**, **Weyand NJ**, **Rhodes KA**, **Rendón MA**, **Frelinger JA**, **So M**. 2018. A mouse model for *Neisseria* colonization. Infect Immun doi:10.1128/IAI.00839-17.
43. **Rosenthal RS**. 1979. Release of soluble peptidoglycan from growing gonococci: hexaminidase and amidase activities. Infect Immun **24**:869–878.
44. **Mavrogiorgos N**, **Mekasha S**, **Yang Y**, **Kelliher MA**, **Ingalls RR**. 2014. Activation of NOD receptors by *Neisseria gonorrhoeae* modulates innate immune response. Innate Immun **20**:377–389.
45. **Lenz JD**, **Hackett KT**, **Dillard JP**. 2017. A single dual-function enzyme controls the production of inflammatory NOD agonist peptidoglycan fragments by *Neisseria gonorrhoeae*. MBio **8**:e01464-17.
46. **Melly MA**, **McGee ZA**, **Rosenthal RS**. 1984. Ability of monomeric peptidoglycan fragments from *Neisseria gonorrhoeae* to damage human Fallopian-tube. J Infect Dis **149**:378–386.
47. **Goldman WE**, **Klapper DG**, **Baseman JB**. 1982. Detection, isolation, and analysis of a released *Bordetella pertussis* product toxic to cultured tracheal cells. Infect Immun **36**:782–794.
48. **Cookson BT**, **Cho H**, **Herwaldt LA**, **Goldman WE**. 1989. Biological activities and chemical composition of purified tracheal cytotoxin of *Bordetella pertussis*. Infect Immun **57**:2223–2229.
49. **Koropatnick TA**, **Engle JT**, **Apicella MA**, **Stabb E V**, **Goldman WE**, **McFall-Ngai MJ**. 2004. Microbial factor-mediated development in a host-bacterial mutualism. Science **306**:1186–1188.
50. **Troll J V**, **Adin DM**, **Wier AM**, **Paquette N**, **Silverman N**, **Goldman WE**, **Stadermann**

FJ, **Stabb EV**, **McFall-Ngai MJ**. 2009. Peptidoglycan induces loss of a nuclear peptidoglycan recognition protein during host tissue development in a beneficial animal-bacterial symbiosis. Cell Microbiol **11**:1114–1127.

51. **Woodhams KL**, **Chan JM**, **Lenz JD**, **Hackett KT**, **Dillard JP**. 2013. Peptidoglycan fragment release from *Neisseria meningitidis*. Infect Immun **81**:3490–3498.
52. **Vollmer W**, **Blanot D**, **de Pedro MA**. 2008. Peptidoglycan structure and architecture. FEMS Microbiol Rev **32**:149–167.
53. **Rosenthal RS**, **Wright RM**, **Sinha RK**. 1980. Extent of peptide cross-linking in the peptidoglycan of *Neisseria gonorrhoeae*. Infect Immun **28**:867–875.
54. **Sinha RK**, **Rosenthal RS**. 1980. Release of soluble peptidoglycan from growing gonococci: Demonstration of anhydro-muramyl-containing fragments. Infect Immun **29**:914–925.
55. **Lenz JD**, **Stohl EA**, **Robertson R**, **Hackett KT**, **Fisher K**, **Xiong K**, **Lee M**, **Hesek D**, **Mobashery S**, **Seifert HS**, **Davies C**, **Dillard JP**. 2016. Amidase activity of AmiC controls cell separation and stem-peptide release and is enhanced by NlpD in *Neisseria gonorrhoeae*. J Biol Chem **291**:10916–10933.
56. **Antignac A**, **Rousselle JC**, **Namane A**, **Labigne A**, **Taha MK**, **Boneca IG**. 2003. Detailed structural analysis of the peptidoglycan of the human pathogen *Neisseria meningitidis*. J Biol Chem **278**:31521–31528.
57. **Wolf-Watz H**, **Elmros T**, **Normark S**, **Bloom GD**. 1975. Cell envelope of *Neisseria gonorrhoeae*: Outer membrane and peptidoglycan composition of penicillin-sensitive and -resistant strains. Infect Immun **11**:1332–1341.
58. **Grizot S**, **Buchanan SK**. 2004. Structure of the OmpA-like domain of RmpM from *Neisseria meningitidis*. Mol Microbiol **51**:1027–1037.
59. **Maharjan S**, **Saleem M**, **Feavers IM**, **Wheeler JX**, **Care R**, **Derrick JP**. 2016. Dissection of the function of the RmpM periplasmic protein from *Neisseria meningitidis*. Microbiology 364–375.
60. **Rosenthal RS**, **Blundell JK**, **Perkins HR**. 1982. Strain-related differences in lysozyme sensitivity and extent of *O*-acetylation of gonococcal peptidoglycan. Infect Immun **37**:826–829.
61. **Swim SC**, **Gfell MA**, **Wilde CE**, **Rosenthal RS**. 1983. Strain distribution in extents of lysozyme resistance and *O*-acetylation of gonococcal peptidoglycan determined by high-performance liquid chromatography. Infect Immun **42**:446–452.
62. **Dillard JP**, **Hackett KT**. 2005. Mutations affecting peptidoglycan acetylation in *Neisseria gonorrhoeae* and *Neisseria meningitidis*. Infect Immun **73**:5697–5705.
63. **Moynihan PJ**, **Clarke AJ**. 2010. *O*-acetylation of peptidoglycan in Gram-negative bacteria: Identification and characterization of peptidoglycan *O*-acetyltransferase in *Neisseria gonorrhoeae*. J Biol Chem **285**:13264–13273.
64. **Schaub RE**, **Chan YA**, **Lee M**, **Hesek D**, **Mobashery S**, **Dillard JP**. 2016. Lytic transglycosylases LtgA and LtgD perform distinct roles in remodeling, recycling, and releasing peptidoglycan in *Neisseria gonorrhoeae*. Mol Microbiol **102**:865–881.
65. **Garcia DL**, **Dillard JP**. 2006. AmiC functions as an *N*-acetylmuramyl-L-alanine amidase necessary for cell separation and can promote autolysis in *Neisseria gonorrhoeae*. J Bacteriol **188**:7211–7221.
66. **Schaub RE**, **Lenz JD**, **Dillard JP**. 2016. Analysis of peptidoglycan fragment release. Methods Mol Biol **1440**:185–200.

67. **Rosenthal RS**, **Nogami W**, **Cookson BT**, **Goldman WE**, **Folkening WJ**. 1987. Major fragment of soluble peptidoglycan released from growing *Bordetella pertussis* is tracheal cytotoxin. Infect Immun **55**:2117–2120.
68. **Sinha RK**, **Rosenthal RS**. 1981. Effect of penicillin G on release of peptidoglycan fragments by *Neisseria gonorrhoeae*: Characterization of extracellular products. Antimicrob Agents Chemother **20**:98–103.
69. **Goodell EW**, **Schwarz U**. 1985. Release of cell wall peptides into culture medium by exponentially growing *Escherichia coli*. J Bacteriol **162**:391–397.
70. **Fleming TJ**, **Wallsmith DE**, **Rosenthal RS**. 1986. Arthropathic properties of gonococcal peptidoglycan fragments : implications for the pathogenesis of disseminated gonococcal disease. Infect Immun **52**:600–608.
71. **Johannsen L**, **Toth LA**, **Rosenthal RS**, **Opp MR**, **Obal F**, **Cady AB**, **Krueger JM**. 1990. Somnogenic, pyrogenic, and hematologic effects of bacterial peptidoglycan. Am J Physiol **258**:R182–R186.
72. **Biberstine KJ**, **Darr DS**, **Rosenthal RS**. 1996. Tolerance to appetite suppression induced by peptidoglycan. Infect Immun **64**:3641–3645.
73. **Krueger J**, **Opp M**. 2016. Sleep and microbes. Int Rev Neurobiol **131**:207–225.
74. **García KP**, **Rubilar PS**, **Vargas MF**, **Cardenas H**, **Rios MA**, **Orihuela PA**, **Vargas RH**, **Fuhrer J**, **Heckels JE**, **Christodoulides M**, **Velásquez LA**. 2010. Nitric oxide is not involved in *Neisseria gonorrhoeae*-induced cellular damage of Fallopian tubes *in vitro*. Biol Res **43**:39–50.
75. **McGee ZA**, **Jensen RL**, **Clements CM**, **Taylor-Robinson D**, **Johnson AP**, **Gregg CR**. 1999. Gonococcal infection of human Fallopian tube mucosa in organ culture: relationship of mucosal tissue TNF-α concentration to sloughing of ciliated cells. Sex Transm Dis **26**:160–165.
76. **Dagil YA**, **Arbatsky NP**, **Alkhazova BI**, **L'vov VL**, **Mazurov D V**, **Pashenkov M V**. 2016. The dual NOD1/NOD2 agonism of muropeptides containing a meso-diaminopimelic acid residue. PLoS One **11**:e0160784.
77. **Philpott DJ**, **Sorbara MT**, **Robertson SJ**, **Croitoru K**, **Girardin SE**. 2014. NOD proteins: regulators of inflammation in health and disease. Nat Rev Immunol **14**:9–23.
78. **Girardin SE**, **Boneca IG**, **Carneiro LAM**, **Antignac A**, **Jehanno M**, **Viala J**, **Tedin K**, **Taha M-K**, **Labigne A**, **Zahringer U**, **Coyle AJ**, **DiStefano PS**, **Bertin J**, **Sansonetti PJ**, **Philpott DJ**. 2003. Nod1 detects a unique muropeptide from Gram-negative bacterial peptidoglycan. Science **300**:1584–1587.
79. **Laroui H**, **Yan Y**, **Narui Y**, **Ingersoll SA**, **Ayyadurai S**, **Charania MA**, **Zhou F**, **Wang B**, **Salaita K**, **Sitaraman S V**, **Merlin D**. 2011. L-Ala-γ-D-Glu-meso-diaminopimelic acid (DAP) interacts directly with leucine-rich region domain of nucleotide-binding oligomerization domain 1, increasing phosphorylation activity of receptor-interacting serine/threonine-protein kinase 2 and its interaction with nucleotide-binding oligomerization domain 1. J Biol Chem **286**:31003–31013.
80. **Caruso R**, **Warner N**, **Inohara N**, **Nunez G**. 2014. NOD1 and NOD2: Signaling, host defense, and inflammatory disease. Immunity **41**:898–908.
81. **Girardin SE**, **Boneca IG**, **Viala J**, **Chamaillard M**, **Labigne A**, **Thomas G**, **Philpott DJ**, **Sansonetti PJ**. 2003. Nod2 is a general sensor of peptidoglycan through muramyl dipeptide (MDP) detection. J Biol Chem **278**:8869–8872.
82. **Inohara N**, **Ogura Y**, **Fontalba A**, **Gutierrez O**, **Pons F**, **Crespo J**, **Fukase K**, **Inamura**

S, **Kusumoto S**, **Hashimoto M**, **Foster SJ**, **Moran AP**, **Fernandez-Luna JL**, **Nunez G**. 2003. Host recognition of bacterial muramyl dipeptide mediated through NOD2: Implications for Crohn's disease. J Biol Chem **278**:5509–5512.

83. **Grimes CL**, **Ariyananda LDZ**, **Melnyk JE**, **O' Shea EK**. 2012. The innate immune protein Nod2 binds directly to MDP, a bacterial cell wall fragment. J Am Chem Soc **134**:13535–13537.
84. **Mo J**, **Boyle JP**, **Howard CB**, **Monie TP**, **Davis BK**, **Duncan JA**. 2012. Pathogen sensing by nucleotide-binding oligomerization domain-containing protein 2 (NOD2) is mediated by direct binding to muramyl dipeptide and ATP. J Biol Chem **287**:23057–23067.
85. **Knilans KJ**, **Hackett KT**, **Anderson JE**, **Weng C**, **Dillard JP**, **Duncan JA**. 2017. *Neisseria gonorrhoeae* lytic transglycosylases LtgA and LtgD reduce host innate immune signaling through TLR2 and NOD2. ACS Infect Dis **3**:624–633.
86. **Magalhaes JG**, **Philpott DJ**, **Nahori M-A**, **Jéhanno M**, **Fritz J**, **Le Bourhis L**, **Viala J**, **Hugot J-P**, **Giovannini M**, **Bertin J**, **Lepoivre M**, **Mengin-Lecreulx D**, **Sansonetti PJ**, **Girardin SE**. 2005. Murine Nod1 but not its human orthologue mediates innate immune detection of tracheal cytotoxin. EMBO Rep **6**:1201–1207.
87. **Dokter WHA**, **Dijkstra AJ**, **Koopmans SB**, **Stulp BK**, **Keck W**, **Halie MR**, **Vellenga E**. 1994. G(Anh)MTetra, a natural bacterial cell wall breakdown product, induces interleukin-1beta and interleukin-6 expression in human monocytes: A study of the molecular mechanisms involved in inflammatory cytokine expression. J Biol Chem **269**:4201–4206.
88. **Nigro G**, **Fazio LL**, **Martino MC**, **Rossi G**, **Tattoli I**, **Liparoti V**, **De Castro C**, **Molinaro A**, **Philpott DJ**, **Bernardini ML**. 2008. Muramylpeptide shedding modulates cell sensing of *Shigella flexneri*. Cell Microbiol **10**:682–695.
89. **Simons MP**, **Nauseef WM**, **Apicella MA**. 2005. Interactions of *Neisseria gonorrhoeae* with adherent polymorphonuclear leukocytes. Infect Immun **73**:1971–1977.
90. **Criss AK**, **Katz BZ**, **Seifert HS**. 2009. Resistance of *Neisseria gonorrhoeae* to non-oxidative killing by adherent human polymorphonuclear leucocytes. Cell Microbiol **11**:1074–1087.
91. **Criss AK**, **Seifert HS**. 2012. A bacterial siren song: intimate interactions between *Neisseria* and neutrophils. Nat Rev Microbiol **10**:178–90.
92. **Ekman A-K**, **Cardell LO**. 2009. The expression and function of Nod-like receptors in neutrophils. Immunology **130**:55–63.
93. **Ragland SA**, **Schaub RE**, **Hackett KT**, **Dillard JP**, **Criss AK**. 2017. Two lytic transglycosylases in *Neisseria gonorrhoeae* impart resistance to killing by lysozyme and human neutrophils. Cell Microbiol **19**:e12662.
94. **Chan JM**, **Dillard JP**. 2016. *Neisseria gonorrhoeae* crippled its peptidoglycan fragment permease to facilitate toxic peptidoglycan monomer release. J Bacteriol **198**:3029–3040.
95. **Chan YA**, **Hackett KT**, **Dillard JP**. 2012. The lytic transglycosylases of *Neisseria gonorrhoeae*. Microb Drug Resist **18**:271–279.
96. **Engel H**, **Smink AJ**, **Wijngaarden L Van**, **Keck W**. 1992. Murein-metabolizing enzymes from *Escherichia coli*: Existence of a second lytic transglycosylase. J Bacteriol **174**:6394–6403.
97. **Thunnissen A-MWH**, **Dijkstra AJ**, **Kalk KH**, **Rozeboom H**, **Engel H**, **Keck W**, **Dijkstra BW**. 1994. Doughnut-shaped structure of a bacterial muramidase revealed by X-

ray crystallography. Nature **367**:750–753.
98. **Cloud KA**, **Dillard JP**. 2002. A lytic transglycosylase of *Neisseria gonorrhoeae* is involved in peptidoglycan-derived cytotoxin production. Infect Immun **70**:2752–2757.
99. **Cloud-Hansen KA**, **Hackett KT**, **Garcia DL**, **Dillard JP**. 2008. *Neisseria gonorrhoeae* uses two lytic transglycosylases to produce cytotoxic peptidoglycan monomers. J Bacteriol **190**:5989–5994.
100. **Heidrich C**, **Templin MF**, **Ursinus A**, **Merdanovic M**, **Berger J**, **Schwarz H**, **de Pedro MA**, **Höltje J-V**. 2001. Involvement of *N*-acetylmuramyl-L-alanine amidases in cell separation and antibiotic-induced autolysis of *Escherichia coli*. Mol Microbiol **41**:167–178.
101. **Uehara T**, **Park JT**. 2007. An anhydro-*N*-acetylmuramyl-L-alanine amidase with broad specificity tethered to the outer membrane of *Escherichia coli*. J Bacteriol **189**:5634–5641.
102. **Uehara T**, **Dinh T**, **Bernhardt TG**. 2009. LytM-domain factors are required for daughter cell separation and rapid ampicillin-induced lysis in *Escherichia coli*. J Bacteriol **191**:5094–5107.
103. **Uehara T**, **Parzych KR**, **Dinh T**, **Bernhardt TG**. 2010. Daughter cell separation is controlled by cytokinetic ring-activated cell wall hydrolysis. EMBO J **29**:1412–22.
104. **Stohl EA**, **Lenz JD**, **Dillard JP**, **Seifert HS**. 2016. The gonococcal NlpD protein facilitates cell separation by activating peptidoglycan cleavage by AmiC. J Bacteriol **198**:615–622.
105. **Yang DC**, **Tan K**, **Joachimiak A**, **Bernhardt TG**. 2012. A conformational switch controls cell wall-remodelling enzymes required for bacterial cell division. Mol Microbiol **85**:768–781.
106. **Bernhardt TG**, **Boer PAJ De**. 2003. The *Escherichia coli* amidase AmiC is a periplasmic septal ring component exported via the twin-arginine transport pathway. Mol Microbiol **48**:1171–1182.
107. **Olrichs NK**, **Aarsman MEG**, **Verheul J**, **Arnusch CJ**, **Martin NI**, **Herve M**, **Vollmer W**, **Kruijff B De**, **den Blauuwen T**. 2011. A novel in vivo cell-wall labeling approach sheds new light on peptidoglycan synthesis in *Escherichia coli*. ChemBioChem **12**:1124–1133.
108. **Cloud KA**, **Dillard JP**. 2004. Mutation of a single lytic transglycosylase causes aberrant septation and inhibits cell separation of *Neisseria gonorrhoeae*. J Bacteriol **186**:7811–7814.
109. **Jennings GT**, **Savine S**, **Marchetti E**, **Arico B**, **Kast T**, **Baldi L**, **Ursinus A**, **Höltje J-V**, **Nicholas RA**, **Rappuoli R**, **Grandi G**. 2002. GNA33 from *Neisseria meningitidis* serogroup B encodes a membrane-bound lytic transglycosylase (MltA). Eur J Biochem **269**:3722–3731.
110. **Adu-Bobie J**, **Lupetti P**, **Brunelli B**, **Granoff D**, **Norais N**, **Ferrari G**, **Grandi G**, **Rappuoli R**, **Pizza M**. 2004. GNA33 of *Neisseria meningitidis* is a lipoprotein required for cell separation , membrane architecture , and virulence. Infect Immun **72**:1914–1919.
111. **Ursinus A**, **Höltje J-V**. 1994. Purification and properties of a membrane-bound lytic transglycosylase from *Escherichia coli*. J Bacteriol **176**:338–343.
112. **Stefanova ME**, **Tomberg J**, **Olesky M**, **Höltje J-V**, **Gutheil WG**, **Nicholas RA**. 2003. *Neisseria gonorrhoeae* penicillin-binding protein 3 exhibits exceptionally high carboxypeptidase and β-Lactam binding activities. Biochemistry **42**:14614–14625.

113. **Stefanova ME**, **Tomberg J**, **Davies C**, **Nicholas RA**, **Gutheil WG**. 2004. Overexpression and enzymatic characterization of *Neisseria gonorrhoeae* penicillin-binding protein. Eur J Biochem **271**:23–32.
114. **Peddi S**, **Nicholas RA**, **Gutheil WG**. 2009. *Neisseria gonorrhoeae* penicillin-binding protein 3 demonstrates a pronounced preference for Nε-acylated substrates. Biochemistry **48**:5731–5737.
115. **Garcia DL**. 2007. Liberation of pro-inflammatory peptidoglycan fragments from the gonococcal cell. PhD thesis. University of Wisconsin-Madison.
116. **Zarantonelli ML**, **Skoczynska A**, **Antignac A**, **El Ghachi M**, **Deghmane AE**, **Szatanik M**, **Mulet C**, **Werts C**, **Peduto L**, **D'Andon MF**, **Thouron F**, **Nato F**, **Lebourhis L**, **Philpott DJ**, **Girardin SE**, **Vives FL**, **Sansonetti P**, **Eberl G**, **Pedron T**, **Taha MK**, **Boneca IG**. 2013. Penicillin resistance compromises Nod1-dependent proinflammatory activity and virulence fitness of *Neisseria meningitidis*. Cell Host Microbe **13**:735–745.
117. **Garcia DL**, **Dillard JP**. 2008. Mutations in *ampG* or *ampD* affect peptidoglycan fragment release from *Neisseria gonorrhoeae*. J Bacteriol **190**:3799–3807.
118. **Rashid Y**, **Azim MK**. 2011. Structural bioinformatics of *Neisseria meningitidis* LD-carboxypeptidase: implications for substrate binding and specificity. Protein J **30**:558–565.
119. **Woodhams KL**. 2013. Characterization of the gonococcal genetic island and peptidoglycan fragment release in *Neisseria meningitidis*. PhD thesis. University of Wisconsin-Madison.
120. **Templin MF**, **Ursinus A**, **Höltje J-V**. 1999. A defect in cell wall recycling triggers autolysis during the stationary growth phase of *Escherichia coli*. EMBO **18**:4108–4117.
121. **Park JT**, **Uehara T**. 2008. How bacteria consume their own exoskeletons (turnover and recycling of cell wall peptidoglycan). Microbiol Mol Biol Rev **72**:211–227.
122. **Lyon RS**. 2001. Tracheal cytotoxin production by the *Bordetellae*. PhD thesis. Washington University in St. Louis.
123. **Adin DM**, **Engle JT**, **Goldman WE**, **McFall-Ngai MJ**, **Stabb E V**. 2009. Mutations in *ampG* and lytic transglycosylase genes affect the net release of peptidoglycan monomers from *Vibrio fischeri*. J Bacteriol **191**:2012–2022.
124. **Höltje J-V**, **Kopp U**, **Ursinus A**, **Wiedemann B**. 1994. The negative regulator of beta-lactamase induction AmpD is a *N*-acetyl-anhydromuramyl-L-alanine amidase. FEMS Microbiol Lett **122**:159–164.
125. **Jacobs C**, **Jorls B**, **Jamin M**, **Klarsou K**, **Van Beeumen J**, **Mengin-Lecreulx D**, **Heijenoort J Van**, **Park JT**, **Normark S**, **Frere J-M**. 1995. AmpD, essential for both beta-lactamase regulation and cell wall recycling, is a novel cytosolic *N*-acetylmuramyl-L-alanine amidase. Mol Microbiol **15**:553–559.
126. **Korfmann G**, **Sanders CC**. 1989. *ampG* is essential for high-level expression of AmpC beta-lactamase in *Enterobacter cloacae*. Antimicrob Agents Chemother **33**:1946–1951.
127. **Tuomanen E**, **Lindquist S**, **Sande S**, **Galleni M**, **Light K**, **Gage D**, **Normark S**. 1991. Coordinate regulation of beta-lactamase induction and peptidoglycan composition by the amp operon. Science **251**:201–204.
128. **Jacobs C**, **Huang L**, **Bartowsky E**, **Normark S**, **Park JT**. 1994. Bacterial cell wall recycling provides cytosolic muropeptides as effectors for beta-lactamase induction. EMBO J **13**:4684–4694.
129. **Jacobs C**, **Frère JM**, **Normark S**. 1997. Cytosolic intermediates for cell wall

biosynthesis and degradation control inducible β-lactam resistance in gram-negative bacteria. Cell **88**:823–832.

130. **Dietz H**, **Pfeifle D**, **Wiedemann B**. 1997. The signal molecule for β-lactamase induction in *Enterobacter cloacae* is the anhydromuramyl-pentapeptide. Antimicrob Agents Chemother **41**:2113–2120.
131. **Beachey EH**, **Keck W**, **Pedro MA**, **Schwarz U**. 1981. Exoenzymatic activity of transglycosylase isolated from *Escherichia coli*. Eur J Biochem **116**:355–358.
132. **Höltje J-V**. 1998. Growth of the stress-bearing and shape-maintaining murein sacculus of *Escherichia coli*. Microbiol Mol Biol Rev **62**:181–203.
133. **Typas A**, **Banzhaf M**, **Gross CA**, **Vollmer W**. 2012. From the regulation of peptidoglycan synthesis to bacterial growth and morphology. Nat Rev Microbiol **10**:123–136.
134. **Park JT**. 1995. Why does *Escherichia coli* recycle its cell wall peptides? Mol Microbiol **17**:421–426.
135. **Folster JP**, **Johnson PJT**, **Jackson L**, **Dhulipali V**, **Dyer DW**, **Shafer WM**. 2009. MtrR modulates *rpoH* expression and levels of antimicrobial resistance in *Neisseria gonorrhoeae*. J Bacteriol **191**:287–297.
136. **Veyrier FJ**, **Williams AH**, **Mesnage S**, **Schmitt C**, **Taha M-K**, **Boneca IG**. 2013. De-*O*-acetylation of peptidoglycan regulates glycan chain extension and affects *in vivo* survival of *Neisseria meningitidis*. Mol Microbiol **87**:1100–1112.
137. **Williams AH**, **Wheeler R**, **Thiriau C**, **Haouz A**, **Taha M-K**, **Boneca IG**. 2017. Bulgecin A: The key to a broad-spectrum inhibitor that targets lytic transglycosylases. Antibiotics **6**:doi:10.3390.

CHAPTER 2

Neisseria gonorrhoeae crippled its peptidoglycan fragment permease to facilitate toxic peptidoglycan monomer release

Jia Mun Chan and Joseph P. Dillard

JM Chan and JP Dillard designed the experiments and wrote the manuscript.

JM Chan performed the experiments and analyzed the data.

Originally published as

Chan JM, Dillard JP. 2016. *Neisseria gonorrhoeae* crippled its peptidoglycan fragment permease to facilitate toxic peptidoglycan monomer release. J Bacteriol **198**: 3029-3040.

ABSTRACT

Neisseria gonorrhoeae (gonococci) and *Neisseria meningitidis* (meningococci) are human pathogens that cause gonorrhea and meningococcal meningitis respectively. Both *N. gonorrhoeae* and *N. meningitidis* release a number of small peptidoglycan (PG) fragments, including proinflammatory PG monomers, although *N. meningitidis* releases less of the PG monomers. The PG fragments released by *N. gonorrhoeae* and *N. meningitidis* are generated in the periplasm during cell wall remodeling, and a majority of these fragments are transported into the cytoplasm by an inner membrane permease, AmpG; however, a portion of the PG fragments are released into the extracellular environment through unknown mechanisms. We previously reported that expression of meningococcal *ampG* in *N. gonorrhoeae* reduced PG monomer release by gonococci. This finding suggested that the efficiency of AmpG-mediated PG fragment recycling regulates the amount of PG fragments released into the extracellular milieu. We determined that three AmpG residues near the C-terminal end of the protein modulate AmpG's efficiency. We also investigated the association between PG fragment recycling and release in two species of human-associated nonpathogenic *Neisseria*, *N. sicca* and *N. mucosa*. Both *N. sicca* and *N. mucosa* release lower levels of PG fragments and are more efficient at recycling PG fragments compared to *N. gonorrhoeae*. Our results suggest that *N. gonorrhoeae* has evolved to increase the amounts of toxic PG fragments released by reducing its PG recycling efficiency.

INTRODUCTION

Ten species in the genus *Neisseria* are found associated with humans. *Neisseria gonorrhoeae* (gonococci, GC) and *Neisseria meningitidis* (meningococci, MC) are considered human restricted pathogens, while *N. cinerea*, *N. elongata*, *N. flavescens*, *N. lactamica*, *N. mucosa*, *N. polysaccharea*, *N. sicca*, and *N. subflava* are considered nonpathogenic. The nonpathogenic species colonize the nasopharynx and oral cavity of healthy people (1–3). In rare cases, these species disseminate to cause endocarditis or septic infection in immunocompromised individuals or trauma patients (4). *N. gonorrhoeae* and *N. meningitidis* share many infection-related factors with the nonpathogenic species including type IV pili, adhesins, and certain iron transport proteins (5). Unlike *N. gonorrhoeae* and *N. meningitidis*, nonpathogenic *Neisseria* are considered to be non-inflammatory, and very rarely elicit a symptomatic inflammatory response (6).

N. gonorrhoeae commonly infects the genitourinary tract, causing urethritis in men and cervicitis in women. In women, the bacteria can spread to the uterus and Fallopian tubes, leading to highly inflammatory conditions, endometritis, pelvic inflammatory disease, and ectopic pregnancy. Gonococci can also disseminate to cause sepsis, tenosynovitis, and meningitis (7). Disease manifestations are due to the host inflammatory response. In pelvic inflammatory disease, release of peptidoglycan (PG) fragments and endotoxin by gonococci in the Fallopian tubes induces an inflammatory response that kills the ciliated cells, and the cells come out of the epithelium and are sloughed off (8, 9). The loss of ciliated cells and the tissue damage results in tubal factor infertility or predisposes the woman to ectopic pregnancy.

N. gonorrhoeae is unusual among Gram-negative bacteria in that it releases significant amounts of PG fragments during growth (10). The most abundant fragments released are the PG

monomers. These are disaccharide-tripeptide and disaccharide-tetrapeptide fragments carrying a 1,6-anhydro bond on the *N*-acetylmuramic acid residue (11). The disaccharide-tetrapeptide is identical to tracheal cytotoxin (TCT), the PG fragment released by *Bordetella pertussis* that induces death and sloughing of ciliated cells in the trachea (12–14). The disaccharide-tripeptide stimulates activation of the human pattern-recognition receptor NOD1 (15). When added to Fallopian tube tissue in organ culture, a mixture of the two monomers caused death and sloughing of ciliated cells, mimicking the tissue damage of pelvic inflammatory disease (8).

Although commonly considered a pathogen, *N. meningitidis* is a normal colonizer of the human nasopharynx and is carried asymptomatically by 10-40% of the population (16). The bacteria can spread to cause sepsis or meningitis, and approximately 550 cases of invasive meningococcal disease occur in the US every year (17). In these invasive infections, meningococci elicit a large inflammatory response that frequently results in septic shock and death of the patient within a few days of the onset of symptoms. However, *N. meningitidis* may not be inflammatory during the carriage state, only upregulating expression of virulence factors required for invasion and immune evasion under certain conditions (18).

We have investigated the mechanisms involved in the generation and release of proinflammatory PG fragments by *N. gonorrhoeae* and *N. meningitidis*. The PG monomers are generated by lytic transglycosylases, which in *Neisseria* species, are predicted outer-membrane lipoproteins (19, 20). As the bacteria grow and divide, they must degrade PG strands to make space for the incorporation of additional PG strands and remodel the cell wall to build and then split the septum for cell division and separation. Most of the PG fragments generated by these processes are taken up from the periplasm and transported to the cytoplasm by the inner membrane permease AmpG (21–25). However, in *N. gonorrhoeae*, 15% of the PG monomers

escape from the cell and are released into the milieu (22). By comparison, only 4% of the PG monomers generated by *N. meningitidis* are released from the bacteria (23). We previously demonstrated that replacement of gonococcal *ampG* with meningococcal *ampG* led to reduced PG fragment release, suggesting that meningococcal AmpG is more efficient at PG fragment import (23).

In the present study, we examine the differences between gonococcal AmpG and meningococcal AmpG and characterize PG fragment release in *N. sicca* and *N. mucosa*. Replacement of meningococcal *ampG* with gonococcal *ampG* resulted in increased PG fragment release. Also, the nonpathogenic species exhibited highly-efficient PG recycling and failed to release certain PG fragments that the pathogens do release, which may indicate additional differences in PG fragment degradation, recycling, and release in nonpathogenic *Neisseria*. Overall, these data show that *Neisseria* species that are usually asymptomatic colonizers, i.e., *N. meningitidis*, *N. sicca*, and *N. mucosa*, are more efficient at PG recycling by comparison with *N. gonorrhoeae*. Thus *N. gonorrhoeae* has evolved an inefficient PG recycling system as it has moved to a proinflammatory infection lifestyle.

MATERIALS AND METHODS

Bacterial strains and growth conditions. All bacterial strains used in this study are listed in Table 1. *Neisseria* strains (*N. gonorrhoeae, N. meningitidis, N. sicca* and *N. mucosa*) were grown on either gonococcal base medium (GCB) agar plates (Difco) at 37°C with 5% CO_2 or in gonococcal base liquid medium (GCBL) containing Kellogg's supplements (26) and 0.042% $NaHCO_3$ (complete GCBL or cGCBL) at 37°C with aeration. *Escherichia coli* cells were grown either on LB agar plates (Difco) at 37°C or in LB broth at 37°C with aeration. When necessary, media were supplemented with antibiotics for selection. Chloramphenicol was used at concentrations of 10 μg/ml (*Neisseria*) or 25 μg/ml (*E. coli*), while erythromycin was used at concentrations of 10 μg/ml (*Neisseria*) or 500 μg/ml (*E. coli*). Kanamycin was used at concentrations of 80 μg/ml (*Neisseria*) or 40 μg/ml (*E. coli*).

Strain construction. Mutant or complemented strains of *N. gonorrhoeae, N. meningitidis, N. sicca* and *N. mucosa* were generated using spot transformation (27). Briefly, 1 – 20 μg linearized plasmid DNA or chromosomal DNA were spotted onto GCB plates. 3-10 piliated colonies were then streaked over the spots, and the plates incubated overnight at 37°C with 5% CO_2. Transformants were screened by colony PCR and restriction enzyme digestion where applicable, and confirmed by sequencing (28).

Plasmid construction. All plasmids used in this study are listed in Table 2, while all primers used to generate the constructs are listed in Table 3. pIDN3 is a cloning plasmid that contains the gonococcal and meningococcal DNA uptake sequence (DUS) (GCCGTCTGAA), and was used as a vector backbone to generate most of the plasmids used in this study (29, 30). However,

transformation into *N. sicca* and *N. mucosa* may have higher efficiency with an alternate DNA uptake sequence (GTCGTCTGAA), which is more commonly found in *N. sicca* ATCC 29256 and *N. mucosa* ATCC 25996 (5, 31). Thus, we constructed pEC026, a derivative of pIDN3 that contains the alternate DNA uptake sequence to be used as a vector backbone for transformations into *N. sicca* and *N. mucosa*. Primers Alt-DUS AvrII F and Alt-DUS AvrII R, which contain the alternate DUS sequence and an AvrII restriction enzyme site, were used to PCR around pIDN3. The resulting PCR product was digested with AvrII, ligated and transformed into *E. coli* to generate pEC026.

To facilitate screening of transformants, we introduced a silent mutation at base 993 (L331, CTG-> CTA) of gonococcal and meningococcal *ampG* to generate an *Nhe*I site. For clarity and simplicity, constructs that have WT *ampG* coding sequence are referred to as $ampG_{GC\ WT}$ or $ampG_{MC\ WT}$, while constructs with the screening site are referred to as $ampG_{GC}$ or $ampG_{MC}$.

All plasmids were constructed with one of three methods: (i) PCR around the plasmid (pEC026), (ii) two-way ligation of two PCR inserts into a plasmid (pEC007, pEC008 and pEC013) and (iii) ligation of one PCR product into the plasmid (all other plasmids). Inserts for the plasmids were generated by PCR and/or with overlap extension PCR. For overlap extension PCR, two or three PCR products were used as templates in PCR to make a larger PCR product. The final PCR products were digested with restriction enzymes, ligated into either a pIDN3 or pEC026-based vector, and transformed into *E. coli* RapidTrans™ (Active Motif) TAM1 chemical competent cells. Successful transformants were checked by PCR and sequencing.

To generate pEC005 ($ampG_{MC}p$-$ampG_{GC\ WT}$ cloned into pIDN3), $ampG_{MC\ WT}$ was amplified by PCR using primer pairs ampG F2 and ampG1325R and ATCC 13102 chromosomal DNA as template. Approximately 600bp of the gonococcal 5' and 3' *ampG* flanking region were

amplified using primer pairs MC ampG SacI F3/ampG 5' flank R and ampG 3' flank F/ampG 3' flank R BamHI and MS11 chromosomal DNA as template. The three pieces of DNA were joined by overlap extension PCR using primers MC ampG SacI F3 and ampG 3' flank R BamHI. The resulting PCR product was cloned into pIDN3. pEC006 (*ampG*$_{GC}$*p-ampG*$_{MC\ WT}$ cloned into pIDN3) was generated similarly, although MS11 chromosomal DNA and ATCC 13102 chromosomal DNA were used as templates for amplifying *ampG*$_{GC\ WT}$ and meningococcal 5' and 3' flanking regions, respectively.

To facilitate screening of successful transformants, we created three constructs with a silent point mutation at base 993 (Leu^{331},CTG->CTA) of the gonococcal and meningococcal *ampG* coding sequence to introduce a NheI digestion site. To generate pEC007 (*ampG*$_{GC}$*p-ampG*$_{GC}$ cloned into pIDN3), two fragments of *ampG*$_{GC\ WT}$ were amplified using primer pairs MC ampG SacI F3/ampG NheI 990bp R and ampG NheI 990bp R/ampG 3' flank R BamHI using MS11 chromosomal DNA as a template. We then digested the first *ampG* fragment with the restriction enzymes SacI and NheI, the second *ampG* fragment with NheI and BamHI, and pIDN3 with SacI and BamHI, and performed a three-way ligation. pEC008 (*ampG*$_{MC}$*p-ampG*$_{GC}$ cloned into pIDN3) and pEC013 (*ampG*$_{GC}$*p ampG*$_{MC}$ cloned into pIDN3) were generated similarly, using pEC005 and pEC006 respectively as templates for PCR.

The chimeric *ampG* constructs (pEC016-pEC019) were generated with pEC013 as a base. The *ampG* coding sequence was divided into four unequal quarters (also called *ampG* regions 1-4), in which each region contains at least one nonsynonymous nucleotide polymorphism in GC and MC. The *ampG* coding region is 1284 base pairs long. Region 1 encompassed base pairs 1-150, while region 2 contained base pairs 151-788. Region 3 is comprised of base pairs 789-992, while region 4 included base pairs 993-1284. The chimeric

ampG constructs also contained ~600bp $ampG_{GC}$ 5' and 3' flanking region to facilitate double crossover homologous recombination when transformed into *Neisseria.*

To generate pEC016 ($ampG_{GC}p\ ampG_{Chimera\ 1}$ cloned into pIDN3), $ampG_{GC}$ region 1 was amplified from pEC008 using primers ampG F2 and ampG internal 1R. $ampG_{GC}$ 5' flanking region and $ampG_{MC}$ region 2-4 with $ampG_{GC}$ 3' flanking region were amplified from pEC007 using primer pairs MC ampG SacI F3/ampG 5' flank R and ampG internal 1F and ampG 3' flank R BamHI respectively. The three DNA pieces were joined by overlap extension PCR using primers MC ampG SacI F3 and ampG 3' flank R BamHI, and the resulting PCR product cloned into pIDN3. pEC017 ($ampG_{GC}p\ ampG_{Chimera\ 2}$ cloned into pIDN3) was generated similarly using primer pairs ampG internal 1F/ampG internal 2R to amplify $ampG_{GC}$ region 2 from pEC008 and using primer pairs MC ampG SacI F3/ampG internal 1R and ampG internal 2F/ampG 3' flank R BamHI to amplify $ampG_{MC}$ region 1 with $ampG_{GC}$ 5' flanking region and $ampG_{MC}$ regions 3-4 with $ampG_{GC}$ 3' flanking region from pEC013. pEC018 ($ampG_{GC}p\ ampG_{Chimera\ 3}$ cloned into pIDN3) was generated similarly using primer pairs ampG internal 2F/ampG 990bp NheI R to amplify $ampG_{GC}$ region 3 from pEC008 and using primer pairs MC ampG SacI F3/ampG internal 2R and ampG 990bp NheI F/ampG 3' flank R BamHI to amplify $ampG_{MC}$ region 1-2 with $ampG_{GC}$ 5' flanking region and $ampG_{MC}$ regions 4 with $ampG_{GC}$ 3' flanking region from pEC013. pEC019 ($ampG_{GC}p\ ampG_{Chimera\ 4}$ cloned into pIDN3) was generated similarly using primer pairs ampG 990bp NheI F/ampG 1325R to amplify $ampG_{GC}$ region 4 from pEC008 and using primer pairs MC ampG SacI F3/ampG 990bp NheI R and ampG 3' flank F/ampG 3' flank R BamHI to amplify $ampG_{MC}$ region 1-3 with $ampG_{GC}$ 5' flanking region and $ampG_{GC}$ 3' flanking region from pEC013.

To construct pEC028 (*ampG*$_{GC}$-FLAG3 cloned into pIDN3), the triple FLAG epitope (FLAG3) was amplified from pMR100 (C-terminal FLAG3 in pIDN3) using primers ampG-FLAG3 F and ampGend-FLAG3 R. *ampG*$_{GC}$ was amplified by PCR using MS11 chromosomal DNA as a template and primers SacI ampG F and (Gc) FLAG3-ampGend R, while the *ampG*$_{GC}$ 3' flanking region was amplified using the same template and primers (Gc) FLAG3-ampGend F and ampG 3' flank R BamHI. The three pieces of DNA were joined with overlap extension PCR using primers SacI ampG F and ampG 3' flank R BamHI. pEC029 (*ampG*$_{MC}$-FLAG3 cloned into pIDN3) was constructed similarly, although ATCC 13102 chromosomal DNA was used instead of MS11 chromosomal DNA as a template, and primers (Mc) FLAG3-ampGend F and (Mc) FLAG3-ampGend R were used instead of (Gc) FLAG3-ampGend F and (Gc) FLAG3-ampGend R where appropriate for PCR amplification.

Complementary primers that contain the specific mutation of interest were used in the generation of *ampG* site-directed mutagenesis constructs. To generate pEC037 (*ampG*$_{GC}$*p-ampG*$_{GC}$^{M391L} cloned into pIDN3), two *ampG*$_{GC}$ fragments were amplified using primer pairs MC ampG SacI F3/MS11 ampG M391L R and MS11 ampG M391L F/ampG 3' flank R BamHI with pEC007 as a template, and joined by overlap extension PCR using primers MC ampG SacI F3 and ampG 3' flank R BamHI. pEC038 (*ampG*$_{GC}$*p-ampG*$_{GC}$^{R398Q} cloned into pIDN3) was constructed similarly, using primers MS11 ampG R398Q F and MS11 ampG R398Q R instead of MS11 ampG M391L F and MS11 ampG M391L R for PCR where appropriate. pEC039 (*ampG*$_{GC}$*p-ampG*$_{GC}$^{I402A} cloned into pIDN3) was also constructed using the same strategy, using primers MS11 ampG I402A F and MS11 ampG I402A R for PCR where appropriate.

Plasmids pEC042, pEC043, pEC054 and pEC058 were also constructed using a similar strategy as pEC037. To generate pEC042 (*ampG*$_{GC}$*p-ampG*$_{GC}$$^{M391L\ R398Q}$ cloned into pIDN3),

two *ampG*$_{GC}$ fragments were amplified using primer pairs SacI ampG F/MS11 ampG R398Q R and MS11 ampG R398Q F/ampG 3' flank R BamHI and pEC037 as a template, and joined by overlap extension PCR using primers SacI ampG F and ampG 3' flank R BamHI. To generate pEC043 (*ampG*$_{GC}$*p-ampG*$_{GC}$ $^{M391L\ I402A}$ cloned into pIDN3), primers MS11 ampG I402A F and MS11 ampG I402 R were used instead of MS11 ampG R398Q F and MS11 ampG R398Q R during PCR. pEC054 (G *ampG*$_{GC}$*p-ampG*$_{GC}$ $^{R398Q\ I402A}$ cloned into pIDN3), primers MS11 ampG R398Q I402A F and MS11 ampG R398Q I402A R were used for PCR, with pEC007 as a template. pEC058 was constructed similarly using pEC054 as a template, and MS11 ampG M391L F and MS11 ampG M391L as primers for PCR.

N. sicca and *N. mucosa ampG* deletion constructs were generated with a two-step approach. *N. sicca ampG* coding region was first amplified using primers NSi ampG SacIF and NSi ampG BamHI R2 and cloned into pEC026 to generate pEC063 (*ampG*$_{N.\ sicca}$ cloned into pEC026). A kanamycin resistance cassette was excised from pHSS6 with AvaI and PciI and subcloned into pEC063, which was digested with NgoMIV and BspHI to excise 271bp (bp 530-801) of *ampG* coding sequence, to generate pEC081 (*ampG*$_{N.\ sicca}$::*kan* cloned into pEC026). *N. mucosa ampG* coding region was first amplified using primers NMu ampG SacIF and NMu ampG BamHI R, and cloned into pIDN3 to generate pEC064 (*ampG*$_{N.\ mucosa}$ cloned into pIDN3). An AvaI and PciI digested DNA fragment containing a kanamycin resistance cassette from pHSS6 was subcloned into pEC064, which was digested with NgoMIV and BspHI to excise 271bp (bp 636-907) of *ampG* coding sequence, to generate pEC067 (*ampG*$_{N.\ mucosa}$::*kan* cloned into pIDN3). The *ampG*::*kan* insert was then excised from pIDN3 by digestion with SacI and BamHI, and subcloned into pEC026 digested with the same enzymes to generate pEC070 (*ampG*$_{N.\ mucosa}$::*kan* cloned into pEC026).

Plasmids pEC098, pEC099, pEC100, pEC102 and pEC103 were generated using a similar strategy as pEC028 and pEC029. The FLAG3 epitope was amplified from pMR100 using primers ampG-FLAG3 F and ampGend-FLAG3 R, and *ampG*$_{GC}$ 3' flanking region was amplified from MS11 chromosomal DNA using primers (Gc) ampGend-FLAG3 F and ampG 3' flank R BamHI. For pEC098 (*ampG*$_{MC\ WT}$-FLAG3 cloned into pIDN3), *ampG*$_{MC}$ was amplified from EC505 using primers SacI ampG F and (Mc) ampGend-FLAG3 R. The *ampG* coding sequence for generating pEC100 (*ampG*$_{GC}$ ^{M391L}-FLAG3 cloned into pIDN3), pEC102 (*ampG*$_{GC}$ ^{I402A}-FLAG3 cloned into pIDN3) and pEC103 (*ampG*$_{GC}$ $^{M391L\ R398Q\ I402A}$-FLAG3 cloned into pIDN3) were amplified using the same primers as for pEC099, using EC515, EC517 and EC523 chromosomal DNA as templates. As described with the construction of pEC028 and pEC029, the three piece of PCR products were joined using overlap extension PCR and cloned into pIDN3.

Characterization of released PG fragments. Metabolic labeling of PG using [6-^{3}H]-glucosamine was performed as described by Rosenthal and Dziarski (32) with modifications from Cloud and Dillard (33). Quantitative PG fragment release analysis was performed as described by Garcia and Dillard (22). Briefly, *Neisseria* strains were pulse-labeled using 10 μCi/ml [6-^{3}H]-glucosamine in GCBL lacking glucose and supplemented with 0.042% $NaHCO_3$ and pyruvate as a carbon source to label the sugar backbone, or using 25 μCi/ml [2,6-^{3}H]-diaminopimelic acid in DMEM lacking cysteine supplemented with 100 μg/ml methionine and 100 μg/ml threonine to label the peptide stems. For quantitative PG fragment release, an aliquot of the culture was removed after labeling for determination of the number of radioactive counts per minute (CPM) by liquid scintillation counting. The number of CPM was then normalized to obtain equal numbers of CPM in the bacteria in each culture. Pulse-labeling was then followed

by a 2 hr (*N. meningitidis*) or 2.5 hr chase (*N. gonorrhoeae, N. sicca* and *N. mucosa*) period in cGCBL to achieve an equal number of generations. At the end of the chase period, culture supernatant was obtained by centrifugation at 3000 x *g* for 10 mins and filter-sterilization of the supernatant using a 0.22 μm pore filter. Radiolabeled PG fragments in the supernatant were separated by size using tandem size-exclusion chromatography and detected by liquid scintillation counting. Relative amounts of PG fragments released were determined by calculating the area under the curve.

Immunoblotting and detection of AmpG-FLAG3. 10 μg whole-cell lysates were electrophoresed on 12% SDS-PAGE gels. The proteins were then transferred onto polyvinylidene fluoride (PVDF) membrane (Bio-Rad) either at 100 V for 1 hr or at 20 V overnight. Membranes were blocked with 5% milk in Tris-buffered saline (TBS) for 1 hr at room temperature (RT), and then incubated with anti-FLAG® M2 primary antibody (Sigma-Aldrich) in TBS with 0.05% Tween-20 (TTBS) with 5% milk either for 1 hr at RT or overnight at 4°C. Membranes were washed 4x with TTBS for 5 mins each at RT, incubated with goat anti-mouse IgG-HRP secondary antibody (Santa Cruz) in TTBS for 1 hr, and washed 5x with TTBS for 5 mins each. Blots were developed using an Immun-Star horseradish peroxidase substrate kit (Bio-Rad), and imaged using the Odyssey® Fc Imagining System (LI-COR). Band intensities and protein concentrations were determined using Odyssey® Fc.

Quantitative RT-PCR. Quantitative RT-PCR was performed according to Salgado-Pabón (34). Briefly, gonococcal strains were grown in cGCBL until mid-log phase. RNA from 2 ml of culture was isolated using TRIzol® reagent and treated with TURBO DNAse to remove DNA

contaminants (Life Technologies). Reverse transcription was then performed using the iScript cDNA synthesis kit (Bio-Rad). The resulting cDNA samples were then used for quantitative real-time PCR using the iQ SYBR Green supermix (Bio-Rad) with primers ampG-RT-F (GTGCGTGCTGCTGTTTATC) and ampG-RT-R (GTCTTGCTGAAACCCATATCC) to measure *ampG* transcript levels and primers rmp-RT-F (CGAAGGCCATACCGACTTTATGG) and rmp-RT-R (GTTGCTGACCAGGTTGTTTGC) to measure *rmp* transcript levels as a control. Rmp was chosen as a control because it is a constitutively expressed protein that is not regulated by iron levels, and *rmp* levels have been used to normalize RT-PCR data (35–37). Quantitative RT-PCR results were analyzed using the StepOnePlus™ System (Applied Biosciences). Statistical analyses were performed using Student two-tailed *t* test.

Model of gonococcal AmpG structure. The predicted structure of gonococcal AmpG was modeled using I-TASSER server (38–41) with multiple threading templates and using Phyre2 with a multi-template/*ab initio* template (42). Structures of the following proteins were used as templates for I-TASSER: *E. coli* glycerol-3-transporter GlpT (PDB ID 1PW4), MdfA multidrug transporter (PDB ID 4ZOW), *E. coli* YajR transporter (PDB ID 3WDO) and *E. coli* lactose permease LacY (PDB ID 1PV6). Structures of the following proteins were used as templates for Phyre2: human glucose transporter GLUT3/SLC2A3 (PDB ID 5C6C), *E. coli* glycerol-3-phosphate transporter GlpT (PDB ID 1PW4), *E. coli* YajR transporter (PDB ID 3WDO), *E. coli* lactose permease LacY (PDB ID 1PV7), a eukaryotic phosphate transporter (PDB ID 4J05) and a *Staphylococcus epidermidis* glucose transporter (PDB ID 4LDS).

Phylogeny of *Neisseria* based on *ampG* and *gdh* (glucose-6-phosphate dehydrogenase) sequences. The coding sequence of *ampG* and the housekeeping gene *gdh* for various human associated *Neisseria* species, with the exception of *N. meningitidis* ATCC 13102 and *N. lactamica* ATCC 49142, were obtained from Genbank or the *Neisseria* Multi Locus Sequence Typing (MLST) website (http://pubmlst.org/neisseria/) (43–45). The GenBank accession number (AN) or *Neisseria* MLST ID number (ID) for the whole genome sequence data used to extract and compile the *ampG* and *gdh* alleles from 29 species of *Neisseria* are listed in parenthesis following the strain name. Sequences from the following strains were used for phylogeny analyses: gonococcal strains MS11 (AN CP003909.1), FA1090 (AN AE004969.1), FA19 (AN CP012026.1), F62 (ID 2856), DGI2 (ID 15698), DGI18 (ID 15698), NCCP11945 (AN CP001050.1) and 1291 (ID 15700), *N. meningitidis* strains FAM18 (AN AM421808.1), WUE 2594 (AN FR774048.1), MC58 (AN AE002098.2), alpha 710 (AN CP001561.1), alpha 14 (AN AM889136.1), 8013 (AN FM999788.1), Z2491 (AN AL157959.1), H44/76 (CP002420.1) and M10-240473 (ID 19023), *N. lactamica* strains 020-06 (AN FN995097.1), ATCC 23970 (ID 5544), Y92-1009 (ID 4945) and 049-12 (ID 1777), *N. cinerea* strain ATCC 14685 (ID 14731), *N. polysaccharea* strains ATCC 43768 (ID 14730) and 12030-2014 (ID 36153), *N. subflava* strain NJ9703 (ID 14733), *N. flavescens* strain NRL30031 (ID 14732), *N. sicca* strain ATCC 29256 (ID 2863), *N. mucosa* strain ATCC 25996 (ID 3565), and *N. elongata* strain ATCC 29315 (ID 14740).

The coding sequence of *ampG* and *gdh* for *N. meningitidis* ATCC 13102 and *N. lactamica* ATCC 49142 were obtained by PCR amplification and sequence. Primers SacI *ampG* F (CGGGAGCTCGCGATATTTGCTACAATAGGC) and XbaI *ampG* R

(GCCCTCTAGACACAATATCAGGTAAACGCTCC) were used to amplify and sequence *ampG*. The *gdh* coding sequences from *N. meningitidis* ATCC 13102 was obtained similarly using primers gdh-F2 (GTAGCGATGAGTAGTATTAC), gdh-R1 (GCCGTACTATTTGTACTGTC) and gdh-internal-F (GGCAAAGAAAGCCTGC). The *gdh* coding sequence from *N. lactamica* ATCC 49142 was obtained similarly using primers gdh-F2, gdh-R2 (GTGATTTCAGACGGCATATC) and gdh-internal-F. All newly acquired sequences were uploaded onto GenBank. The accession numbers for the *ampG* sequences of ATCC 13102, NM00268, and ATCC 49142 are KX289600, KX289601 and KX289603 respectively. The accession numbers for the *gdh* sequences of ATCC 13102, NM00268 and ATCC 49142 are KX289604, KX289605 and KX289607 respectively. Using MEGA7, the coding sequences of *ampG* and *gdh* were translated into amino acid sequences, aligned with ClustalW and used to construct neighbor-joining trees.

RESULTS

Meningococcal AmpG is more efficient at PG fragment recycling compared to gonococcal AmpG. We previously generated a gonococcal strain that expresses meningococcal *ampG* (EC505) and characterized the PG fragment profile of this gene replacement mutant (23). The native gonococcal *ampG* (*ampG*$_{\text{GC WT}}$) was replaced with meningococcal *ampG* (*ampG*$_{\text{MC WT}}$) coding region through double crossover homologous recombination to generate EC505. Using metabolic labeling of PG with [6-^{3}H]-glucosamine and quantitative fragment release in three independent experiments, we determined that EC505 released 52% of PG monomers, and 33% disaccharide compared to wild-type (WT) *N. gonorrhoeae* (MS11) (Figure 1A and 1C) in agreement with previous observations (23). We employed a similar strategy to generate a meningococcal strain that expresses gonococcal *ampG* (EC1001), and determined EC1001 released ~39% more PG monomers compared to WT MC (ATCC 13102) (Figure 1B and 1C). The differences in the amounts of PG monomers released in the gene replacement mutants compared to WT GC and WT MC are not identical to each other, or to the differences seen between WT GC and WT MC (2.8-fold less in WT MC). This discrepancy is likely due to the increased degradation of PG fragments in MC compared to GC, as previously described (23). Our results suggest that meningococcal AmpG is more efficient at PG fragment recycling compared to gonococcal AmpG. Thus, expression of meningococcal AmpG by *N. gonorrhoeae* reduced the amount of proinflammatory PG monomers released into the extracellular milieu, and vice versa.

AmpG from gonococcal strain MS11 and meningococcal strain ATCC 13102 have 97% identity and differ only by nine amino acid residues (Figure 3A, Supplementary Figure 1). We sought to determine if the difference in PG recycling efficiency is caused by differences in *ampG*

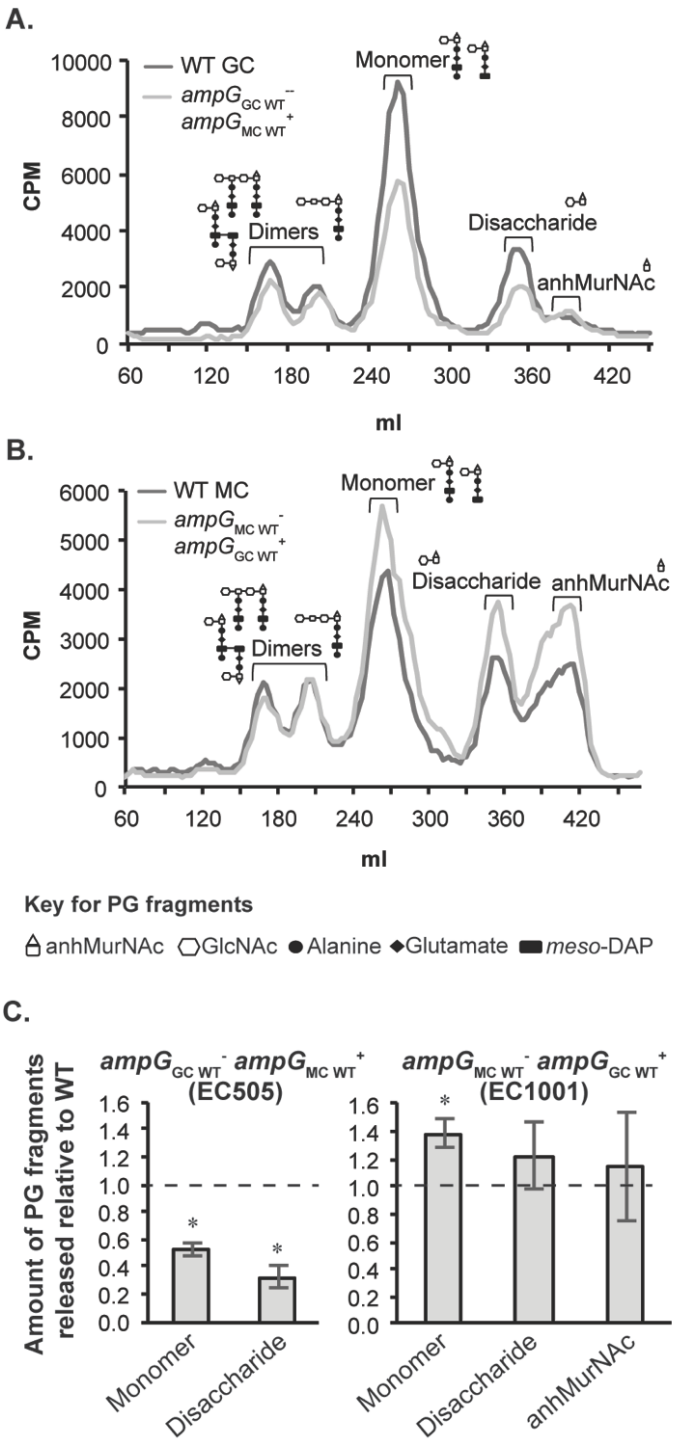

Figure 1. Expression of non-native *Neisseria ampG* in *N. gonorrhoeae* and *N. meningitidis* altered peptidoglycan fragment release. Released [^{3}H]-glucosamine labeled PG fragments were separated by size-exclusion chromatography and detected by liquid scintillation counting to

generate a PG fragment release profile. Symbols for PG sugars and amino acids are based on Jacobs *et al*. (24). A) Comparison of WT GC (MS11, dark grey line) to a gonococcal *ampG* replacement mutant expressing $ampG_{\text{MC WT}}$ (EC505, light grey line). B) Comparison of WT MC (ATCC 13102, dark grey line) to a meningococcal *ampG* replacement mutant expressing $ampG_{\text{GC WT}}$ (EC1001, light grey line). C) Quantification of the amount of PG fragments released by the *ampG* replacement mutants compared to WT in three independent experiments. * indicates that the amount of PG fragments released by the gene replacement mutant was significantly different compared to WT by Student two-tailed *t* test ($p<0.05$).

expression levels, or if small differences in protein sequence impact AmpG function. We performed quantitative RT-PCR on RNA samples isolated from WT GC (MS11), WT MC (ATCC 13102), GC expressing meningococcal *ampG* (EC505) and MC expressing gonococcal *ampG* (EC1001). If the difference in recycling efficiency is a direct consequence of differences in *ampG* expression, we would expect to see higher levels of *ampG* transcript expressed by strains that release lower levels of PG fragments, such as ATCC 13102 and EC505, compared to strains that release higher levels of PG fragments, such as MS11 and EC1001. Interestingly and contrary to this hypothesis, bacterial strains that are more efficient at recycling produced lower levels of *ampG* transcript compared to the strains that are less efficient at recycling. Gonococcal strain MS11 produced higher levels of *ampG* transcript compared to meningococcal strain ATCC 13102 (Figure 2A). EC505, which is more efficient at recycling compared to MS11 produced lower levels of *ampG* transcript compared to MS11 (Figure 2B). ATCC 13102, which is more efficient at recycling compared to EC1001, did not show increased *ampG* transcript compared to the latter strain (Figure 2C).

To determine levels of AmpG protein in WT gonococci and in WT meningococci, we raised polyclonal antibodies against a short AmpG epitope (FRREILSDEELGLG) (Genscript). Unfortunately, this antibody was not specific enough to detect AmpG levels in an immunoblot (data not shown). As an alternative, we generated strains expressing AmpG fused to a C-terminal triple FLAG tag ((DYKDDDDK)$_3$) and performed immunoblotting using anti-FLAG® M2 primary antibody. There was no significant difference in the amount of AmpG-FLAG3 expressed by WT gonococci and WT meningococci (Figure 2D and 2E). Taken together, these results suggested that the difference in PG fragment release between *N. gonorrhoeae* and

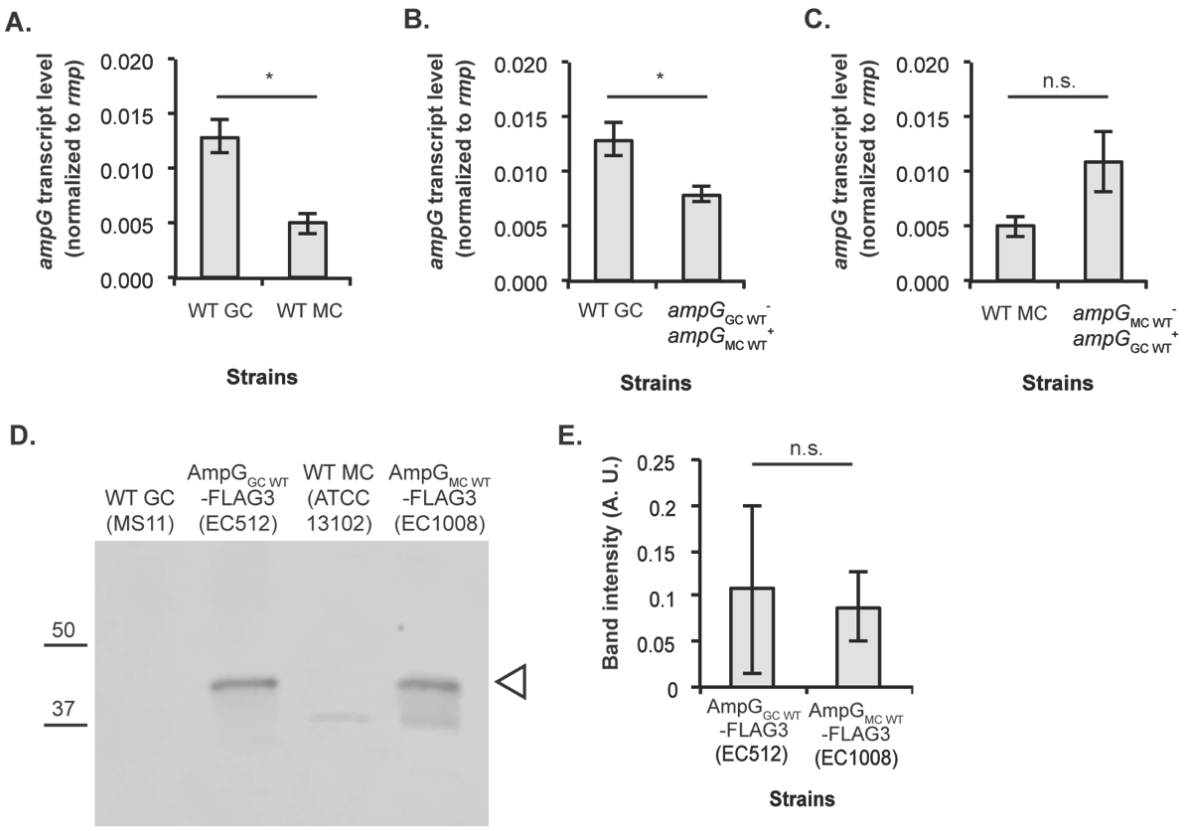

Figure 2. *Neisseria* strains that were more efficient at recycling PG fragments did not express higher levels of *ampG*. Transcript levels for *ampG* were determined comparing: A) WT MC (ATCC 13102) to WT GC (MS11), B) $ampG_{GC\ WT}^{-}$ $ampG_{MC\ WT}^{+}$ (EC505) to WT GC, and C) WT MC to $ampG_{MC\ WT}^{-}$ $ampG_{GC\ WT}^{+}$ (EC1001). RT-PCR results are from three biological replicates with technical triplicates. D) Protein levels of AmpG-FLAG3 were determined for GC and MC strains by Western blot. WT gonococci and meningococci that did not express FLAG3 tagged AmpG protein were included as negative controls. E) Quantification of the AmpG-FLAG3 bands from three independent experiments was performed using LiCor Odyssey Fc. Statistical significance was determined using Student two-tailed *t* test. * indicates statistical significance, with $p<0.05$, while n.s. indicates not significant.

N. meningitidis was not due to higher *ampG* expression levels or AmpG protein levels in strains that are more efficient at recycling.

Three residues near the C-terminal end of AmpG modulate AmpG recycling efficiency. Although AmpG sequences from *N. gonorrhoeae* strain MS11 and *N. meningitidis* ATCC 13102 are 97% identical, the nine amino acid residues that differ may impact protein function. To determine which residues affect AmpG efficiency, we designed four chimeric *ampG* constructs to be expressed in *N. gonorrhoeae* (Figure 3A). We divided AmpG into four unequal regions – region 1 (N-terminal end, bp 1-150), region 2 (mid gene, closer to N-terminal end, bp 151-788), region 3 (mid gene, closer to C-terminal end, bp 789-992) and region 4 (C-terminal end, bp 993-1284) – in which each region contained at least one residue that differs between MS11 and ATCC 13102. Each chimeric gene construct is comprised of approximately one-quarter gonococcal *ampG* coding region and approximately three-quarters meningococcal *ampG* coding region, so that each chimeric protein expressed would contain a mixture of gonococcal and meningococcal AmpG residues. We would expect to see a WT GC-like phenotype for PG fragment release in strains that express the gonococcal region(s) that codes for AmpG residues important for function, while the other strains would phenocopy a strain that expresses $ampG_{MC}$ $_{WT}$ (EC505). Only expression of a chimeric AmpG protein with meningococcal region 1-3 and gonococcal region 4 (EC511) resulted in a WT GC-like phenotype (Figure 3B). This strain showed a large increase in release of PG monomers as well as increased release of the other small PG fragments compared to strains that express the other chimeric AmpG proteins with gonococcal *ampG* regions 1, 2 or 3. We also produced a GC strain expressing *ampG* carrying gonococcal regions 1-3 and meningococcal region 4. This strain phenocopied EC505, indicating

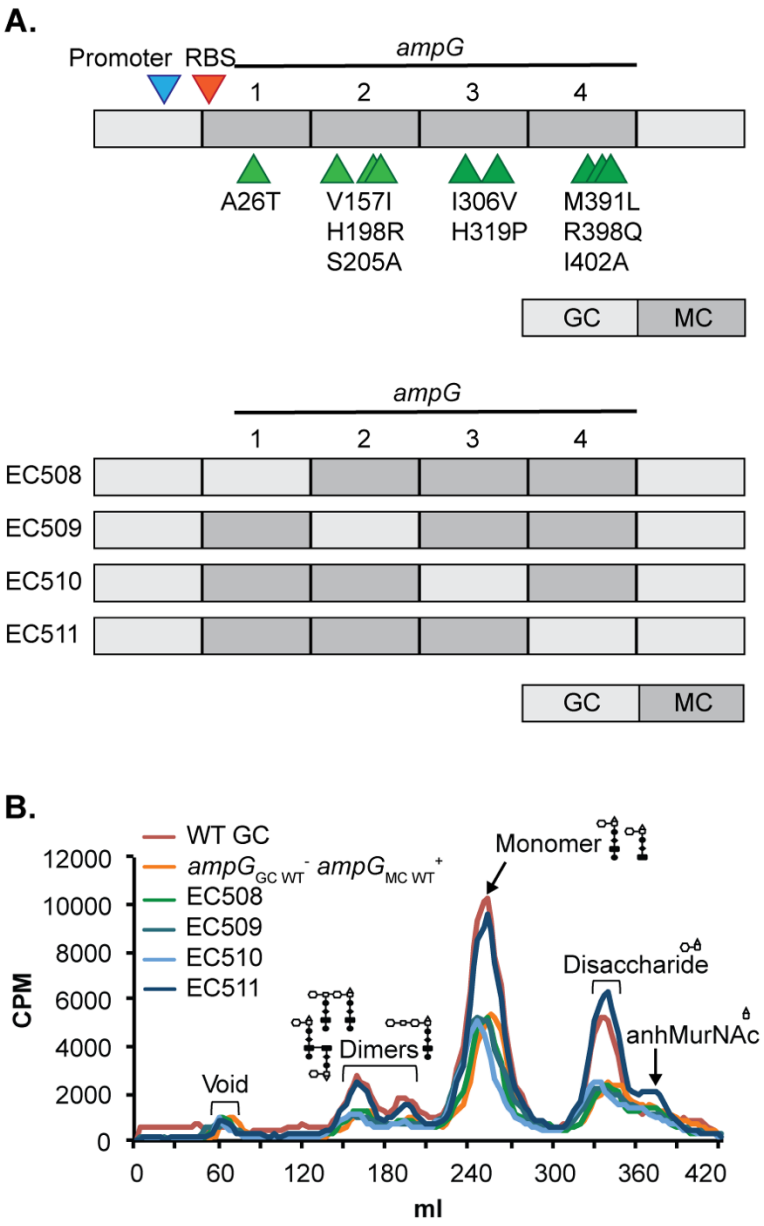

Figure 3. Residues near the C-terminal end of AmpG (AmpG region 4) modulated AmpG recycling efficiency. A) Cartoon depiction of the AmpG replacement and AmpG chimera constructs expressed in *N. gonorrhoeae* (not to scale). The AmpG replacement construct (top) was used as a base to generate the chimera constructs. Residues that differ between GC AmpG and MC AmpG are indicated in this format: [gonococcal residue][residue number][meningococcal residue]. Each chimera construct contained approximately one-quarter

gonococcal *ampG* coding region and three-quarters meningococcal *ampG* coding region, and contained a mixture of gonococcal and meningococcal residues. B) PG fragment release profiles for *N. gonorrhoeae* strains expressing different versions of *ampG*.

that the six changes in these three regions do not decrease AmpG function (data not shown). Our results suggest that residues in AmpG region 4 modulate AmpG efficiency.

Three residues in AmpG region 4 that differ between gonococcal and meningococcal AmpG are residues 391 (methionine in GC, leucine in MC), 398 (arginine in GC, glutamine in MC), and 402 (isoleucine in GC, alanine in MC). To determine which residues are most important for modulating AmpG function, we utilized site-directed mutagenesis to perform single, double and triple substitutions of gonococcal AmpG residues 391, 398 and 402 with the corresponding meningococcal residues. Expression of *ampG*$_{GC}^{M391L}$ and *ampG*$_{GC}^{I402A}$ reduced PG monomer release in *N. gonorrhoeae*, although not to the levels seen in the gene replacement mutant, EC505 (Figure 4A). Expression of *ampG*$_{GC}^{R398Q}$ resulted in a WT GC-like phenotype (Figure 4A).

We next asked if double substitutions of residues 391 and 402 from the gonococcal to the meningococcal residues would result in an additive effect, leading to PG monomer release levels similar to that of gonococci expressing meningococcal *ampG*. Gonococcal strains that expressed *ampG*$_{GC}^{M391L\ I402A}$ phenocopied strains that expressed the *ampG*$_{GC}^{M391L}$ and *ampG*$_{GC}^{I402A}$ single substitution mutants, releasing an intermediate level of PG monomers (Figure 4B). Double substitutions of any of the three residues resulted in PG monomer release levels similar to that of gonococcal strains expressing *ampG*$_{GC}^{M391L}$ or *ampG*$_{GC}^{I402A}$, suggesting that double mutations did not have an additive effect on PG recycling efficiency (Figure 4B). Substitutions of all three residues 391, 398 and 402 from the gonococcal to the meningococcal residues resulted in PG monomer release levels similar to that of gonococci expressing meningococcal *ampG* (Figure 4C). Our results suggested that residues 391, 398 and 402 work cooperatively to modulate AmpG function.

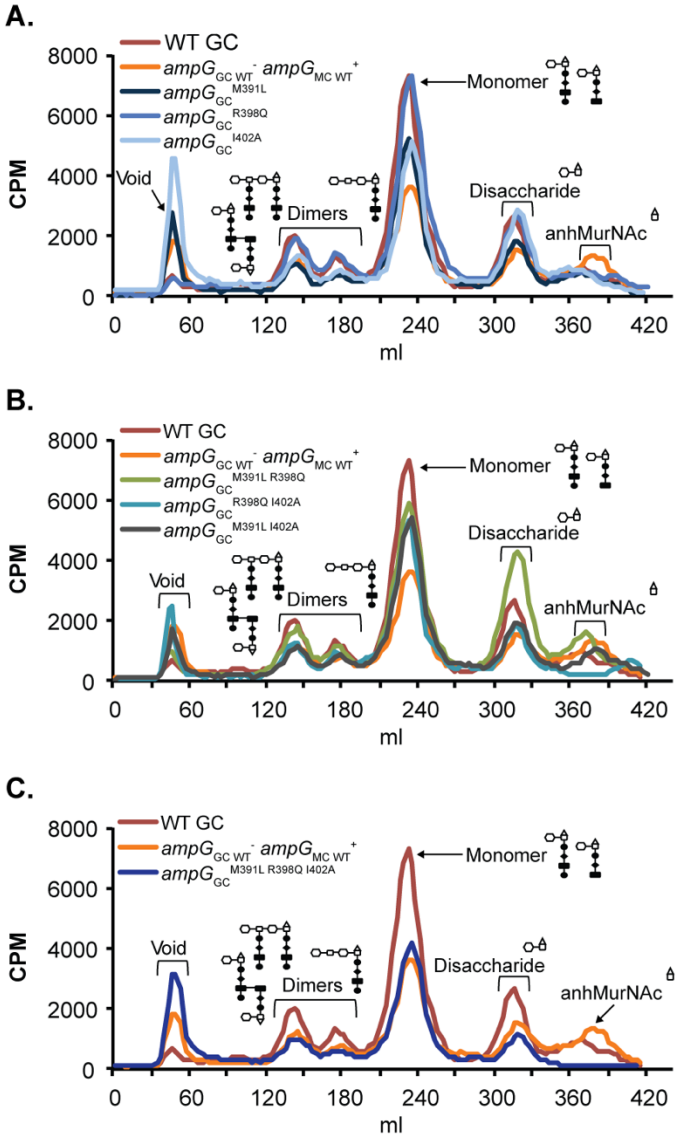

Figure 4. AmpG residues 391, 398 and 402 worked cooperatively to modulate AmpG recycling efficiency. PG fragment release profiles are shown for: A) Single substitutions of AmpG residues 391, 398 and 402 (EC515, EC516, EC517) compared to the whole gene replacement mutant (EC505) and wild type (MS11), B) Double substitutions of AmpG residues 391, 398 and 402 (EC518, EC519, EC521) compared to WT and EC505, and C) Triple substitutions of AmpG residues 391, 398 and 402 (EC523) compared to WT and EC505.

AmpG residues 391, 398 and 402 do not regulate levels of AmpG protein. We hypothesized that substitutions of residues 391, 398, and 402 from the gonococcal to the meningococcal variants might stabilize the protein. Thus, increased recycling efficiency in the gonococcal strain that expressed *ampG*$_{GC}^{M391L\ R398Q\ I402A}$ could be a result of increased AmpG protein levels. To test this idea, we tagged various gonococcal *ampG* substitution mutants that were more efficient at recycling compared to WT GC with the C-terminal triple FLAG epitope and measured AmpG protein levels by immunoblot. There was no significant difference in the amounts of AmpG-FLAG3 protein in any of the mutant strains tested (Figure 5). Thus, strains that expressed *ampG* variants that are more efficient at recycling PG fragments did not produce more AmpG-FLAG3 protein compared to WT gonococci. The immunoblot results suggested that substitutions of residues 391, 398, and 402 from the gonococcal to the meningococcal variants do not increase AmpG stability and levels.

***Neisseria sicca* and *Neisseria mucosa* are more efficient at PG recycling, and release lower levels of PG fragments compared to *N. gonorrhoeae*.** There are eight species of human associated, nonpathogenic *Neisseria* that asymptomatically colonize the human nasopharyngeal and oropharyngeal space. They include *N. sicca, N. mucosa, N. lactamica, N. polysaccharea, N. subflava, N. flavescens, N. cinerea* and *N. elongata* (46). We hypothesized that nonpathogenic *Neisseria* would release lower levels of PG fragments to evade immune clearance and maintain asymptomatic carriage in human hosts. We found that both *N. sicca* and *N. mucosa* released lower levels of PG monomers compared to *N. gonorrhoeae* (Figure 6). Intriguingly, both *N. sicca* and *N. mucosa* also released very small amounts or possibly no PG dimers (Figure 6).

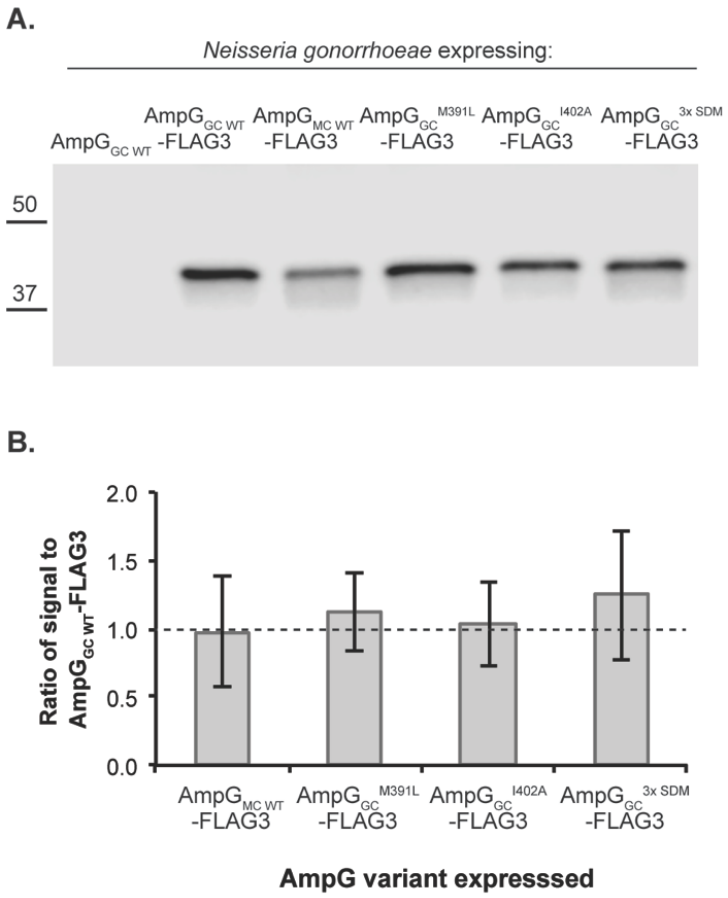

Figure 5. Increased recycling efficiency of gonococcal *ampG* mutants was not a consequence of increased AmpG protein levels. A) AmpG was tagged with a C-terminal triple FLAG (FLAG3) epitope to determine AmpG levels made by *N. gonorrhoeae* via immunoblotting, comparing the levels of AmpG-FLAG3 expressed by different *ampG* mutant strains that have GC WT-like (EC512) or more efficient PG recycling (EC546, EC548, EC550). B) Quantification of band intensities from three independent experiments using LiCor Odyssey Fc.

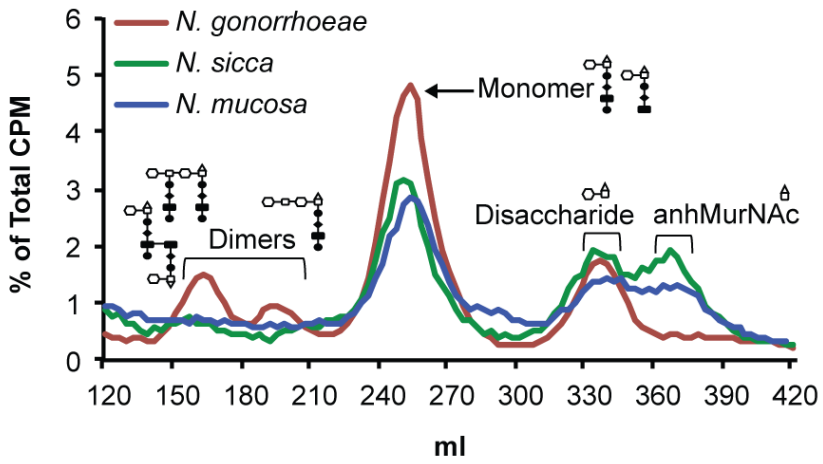

Figure 6. PG fragment release from nonpathogenic *N. sicca* (ATCC 29256, green line) and *N. mucosa* (ATCC 25996, blue line) compared to *N. gonorrhoeae* (MS11, red line).

To determine AmpG recycling efficiency in *N. sicca* and in *N. mucosa*, we compared the amounts of PG fragments released by WT and an *ampG* mutant that is unable to recycle PG fragments. We mutated *N. sicca* and *N. mucosa ampG* by interrupting the *ampG* coding sequence with a kanamycin resistance cassette. Since there are currently no complementation constructs available for *N. sicca* and *N. mucosa*, we generated backcrossed strains by transforming WT *N. sicca* and *N. mucosa* with chromosomal DNA isolated from the *ampG* deletion mutants. We calculated the recycling efficiency in *N. sicca* and *N. mucosa* by determining the area under the monomer curve for WT and *ampG* mutants. Both *N. sicca* and *N. mucosa* released 5% and recycled 95% of PG monomers liberated during PG turnover (Figure 7). This level of PG monomer release is very similar to that of *N. meningitidis*, which releases 4% of PG monomers (23). Free disaccharide release was also increased in the *N. sicca* and *N. mucosa ampG* mutants, suggesting that the permease also transports these PG molecules, in agreement with previous reports (23, 47).

Bioinformatic analyses demonstrate that all gonococci encode M391, R398, and I402 in *ampG*. We compiled and aligned *ampG* alleles expressed by 31 strains from 9 species of *Neisseria* and found that all gonococcal strains surveyed have methionine, arginine and isoleucine at AmpG positions 391, 398 and 402 (Supplementary Figure 1). A query of the sequences in the *Neisseria* Multi Locus Sequence Typing website (http://pubmlst.org/neisseria) and the Meningitis Research Foundation (MRF) Meningococcus Genome Library database (http://meningitis.org/research/genome) revealed that while no gonococcal strains (out of 1,847 sequences) had leucine, glutamine and alanine at the three positions, there were two strains of *N. polysaccharea* (out of 19 sequences) (44), eight strains of *N. lactamica* (out of 130 sequences)

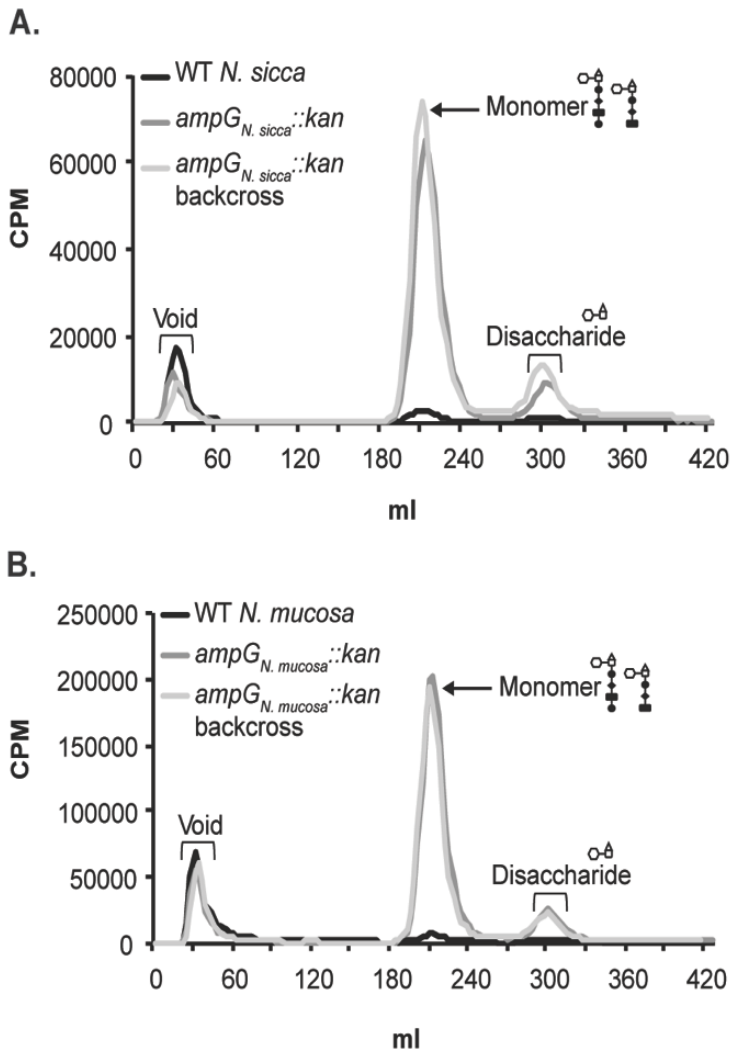

Figure 7. *N. sicca and N. mucosa* possess functional AmpG proteins. PG fragment release was examined for mutants carrying a kanamycin resistance cassette interrupting *ampG* in *N. sicca* (EC2004) (A) and *N. mucosa* (EC2003) (B) (dark grey lines) compared to WT *N. sicca* and *N. mucosa* (black lines). PG fragment release profiles for backcrossed mutants (EC2004BC/ EC2003BC, light grey lines) are also shown. Quantification of the peaks was performed with data obtained from three independent experiments.

and around 420 meningococcal strains (out of 7,141 sequences), predominantly of the ST-269 and to a lesser extent, the ST41/44 subtypes, that had methionine, arginine and isoleucine at AmpG residues 391, 398 and 402 (data not shown). These three amino acid changes were found in 5.88% of meningococcal strains. One example each of *N. polysaccharea* (strain 12030-2014), *N. lactamica* (strain 049-12) and *N. meningitidis* (strain M10-240473) are shown in Supplementary Figure 1.

We also sequenced *ampG* from several meningococcal clinical isolates, and found an isolate, *N. meningitidis* strain NM00268, that codes for the gonococcal-like residues arginine and isoleucine at AmpG positions 398 and 402 (Supplementary Figure 1). NM00268 labels poorly with [^{3}H]-glucosamine, and thus was labeled with [^{3}H]-diaminopimelic acid instead. In accordance to our model, NM00268 released approximately 1.7 times more PG monomers compared to ATCC 13102 (Figure 8), providing support to our hypothesis that having gonococcal-like residues at AmpG positions 391, 398 and/or 402 contribute to increased PG monomer release. There were no significant differences in the amount of peptides released by NM00268 and ATCC 13102.

We constructed a neighbor-joining tree based on AmpG sequences, and found that while gonococcal strains tend to cluster together, strains of *N. lactamica* and *N. polysaccharea* that expressed GC-like AmpG residues 391, 398 and 402, did not cluster with *N. gonorrhoeae* or with each other. While *N. meningitidis* strains NM00268 and M10-240473 cluster close to each other, they did not cluster with *N. gonorrhoeae* or with *N. lactamica* strain 049-12 or *N. polysaccharea* strain 12030-2014. In addition, *N. polysaccharea* strain 12030-2014 did not cluster well with other strains from the same species, suggesting that the AmpG sequences in these non-gonococcal strains evolved independently or resulted from horizontal gene transfer

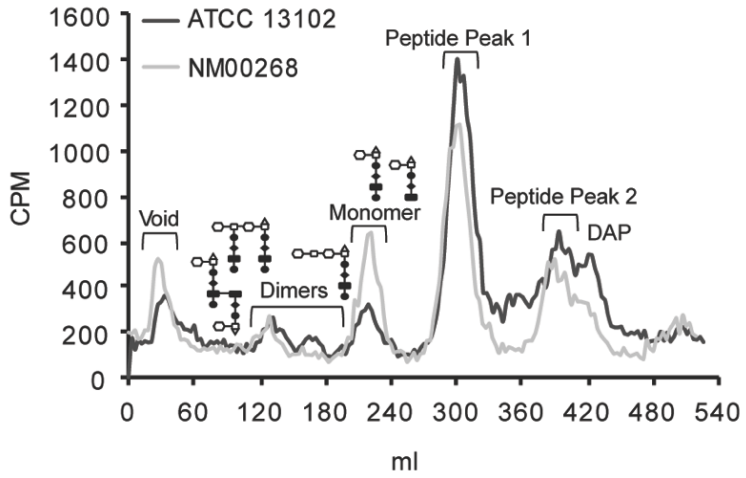

Figure 8. PG fragment release from a meningococcal strain with naturally-occurring GC-like AmpG residues 398 and 402 (NM00268). ATCC 13102 and NM00268 were labeled with [^{3}H]-diaminopimelic acid, which labels the peptide stem of PG fragments. Quantification of the area under the curve was performed with data from three independent experiments.

events creating mosaic AmpG sequences, as is seen for *N. meningitidis* PBP2 (48). As a control, we also constructed a neighbor-joining tree based on Gdh sequences (Supplementary Figure 2). With the exception of *N. meningitidis* strain 8013, all other strains clustered with members of the same species. Overall, these results demonstrated that while M391, R398 and I402 are present in a small fraction of meningococcal or nonpathogenic *Neisseria* strains, these AmpG-crippling mutations are universally present in *N. gonorrhoeae*, making it likely that all *N. gonorrhoeae* isolates release high levels of PG fragments.

AmpG residues 391, 398 and 402 are predicted to be located on a transmembrane helix near the periplasmic face of the protein. We used I-TASSER and Phyre2 servers to predict the structure of AmpG, and obtained two different putative AmpG structures (38–42). The model of AmpG structure obtained by I-TASSER showed an inward facing conformation, in which irregularly arranged helices surround a substrate binding cavity that opens towards the cytoplasm (Figure 9A). On the other hand, the predicted structure of AmpG using Phyre2 showed an occluded conformation that may be a transitional state between the inward facing and the outward (periplasmic) facing conformations during transport (Fig 9B). In both models, AmpG residues 391, 398 and 402 are located near the periplasmic face of the protein at the start of the last transmembrane helix.

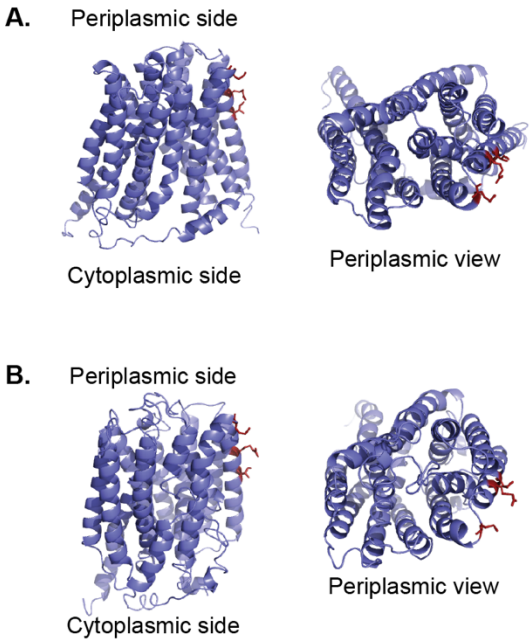

Figure 9. Prediction of gonococcal AmpG structure. The predicted structure of gonococcal AmpG was determined using I-TASSER server with multiple threading templates (A) and using Phyre2 with a multi-template/*ab initio* template (B). Side view (left), and the view from the periplasmic face (right) of the AmpG structure are shown here, with residues 391, 398 and 402 displayed as dark red sticks. Residues 391, 398 and 402 are located close to the periplasmic face of the protein.

DISCUSSION

The release of PG fragments is not unique to *Neisseria,* although few genera besides *Neisseria* release mainly toxic anhydro-PG monomers. PG moieties released by bacteria have been implicated in resuscitation of dormant mycobacteria, development of *Myxococcus* fruiting bodies, germination of *Bacillus subtilis* spores and establishment of mutualism between *Bacillus cereus* and *Flavobacterium johnsoniae* (reviewed in (49), (50) and (51)). Nonetheless, the release of PG monomers by bacteria tends to lead to inflammation and death of animal host cells, whether this interaction leads to beneficial or detrimental effects at the organismal level. Tetrapeptide monomer (also known as TCT) and lipopolysaccharide (LPS) released by *Vibrio fischeri* work synergistically to induce regression of ciliated epithelial cells near the light organ of the Hawaiian bobtail squid to allow establishment of squid-*Vibrio* symbiosis (21, 52, 53). The production of PG fragments is also thought to be important for the pathogenesis of multiple bacterial species, including but not limited to human pathogens like *Helicobacter pylori* and *Shigella flexneri,* as well as plant pathogens like *Pseudomonas syringae* and *Erwinia amylovora* (reviewed in (50)).

Besides *N. gonorrhoeae*, the effects of released PG fragments on host fitness is most well studied with respect to the human pathogen *Bordetella pertussis,* which causes whooping cough. Unlike *Neisseria,* which releases a mixture of tripeptide monomer and TCT, *B. pertussis* releases exclusively TCT. TCT causes the sloughing and death of ciliated tracheal cells in *ex vivo* hamster tracheal tissue studies (14, 54, 55). An insertion element (IS*481*) ~90bp upstream of *B. pertussis ampG* reduced *ampG* expression in *B. pertussis* and results in high levels of TCT released (56). When IS*481* is deleted, or when *E. coli ampG* is expressed in *B. pertussis* instead, the amount of TCT released is significantly lowered (56). Collectively, these findings suggest that both human

pathogens *B. pertussis* and *N. gonorrhoeae* evolved different strategies to reduce PG fragment recycling efficiency to release more PG monomers. This process generates an inflammatory environment that may be favorable for bacterial growth and invasion.

In this work, we showed that *N. gonorrhoeae* releases more PG monomer and is less efficient at recycling PG monomers compared to *N. meningitidis*, *N. sicca* and *N. mucosa*, three species of *Neisseria* that can asymptomatically colonize the human nasopharyngeal space. With *N. gonorrhoeae* and *N. meningitidis*, the difference in the recycling efficiency is not due to higher expression of *ampG* in *N. meningitidis* compared to *N. gonorrhoeae*. In fact, gonococcal and meningococcal strains that are more efficient at recycling consistently produced lower levels of *ampG* transcript compared to strains that are less efficient at recycling. Furthermore, we did not see significant differences in the amount of various AmpG-FLAG3 proteins expressed by *N. gonorrhoeae*, and amino acid substitutions to make gonococcal AmpG more like meningococcal AmpG did not increase AmpG protein levels. These data indicated that it is not reduced amounts of *ampG* transcript or AmpG protein that makes *N. gonorrhoeae* deficient at recycling, but rather the reduced function of gonococcal AmpG in facilitating PG fragment recycling.

We also showed that reduced recycling efficiency in *N. gonorrhoeae* can be accounted for by the amino acid identity of residues 391, 398 and 402, which are close to the C-terminal end of AmpG (Figure 9). Although we do not yet understand how these three residues modulate AmpG function, beyond that the three residues do not change AmpG protein levels, we have several hypotheses. One hypothesis is that residues 391, 398, and 402 may directly bind to PG, and the gonococcal residues are either less able to bind PG fragments, or bind PG fragments too tightly, making transport of PG fragments less efficient compared to the meningococcal, *N. sicca* or *N. mucosa* AmpG counterparts.

The *E. coli* AmpG homolog is powered by proton motive force (47), although it is unknown if AmpG functions as a H^+/PG fragment symporter or if AmpG interacts with a proton transducing protein that powers the permease. It is also unknown if PG-degrading enzymes work together in a complex to remodel the PG layer, and if such complexes co-localize or interact with AmpG to ensure efficient recycling. Lytic transglycosylases are PG-degrading enzymes that cleave the glycan backbone to generate PG monomers (20). *N. gonorrhoeae* has two lytic transglycosylases, LtgA and LtgD, that generate all or nearly all the PG monomers released by the bacterium. Deletion of *ltgD* leads to a larger reduction in the amount of PG monomers released compared to deletion of *ltgA* (62% reduction vs 38% reduction) (19). However, LtgA generates more PG monomers than LtgD and LtgA-generated monomers are preferentially taken up into the cytoplasm for recycling (57). Thus, it is also possible that residues 391, 398 and 402 facilitate protein-protein interaction with hypothetical accessory protein(s), or with PG-degrading enzymes like LtgA in the periplasm to power AmpG function or ensure efficient PG recycling.

Another hypothesis is that the residues at these positions are important for facilitating conformational changes required for the import of PG fragments into the cytoplasm. AmpG belongs to major facilitator superfamily (MFS). MFS proteins are typically membrane transport proteins with 12 or 14 transmembrane α-helices that can function as uniporters, symporters and antiporters and can be found in bacteria, eukaryotes and archaea (58, 59). The most well-studied MFS protein, LacY, is a lactose/H^+ symporter that can assume one of at least two conformations, as determined by X-ray crystallography studies. LacY can assume a conformation with two-fold pseudosymmetry with a large aqueous, substrate-binding cavity that opens towards the cytoplasm (PDB ID 1PV7, 2V8N) (60, 61). It is proposed that LacY can assume a similar conformation in which the aqueous cavity opens towards the periplasm for substrate binding

(62). LacY can also form an occluded conformation with a narrow cavity that opens slightly towards the periplasm that is thought to be an intermediate conformation during substrate transport (PDB ID 4OAA, 4ZYR) (63, 64). Given that the two predicted AmpG structures resembled the two structurally determined conformations of LacY, AmpG may function similarly to LacY. As such, residues at positions 391, 398 and 402 might impact the rate of conformational changes required for transport. The crystal structure of AmpG and the exact mechanism of action that AmpG uses to transport PG fragments are currently unknown. A crystal structure of AmpG would help inform studies of AmpG's mechanism of action and provide insight into how residues 391, 398 and 402 impact AmpG efficiency.

We hypothesize that the differences in AmpG function and PG fragment release between the asymptomatic colonizers and *N. gonorrhoeae* contribute to the differences in the inflammatory responses to these species at their different infection sites. It should be noted that *ampG* is not the only factor affecting PG fragment release. Comparing *N. meningitidis* to *N. gonorrhoeae*, expression of meningococcal *ampG* in gonococci results in a near two-fold decrease in PG release, but expression of gonococcal *ampG* in meningococci only resulted in a 39% increase in PG monomer release (Figure 1). These results suggest that additional features of PG fragment metabolism in *N. gonorrhoeae* may favor PG fragment release, and that *N. meningitidis* and the nonpathogenic *Neisseria* species may have additional mechanisms for increasing PG fragment recycling and diminishing PG fragment release. Increased PG fragment breakdown by *N. meningitidis* as well as *N. mucosa* and *N. sicca* as compared to *N. gonorrhoeae* can be seen in the PG fragment release profiles (Figure 1, Figure 6) (23). Less PG dimers and monomers are released but more anhMurNAc is released as compared to *N. gonorrhoeae*. In addition to the reduced PG fragment release we have shown here, nonpathogenic *Neisseria* are

also known to produce a lipid A structure that is less inflammatory (6). Together with differences in the responsiveness of the different tissues infected by these species, the differences in lipid A and PG fragment release may explain how nonpathogenic *Neisseria* are able to maintain asymptomatic colonization while *N. gonorrhoeae* usually induces a strong inflammatory response and disease.

ACKNOWLEDGEMENTS

We thank Nate Weyand for the gift of *N. sicca* ATCC 29256 and *N. mucosa* ATCC 25996. We are grateful to Katie Hackett, Jon Lenz and Ryan Schaub for experimental support and discussions.

Table 1. Strains used in this study.

Strain	Description	Reference or source
N. gonorrhoeae		
MS11	WT *N. gonorrhoeae*	(65)
EC505	$ampG_{GC}^{-}$ $ampG_{MC\ WT}^{+}$	(23)
EC508	MS11 transformed with pEC016; $ampG_{GC}^{-}$ $ampG_{GC\ Chimera\ 1}^{+}$	This work
EC509	MS11 transformed with pEC017; $ampG_{GC}^{-}$ $ampG_{GC\ Chimera\ 2}^{+}$	This work
EC510	MS11 transformed with pEC018; $ampG_{GC}^{-}$ $ampG_{GC\ Chimera\ 3}^{+}$	This work
EC511	MS11 transformed with pEC019; $ampG_{GC}^{-}$ $ampG_{GC\ Chimera\ 4}^{+}$	This work
EC512	MS11 transformed with pEC028; $ampG_{GC\ WT}$-FLAG3	This work
EC515	MS11 transformed with pEC037; $ampG_{GC}^{M391L}$	This work
EC516	MS11 transformed with pEC038; $ampG_{GC}^{R398Q}$	This work
EC517	MS11 transformed with pEC039; $ampG_{GC}^{I402A}$	This work
EC518	MS11 transformed with pEC042; $ampG_{GC}^{M391L\ R398Q}$	This work
EC519	MS11 transformed with pEC043; $ampG_{GC}^{M391L\ I402A}$	This work
EC521	MS11 transformed with pEC054; $ampG_{GC}^{R398Q\ I402A}$	This work
EC523	MS11 transformed with pEC058; $ampG_{GC}^{M391L\ R398Q\ I402A}$	This work
EC546	MS11 transformed with pEC100; $ampG_{GC}^{M391L}$-FLAG3	This work
EC548	MS11 transformed with pEC102; $ampG_{GC}^{I402M}$-FLAG3	This work
EC549	MS11 transformed with pEC103; $ampG_{GC}^{M391L\ R398Q\ I402M}$-FLAG3	This work
EC550	MS11 transformed with pEC098; $ampG_{GC}^{-}$ $ampG_{MC\ WT}$-$FLAG^{+}$	This work
N. meningitidis		
ATCC 13102 *cap*$^{-}$	ATCC 13102 *rpsL* (K43R) *siaD::cat* (WT *N. meningitidis*)	(23)
NM00268	Serogroup B clinical isolate	(66)
EC1001	ATCC 13102 *cap*$^{-}$ transformed with pEC008; $ampG_{MC}^{-}$ $ampG_{GC\ WT}^{+}$	This work
EC1008	ATCC 13102 *cap*$^{-}$ transformed with pEC029; $ampG_{MC\ WT}$-FLAG3	This work
N. sicca		
ATCC 29256	Pharyngeal mucosa isolate (WT *N. sicca*)	N. Weyand
EC2004	ATCC 29256 transformed with pEC081; $ampG_{N.\ sicca}$::*kan*	This work
EC2004BC	ATCC 29256 transformed with EC2004 chromosomal DNA; $ampG_{N.\ sicca}$::*kan* backcross	This work
N. mucosa		
ATCC 25996	Pharyngeal mucosa isolate (WT *N. mucosa*)	N. Weyand
EC2003	ATCC 25996 transformed with pEC070; $ampG_{N.\ mucosa}$::*kan*	This work
EC2003BC	ATCC 25996 transformed with EC2003 chromosomal DNA; $ampG_{N.\ mucosa}$::*kan*	This work

Table 2. Plasmids used in this study.

Plasmid	Description	Reference or source
pIDN3	Cloning plasmid containing GC/MC DNA uptake sequences	(30)
pHSS6	Cloning plasmid, source of *kanR*	(67)
pEC026	pIDN3 containing *N. sicca/N.mucosa* DNA uptake sequences	This work
pEC005	*ampG*$_{MC}$*p-ampG*$_{GC\ WT}$ cloned into pIDN3	This work
pEC006	*ampG*$_{GC}$*p-ampG*$_{MC\ WT}$ cloned into pIDN3	(23)
pEC007	*ampG*$_{GC}$*p-ampG*$_{GC}$ cloned into pIDN3	This work
pEC008	*ampG*$_{MC}$*p-ampG*$_{GC}$ cloned into pIDN3	This work
pEC013	*ampG*$_{GC}$*p ampG*$_{MC}$ cloned into pIDN3	This work
pEC016	*ampG*$_{GC}$*p ampG*$_{Chimera\ 1}$ cloned into pIDN3	This work
pEC017	*ampG*$_{GC}$*p ampG*$_{Chimera\ 2}$ cloned into pIDN3	This work
pEC018	*mpG*$_{GC}$*p ampG*$_{Chimera\ 3}$ cloned into pIDN3	This work
pEC019	*ampG*$_{GC}$*p ampG*$_{Chimera\ 4}$ cloned into pIDN3	This work
pEC028	*ampG*$_{GC}$-FLAG3 cloned into pIDN3	This work
pEC029	*ampG*$_{MC}$-FLAG3 cloned into pIDN3	This work
pEC037	*ampG*$_{GC}$*p-ampG*$_{GC}^{M391L}$ cloned into pIDN3	This work
pEC038	*ampG*$_{GC}$*p-ampG*$_{GC}^{R398Q}$ cloned into pIDN3	This work
pEC039	*ampG*$_{GC}$*p-ampG*$_{GC}^{I402A}$ cloned into pIDN3	This work
pEC042	*ampG*$_{GC}$*p-ampG*$_{GC}^{M391L\ R398Q}$ cloned into pIDN3	This work
pEC043	*ampG*$_{GC}$*p-ampG*$_{GC}^{M391L\ I402A}$ cloned into pIDN3	This work
pEC054	*ampG*$_{GC}$*p-ampG*$_{GC}^{R398Q}$ I402A cloned into pIDN3	This work
pEC058	*ampG*$_{GC}$*p-ampG*$_{GC}^{M391L}$ cloned into pIDN3	This work
pEC063	*ampG*$_{N.\ sicca}$ cloned into pEC026	This work
pEC064	*ampG*$_{N.\ mucosa}$ cloned into pIDN3	This work
pEC067	*ampG*$_{N.\ mucosa}$::*kan* cloned into pIDN3	This work
pEC070	*ampG*$_{N.\ mucosa}$::*kan* cloned into pEC026	This work
pEC081	*ampG*$_{N.\ sicca}$::*kan* cloned into pEC026	This work
pEC098	*ampG*$_{MC\ WT}$-FLAG3 cloned into pIDN3	This work
pEC100	*ampG*$_{GC}^{M391L}$-FLAG3 cloned into pIDN3	This work
pEC102	*ampG*$_{GC}^{I402A}$-FLAG3 cloned into pIDN3	This work
pEC103	*ampG*$_{GC}^{M391L\ R398Q\ I402A}$-FLAG3 cloned into pIDN3	This work

Table 3. Primers used in this study.

Primer name	Sequence (5' to 3')
MC ampG sacI F3	ATTCAGAGCTCCATCGGCGGCATCATCAAAC
SacI ampG F	CGGGAGCTCGCGATATTTGCTACAATAGGC
XbaI ampG R	GCCCTCTAGACACAATATCAGGTAAACGCTCC
ampG 5' flank R	AGCCTATTGTAGCAAATATCGCC
ampG F2	GGCGATATTTGCTACAATAGGCT
ampG 3' flank F	TCAAACTGGAGCGTTTACCTGATATTG
ampG1325R	CAATATCAGGTAAACGCTCCAGTTTGA
ampG 3' flank R BamHI	CTCAGGATCCGTTCTTTATATGAGCGGCAGG
ampG 990bp NheI F	GTAAGCTAGCGGCAGTTATCGGCGCGGAAG
ampG 990bp NheI R	CTAAGCTAGCATCAGCCTCTCGCCTGTG
ampG internal 1 F	CAGCGAGCAGGTGGATTTGAAG
ampG internal 1 R	CTTCAAATCCACCTGCTCGCTG
ampG internal 2 F	GGATATGGGTTTCAGCAAGAC
ampG internal 2 R	GTCTTGCTGAAACCCATATCC
Alt-DUS AvrII F	GGCTGCCTAGGTTCAGACGACAAGCTAATT
Alt-DUS AvrII R	GGTTGCCTAGGTTCAGACGACATGCAGC
ampG-FLAG3 F	CAGGCAGAGGTTCCGCTGGCTCCGCT
ampGend-FLAG3 R	CCTGCATCCTTATGAGAAAGTAAGTTC
(Gc) FLAG3-ampGend F	TTCTCATAAGAGAAAACCCAGGATGCAGG
(Gc) FLAG3-ampGend R	AGCGGAACCTCTGCCTGCATCCTGGG
(Mc) FLAG3-ampGend F	TTCTCATAAGAGAAAACTCAGGATGCAGG
(Mc) FLAG3-ampGend R	AGCGGAACCTCTGCCTGCATCCTGAG
MS11 AmpG R398Q F	GTACCGTTTTTCCAGTTGTGTTTCATAC
MS11 AmpG R398Q R	GTATGAAACACAACTGGAAAAACGGTAC
MS11 AmpG M391L F	CTGATCGAATGGCTGGGTTATGTACCG
MS11 AmpG M391L R	CGGTACATAACCCAGCCATTCGATCAG
MS11 AmpG I402A F	GGCTGTGTTTCGCACTTGCCCTG
MS11 AmpG I402A R	CAGGGCAAGTGCGAAACACAGCC
MS11 AmpG R398Q I402A F	CAGTTGTGTTTCGCACTTGCCCTG
MS11 AmpG R398Q I402A R	CAGGGCAAGTGCGAAACACAACTG
NSi ampG SacIF	CAGGAGAGCTCGTACTGCTCATCCATTATGAC
NSi ampG down BamHI R2	CATTAGGATCCCAATCGGCGTGTCTGCGATG
NMu ampG SacIF	CGCCGAGAGCTCGATGTTGTTCTCCCATTATGAC
Nmu ampG BamHI R	GACGAGGATCCCTACCGATACATTCAAACG
rmp-RT-F	CGAAGGCCATACCGACTTTATGG
rmp-RT-R	GTTGCTGACCAGGTTGTTTGC
ampG-RT-F	GTGCGTGCTGCTGTTTATC
ampG-RT-R	GTCTTGCTGAAACCCATATCC
gdh-F2	GTAGCGATGAGTAGTATTAC
gdh-R1	GCCGTACTATTTGTACTGTC
gdh-R2	GTGATTTCAGACGGCATATC
gdh-internal-F	GGCAAAGAAAGCCTGC

REFERENCES

1. **Dewhirst FE**, **Chen T**, **Izard J**, **Paster BJ**, **Tanner ACR**, **Yu WH**, **Lakshmanan A**, **Wade WG**. 2010. The human oral microbiome. J Bacteriol **192**:5002–5017.
2. **Zaura E**, **Keijser BJ**, **Huse SM**, **Crielaard W**. 2009. Defining the healthy "core microbiome" of oral microbial communities. BMC Microbiol **9**:259.
3. **Liu G**, **Tang CM**, **Exley RM**. 2015. Non-pathogenic *Neisseria*: members of an abundant, multi-habitat, diverse genus. Microbiology **161**:1297–1312.
4. **Johnson AP**. 1983. The pathogenic potential of commensal species of *Neisseria*. J Clin Pathol **36**:213–23.
5. **Marri PR**, **Paniscus M**, **Weyand NJ**, **Rendon MA**, **Calton CM**, **Hernandez DR**, **Higashi DL**, **Sodergren E**, **Weinstock GM**, **Rounsley SD**, **So M**. 2010. Genome sequencing reveals widespread virulence gene exchange among human *Neisseria* species. PLoS One **5**:e11835.
6. **John CM**, **Liu M**, **Phillips NJ**, **Yang Z**, **Funk CR**, **Zimmerman LI**, **Griffiss M**, **Stein DC**, **Jarvis GA**. 2012. Lack of lipid A pyrophosphorylation and functional *lptA* reduces inflammation by *Neisseria* commensals. Infect Immun **80**:4014–4026.
7. **Mayor MT**, **Roett MA**, **Uduhiri KA**. 2012. Diagnosis and management of gonococcal infections. Am Fam Physician **86**:931–938.
8. **Melly MA**, **McGee ZA**, **Rosenthal RS**. 1984. Ability of monomeric peptidoglycan fragments from *Neisseria gonorrhoeae* to damage human Fallopian-tube. J Infect Dis **149**:378–386.
9. **McGee ZA**, **Jensen RL**, **Clements CM**, **Taylor-Robinson D**, **Johnson AP**, **Gregg CR**. 1999. Gonococcal infection of human Fallopian tube mucosa in organ culture: relationship of mucosal tissue TNF-α concentration to sloughing of ciliated cells. Sex Transm Dis **26**:160–165.
10. **Rosenthal RS**. 1979. Release of soluble peptidoglycan from growing gonococci: hexaminidase and amidase activities. Infect Immun **24**:869–878.
11. **Sinha RK**, **Rosenthal RS**. 1980. Release of soluble peptidoglycan from growing gonococci: Demonstration of anhydro-muramyl-containing fragments. Infect Immun **29**:914–925.
12. **Rosenthal RS**, **Nogami W**, **Cookson BT**, **Goldman WE**, **Folkening WJ**. 1987. Major fragment of soluble peptidoglycan released from growing *Bordetella pertussis* is tracheal cytotoxin. Infect Immun **55**:2117–2120.
13. **Goldman WE**, **Klapper DG**, **Baseman JB**. 1982. Detection, isolation, and analysis of a released *Bordetella pertussis* product toxic to cultured tracheal cells. Infect Immun **36**:782–794.
14. **Cookson BT**, **Cho H**, **Herwaldt LA**, **Goldman WE**. 1989. Biological activities and chemical composition of purified tracheal cytotoxin of *Bordetella pertussis*. Infect Immun **57**:2223–2229.
15. **Girardin SE**, **Boneca IG**, **Carneiro LAM**, **Antignac A**, **Jehanno M**, **Viala J**, **Tedin K**, **Taha M-K**, **Labigne A**, **Zahringer U**, **Coyle AJ**, **DiStefano PS**, **Bertin J**, **Sansonetti PJ**, **Philpott DJ**. 2003. Nod1 detects a unique muropeptide from Gram-negative bacterial peptidoglycan. Science **300**:1584–1587.
16. **Stephens DS**, **Greenwood B**, **Brandtzaeg P**. 2007. Epidemic meningitis, meningococcaemia, and *Neisseria meningitidis*. Lancet **369**:2196–2210.

17. **Centers for Disease Control and Prevention**. 2015. Meningococcal disease: Technical & clinical information. Accessed from <http://www.cdc.gov/meningococcal /clinical-info.html>.
18. **Loh E**, **Kugelberg E**, **Tracy A**, **Zhang Q**, **Gollan B**, **Ewles H**, **Chalmers R**, **Pelicic V**, **Tang CM**. 2013. Temperature triggers immune evasion by *Neisseria meningitidis*. Nature **502**:237–40.
19. **Cloud-Hansen KA**, **Hackett KT**, **Garcia DL**, **Dillard JP**. 2008. *Neisseria gonorrhoeae* uses two lytic transglycosylases to produce cytotoxic peptidoglycan monomers. J Bacteriol **190**:5989–5994.
20. **Chan YA**, **Hackett KT**, **Dillard JP**. 2012. The lytic transglycosylases of *Neisseria gonorrhoeae*. Microb Drug Resist **18**:271–279.
21. **Adin DM**, **Engle JT**, **Goldman WE**, **McFall-Ngai MJ**, **Stabb EV**. 2009. Mutations in *ampG* and lytic transglycosylase genes affect the net release of peptidoglycan monomers from *Vibrio fischeri*. J Bacteriol **191**:2012–2022.
22. **Garcia DL**, **Dillard JP**. 2008. Mutations in *ampG* or *ampD* affect peptidoglycan fragment release from *Neisseria gonorrhoeae*. J Bacteriol **190**:3799–3807.
23. **Woodhams KL**, **Chan JM**, **Lenz JD**, **Hackett KT**, **Dillard JP**. 2013. Peptidoglycan fragment release from *Neisseria meningitidis*. Infect Immun **81**:3490–3498.
24. **Jacobs C**, **Huang L**, **Bartowsky E**, **Normark S**, **Park JT**. 1994. Bacterial cell wall recycling provides cytosolic muropeptides as effectors for beta-lactamase induction. EMBO J **13**:4684–4694.
25. **Korfmann G**, **Sanders CC**. 1989. *ampG* is essential for high-level expression of AmpC beta-lactamase in *Enterobacter cloacae*. Antimicrob Agents Chemother **33**:1946–1951.
26. **Kellogg DS**, **Peacock WL**, **Deacon WE**, **Brown L**, **Pirkle CI**. 1963. *Neisseria gonorrhoeae*: Virulence genetically linked to clonal variation. J Bacteriol **85**:1274–1279.
27. **Dillard JP**. 2011. Genetic manipulation of *Neisseria gonorrhoeae*. Curr Protoc Microbiol **4**:Unit4A.2.
28. **Wright CJ**, **Jerse AE**, **Cohen MS**, **Cannon JG**, **Seifert HS**. 1994. Nonrepresentative PCR amplification of variable gene sequences in clinical specimens containing dilute, complex mixture of microorganisms. J Clin Microbiol **32**:464–468.
29. **Goodman SD**, **Scocca JJ**. 1988. Identification and arrangement of the DNA sequence recognized in specific transformation of *Neisseria gonorrhoeae*. Proc Natl Acad Sci U S A **85**:6982–6986.
30. **Hamilton HL**, **Schwartz KJ**, **Dillard JP**. 2001. Insertion-duplication mutagenesis of *Neisseria*: Use in characterization of DNA transfer genes in the gonococcal genetic island. J Bacteriol **183**:4718–4726.
31. **Frye SA**, **Nilsen M**, **Tonjum T**, **Ambur OH**. 2013. Dialects of the DNA Uptake Sequence in *Neisseriaceae*. PLoS Genet **9**:e1003458.
32. **Rosenthal RS**, **Dziarski R**. 1994. Isolation of peptidoglycan and soluble peptidoglycan fragments. Methods Enzymol **235**:253–285.
33. **Cloud KA**, **Dillard JP**. 2002. A lytic transglycosylase of *Neisseria gonorrhoeae* is involved in peptidoglycan-derived cytotoxin production. Infect Immun **70**:2752–2757.
34. **Salgado-Pabon W**, **Du Y**, **Hackett KT**, **Lyons KM**, **Arvidson CG**, **Dillard JP**. 2010. Increased expression of the type IV secretion system in piliated *Neisseria gonorrhoeae* variants. J Bacteriol **192**:1912–1920.
35. **Shaik YB**, **Grogan S**, **Davey M**, **Sebastian S**, **Goswami S**, **Szmigielski B**, **Genco CA**.

2007. Expression of the iron-activated *nspA* and *secY* genes in *Neisseria meningitidis* group B by Fur-dependent and -independent mechanisms. J Bacteriol **189**:663–669.
36. **Agarwal S**, **King CA**, **Klein EK**, **Soper DE**, **Rice PA**, **Wetzler LM**, **Genco CA**. 2005. The gonococcal Fur-regulated *tbpA* and *tbpB* genes are expressed during natural mucosal gonococcal infection. Infect Immun **73**:4281–4287.
37. **Grifantini R**, **Sebastian S**, **Frigimelica E**, **Draghi M**, **Bartolini E**, **Muzzi A**, **Rappuoli R**, **Grandi G**, **Genco CA**. 2003. Identification of iron-activated and -repressed Fur-dependent genes by transcriptome analysis of *Neisseria meningitidis* group B. Proc Natl Acad Sci U S A **100**:9542–9547.
38. **Zhang Y**. 2008. I-TASSER server for protein 3D structure prediction. BMC Bioinformatics **9**:40.
39. **Roy A**, **Kucukural A**, **Zhang Y**. 2010. I-TASSER: a unified platform for automated protein structure and function prediction. Nat Protoc **5**:725–738.
40. **Yang J**, **Zhang Y**. 2015. I-TASSER server: new development for protein structure and function predictions. Nucleic Acids Res **43**:W174-181.
41. **Yang J**, **Yan R**, **Roy A**, **Xu D**, **Poisson J**, **Zhang Y**. 2015. The I-TASSER Suite: Protein structure and function prediction. Nat Methods **12**:7–8.
42. **Kelley LA**, **Mezulis S**, **Yates CM**, **Wass MN**, **Sternberg MJE**. 2015. The Phyre2 web portal for protein modelling, prediction, and analysis. Nat Protoc **10**:845–858.
43. **Benson DA**, **Karsch-Mizrachi I**, **Lipman DJ**, **Ostell J**, **Sayers EW**. 2009. GenBank. Nucleic Acids Res **37**:D26–D31.
44. **Jolley KA**, **Maiden MCJ**. 2010. BIGSdb: Scalable analysis of bacterial genome variation at the population level. BMC Bioinformatics **11**:595.
45. **Sayers EW**, **Barrett T**, **Benson DA**, **Bryant SH**, **Canese K**, **Chetvernin. V**, **Church DM**, **Dicuccio M**, **Edgar R**, **Federhen S**, **Feolo M**, **Geer LY**, **Helmberg W**, **Kapustin Y**, **Landsman D**, **Lipman DJ**, **Madden TL**, **Maglott DR**, **Miller V**, **Mizrachi I**, **Ostell J**, **Pruitt KD**, **Schuler GD**, **Sequeira E**, **Sherry ST**, **Shumway M**, **Sirotkin K**, **Souvorov A**, **Starchenko G**, **Tatusova TA**, **Wagner L**, **Yaschenko E**, **Ye J**. 2009. Database resources of the National Center for Biotechnology Information. Nucleic Acids Res **37**:5–15.
46. **Tonjum T**. 2015. *Neisseria*. Bergey's Man Syst Archaea Bact 1–48.
47. **Cheng Q**, **Park JT**. 2002. Substrate specificity of the AmpG permease required for recycling of cell wall anhydro-muropeptides. J Bacteriol **184**:6434–6436.
48. **Bowler LD**, **Zhang QY**, **Riou JY**, **Spratt BG**. 1994. Interspecies recombination between the *penA* genes of *Neisseria meningitidis* and commensal *Neisseria* species during the emergence of penicillin resistance in *N. meningitidis*: Natural events and laboratory simulation. J Bacteriol **176**:333–337.
49. **Bertsche U**, **Mayer C**, **Götz F**, **Gust AA**. 2015. Peptidoglycan perception — Sensing bacteria by their common envelope structure. Int J Med Microbiol **305**:217–223.
50. **Cloud-Hansen KA**, **Peterson SB**, **Stabb E V**, **Goldman WE**, **McFall-Ngai MJ**, **Handelsman J**. 2006. Breaching the great wall: peptidoglycan and microbial interactions. Nat Rev Microbiol **4**:710–716.
51. **Dworkin J**. 2014. The medium is the message: interspecies and interkingdom signaling by peptidoglycan and related bacterial glycans. Annu Rev Microbiol **68**:137–154.
52. **Koropatnick TA**, **Engle JT**, **Apicella MA**, **Stabb E V**, **Goldman WE**, **McFall-Ngai MJ**. 2004. Microbial factor-mediated development in a host-bacterial mutualism. Science

306:1186–1188.
53. **Troll J V**, **Adin DM**, **Wier AM**, **Paquette N**, **Silverman N**, **Goldman WE**, **Stadermann FJ**, **Stabb EV**, **McFall-Ngai MJ**. 2009. Peptidoglycan induces loss of a nuclear peptidoglycan recognition protein during host tissue development in a beneficial animal-bacterial symbiosis. Cell Microbiol **11**:1114–1127.
54. **Cole PJ**, **Wilson R**. 1994. Effect of tracheal cytotoxin from *Bordetella pertussis* on human neutrophil function *in vitro*. Infect Immun **62**:639–643.
55. **Luker KE**, **Tyler AN**, **Marshall GR**, **Goldman WE**. 1995. Tracheal cytotoxin structural requirements for respiratory epithelial damage in pertussis. Mol Microbiol **16**:733–743.
56. **Lyon RS**. 2001. Tracheal cytotoxin production by the *Bordetellae*. PhD thesis. Washington University in St. Louis.
57. **Schaub RE**, **Chan YA**, **Lee M**, **Hesek D**, **Mobashery S**, **Dillard JP**. 2016. Lytic transglycosylases LtgA and LtgD perform distinct roles in remodeling, recycling, and releasing peptidoglycan in *Neisseria gonorrhoeae*. Mol Microbiol **102**:865–881.
58. **Reddy VS**, **Shlykov MA**, **Castillo R**, **Sun EI**, **Saier MH**. 2012. The major facilitator superfamily (MFS) revisited. FEBS J **279**:2022–2035.
59. **Yan N**. 2015. Structural biology of the major facilitator superfamily transporters. Annu Rev Biophys **44**:257–283.
60. **Abramson J**, **Smirnova I**, **Kasho V**, **Verner G**, **Kaback HR**, **Iwata S**. 2003. Structure and mechanism of the lactose permease of *Escherichia coli*. Science **301**:610–615.
61. **Guan L**, **Mirza O**, **Verner G**, **Iwata S**, **Kaback HR**. 2007. Structural determination of wild-type lactose permease. Proc Natl Acad Sci United States **104**:15294–15298.
62. **Smirnova I**, **Kasho V**, **Choe J-Y**, **Altenbach C**, **Hubbell WL**, **Kaback HR**. 2007. Sugar binding induces an outward facing conformation of LacY. Proc Natl Acad Sci U S A **104**:16504–16509.
63. **Kumar H**, **Kasho V**, **Smirnova I**, **Finer-Moore JS**, **Kaback HR**, **Stroud RM**. 2014. Structure of sugar-bound LacY. Proc Natl Acad Sci United States **111**:1784–1788.
64. **Kumar H**, **Finer-Moore JS**, **Kaback HR**, **Stroud RM**. 2015. Structure of LacY with an α-substituted galactoside: Connecting the binding site to the protonation site. Proc Natl Acad Sci U S A **112**:9004–9009.
65. **Swanson J**. 1972. Studies on gonococcus infection. II. Freeze-fracture, freeze-etch studies on gonococci. J Exp Med **136**:1258–1271.
66. **Woodhams KL**, **Benet ZL**, **Blonsky SE**, **Hackett KT**, **Dillard JP**. 2012. Prevalence and detailed mapping of the gonococcal genetic island in *Neisseria meningitidis*. J Bacteriol **194**:2275–2285.
67. **Mehr IJ**, **Long CD**, **Serkin CD**, **Seifert HS**. 2000. A homologue of the recombination-dependent growth gene, *rdgC*, is involved in gonococcal pilin antigenic variation. Genetics **154**:523–532.

Supplementary Figure 1, Page 1

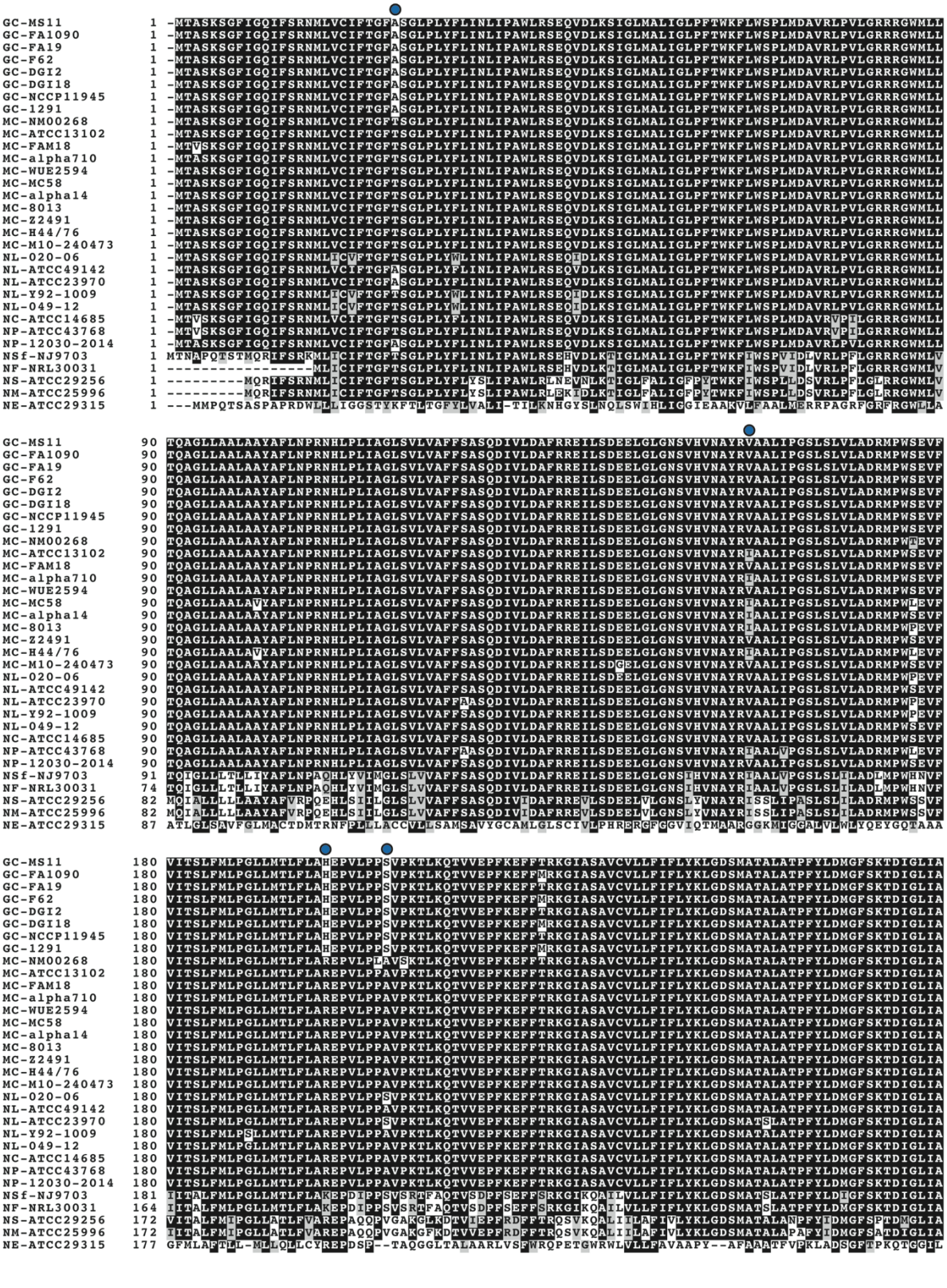

Supplementary Figure 1, Page 2

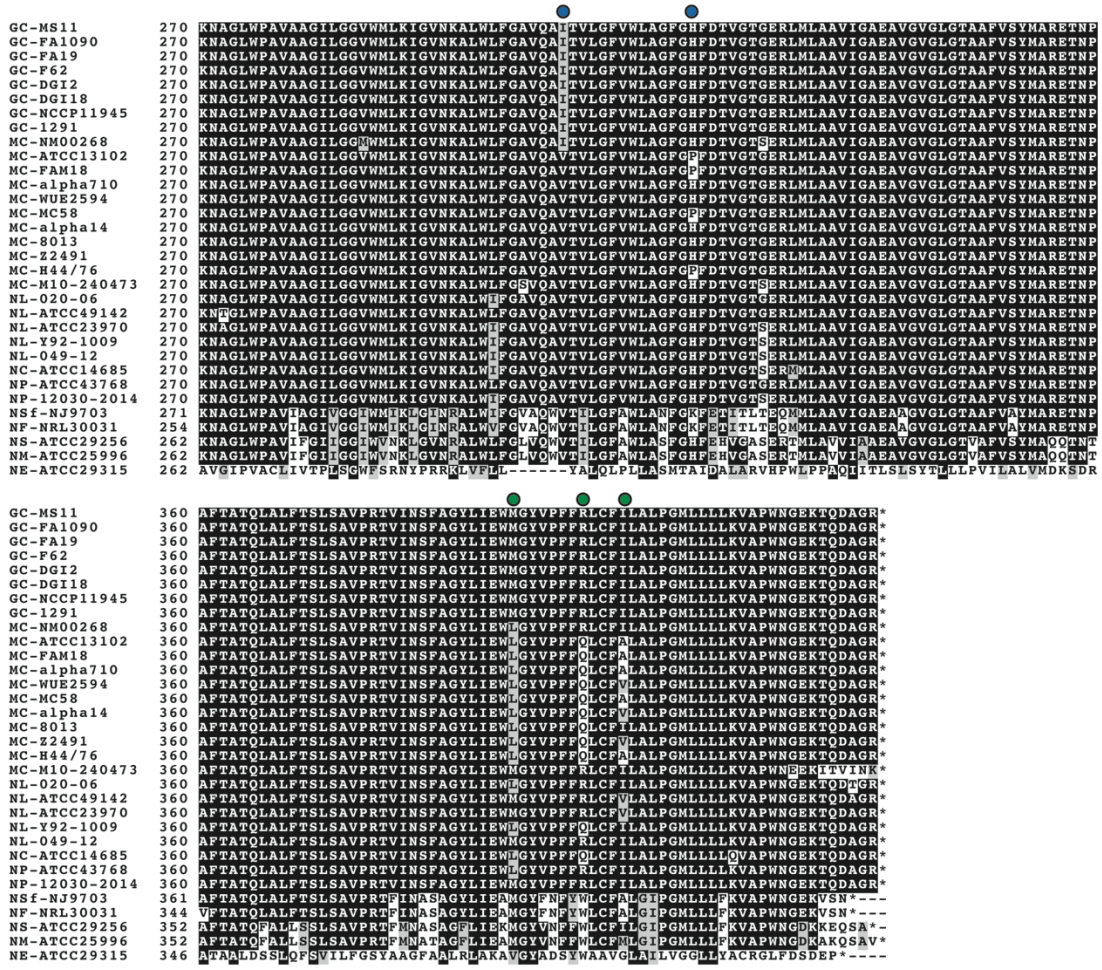

Supplementary Figure 1. Alignment of AmpG protein sequences. The coding sequences of *ampG* from different species of human associated Neisseria were translated using MEGA7, aligned using ClustalW, and shaded using BoxShade. Blue circles were used to mark residues that differ between *N. gonorrhoeae* strain MS11 (WT GC) and *N. meningitidis* ATCC 13102 (WT MC) but did not appear to modulate AmpG function, while green circles were used to mark residues that do affect AmpG function (AmpG residues 391, 398, 402). The *ampG* sequence from the following species were used in this alignment: *N. gonorrhoeae* (abbreviated GC, strains MS11, FA1090, FA19, F62, DGI2, DGI18, NCCP11945 and 1291), *N. meningitidis* (abbreviated MC, strains ATCC 13102, FAM18, WUE 2594, MC58, alpha 710, alpha 14, 8013, Z2491, H44/76, M10-240473 and NM00268), *N. lactamica* (abbreviated NL, strains 020-06, ATCC 49142, ATCC 23970, Y92-1009 and 049-12), *N. cinerea* (abbreviated NC, strain ATCC 14685), *N. polysaccharea* (abbreviated NP, strains ATCC 43768 and 12030-2014), *N. subflava* (abbreviated NSf, strain NJ9703), *N. flavescens* (abbreviated NF, strain NRL30031), *N. sicca* (abbreviated NS, strain ATCC 29256), *N. mucosa* (abbreviated NM, strain ATCC 25996) and *N. elongata* (abbreviated NE, strain ATCC 29315).

Supplementary Figure 2

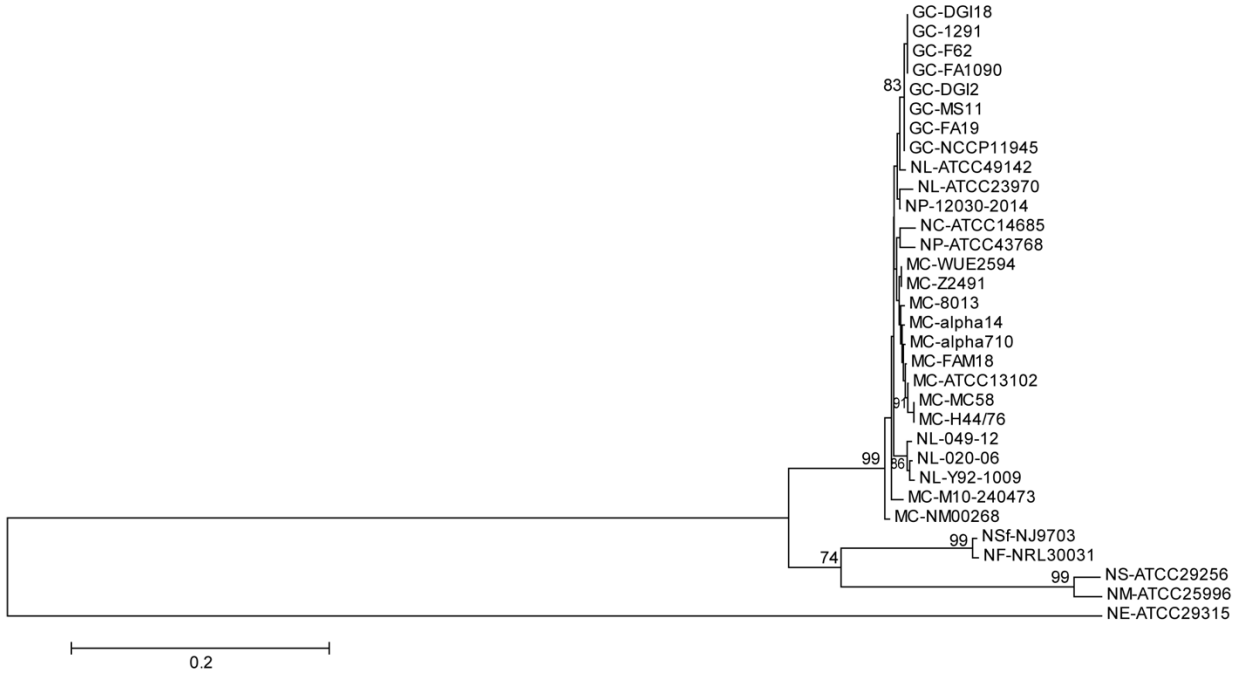

Supplementary Figure 2. Neighbor-joining tree based on AmpG sequences. The coding sequences of *ampG* from different species of human associated *Neisseria* were translated using MEGA7, aligned using ClustalW and used to construct a neighbor-joining tree using MEGA7. Bootstrap values from 1000 replications that were above 70% were indicated on the tree. Scale bar indicates branch length. The *ampG* sequence from the following species were used in generating this tree: *N. gonorrhoeae* (abbreviated GC, strains MS11, FA1090, FA19, F62, DGI2, DGI18, NCCP11945 and 1291), *N. meningitidis* (abbreviated MC, strains ATCC 13102, FAM18, WUE 2594, MC58, alpha 710, alpha 14, 8013, Z2491, H44/76, M10-240473 and NM00268), *N. lactamica* (abbreviated NL, strains 020-06, ATCC 49142, ATCC 23970, Y92-1009 and 049-12), *N. cinerea* (abbreviated NC, strain ATCC 14685), *N. polysaccharea* (abbreviated NP, strains ATCC 43768 and 12030-2014), *N. subflava* (abbreviated NSf, strain NJ9703), *N. flavescens* (abbreviated NF, strain NRL30031), *N. sicca* (abbreviated NS, strain ATCC 29256), *N. mucosa* (abbreviated NM, strain ATCC 25996) and *N. elongata* (abbreviated NE, strain ATCC 29315).

Supplementary Figure 3

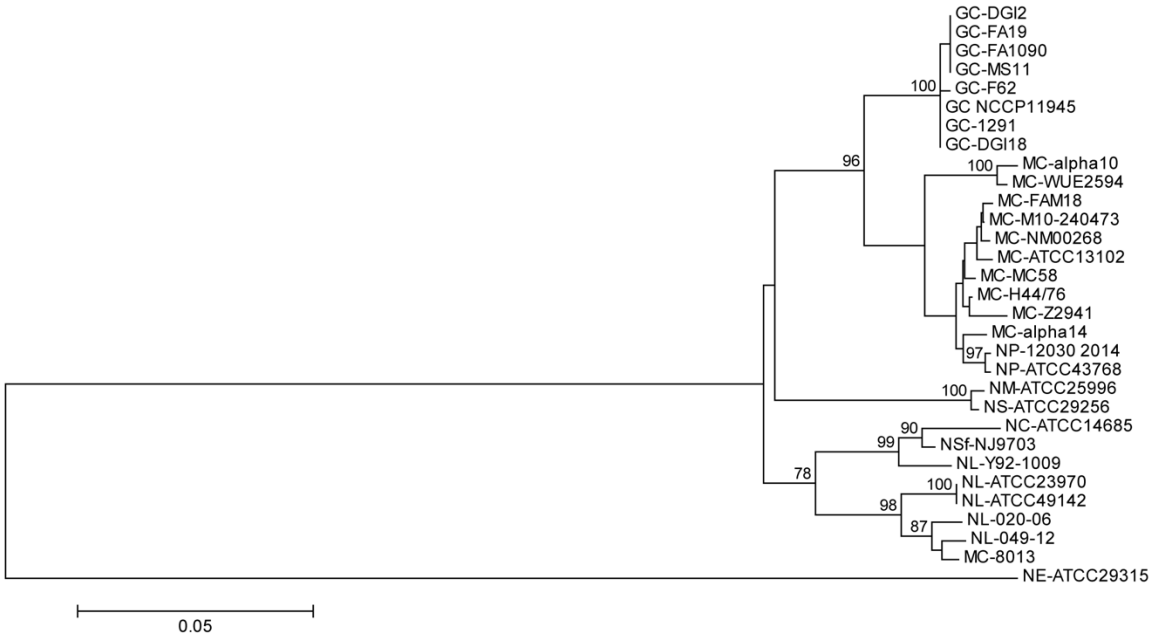

Supplementary Figure 3. Neighbor-joining tree based on Gdh (glucose-6-phosphate dehydrogenase) sequences. The coding sequences of the housekeeping gene, *gdh* from different species of human associated *Neisseria* were translated using MEGA7, aligned using ClustalW and used to construct a neighbor-joining tree using MEGA7. Bootstrap values from 1000 replications that were above 70% were indicated on the tree. The gdh sequence from the following species were used in constructing this tree: *N. gonorrhoeae* (abbreviated GC, strains MS11, FA1090, FA19, F62, DGI2, DGI18, NCCP11945 and 1291), *N. meningitidis* (abbreviated MC, strains ATCC 13102, FAM18, WUE 2594, MC58, alpha 710, alpha 14, 8013, Z2491, H44/76, M10-240473, NM00268 and NM00329), *N. lactamica* (abbreviated NL, strains 020-06, ATCC 49142, ATCC 23970, Y92-1009 and 049-12), *N. cinerea* (abbreviated NC, strain ATCC 14685), *N. polysaccharea* (abbreviated NP, strains ATCC 43768 and 12030-2014), *N. subflava* (abbreviated NSf, strain NJ9703), *N. flavescens* (abbreviated NF, strain NRL30031), *N. sicca* (abbreviated NS, strain ATCC 29256), *N. mucosa* (abbreviated NM, strain ATCC 25996) and *N. elongata* (abbreviated NE, strain ATCC 29315).

CHAPTER 3

Neisseria meningitidis uses AmiC and NlpD to liberate hNOD1 agonists in the form of peptidoglycan-derived peptides

Jia Mun Chan, Katelynn L. Woodhams, Kathleen T. Hackett and Joseph P. Dillard

JM Chan, KL Woodhams and JP Dillard designed the experiments.

KL Woodhams constructed *amiC* and *nlpD* inactivation mutants and performed preliminary peptidoglycan fragment release and TEM experiments. KT Hackett assisted in the preparation of samples for TEM. JM Chan constructed complementation and FLAG3 tagged mutants, and performed all other experiments.

JM Chan and KL Woodhams analyzed the data.

JM Chan and JP Dillard wrote the manuscript with input from KL Woodhams.

ABSTRACT

The human-restricted pathogen *Neisseria meningitidis*, which is best known for causing invasive meningococcal disease, has a nonpathogenic lifestyle as an asymptomatic colonizer of the human naso- and oropharyngeal space. *N. meningitidis* releases small peptidoglycan (PG) fragments during normal growth in laboratory conditions. It was demonstrated previously that *N. meningitidis* releases low levels of tripeptide PG monomer, which is an inflammatory molecule recognized by the human intracellular innate immune receptor NOD1 (hNOD1). In this present study, we demonstrated that *N. meningitidis* released more PG-derived peptides compared to PG monomers. Using a HEK293 reporter cell line overexpressing hNOD1, we showed that PG-derived peptides released by *N. meningitidis* are capable of activating hNOD1. Generation of such peptides required the presence of the periplasmic *N*-acetylmuramyl-L-alanine amidase AmiC, and the outer membrane lipoprotein, NlpD. AmiC and NlpD function in cell separation, and mutation of either *amiC* or *nlpD* resulted in large clumps of cells instead of the characteristic diplococci presentation of *N. meningitidis.* Using stochastic optical reconstruction microscopy (STORM), we demonstrated that AmiC:FLAG3$^+$ and NlpD:FLAG3$^+$ localized to the septum in a subset of cells, and were found distributed around the cell in a subset of cells. Thus, *N. meningitidis* generates and releases hNOD1 agonists using the cell separation proteins AmiC and NlpD.

INTRODUCTION

Neisseria meningitidis, also known as meningococcus, is an obligate colonizer of the human nasopharyngeal space. Meningococcus occasionally disseminates to cause invasive disease such as meningitis and septicemia. Invasive disease has a fatality rate of 10-15% even with early treatment, and 11-19% of survivors develop lifelong sequelae (1, 2). *N. meningitidis* colonizes up to 25% of the population at any one time (3). The carriage rate of *N. meningitidis* can be as high as 70% in areas of high density such as military barracks, college dormitories and during the Hajj pilgrimage (3, 4); prolonged exposure to carriers increases the risk of invasive meningococcal disease for non-carriers (4). During major epidemics, as many as 1,000 infection cases in a population of 100,000 people have been reported (5, 6). *N. meningitidis* encodes multiple virulence factors that allow it to invade the bloodstream and cross the blood-brain barrier, cause a large inflammatory response, and evade clearance by the immune system (Reviewed in (7–11)). Much of the tissue damage sustained during meningococcal disease is a result of a strong inflammatory immune response (3, 10, 11). One class of immunostimulatory molecules made and released by *N. meningitidis* is diaminopimelic acid (DAP)-type peptidoglycan fragments (12).

Peptidoglycan (PG) is a structural macromolecule that confers cell shape and protects the cell against turgor pressure. It is made of repeating subunits of *N*-acetylglucosamine (GlcNAc) and *N*-acetylmuramic acid (MurNAc), with peptide chains attached to the *N*-acetylmuramic acid moiety (13). The third amino acid on this peptide chain is DAP in Gram-negative bacteria (DAP-type PG), and lysine in many Gram-positive bacteria (Lys-type PG). Breakdown of existing PG strands and incorporation of newly synthesized PG strands allow for cell enlargement and cell separation. Digestion of the sacculi by peptidoglycanases generate small PG fragments (14, 15).

Owing to the presence of an outer membrane, most Gram-negative bacteria release very little PG fragments; instead, PG fragments are typically contained in the periplasmic space and efficiently taken back into the cytoplasm by a PG fragment permease to be reused in cellular processes (15, 16). A limited group of Gram-negative bacteria, including but not limited to *N. meningitidis,* the closely related pathogen *N. gonorrhoeae*, the etiological agent of whooping cough *Bordetella pertussis*, and the squid symbiont *Vibrio fischeri* release cytotoxic PG monomers (GlcNAc-anhydroMurNAc-peptide) with no overt effects on bacterial growth in the laboratory (12, 14, 17, 18). *N. meningitidis* also releases inflammatory PG dimers (two glycosidically- or peptide-linked monomers), and PG-derived sugars such as GlcNAc-anhydroMurNAc disaccharide and anhydroMurNAc (12). The release of PG-derived peptides by *N. meningitidis* has not been characterized.

Host organisms such as humans have evolved strategies to detect and respond to microbe associated molecular patterns (MAMPs) to either prevent or resolve an infection. One such intracellular innate immune receptor is human NOD1 (hNOD1). hNOD1 induces a proinflammatory response upon recognition of PG fragments with a terminal DAP, which includes tripeptide PG monomers (GlcNAc-anhydroMurNAc-L-ala-D-glu-*meso*DAP) and PG derived tripeptide (L-ala-D-glu-*meso*DAP) (19–22). hNOD1 does not respond well to amidated PG fragments; some species of Gram-positive bacteria that have DAP-type PG, such as *Bacillus subtilis*, amidate the DAP moiety of their PG stems (19, 21, 23). Thus, hNOD1 predominantly detects the presence of Gram-negative bacteria, which includes *N. meningitidis*. In this study, we characterized PG-derived peptides released by *N. meningitidis* and found that meningococcus releases immunologically relevant amounts of hNOD1 activating PG-derived peptides.

MATERIALS AND METHODS

Bacterial strains and growth conditions. All strains used in this study are listed in Table 1. All meningococcal strains used in the experiments are unencapsulated strains of *N. meningitidis* (ATCC 13102 *cap*-), in which the capsule biosynthesis gene *siaD* has been interrupted with a chloramphenicol marker (12). All meningococcal strains also have a point mutation in *rpsL* conferring streptomycin resistance (12). *Neisseria meningitidis* strains were grown on gonococcal base medium (GCB) agar (Difco) plates at 37°C with 5% CO_2 or in gonococcal base liquid medium (Difco) with 0.042% bicarbonate (24) and Kellogg's supplement (25) (cGCBL) at 37°C with aeration. *Escherichia coli* strains were grown on LB agar (Difco) plates at 37°C or in LB liquid medium at 37°C. When needed, 10 μg/ml chloramphenicol, 10 μg/ml erythromycin or 80 μg/ml kanamycin was added to *N. meningitidis* cultures. For *E. coli*, 100 μg/ml ampicillin, 25 μg/ml chloramphenicol, 500 μg/ml erythromycin or 40 μg/ml kanamycin was added to the media when appropriate. When necessary, 0.1 mM or 1 mM IPTG, or 2 ng/ml anhydrotetracycline was added to the media to induce expression of a target gene.

Strain construction. *Neisseria meningitidis* mutants were generated by spot transformation (26). Briefly, 20 μg linearized plasmid DNA or PCR product was spotted onto a GCB agar plate and allowed to dry. Subsequently, 5-10 piliated colonies were streaked over the DNA spots, and the plate was incubated overnight at 37°C with 5% CO_2. Successful transformants were either selected using antibiotics, or identified by PCR screening. All transformants were confirmed by PCR and DNA sequencing. Due to difficulty of transforming *amiC* and *nlpD* mutants, complementation strains were constructed by first transforming WT with the complementation construct, followed by transformation of the resulting strains with the deletion construct. EC1026

is the only strain generated by transformation with a PCR product. This PCR product was generated by PCR amplification of *nlpD* from WT *N. meningitidis* chromosomal DNA using primer NlpD DUS F and NlpD DUS R (Table 2), which resulted in a DNA fragment containing the *nlpD* coding sequence flanked by DNA uptake sequences (DUS) to facilitate uptake and recombination (27).

Plasmid construction. All plasmids used in this study are listed in Table 1 and were verified by PCR and sequencing as necessary. All primers are listed in Table 2. Plasmids were generated by ligation of a vector backbone and an insert, and transformed into Rapid Trans™ chemically competent TAM1 cells (Active Motif).

Two plasmids, pKL24 and pKL25, were generated to create an in-frame deletion of *amiC*. To make pKL24 (*amiC* deletion in pKH6), pDG005 and pKH6 were digested with XmaI and SacI. The *amiC* deletion insert from pDG005 was ligated into pKH6 generating pKL24. To generate pKL25 (*ermC rpsL* in pKL24; final construct Δ*amiC::ermCrpsL*), the *ermC rpsL* positive/negative selection cassette was first excised from pKC1 by digestion with NheI and EcoRV. The insert from pKC1 was blunted with T4 polymerase and ligated into the blunted BspHI site from pKL24 to create pKL25.

Three plasmids were generated to create a *nlpD* insertional inactivation mutant. To create pKL28 (*nlpD* and flanking DNA in pKH6), PCR was used to amplify *nlpD* and flanking DNA with primers SacII nlpD F and SacI nlpD R. The PCR product and pKH6 were digested with SacI and SacII, then ligated. To generate pKL29 (*nlpD* deletion in pKH6), primers BglII nlpD del F and BglII nlpD del R were used in a PCR with pKL28 as a template. The product was digested with BglII and self-ligated to make pKL29, which contains a markerless *nlpD* deletion

with flanking DNA. To build pKL38 (Δ*nlpD::kan* allelic replacement in pKH6), the kanamycin resistance marker from pKH99 was excised by digestion with EcoRV and Ecl136II and inserted into the blunted BglII site of pKL29.

Two plasmids, pKL45 and pKL49, were constructed to complement an *nlpD* mutation at an ectopic site. Plasmid pKL45 (*nlpD** in pMR68; K3*) was made by first amplifying *nlpD* from WT *N. meningitidis* chromosomal DNA with primers SacI nlpD F2 and SpeI nlpD R. The PCR product and pMR68 were subsequently digested with SacI and SpeI and ligated to each other. Despite repeated attempts, the resulting plasmid contained one or more mutations in the *nlpD* coding sequence. We deduce that the presence of a second copy of *nlpD* in *E. coli* is toxic to the bacterium, and saved one of the plasmids as pKL45. pKL45 has a nonsense mutation leading to a premature stop codon at the third codon. Plasmid pKL49 (*nlpD*-rpsL* in pMR68) was generated by insertion of *rpsL* into pKL48. *rpsL* was amplified from pKC1 using primers MluI rspL F and MluI rpsL R; the PCR product and pKL45 were digested with MluI and subsequently ligated to each other to generate pKL49.

Plasmid pKL50 was generated to complement an *amiC* mutation at an ectopic site. To make pKL50 (*amiC* in pMR33), *amiC* was amplified from WT *N. meningitidis* chromosomal DNA with primers SacI MC amiC F and SpeI MC amiC R and digested with SacI and SpeI. pMR33 was digested similarly, and ligated with the digested *amiC* PCR product.

Plasmid pEC140 was built to create an *amiC* insertional inactivation mutant. To generate pEC140 (*amiC::kan* in pIDN3), pDG005 was first digested with BspHI and subsequently blunted with T4 DNA polymerase. The *aph3* gene conferring resistance against kanamycin (referred to as kan^R) was amplified from pHSS6 using primers kan F BamHI and kan R BamHI and blunt-ligated with the blunted, BspHI digested pDG005 to form pEC140.

Plasmid pEC169 (*amiC':FLAG3*$^{+}$ -3' flank in pIDN3) was constructed in multiple steps. First, *amiC* 3' flank region was amplified using primers HindIII MC amiC down F and XhoI MC amiC down R and WT *N. meningitidis* chromosomal DNA as a template. pMR100 and the PCR product were digested with HindIII and XhoI, and ligated to make pEC167 (*amiC* 3' flank in pMR100). The partial coding sequence of *amiC* lacking the start codon, signal sequence and stop codon (*amiC'*) was amplified from WT *N. meningitidis* chromosomal DNA using primers SacI MC amiC –sigseq F and EcoRI MC amiC –stop codon R, digested with SacI and EcoRI and ligated into similarly digested pEC167 to form pEC169.

Plasmid pEC173 (*nlpD':FLAG3*$^{+}$*-kan*^{R}-3' flank in pIDN3) was generated with a similar strategy as pEC169, with several modifications. *nlpD* 3' flank region was amplified using primers HindIII MC nlpD down F and XhoI MC nlpD down R instead, digested with HindIII and XhoI and ligated with similarly digested pMR100 to form pEC168 (*nlpD* 3' flank in pMR100). The partial coding sequence of *nlpD* lacking the start codon, signal sequence and stop codon (*nlpD'*) was amplified with primers SacI MC nlpD –sigseq F and EcoRI MC nlpD –stop codon R, digested with SacI and EcoRI and ligated into similarly digested pEC168 to form pEC170. pEC170 was digested with HindIII, blunted with T4 polymerase and ligated with *kan*^{R} to form pEC173.

Metabolic labeling of peptidoglycan and quantitative fragment release. Metabolic labeling of PG and quantitative fragment release was performed as described previously (28–31). Strains were pulse-chased labeled with 25 μg/ml [2,6-^{3}H] DAP in DMEM lacking cysteine supplemented with 100 μg/ml methionine and 100 μg/ml threonine for 45 minutes. A sample of the culture was removed to determine the number of radioactive counts per minute (CPM) by

liquid scintillation counting, and the number of CPM is normalized to obtain equal CPM in each culture. After a 2 hour chase period, supernatant was harvested by centrifugation at 3,000 x *g* for 10 mins, and filter-sterilized with a 0.22 μm filter. [2,6-^{3}H] DAP labeled molecules in the filtered supernatant were then separated using tandem size-exclusion chromatography with 0.1 M LiCl as the mobile phase, and detected by liquid scintillation counting. The growth medium for the *amiC* and *nlpD* complementation strains was supplemented with 0.1 mM IPTG and 2 ng/ml anhydrotetracyline, respectively.

Thin section electron microscopy. *N. meningitidis* strains were grown in cGCBL until mid-log phase, when cells were harvested by centrifugation at 17, 000 x *g* for 1 minute. Growth medium for the *amiC* and *nlpD* complementation strains contained 0.1 mM IPTG and 2 ng/ml anhydrotetracyline, respectively, for gene induction. Cells were washed once with PBS and resuspended in fixative solution (2% paraformaldehye, 2.5% glutaraldehye in 0.1M phosphate buffer). Thin section electron microscopy of fixed samples was done at the University of Wisconsin-Madison Medical School Electron Microscope Facility. Enumeration of meningococci in cell clusters were done by counting the number of complete, in plane cells presenting as monococci, diplococci, tetrads or clusters of five or more cells in 16-24 fields/strain containing an average of 30 cells/field.

Treatment of HEK293 reporter cell line with filtered supernatant from meningococcal cultures. HEK293-Blue cells that encode secreted alkaline phosphatase (SEAP) under the control of an NF-κB promoter (parental cell lines NULL1 and NULL2) and hNOD1 or hNOD2 receptors (NOD and NOD2 cell lines) were grown, maintained and treated according to the

manufacturer's instructions (InvivoGen). Supernatant samples were harvested from meningococcal cultures started at OD_{540} of 0.2 and grown for 2 hours by centrifugation at 17,000 x *g* for a minute and filter sterilized using a 0.22 μm pore filter. Cultures were supplemented with 1 mM IPTG or 2 ng/ml anhydrotetracycline as needed. Supernatant samples were normalized to total cellular protein. HEK293 cells that were seeded at a density of 2.8 x 10^5 cells/ml (NOD1/NULL1) or 1.4 x 10^5 cells/ml (NOD2/NULL2) in 180 μl DMEM with 4.5g/L glucose, 2 mM L-glutamine and 10% heat inactivated fetal bovine serum (FBS) were treated with 20 μl supernatant for 18 hours at 37°C with 5% CO_2. A total volume of 20 μl each of cGCBL (media only control), 10 μg/ml TriDAP (positive control for NOD1/NULL1) (InvivoGen) or 10 μg/ml muramyl dipeptide (MDP; positive control for NOD2/NULL2) (InvivoGen), 10 μg/ml Tri-Lys (negative control for NOD1/NULL1) or 10 μg/ml MDP-control (MDP-c; negative control for NOD2/NULL2) (InvivoGen) were used as treatment controls. After 18 hours of treatment, 20 μl HEK293 culture supernatant was added to 180 μl QUANTI-Blue reagent (InvivoGen) and incubated at 37°C for 4 hours. Secreted alkaline phosphatase activity was determined by measuring absorbance at 650 nm. To calculate NF-κB dependent hNOD activation (graphed SEAP levels (A_{650})), A_{650} values from NULL1 or NULL2 controls were subtracted from the corresponding A_{650} values from NOD1 or NOD2 treatments. Summarized results are from four independent experiments, and statistical tests were performed using Student's *t*-test.

Stochastic optical reconstruction microscopy (STORM). Sample preparation and imaging was done as described previously (32). Meningococcal cultures were grown to mid-log phase and harvested by centrifugation at 17,000 x *g* for 2 minutes. Cells were washed once with PBS, and suspended in 400 μl fixative solution (4% methanol-free formaldehyde in PBS). The cell

suspensions were first incubated at RT for 15 minutes, and then on ice for 15 minutes. The cell suspensions were then centrifuged at 6,000 x *g* and the fixative solution discarded. Cells were quickly washed thrice with cold PBS to ensure thorough removal of fixative solution, and resuspended in cold GTE buffer (50 mM glucose, 1mM EDTA, 20 mM Tris-HCl pH 7.5) and incubated on ice for 10 minutes. Cells were quickly washed with PBS-T (0.3% Triton-X100 in PBS), suspended in cold methanol and incubated at -20°C for a minimum of 10 minutes. Methanol was removed, after which cells were washed with PBS-T for 5 minutes, blocked with 400 µl 5% goat serum in PBS-T for 15 minutes, and incubated with 1:150 diluted M2 primary antibody (Sigma) in PBS for 1 hour. Cells were subsequently washed with PBS thrice, and incubated with 200 µl 1:100 diluted AlexaFluor-647 (Thermo Fisher) secondary antibody, 100 ng/ml DAPI and 5% goat serum in PBS for 1 hour at RT or O/N at 4°C. Cells were washed with PBS five times and suspended in 200 µl PBS to remove unbound antibody and dye. Around 2 µl volumes of the samples were spotted onto poly-L-lysine coated coverslips, mounted with VECTASHIELD^{TM} H-1000 mounting media (Vector laboratories) and visualized using a Nikon N-STORM microscope. Images were analyzed using the software NIS-Elements AR with N-STORM analysis. Linear brightness/contrast adjustments and false-coloring was performed using FIJI.

RESULTS

***Neisseria meningitidis* releases higher levels of PG-derived peptides compared to PG monomers.** The peptide stems of meningococcal sacculi are comprised of three to five amino acids in the following order: L-alanine, D-glutamate, *meso*DAP, D-alanine, D-alanine (33). Metabolic labeling of PG using [2,6-^{3}H] DAP and subsequent fragment release analysis revealed that *N. meningitidis* released at least five types of DAP-containing PG fragments that elute as five distinct peaks when subjected to size-exclusion chromatography (Figure 1A). Peak I is of PG dimers, while peak II is of tetrasaccharide peptide (glycosidically-linked PG dimers with only one peptide stem). Peak III, which is the major PG fragment released by *N. gonorrhoeae*, consists of tripeptide and tetrapeptide PG monomers. *N. meningitidis* releases about twice as much tripeptide monomers (anhydro-disaccharide-L-Ala-D-Glu-*meso*DAP; hNOD1 agonist) compared to tetrapeptide monomers (anhydro-disaccharide-L-Ala-D-Glu-*meso*DAP-D-Ala) (12). By comparison to the PG fragment release characteristics of *N. gonorrhoeae* (34), the last two peaks (peaks **a** and **b**) are most likely free PG-derived peptides. Supporting this conclusion is the observation that these molecules contain *meso*DAP but not GlcNAc (14). The penultimate peak (peak **a**) is the major species of PG fragment released by *N. meningitidis*.

"PG-derived peptides" (also referred to as simply "peptides" hereafter) is a catch-all term for any configuration of PG peptide stems that can be liberated during PG remodeling. *N. meningitidis* encodes putative amidases that cleave the peptide backbone, putative endopeptidases that sever cross-links and carboxypeptidases that digest pentapeptide stems to tetrapeptides and tetrapeptide stems to tripeptides respectively. As such, these peptides may include but are not limited to dipeptides (D-Glu-DAP, DAP-D-Ala), tripeptide (L-Ala-D-Glu-DAP), tetrapeptide (L-Ala-D-Glu-DAP-D-Ala), and pentapeptide (L-Ala-D-Glu-DAP-D-Ala-D-

Ala (Figure 1B). The corresponding peak **a** released by *N. gonorrhoeae* does not contain crosslinked peptides (34). Gonococcus and meningococcus both release PG dimers, tetrasaccharide peptide, tripeptide and tetrapeptide monomers, albeit at different amounts (12). Given the similarity in the types of PG fragments released by *N. gonorrhoeae* and *N. meningitidis* characterized thus far (12), we infer that peaks **a** and **b** also contain free peptides and not crosslinked peptides.

Mutation of *amiC* or *nlpD* abolishes peptide release. *N. meningitidis* encodes one periplasmic *N*-acetylmuramyl-L-alanine amidase, AmiC (36, 37). Meningococcal AmiC is predicted to be a 417-amino acid zinc-dependent metalloprotease with a Tat signal sequence, an N-terminal AMIN domain that binds PG, and a C-terminal catalytic domain that cleaves peptide stems. AmiC homologues in *E. coli* and *N. gonorrhoeae* function as cell separation amidases (37, 38). To examine the role of meningococcal AmiC in PG fragment production and release, we generated an in-frame markerless deletion of *amiC*. Mutation of *amiC* abolished PG peptide release with an increase in PG multimer release (Figure 2A). If AmiC is able to cleave PG monomers, we expect to see a proportional increase in PG monomer release (peak III) with the decrease in peptide release (peaks **a** and **b**) by the *amiC* mutant. However, there is no significant difference in PG monomer release by WT and the *amiC* mutant. Complementation of *amiC* from an ectopic locus restored almost WT-like distributions of fragment release. Our results suggest that meningococcal AmiC liberates peptide stems from the sacculi, but does not act on PG monomers. This is consistent with the known substrate specificity of other AmiC homologues (31, 39, 40).

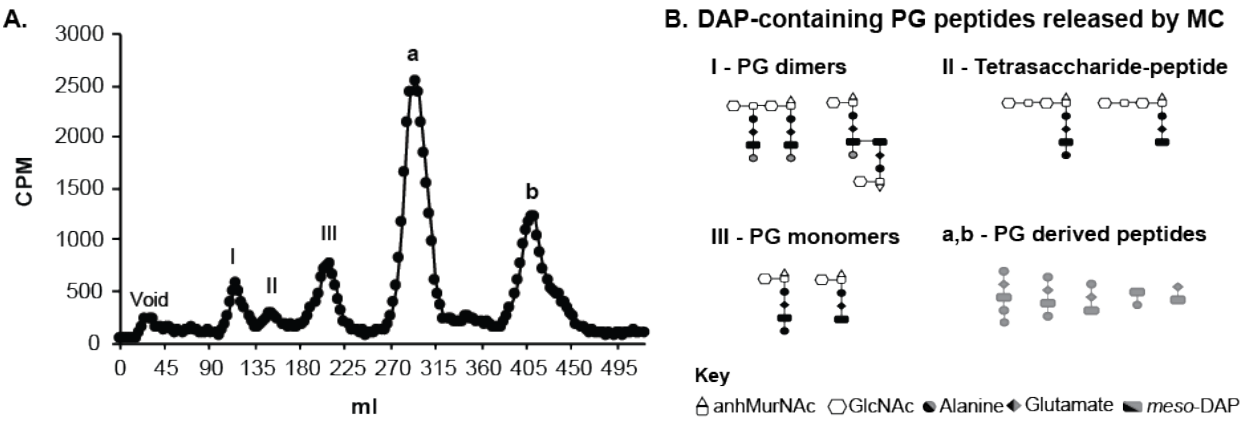

Figure 1. *N. meningitidis* releases more PG-derived peptides compared to PG monomers. A) [2,6-^{3}H] DAP-labeled PG fragments released by WT *N. meningitidis* (ATCC 13102 *cap*-) were separated by size-exclusion chromatography, resolving into five distinct peaks. B) Cartoon depictions of PG fragments found in peaks I, II, III, **a** and **b**. Peaks I, II and III have been determined previously by HPLC and mass spectrometry analyses to be PG dimers, tetrasaccharide peptide and PG monomer, respectively. Peaks **a** and **b** are of PG-derived peptides, and the structures shown represent possible peptide configurations. Empty symbols represent sugar moieties, while filled symbols represent amino acids. Structures drawn in black have been determined by mass spectrometry while structures in grey are predicted based on size and known peptidoglycanase activities. Symbols used are based on Jacobs *et al.* (35)

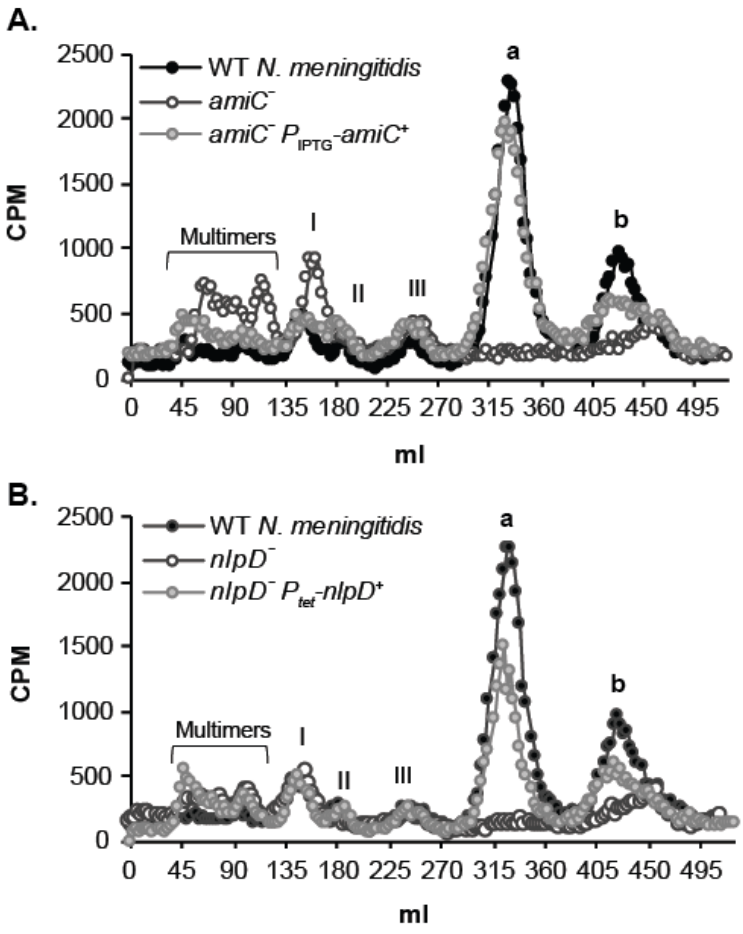

Figure 2. Mutation of *amiC* or *nlpD* abolishes peptide release. Supernatant from [2,6-^{3}H] DAP-labeled WT *N. meningitidis* (A,B), *amiC* mutant (KL1065) and *amiC* complementation (EC1020) (A), and *nlpD* mutant (KL1072) and *nlpD* complementation (EC1026) (B) strains were subjected to size-exclusion chromatography. Mutation of *amiC* (A) or *nlpD* (B) abolished the release of PG-derived peptides, as seen by the absence of peaks **a** and **b**. Genetic complementation of the *amiC* (A) and *nlpD* (B) mutations partially restored release of PG-derived peptides. Results depicted are representative of three experiments.

NlpD is a putative AmiC activator protein, and functions to potentiate the amidase activity of AmiC in *N. gonorrhoeae* and *E. coli* (31, 41–44). Meningococcal NlpD is predicted to be a 415-amino acid outer membrane lipoprotein with two LysM PG binding domains and a degenerate LytM/M23 peptidase domain. Like NlpD homologues from *N. gonorrhoeae* and *E. coli*, only 2/4 of the active site residues in the M23 peptidase domain of meningococcal NlpD are conserved (42, 44). Analyses in *N. gonorrhoeae* and *E. coli* indicate that their NlpD homologues do not have enzymatic function, but instead act as activator proteins for the amidases (31, 41, 42, 44). Mutation of *nlpD* in *N. meningitidis* abolished peak **a** and peak **b**, without affecting release of PG monomer (peak III) and dimers (peak I) (Figure 2B). Complementation of *nlpD* at an ectopic site partially rescued peptide release. We conclude that AmiC and NlpD are indispensable for PG-derived peptide release in *N. meningitidis*. Based on known AmiC and NlpD functions in gonococcus and *E. coli*, we deduce that AmiC activity is dependent on the presence of NlpD in *N. meningitidis*.

PG-derived peptides released by *N. meningitidis* stimulate hNOD1 activation. HEK293 reporter cell lines overexpressing hNOD receptors were used to determine if peptide release by meningococcus is necessary for induction of a hNOD-dependent response. In this assay, hNOD activation is measured by determining the amount of NF-κB controlled secreted alkaline phosphatase (SEAP) detected in the medium via a colorimetric assay. HEK293 cells overexpressing hNOD1 were treated with cell-free supernatant from WT, *amiC* mutant, *nlpD* mutant, induced or uninduced cultures of the respective *amiC* and *nlpD* complementation strains (Figure 3A). As described previously and demonstrated here, supernatant from *N. meningitidis* engenders a hNOD1-dependent response (Figure 3, (12)). We found that supernatant from WT

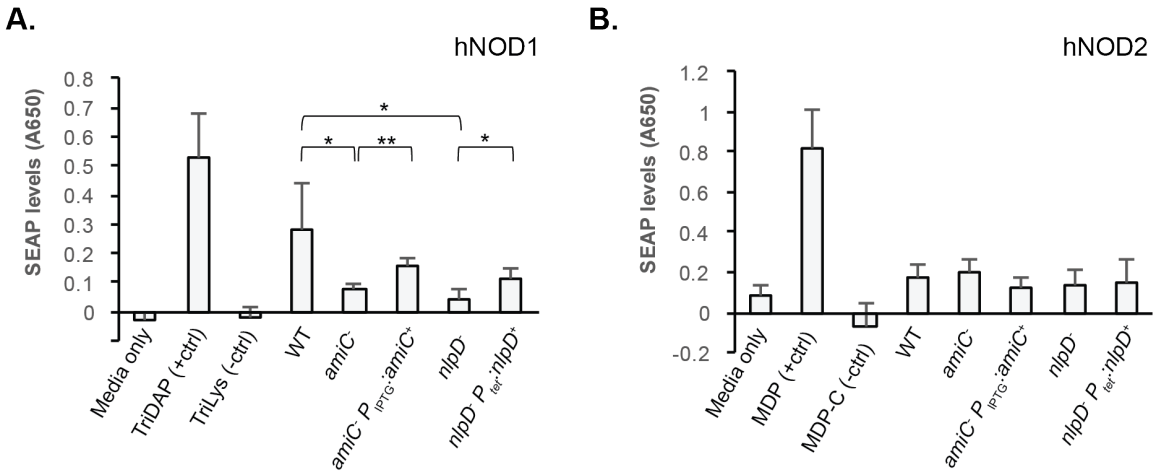

Figure 3. Conditioned media from mutants that do not release peptides stimulated lower levels of hNOD1 but not hNOD2 activation in HEK293 reporter cell lines overexpressing NOD receptors. Supernatant from WT (ATCC 13102 *cap*-), *amiC* mutant (KL1065), *amiC* complementation (EC1020), *nlpD* mutant (KL1072) and *nlpD* complementation (EC1026) strains were harvested, normalized to total cellular protein and used to treat HEK293 reporter cell lines overexpressing hNOD1 (A) or hNOD2 (B), as well as parental HEK293 cell lines. hNOD activation was determined by measuring the amount of secreted alkaline phosphatase in the media. Results are from three independent experiments, with technical triplicates for each biological replicate. Statistical significance was determined by Student's *t*-test, in which * indicates $p<0.05$.

N. meningitidis induced 3.6x and 7.5x higher levels of hNOD1 activation compared to an *amiC* or a *nlpD* mutant, respectively (Figure 3A). Supernatant from induced *amiC* and *nlpD* complementation strains showed a partial phenotypic complementation, with 2x and 3x higher hNOD1 responses compared to supernatant from the mutant strains, respectively ($p < 0.05$) (Figure 3A).

We also treated an HEK293 cell line overexpressing hNOD2 in parallel with the same supernatant samples (Figure 3B). The intracellular innate immune receptor hNOD2 recognizes muramyl-dipeptide (MDP) and responds to reducing end PG monomers and thus would not be expected to be differentially affected by amounts of free peptides (45–47). As predicted, treatment with supernatant from *amiC* and *nlpD* mutants did not alter hNOD2 activation levels. Thus, we conclude that PG-derived peptides generated by the action of AmiC and NlpD in *N. meningitidis* induce a hNOD1 response, but do not activate hNOD2 in a human cell line.

AmiC and NlpD are required for cell separation. Periplasmic *N*-acetylmuramyl-L-alanine amidases that act on the sacculi cleave septal PG to allow for proper cell separation (36). To examine the role of meningococcal AmiC in cell-separation, we performed thin-section electron microscopy (TEM) to visualize the cell morphology of WT, *amiC* mutant and *amiC* complementation strains. We counted the numbers of cells presenting as monococci, diplococci, tetrads and 5+ cell clusters in 16-24 fields/strain. Each field used in quantification had an average of 30 cells; an example of a field for each strain used for quantification is shown in Figure 4. A larger field of image demonstrating the size of the multi-cell clumps of the *amiC* and *nlpD* mutants is also included.

WT cells predominantly presented as diplococci (60%) and monococci (26%), with few cells found as tetrads (13%) and 5+ cell clusters (1%). In contrast, both *amiC* and *nlpD* mutants

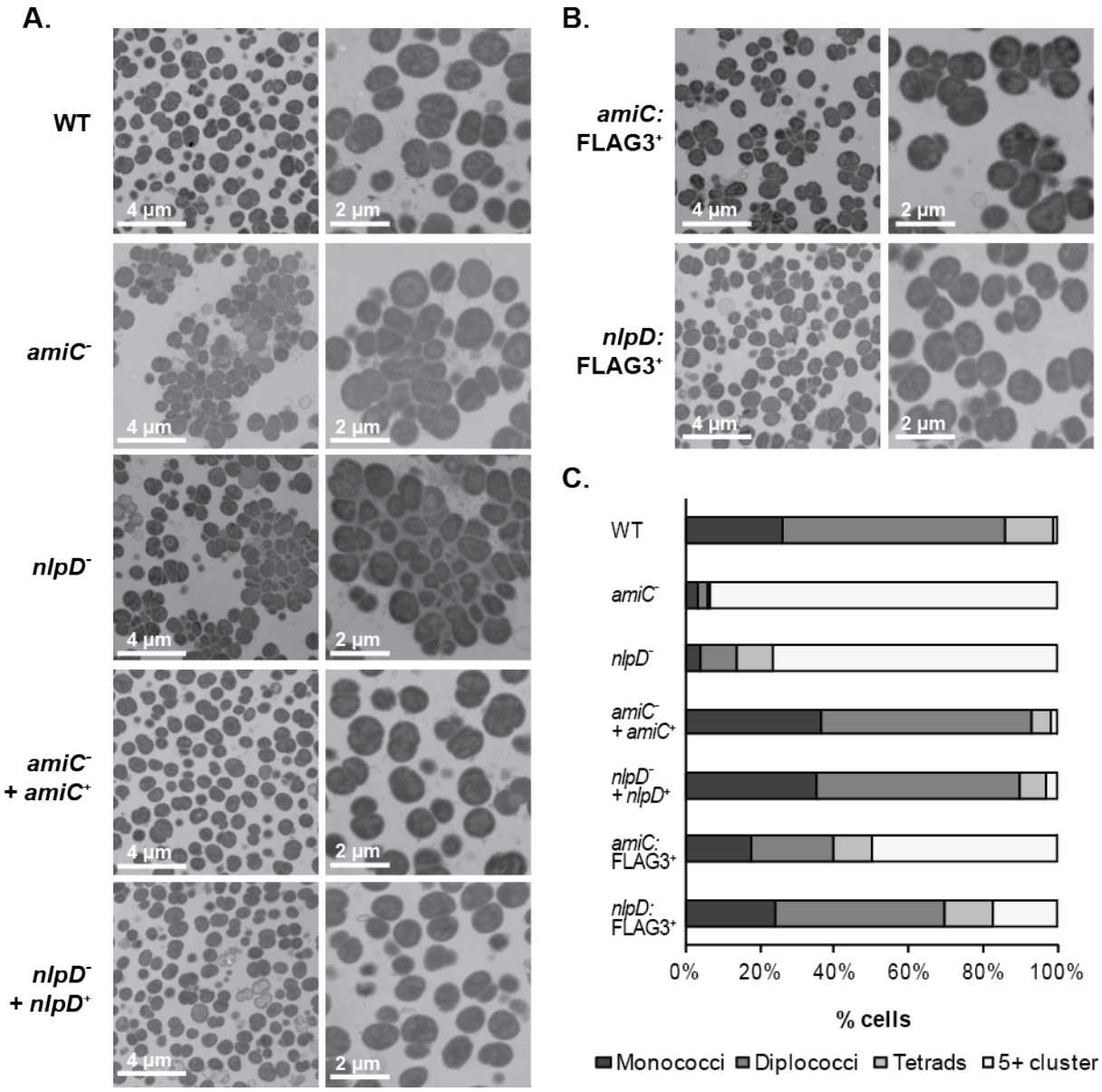

Figure 4. Mutation of *amiC* or *nlpD* results in cell separation defects. A) WT, *amiC* mutant and complementation strains (KL1065, EC1020), *nlpD* mutant and complementation strains (KL1072, EC1026), as well as B) strains expressing *amiC:FLAG3*$^+$ (EC1032) and *nlpD:FLAG3*$^+$ (EC1033) were imaged by thin section electron microscopy (TEM). C) Quantification of the number of cells presenting as monococci, diplococci, tetrads and clumps of 5+ cells in 16-24 fields of view containing an average of 30 cells each were performed, and presented as percent of total cells.

formed large aggregates of 5 cells or more (94% and 76%, respectively). Mutation of *amiC* caused a more severe cell separation defect than did mutation of *nlpD*, as more cells were found in large clusters and fewer cells were found as diplococci or monococci. Only 3% each of *amiC* mutant cells presented as diplococci and monococci, while 10% and 4% of *nlpD* mutants presented as diplococci and monococci, respectively. Both *amiC* and *nlpD* complementation strains showed WT-like cell morphology, with most cells presenting as diplococci (57% and 55%, respectively) and monococci (37% and 35%), respectively. We conclude that AmiC and NlpD are required for proper cell separation in *N. meningitidis*.

C-terminal FLAG3 tagged AmiC and NlpD displayed both septal and distributed localization. We generated C-terminal triple FLAG epitope tagged versions of AmiC and NlpD to visualize localization of these proteins in the cell via stochastic optical reconstruction microscopy (STORM). To determine functionality of these tagged proteins, we performed TEM to look at the cell morphology of the *amiC:FLAG3*$^+$ and *nlpD:FLAG3*$^+$ expressing strains (Figure 4). The *nlpD:FLAG3*$^+$ strain predominantly presented as diplococci (46%) and monococci (24%), although it had more 5+ cell clusters compared to WT (17% vs 1%). In contrast, *amiC:FLAG3*$^+$ cells were more likely to be found in clumps of 5 or more cells (50%) with only 22% and 18% of cells presenting as diplococci and monococci. However, the cell clumps in an *amiC:FLAG3*$^+$ mutant were much smaller and contained fewer cells than the large cell clusters formed by an *amiC* or a *nlpD* mutant, suggesting that AmiC:FLAG3$^+$ is at least partially functional for cell separation.

Localizations of AmiC:FLAG3$^+$ and NlpD:FLAG3$^+$ in *N. meningitidis* were determined using STORM, and chromosomal DNA was counterstained with DAPI and visualized by

epifluorescence microscopy to determine the position of the cells. The presence of a signal band between two adjacent DAPI foci (cells) was interpreted as septal localization. We observed two types of localization patterns for both AmiC:FLAG3$^+$ and NlpD:FLAG3$^+$ (Figure 5). First, as we expected, AmiC:FLAG3$^+$ localized to the putative septum in a small subset of cells (Figure 5, left panel, open triangles). NlpD:FLAG3$^+$ also localized to the septum in a subset of cells (Figure 5, right panel, open triangles). These observations are consistent with the known recruitment of the *E. coli* AmiC and NlpD homologues to the septum during late cell division (37, 49).

Second, we observed peripheral distribution of AmiC:FLAG3$^+$ and NlpD:FLAG3$^+$, with minor enrichment of the proteins at sites around the cell (Figure 5, closed triangles). Peripheral distribution of AmiC and NlpD homologues in *E. coli* are also seen in non-dividing cells, with a minor enrichment of *E. coli* AmiC at the poles of such cells (37). Our findings suggest that AmiC:FLAG3$^+$ and NlpD:FLAG3$^+$ localizes to the septum in dividing cells, and is distributed around the cell in non-dividing cells.

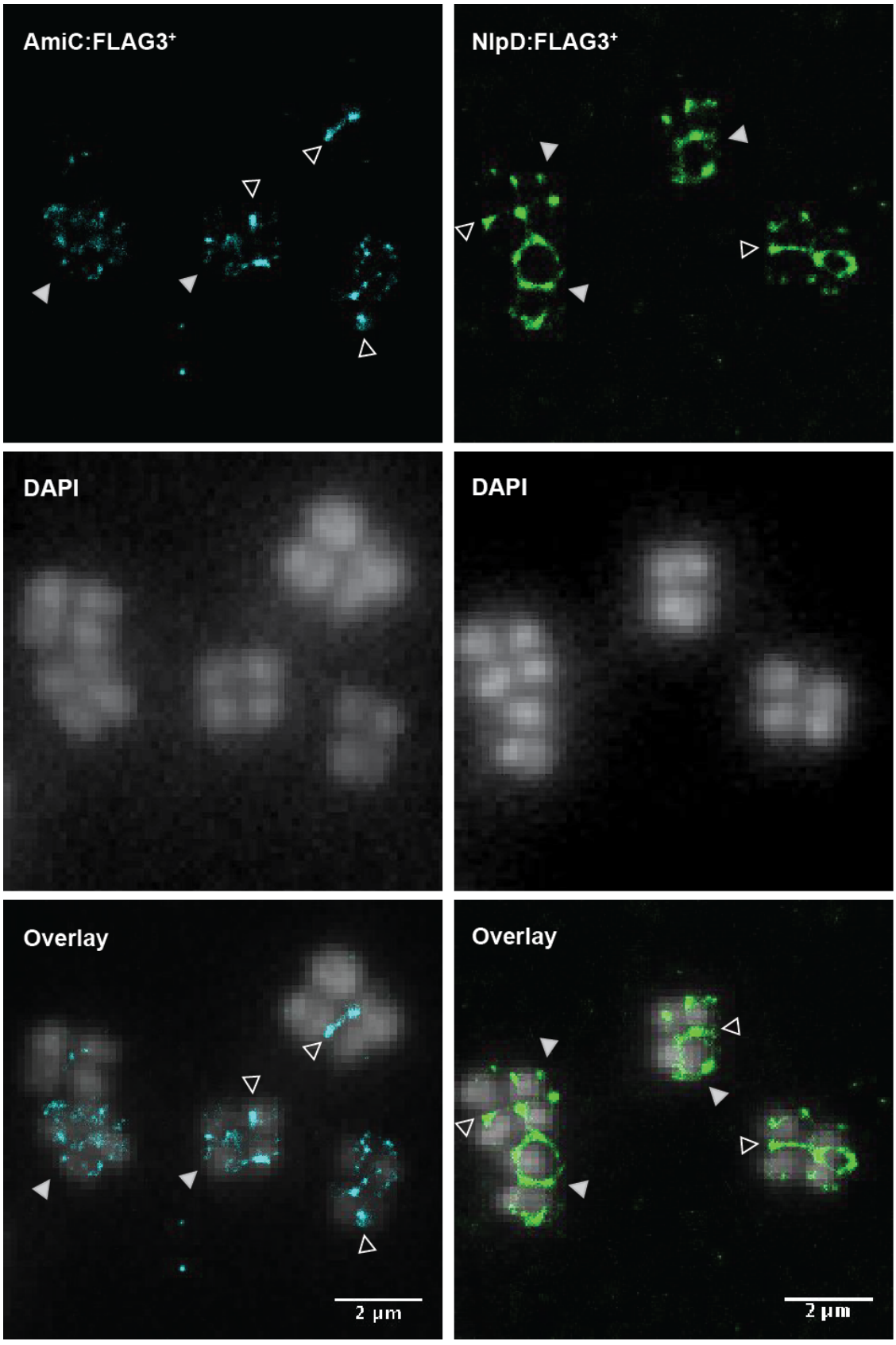
AmiC:FLAG3+
NlpD:FLAG3+
DAPI
DAPI
Overlay
Overlay
2 µm
2 µm

Figure 5. Localization of AmiC:FLAG3$^+$ and NlpD:FLAG3$^+$ in the cell. Localizations of AmiC:FLAG3$^+$ and NlpD:FLAG3$^+$ were determined using STORM. DNA was counterstained with DAPI. Localization of AmiC:FLAG3$^+$ is presented in the left panel, and localization of NlpD:FLAG3$^+$ is presented in the right panel. Septal localization of the proteins is indicated with open triangle, while distributed localization are indicated by closed triangles. AmiC:FLAG3$^+$ signal is false-colored cyan, while NlpD:FLAG3$^+$ signal is false-colored green. DAPI counterstain is in gray. Scale bar is 2 μm.

DISCUSSION

In this study, we demonstrated that the major type of PG fragment released by *N. meningitidis* AmiC is PG-derived peptides. Such peptides are generated from the action of the periplasmic *N*-acetylmuramyl-L-alanine amidase AmiC, which is activated by the outer membrane lipoprotein NlpD. Mutation of either *amiC* or *nlpD* in *N. meningitidis* completely abolished PG-derived peptide release (Figure 2). Abrogation of peptide release was previously observed in *N. gonorrhoeae amiC* mutants (31, 38). Hence, AmiC and NlpD are both necessary for the release of PG-derived peptides by *N. meningitidis*.

Consistent with the role of AmiC as a cell separation amidase, mutation of *amiC* or *nlpD* led to cell separation defects, which manifested as large cell clusters containing more than 10 cells (Figure 4). STORM analyses revealed that in a small subset of cells, AmiC:FLAG3 formed a banding pattern at the septum, suggesting septal localization of this fusion protein. In a different subset of cells, AmiC:FLAG3 was found randomly distributed in the cell. NlpD:FLAG3$^+$ signal was also found to localize to the septum in a subset of cells and was found distributed with enrichment at sites around the cell in a different subset of cells. Such localization patterns suggest that AmiC:FLAG3$^+$ and NlpD:FLAG3$^+$ are recruited to the septum during cell division, as observed in other species of bacteria (37, 49, 50).

Treatments of HEK293-Blue reporter cell lines overexpressing hNOD1 and hNOD2 with cell-free supernatant from WT, *amiC* and *nlpD* mutants suggested that peptide release is necessary for maximal hNOD1, but not hNOD2, activation by *N. meningitidis.* It is well established that hNOD1 responds to natural and synthetic PG fragments with a terminal DAP, in which modification of the DAP moiety by amidation reduces hNOD1 recognition (19–21, 23). As such, we infer that one of the peptides released by meningococcus is the hNOD1 agonist L-

Ala-D-Glu-*meso*DAP tripeptide. We cannot rule out the possibility that deletion of *amiC* or *nlpD* resulted in accumulation of a hNOD1 inhibitor instead of the absence of a hNOD1 agonist. However, since tripeptide is a known hNOD1 agonist and purified gonococcal AmiC have been shown to liberate tripeptide from whole sacculi *in vitro* (31), we deduce that peptide release is necessary for hNOD1 activation by *N. meningitidis*.

In contrast to *N. meningitidis*, abolishment of peptide release alone is not sufficient to reduce hNOD1 activation by supernatant from *N. gonorrhoeae* (31). The release of either PG-derived peptides or PG monomers alone is sufficient to engender WT-like hNOD1 activation by *N. gonorrhoeae* (31). Meningococcus releases lower levels of tripeptide PG monomer compared to gonococcus, and meningococcal supernatant induces lower hNOD1 activation in HEK293 cells and IL-8 production by Fallopian tube explants compared to gonococcal supernatant (12). Taken together with these published observations, our results provide support to the hypothesis that *N. meningitidis* degrades PG fragments more extensively compared to *N. gonorrhoeae* and thereby reduces hNOD1 activation, which may reduce immune clearance during its asymptomatic lifestyle.

It is not currently clear how PG fragment release contributes to meningococcal lifestyle. In response to a synthetic hNOD1 agonist or other inflammatory molecules, oral epithelial cells alter gene expression without inducing an inflammatory response (51). Additionally, treatment of nasopharyngeal tissue explants with meningococcal supernatant or purified PG does not lead to death of ciliated cells (52–54). Still, it is not particularly surprising that PG fragments released by meningococcus do not damage or induce inflammation in nasopharyngeal tissue, since asymptomatic colonization is by definition non-overtly damaging to the host on the organismal level. Released PG fragments may play a role in the establishment of colonization, in the

invasion of the meninges or in exacerbating damage during invasive meningococcal disease, or in colonization of new niches such as the urethra (11, 55). Such questions are challenging to assess because meningococcus does not naturally infect lab animals. Efforts to develop a mouse model using a natural colonizer of mice, *N. musculi*, provides exciting new avenues to study the impact of PG fragment release on colonization and disease in a native host organism (56, 57).

ACKNOWLEDGEMENTS

We are grateful to Ryan Schaub for constructive discussion and technical assistance and Will Vincent for preliminary work on this study. We would also like to acknowledge Ben August from the UW-Madison Medical School EM Facility for assistance with TEM, Elle Kielar-Grevstad from the UW-Madison Biochemistry Optical Core for advice and technical assistance on STORM, and Seamus Holden for advice on STORM.

Table 1. Strains used in this study.

Strain	Description	Reference or source
N. meningitidis		
ATCC 13102 Str	ATCC 13102 *rpsL*K43R	(58)
ATCC 13102 *cap*-	ATCC 13102 *rpsL*K43R *siaD::cat* (WT *N. meningitidis*)	(12)
KL1060	ATCC 13102 Str transformed with pKL25; ATCC 13102 Str Δ*amiC::ermCrpsL*	This study
KL1061	KL1060 transformed with pDG005; ATCC 13102 Str Δ*amiC*	This study
KL1065	KL1061 transformed with pHC10; ATCC 13102 *cap*- Δ*amiC*	This study
KL1071	ATCC 13102 Str transformed with pKL38; ATCC 13102 Str Δ*nlpD::kan*	This study
KL1072	KL1072 transformed with pHC10; ATCC 13102 *cap*- Δ*nlpD::kan*	This study
EC1018	ATCC 13102 *cap*- transformed with pKL50; ATCC 13102 *cap*- P_{IPTG}-*amiC*	This study
EC1020	EC1018 transformed with pEC140; ATCC 13102 *cap*- *amiC::kan* P_{IPTG}-*amiC*	This study
EC1022	ATCC 13102 *cap*- transformed with pKL49; ATCC 13102 *cap*- P_{tet}-*nlpD*-rpsL*	This study
EC1024	EC1022 transformed with pKL38; ATCC 13102 *cap*- *nlpD::kan* P_{tet}-*nlpD*-rpsL*	This study
EC1026	EC1024 transformed with PCR amplified *nlpD*; ATCC 13102 *cap*- Δ*nlpD::kan* P_{tet}-*nlpD*	This study
EC1032	13102 *cap*- transformed with pEC169; ATCC 13102 *cap*- *amiC:FLAG3*$^{+}$	This study
EC1033	13102 *cap*- transformed with pEC173; ATCC 13102 *cap*- *nlpD:FLAG3*$^{+}$-*kan*	This study
N. gonorrhoeae		
MS11	WT *N. gonorrhoeae*	(59)
KH518	*pacA* 26 bp deletion	(60)
Plasmids		
pDG005	Markerless *amiC* deletion in pIDN3	(38)
pHC10	Serogroup C *siaD::cat*	(61)
pHSS6	Cloning vector; source of *aph3* gene (referred to as *kan*^{R})	(62)
pKC1	Positive/negative selection plasmid for *Neisseria* spp.; source of *rpsL*	(29)
pKH6	Cloning vector derived from pIDN1 and pGCC6	(58)
pKH99	Cloning vector derived from pHSS6 and pIDN2; source of *kan*^{R}	(58)
pMR33	Complementation vector; IPTG inducible	(63)
pMR68	Complementation vector; anhydrotetracycline inducible	(63)
pMR100	Cloning vector pIDN3 with a C-terminal FLAG3 sequence	(64)
pKL24	*amiC* deletion insert from pDG005 into pKH6	This study
pKL25	*ermCrpsL* in pKL24; Δ*amiC::ermCrpsL* in pKH6	This study
pKL28	*nlpD* and flanking DNA in pKH6	This study
pKL29	Markerless *nlpD* deletion in pIDN3; Δ*nlpD* in pIDN3	This study
pKL38	*kan*^{R} in pKL29; Δ*nlpD::kan* in pIDN3	This study
pKL45	*nlpD** in pMR68 (has premature stop codon)	This study
pKL49	*nlpD*-rpsL* in pMR68	This study
pKL50	*amiC* in pMR33	This study

pEC140	*kan*^{R} from pHSS6 in pDG005; Δ*amiC::kan* in pIDN3	This study
pEC167	*amiC* 3' flank in pMR100	This study
pEC168	*nlpD* 3' flank in pMR100	This study
pEC169	Partial *amiC* coding sequence (*amiC*') in pEC167; *amiC':FLAG3*$^+$ -3' flank in pIDN3	This study
pEC170	Partial *nlpD* coding sequence (*nlpD*') in pEC168	This study
pEC173	*kan*^{R} in pEC170; *nlpD':FLAG3*$^+$-*kan*^{R}-3' flank in pIDN3	This study

Table 2. Primers used in this study. Restriction enzyme sites are underlined.

Primer	Sequence
SacII nlpD F	TAACCGCGGAGGCACTGTGGACATTGTTG
SacI nlpD R	GATTGAGCTCTCACGATGGTTGCGGTCAAAG
BglII nlpD del F	GCCGAGATCTAGCTATATCGCGTTCTGACTTTC
BglII nlpD del R	GCCCAGATCTCATAAGATAACCTTCATGTTCCG
SacI nlpD F2	GCCGGAGCTCATCGGAACATGAAGGTTATC
SpeI nlpD R	GCCGACTAGTGATTTCAGGCAGAAAGTCAG
MluI rpsL F	AATAACGCGTCCGCTCTTGCCGACATGGTG
MluI rpsL R	AATACGCGTTAGGCGGCCGACGTGCCTAATTG
SacI MC amiC F	TAATGAGCTCCCGAACGAGGACGCGAAAGCC
SpeI MC amiC R	GCCGACTAGTACCGCCTTTTCAATCAACCC
Kan F BamHI	CAGGATCCAAAGCCAGTCCGCAGAAACG
Kan R BamHI	CTGGATCCTGGGCGAAGAACTCCAGCAT
NlpD DUS F	ATGCCGTCTGAACTTTGCGCTTGAGAAGAACG
NlpD DUS R	TCTGTACTGTCTGCGGCTTC
SacI MC amiC -sigseq F	GATTAGAGCTCAAAACGGTACGCGCACCAC
EcoRI MC amiC -stop codon R	GTGCAGAATTCACCCCGCTTCAATACGGATG
HindIII amiC down F	GCACGAAGCTTTAGTTGTCGGATGAAGGCAG
XhoI amiC down R	GACGACTCGAGCAACCATTTCAATTCCGTATCC
SacI MC nlpD -sigseq F	GATTAGAGCTCGCTACCCAGCAGCCTGCC
EcoRI MC nlpD -stop codon R	GCGCAGAATTCGAACGCGATATAGCTGTTC
HindIII nlpD down F	GCAGCAAGCTTCTGCCTGAAATCAAGTTGG
XhoI nlpD down R	GATTACTCGAGATCGGCATCCGTGTCGAAGC

REFERENCES

1. **CDC**. 2017. Meningococcal Disease: Clinical Information. Accessed from < https://www.cdc.gov/meningococcal/clinical-info.html>
2. **Swartz MN**. 2004. Bacterial meningitis — A view of the past 90 years. N Engl J Med **351**:1826–1828.
3. **Stephens DS**, **Greenwood B**, **Brandtzaeg P**. 2007. Epidemic meningitis, meningococcaemia, and *Neisseria meningitidis*. Lancet **369**:2196–2210.
4. **Yezli S**, **Wilder-Smith A**, **Saeed AA**. 2016. Carriage of *Neisseria meningitidis* in the Hajj and Umrah mass gatherings. Int J Infect Dis **47**:65–70.
5. **CDC**. 2017. Meningococcal disease: Meningococcal disease in other countries. Accessed from < https://www.cdc.gov/meningococcal/global.html>.
6. **Roupheal NG**, **Stephens DS**. 2012. *Neisseria meningitidis*: biology, microbiology and epidemiology. Methods Mol Biol **799**:1–20.
7. **McGee ZA**, **Stephens DS**, **Hoffman LH**, **Schlech WF**, **Horn RG**. 2011. Mechanisms of mucosal invasion by pathogenic *Neisseria*. Rev Infect Dis **5 Suppleme**:S708–S714.
8. **Schoen C**, **Kischkies L**, **Elias J**, **Ampattu BJ**. 2014. Metabolism and virulence in *Neisseria meningitidis*. Front Cell Infect Microbiol **4**:114.
9. **Pizza M**, **Rappuoli R**. 2015. *Neisseria meningitidis*: pathogenesis and immunity. Curr Opin Microbiol **23**:68–72.
10. **Doran KS**, **Fulde M**, **Gratz N**, **Kim BJ**, **Nau R**, **Prasadarao N**, **Schubert-Unkmeir A**, **Tuomanen E**, **Valentin-Weigand P**. 2016. Host-pathogen interactions in bacterial meningitis. Acta Neuropathol **131**:185–209.
11. **Johswich K**. 2017. Innate immune recognition and inflammation in *Neisseria meningitidis* infection. Pathog Dis **75**:ftx022.
12. **Woodhams KL**, **Chan JM**, **Lenz JD**, **Hackett KT**, **Dillard JP**. 2013. Peptidoglycan fragment release from *Neisseria meningitidis*. Infect Immun **81**:3490–3498.
13. **Vollmer W**, **Blanot D**, **de Pedro MA**. 2008. Peptidoglycan structure and architecture. FEMS Microbiol Rev **32**:149–167.
14. **Rosenthal RS**. 1979. Release of soluble peptidoglycan from growing gonococci: hexaminidase and amidase activities. Infect Immun **24**:869–878.
15. **Park JT**, **Uehara T**. 2008. How bacteria consume their own exoskeletons (turnover and recycling of cell wall peptidoglycan). Microbiol Mol Biol Rev **72**:211–227.
16. **Johnson JW**, **Fisher JF**, **Mobashery S**. 2013. Bacterial cell-wall recycling. Ann N Y Acad Sci **1277**:54–75.
17. **Rosenthal RS**, **Nogami W**, **Cookson BT**, **Goldman WE**, **Folkening WJ**. 1987. Major fragment of soluble peptidoglycan released from growing *Bordetella pertussis* is tracheal cytotoxin. Infect Immun **55**:2117–2120.
18. **Koropatnick TA**, **Engle JT**, **Apicella MA**, **Stabb E V**, **Goldman WE**, **McFall-Ngai MJ**. 2004. Microbial factor-mediated development in a host-bacterial mutualism. Science **306**:1186–1188.
19. **Girardin SE**, **Boneca IG**, **Carneiro LAM**, **Antignac A**, **Jehanno M**, **Viala J**, **Tedin K**, **Taha M-K**, **Labigne A**, **Zahringer U**, **Coyle AJ**, **DiStefano PS**, **Bertin J**, **Sansonetti PJ**, **Philpott DJ**. 2003. Nod1 detects a unique muropeptide from Gram-negative bacterial

peptidoglycan. Science **300**:1584–1587.
20. **Chamaillard M**, **Hashimoto M**, **Horie Y**, **Masumoto J**, **Qiu S**, **Saab L**, **Ogura Y**, **Kawasaki A**, **Fukase K**, **Kusumoto S**, **Valvano MA**, **Foster SJ**, **Mak TW**, **Nuñez G**, **Inohara N**. 2003. An essential role for NOD1 in host recognition of bacterial peptidoglycan containing diaminopimelic acid. Nat Immunol **4**:702–707.
21. **Girardin SE**, **Travassos LH**, **Herve M**, **Blanot D**, **Boneca IG**, **Philpott DJ**, **Sansonetti PJ**, **Mengin-Lecreulx D**. 2003. Peptidoglycan molecular requirements allowing detection by Nod1 and Nod2. J Biol Chem **278**:41702–41708.
22. **Ghosh M**, **Shen Z**, **Fahey J V.**, **Crist SG**, **Patel M**, **Smith JM**, **Wira CR**. 2013. Pathogen recognition in the human female reproductive tract: expression of intracellular cytosolic sensors NOD1, NOD2, RIG-1, and MDA5 and response to HIV-1 and *Neisseria gonorrhea*. Am J Reprod Immunol **69**:41–51.
23. **Vijayrajratnam S**, **Pushkaran AC**, **Balakrishnan A**, **Vasudevan AK**, **Biswas R**, **Mohan CG**. 2016. Bacterial peptidoglycan with amidated *meso*-diaminopimelic acid evades NOD1 recognition: an insight into NOD1 structure–recognition. Biochem J **473**:4573–4592.
24. **Morse SA**, **Bartenstein L**. 1974. Factors affecting autolysis of *Neisseria gonorrhoeae*. Proc Soc Exp Biol Med **145**:1418–1421.
25. **Kellogg DS**, **Peacock WL**, **Deacon WE**, **Brown L**, **Pirkle CI**. 1963. *Neisseria gonorrhoeae*: Virulence genetically linked to clonal variation. J Bacteriol **85**:1274–1279.
26. **Dillard JP**. 2011. Genetic manipulation of *Neisseria gonorrhoeae*. Curr Protoc Microbiol **4**:Unit4A.2.
27. **Elkins C**, **Thomas CE**, **Seifert HS**, **Sparling PF**. 1991. Species-specific uptake of DNA by gonococci is mediated by a 10-base-pair sequence. J Bacteriol **173**:3911–3913.
28. **Rosenthal RS**, **Dziarski R**. 1994. Isolation of peptidoglycan and soluble peptidoglycan fragments. Methods Enzymol **235**:253–285.
29. **Cloud KA**, **Dillard JP**. 2002. A lytic transglycosylase of *Neisseria gonorrhoeae* is involved in peptidoglycan-derived cytotoxin production. Infect Immun **70**:2752–2757.
30. **Garcia DL**, **Dillard JP**. 2008. Mutations in *ampG* or *ampD* affect peptidoglycan fragment release from *Neisseria gonorrhoeae*. J Bacteriol **190**:3799–3807.
31. **Lenz JD**, **Stohl EA**, **Robertson R**, **Hackett KT**, **Fisher K**, **Xiong K**, **Lee M**, **Hesek D**, **Mobashery S**, **Seifert HS**, **Davies C**, **Dillard JP**. 2016. Amidase activity of AmiC controls cell separation and stem-peptide release and is enhanced by NlpD in *Neisseria gonorrhoeae*. J Biol Chem **291**:10916–10933.
32. **Schaub RE**, **Chan YA**, **Lee M**, **Hesek D**, **Mobashery S**, **Dillard JP**. 2016. Lytic transglycosylases LtgA and LtgD perform distinct roles in remodeling, recycling, and releasing peptidoglycan in *Neisseria gonorrhoeae*. Mol Microbiol **102**:865–881.
33. **Antignac A**, **Rousselle JC**, **Namane A**, **Labigne A**, **Taha MK**, **Boneca IG**. 2003. Detailed structural analysis of the peptidoglycan of the human pathogen *Neisseria meningitidis*. J Biol Chem **278**:31521–31528.
34. **Sinha RK**, **Rosenthal RS**. 1980. Release of soluble peptidoglycan from growing gonococci: Demonstration of anhydro-muramyl-containing fragments. Infect Immun **29**:914–925.
35. **Jacobs C**, **Huang L**, **Bartowsky E**, **Normark S**, **Park JT**. 1994. Bacterial cell wall recycling provides cytosolic muropeptides as effectors for beta-lactamase induction. EMBO J **13**:4684–4694.

36. **Heidrich C**, **Templin MF**, **Ursinus A**, **Merdanovic M**, **Berger J**, **Schwarz H**, **de Pedro MA**, **Höltje J-V**. 2001. Involvement of *N*-acetylmuramyl-L-alanine amidases in cell separation and antibiotic-induced autolysis of *Escherichia coli*. Mol Microbiol **41**:167–178.
37. **Bernhardt TG**, **Boer PAJ De**. 2003. The *Escherichia coli* amidase AmiC is a periplasmic septal ring component exported via the twin-arginine transport pathway. Mol Microbiol **48**:1171–1182.
38. **Garcia DL**, **Dillard JP**. 2006. AmiC functions as an *N*-acetylmuramyl-L-alanine amidase necessary for cell separation and can promote autolysis in *Neisseria gonorrhoeae*. J Bacteriol **188**:7211–7221.
39. **Jensen SE**, **Campbell JN**. 1976. Amidase activity involved in peptidoglycan biosynthesis in membranes of *Micrococcus luteus (sodonensis)*. J Bacteriol **127**:319–326.
40. **Uehara T**, **Park JT**. 2007. An anhydro-*N*-acetylmuramyl-L-alanine amidase with broad specificity tethered to the outer membrane of *Escherichia coli*. J Bacteriol **189**:5634–5641.
41. **Uehara T**, **Dinh T**, **Bernhardt TG**. 2009. LytM-domain factors are required for daughter cell separation and rapid ampicillin-induced lysis in *Escherichia coli*. J Bacteriol **191**:5094–5107.
42. **Uehara T**, **Parzych KR**, **Dinh T**, **Bernhardt TG**. 2010. Daughter cell separation is controlled by cytokinetic ring-activated cell wall hydrolysis. EMBO J **29**:1412–22.
43. **Yang DC**, **Tan K**, **Joachimiak A**, **Bernhardt TG**. 2012. A conformational switch controls cell wall-remodelling enzymes required for bacterial cell division. Mol Microbiol **85**:768–781.
44. **Stohl EA**, **Lenz JD**, **Dillard JP**, **Seifert HS**. 2016. The gonococcal NlpD protein facilitates cell separation by activating peptidoglycan cleavage by AmiC. J Bacteriol **198**:615–622.
45. **Girardin SE**, **Boneca IG**, **Viala J**, **Chamaillard M**, **Labigne A**, **Thomas G**, **Philpott DJ**, **Sansonetti PJ**. 2003. Nod2 is a general sensor of peptidoglycan through muramyl dipeptide (MDP) detection. J Biol Chem **278**:8869–8872.
46. **Inohara N**, **Ogura Y**, **Fontalba A**, **Gutierrez O**, **Pons F**, **Crespo J**, **Fukase K**, **Inamura S**, **Kusumoto S**, **Hashimoto M**, **Foster SJ**, **Moran AP**, **Fernandez-Luna JL**, **Nunez G**. 2003. Host recognition of bacterial muramyl dipeptide mediated through NOD2: Implications for Crohn's disease. J Biol Chem **278**:5509–5512.
47. **Knilans KJ**, **Hackett KT**, **Anderson JE**, **Weng C**, **Dillard JP**, **Duncan JA**. 2017. *Neisseria gonorrhoeae* lytic transglycosylases LtgA and LtgD reduce host innate immune signaling through TLR2 and NOD2. ACS Infect Dis **3**:624–633.
48. **Bendtsen JD**, **Nielsen H**, **Widdick D**, **Palmer T**, **Brunak S**. 2005. Prediction of twin-arginine signal peptides. BMC Bioinformatics **6**:167.
49. **Tsang M-J**, **Yakhnina AA**, **Bernhardt TG**. 2017. NlpD links cell wall remodeling and outer membrane invagination during cytokinesis in *Escherichia coli*. PLoS Genet **13**:e1006888.
50. **Möll A**, **Dörr T**, **Alvarez L**, **Chao MC**, **Davis BM**, **Cava F**, **Waldor MK**. 2014. Cell separation in *Vibrio cholerae* is mediated by a single amidase whose action is modulated by two nonredundant activators. J Bacteriol **196**:3937–3948.
51. **Uehara A**, **Sugawara Y**, **Kurata S**, **Fujimoto Y**, **Fukase K**, **Kusumoto S**, **Satta Y**, **Sasano T**, **Sugawara S**, **Takada H**. 2005. Chemically synthesized pathogen-associated

molecular patterns increase the expression of peptidoglycan recognition proteins via toll-like receptors, NOD1 and NOD2 in human oral epithelial cells. Cell Microbiol **7**:675–686.

52. **Stephens DS**, **Whitney AM**, **Melly MA**, **Hoffman LH**, **Farley MM**, **Frasch CE**. 1986. Analysis of damage to human ciliated nasopharyngeal epithelium by *Neisseria meningitidis*. Infect Immun **51**:579–585.
53. **Stephens DS**, **McGee ZA**, **Cooper MD**. 1987. Cytopathic effects of the pathogenic *Neisseria*. Studies using human fallopian tube organ cultures and human nasopharyngeal organ cultures. Antonie Van Leeuwenhoek **53**:575–584.
54. **Uehara A**, **Sugawara S**, **Tamai R**, **Takada H**. 2001. Contrasting responses of human gingival and colonic epithelial cells to lipopolysaccharides, lipoteichoic acids and peptidoglycans in the presence of soluble CD14. Med Microbiol Immunol **189**:185–192.
55. **Bazan JA**, **Peterson AS**, **Kirkcaldy RD**, **Briere EC**, **Maierhofer C**, **Turner AN**, **Licon DB**, **Parker N**, **Dennison A**, **Ervin M**, **Johnson L**, **Weberman B**, **Hackert P**, **Wang X**, **Kretz CB**, **Abrams AJ**, **Trees DL**, **Del Rio C**, **Stephens DS**, **Tzeng Y-L**, **DiOrio M**, **Roberts MW**. 2016. Notes from the field. Increase in Neisseria meningitidis-associated urethritis among men at two sentinel clinics - Columbus, Ohio, and Oakland County, Michigan, 2015. Morb Mortal Wkly Rep **65**:550–552.
56. **Weyand NJ**, **Ma M**, **Phifer-Rixey M**, **Taku NA**, **Rendón MA**, **Hockenberry AM**, **Kim WJ**, **Agellon AB**, **Biais N**, **Suzuki TA**, **Goodyer-Sait L**, **Harrison OB**, **Bratcher HB**, **Nachman MW**, **Maiden MCJ**, **So M**. 2016. Isolation and characterization of *Neisseria musculi* sp. nov., from the wild house mouse. Int J Syst Evol Microbiol **66**:3585–3593.
57. **Ma M**, **Powell DA**, **Weyand NJ**, **Rhodes KA**, **Rendón MA**, **Frelinger JA**, **So M**. 2018. A mouse model for *Neisseria* colonization. Infect Immun doi:10.1128/IAI.00839-17.
58. **Woodhams KL**, **Benet ZL**, **Blonsky SE**, **Hackett KT**, **Dillard JP**. 2012. Prevalence and detailed mapping of the gonococcal genetic island in *Neisseria meningitidis*. J Bacteriol **194**:2275–2285.
59. **Swanson J**. 1972. Studies on gonococcus infection. II. Freeze-fracture, freeze-etch studies on gonococci. J Exp Med **136**:1258–1271.
60. **Dillard JP**, **Hackett KT**. 2005. Mutations affecting peptidoglycan acetylation in *Neisseria gonorrhoeae* and *Neisseria meningitidis*. Infect Immun **73**:5697–5705.
61. **Ram S**, **Cox AD**, **Wright JC**, **Vogel U**, **Getzlaff S**, **Boden R**, **Li J**, **Plested JS**, **Meri S**, **Gulati S**, **Stein DC**, **Richards JC**, **Moxon ER**, **Rice PA**. 2003. Neisserial lipooligosaccharide Is a target for complement component C4b. J Biol Chem **278**:50853–50862.
62. **Mehr IJ**, **Long CD**, **Serkin CD**, **Seifert HS**. 2000. A homologue of the recombination-dependent growth gene, *rdgC*, is involved in gonococcal pilin antigenic variation. Genetics **154**:523–532.
63. **Ramsey ME**, **Hackett KT**, **Kotha C**, **Dillard JP**. 2012. New complementation constructs for inducible and constitutive gene expression in *Neisseria gonorrhoeae* and *Neisseria meningitidis*. Appl Environ Microbiol **78**:3068–3078.
64. **Ramsey ME**, **Hackett KT**, **Bender T**, **Kotha C**, **Does C Van Der**, **Dillard P**. 2014. TraK and TraB are conserved outer membrane proteins of the *Neisseria gonorrhoeae* Type IV secretion system and are expressed at low levels in wild-type cells. J Bacteriol **196**:2954–2968.

CHAPTER 4

Characterization of peptidoglycan fragment release by nonpathogenic human-associated and animal-associated *Neisseria*

Jia Mun Chan and Joseph P. Dillard

JM Chan and JP Dillard designed the experiments and wrote the manuscript.

JM Chan performed the experiments and analyzed the data.

ABSTRACT

Peptidoglycan (PG) is a structural macromolecule that is important for bacterial survival. Multicellular organisms, such as humans, have evolved ways to detect PG and respond to the presence of bacteria. Human pattern-recognition receptors NOD1 and NOD2 recognize PG intracellularly and induce inflammatory responses upon detection of specific types of PG. A limited number of species of Gram-negative bacteria release PG fragments during normal growth. *Neisseria gonorrhoeae*, a human restricted pathogen and the etiological agent of gonorrhea, releases inflammatory PG fragments that contribute to the pathophysiology of pelvic inflammatory disease (PID). PID is a complication of ascending gonococcal infection in women. In addition to the pathogenic species, the genus *Neisseria* is also home to multiple species of human- or animal-associated *Neisseria* that form part of the normal microbiota of their cognate host organisms. The amounts or types of PG fragments released by these species may influence the inflammatory responses to these symbionts and their abilities to asymptomatically colonize their hosts. In this chapter, we study the human-associated nonpathogenic species *N. sicca*, *N. mucosa* and *N. lactamica*, and animal-associated *Neisseria* isolated from macaques and wild mice, and investigated PG recycling in these species.

INTRODUCTION

The genus *Neisseria* contains multiple species of Gram-negative bacteria with varying cell morphology and niches. *Neisseria* species are almost always found associated with higher order host organisms, which includes multiple species of insects, birds and waterfowl, land and marine mammals, as well as rhinoceros iguana and the marsupial quokka (1, 2). The most infamous of the *Neisseria* species are *Neisseria gonorrhoeae* and *Neisseria meningitidis*, which are human-restricted pathogens and etiological agents for the sexually transmitted infection gonorrhea and invasive meningococcal disease respectively. However, most species in this genus are nonpathogenic colonizers of mucosal surfaces of their respective host organism. In fact, *N. meningitidis* has a nonpathogenic lifestyle as a colonizer of the naso- and oropharyngeal space of healthy adults (3). Like *N. meningitidis*, the major niche occupied by nonpathogenic mammal-associated *Neisseria* (also referred to hereafter as *Neisseria* spp) is the oral and nasopharyngeal space. *Neisseria* is considered part of the core oral microbiome of healthy humans, and constitutes up to 8% of the oral microbiota of humans (4–9).

The five species of *Neisseria* used in this study are all nonpathogenic colonizers of mammals. Three of these species, *Neisseria lactamica*, *N. sicca* and *N. mucosa,* are associated with humans. The newly recognized species, *N. musculi*, was recently isolated from wild house mice. The macaque isolates AP312 and AP678 were isolated from macaques housed in a zoological garden (10, 11). In terms of cell morphology, *N. lactamica*, *N. sicca, N. mucosa* and macaque isolates AP312 and AP678 are all diplococci, while *N. musculi* is a rod-shaped bacterium (2, 11). There are temporal and tissue specific colonization patterns in different species of nonpathogenic *Neisseria.* For example, *N. lactamica* carriage rates are higher in children compared to adults, and nasopharyngeal colonization by *N. lactamica* protects against

colonization by *N. meningitidis* (12–14). In contrast, *N. meningitidis* is more commonly found in the throat of adults (12, 15). *N. sicca* and *N. mucosa* are mostly found in the gingival plaque and tooth surfaces of children and adults, but do not appear to contribute to exacerbating or preventing tooth decay (15, 16). *N. musculi* was isolated from the mouths of wild mice, but is able to colonize both the oral cavity and the gastrointestinal tract of CAST mice in the laboratory (11, 17). While the macaque isolates colonize the nasopharyngeal and oral cavities of rhesus macaques, AP312 was initially isolated from a bite wound (10).

Despite their roles as part of the core oral microbiome, nonpathogenic human-associated *Neisseria* encode a number of virulence-associated factors and in rare cases cause disease in people who are immunocompromised or have pre-existing risk factors, or post-trauma (2, 18, 19). Some diseases caused by *Neisseria* spp include high fatality diseases like meningitis, septicemia, and endocarditis, as well as conjunctivitis, respiratory tract infections and pneumonia (2, 18). Multiple cases of endocarditis by *Neisseria* spp occurred after dental procedures; it is likely that oral wounds sustained from such procedures provided a direct route for the bacteria to transverse from the mouth to the bloodstream (18). Factors that favor colonization by these nonpathogenic Neisseria species while not promoting inflammation and disease are not clear.

The aspect of nonpathogenic *Neisseria* biology that we chose to study is the release of peptidoglycan fragments. Peptidoglycan (PG) is a macromolecular structure that confers cell shape and protection against osmotic shock. PG consists of a glycan backbone made of repeating subunits of *N*-acetylglucosamine (GlcNAc) and *N*-acetylmuramic acid (MurNAc), with peptide stems extending off MurNAc that can be crosslinked to adjacent peptide stems to form a mesh-like structure. As a consequence of PG remodeling to allow for cell enlargement and cell separation, small PG fragments are liberated from the sacculus during growth. In Gram-negative

bacteria, these PG fragments are usually taken back into the cytoplasm to be recycled for cellular metabolism. A limited number of Gram-negative bacteria, including the human pathogens *N. gonorrhoeae* and *N. meningitidis*, release sufficient amounts of pro-inflammatory PG fragments to stimulate production of pro-inflammatory cytokines in tissue explants (20–22). Various species of nonpathogenic human- and animal-associated *Neisseria* encode homologues of *N. gonorrhoeae* PG degrading enzymes and PG recycling proteins (Appendix 5). In this study, we characterized the PG fragments released by nonpathogenic human- and animal-associated *Neisseria*.

MATERIALS AND METHODS

Bacterial strains and growth conditions. All strains used are listed in Table 1. All *Neisseria* strains are grown at 37°C either on gonococcal base medium (Difco) agar plates (GCB) with 5% CO_2 or in gonococcal base liquid medium with 0.042% $NaHCO_3$ (23) and Kellogg's supplements added (cGCBL) (24). When necessary, 80 μg/ml kanamycin was added to the growth medium. *Escherichia coli* strains were grown on LB agar or in LB broth (Difco) at 37°C. The growth medium was supplemented with 40 μg/ml kanamycin, 500 μg/ml erythromycin or 25 μg/ml chloramphenicol as needed.

Strain and plasmid construction. All strains and plasmids used in this study are listed in Table 1, and primers are listed in Table 2. Spot transformation was used to generate *Neisseria* mutants (25). Briefly, around 0.5 - 20 μg plasmid DNA was digested with PciI with a subsequent heat-inactivation step to linearize the plasmid, and the digest reaction was spotted onto a pre-warmed GCB agar plate. Five to ten piliated colonies were then streaked over the DNA spots, and the

plate was incubated at 37°C overnight. Colonies growing on the spots were restreaked onto fresh GCB plates for selection or screening. All transformants were screened by PCR and sequencing.

To construct pEC012 (AP312 *ampG::cat* in pIDN3), AP312 *ampG* was first amplified from macaque isolate AP312 chromosomal DNA with primers AP312 ampG SacI F and AP312 ampG BamHI R, and subsequently digested with SacI, BamHI, DpnI and EarI, resulting in two DNA fragments. The chloramphenicol resistance gene *cat* was excised from pKH6 by digestion with DpnI and EarI. The cloning vector pIDN3 was digested with SacI and BamHI. All four digest products were ligated together to form pEC012. Macaque isolate AP312 was transformed with pEC012 to make EC2000.

The insert for pEC088 (P_{ampGGC}-$ampG_{NL49142}$ in pIDN3) was generated via overlap-extension-PCR (OE-PCR). First, $ampG_{NL49142}$ was amplified from *N. lactamica* ATCC 49142 chromosomal DNA using primers SOE-NL ampG F and SOE-NL ampG R. Approximately 1kb $ampG_{GC}$ upstream and downstream regions, which include the native $ampG_{GC}$ promoter and transcriptional terminator, were amplified from *N. gonorrhoeae* MS11 chromosomal DNA using primer pairs MC ampG SacI F3/NL SOE-MS11 ampG 5' flank R and NL SOE-MS11 ampG 3' flank F/ampG 3' flank R BamHI, respectively. The three PCR products were used as templates in OE-PCR with primes MC ampG SacI F3 and ampG 3' flank R BamHI. The final PCR product was digested with SacI and BamHI, and ligated into similarly digested pIDN3 to form pEC088. pEC089 (P_{ampGGC}-$ampG_{NL23970}$ in pIDN3) was constructed almost exactly as pEC088; the only exception is that $ampG_{NL23970}$ was amplified from *N. lactamica* ATCC 23970 chromosomal DNA. Transformation of *N. gonorrhoeae* MS11 with pEC088 or pEC089 yielded EC544 and EC540, respectively.

To generate pEC095 ($ampG_{Nmus}$ in pIDN3), $ampG_{Nmus}$ was amplified from *N. musculi*

AP2031 chromosomal DNA using primers AP2031 ampG SacI F and AP2031 ampG BamHI R, digested with SacI and BamHI and ligated into similarly digested pIDN3. Plasmid pEC095 was digested with BtsBI and the 5' overhanging DNA ends were filled in with T4 Polymerase (NEB). A kanamycin resistance marker, *kan*, was excised from pHSS6 by digestion with NheI and BamHI, treated with T4 Polymerase and blunt-ligated with the BtsBI digested pEC095 to form pEC096 (*ampG*$_{\text{Nmus}}$*::kan* in pIDN3). Plasmid pEC096 was transformed into *N. musculi* AP2031 to generate EC2005.

Plasmid pEC088 was used as template in two PCR reactions with primer pairs MC ampG SacI F3/NL49142 ampG T272A F and NL49142 ampG T272A R/ampG 3' flank R BamHI. The primer sequences of NL49142 ampG T272A F and NL49142 ampG T272A R contain a missense mutation (ACA->GCA) that would result in substitution of residue 272 from a threonine to an alanine in the final gene product. The two PCR products were used in OE-PCR with primers MC ampG SacI F3 and ampG 3' flank R BamHI, and the final OE-PCR product was digested with SacI and BamHI and ligated into similarly digested pIDN3 to form pEC113 (P$_{ampGGC}$-*ampG*$_{\text{NL49142}}$T272A in pIDN3). pEC116 (P$_{ampGGC}$-*ampG*$_{\text{NL23970}}$A272T in pIDN3) was built with a similar strategy as pEC113, with two variations during the initial PCR reaction. Chromosomal DNA from EC540 was used as template in the PCR reaction, with primer pairs MC ampG SacI F3/NL23970 ampG A272T F and NL23970 ampG A272T R/ampG 3' flank R BamHI instead. *N. gonorrhoeae* MS11 was transformed with pEC113 or pEC116 to form EC561 and EC564, respectively.

Metabolic labeling of peptidoglycan with [^{3}H] glucosamine or [^{3}H] DAP and quantitative fragment release. Metabolic labeling of PG with [^{3}H] glucosamine or [^{3}H] DAP and

quantitative fragment release was performed essentially as described previously for *N. gonorrhoeae* (26–28). For [^{3}H] glucosamine labeling, strains were grown in cGCBL to mid-log phase, diluted to OD_{540} of 0.2 and pulse labeled with 10 μCi/ml [^{3}H] glucosamine in GCBL supplemented with 0.042% $NaHCO_3$ and modified Kellogg's supplements containing pyruvate instead of glucose for 30 minutes. The cells were washed to remove unincorporated label, and were suspended in cGCBL for the chase period. The cells were grown for 2.5 hours, after which cell-free supernatant was harvested by centrifugation at 3,000 x *g* for 10 minutes and filtration using a 0.22 μm filter. For quantitative fragment release, the amount of radiation (counts per minute, CPM) in the cell pellets were determined by liquid scintillation counting prior to the chase period, and normalized to each other. Labeling with [^{3}H] DAP was performed in a similar way as labeling with [^{3}H] glucosamine, with variations in the pulse labeling phase. Strains were grown in DMEM lacking cysteine supplemented with 25 μCi/ml [^{3}H] DAP, 100 μg/ml threonine and 100 μg/ml methionine for 60 minutes for the labeling phase. Released radiolabeled PG fragments are separated by tandem size-exclusion chromatography and detected by liquid scintillation counting.

RESULTS

Nonpathogenic *Neisseria* release PG fragments. PG fragments released by growing *N. gonorrhoeae* and *N. meningitidis* have been previously characterized ((20, 22, 23), Chapter 3) through the method of metabolic pulse-chase labeling of PG with [^{3}H] glucosamine and [^{3}H] diaminopimelic acid (DAP), which labels the glycan backbone and peptide stems of PG, respectively. [^{3}H] glucosamine labeled PG fragments released by WT cells typically resolve into four or five distinct peaks. The fifth peak, consisting of anhydro-*N*-acetylmuramic acid (anhMurNAc), is not always seen due to day-to-day variations. However, the relative amount of anhMurNAc released by different strains grown and subjected to metabolic labeling and quantitative fragment release on the same day are consistent. [^{3}H] DAP labeled PG fragments resolve into five or six distinct peaks, in which the sixth peak (DAP) also displays day-to-day variation and may appear as a shoulder on the fifth peak. The known structures of the PG fragments are summarized in Figure 1I.

We performed metabolic pulse-chase labeling of the PG of *N. sicca*, *N. mucosa*, *N. musculi* and macaque isolates AP312 and AP678 with [^{3}H] glucosamine. Consistent with previous observations, *N. sicca* and *N. mucosa* released PG monomers and disaccharide, with no discernable PG dimer peak (31) (Figure 1A-B). Like *N. sicca* and *N. mucosa*, macaque isolate AP312 released PG monomers and disaccharide but not PG dimers (Figure 1C). In contrast, *N. musculi* and macaque isolate AP678 released PG monomers, disaccharide and PG dimers (Figure 1D-F). Attempts to metabolically label PG of the two *N. lactamica* isolates, *N. lactamica* ATCC 23970 and *N. lactamica* ATCC 49142, with [^{3}H] glucosamine were not successful.

To characterize the PG fragments released by *N. lactamica* ATCC 23970 and *N. lactamica* ATCC 49142, the two isolates were labeled with [^{3}H] DAP. While both isolates

released PG dimers, PG monomers, and PG peptides, the relative amounts of PG fragments released by the two isolates differed (Figure 1G-H). *N. lactamica* ATCC 49142 released similar amounts of PG monomer and PG-derived peptides (Figure 1G), while *N. lactamica* ATCC 23970 released lower levels of PG monomer compared to PG-derived peptides (Figure 1H). Metabolic labeling of *N. musculi* PG with [^{3}H] DAP revealed that in contrast to both *N. lactamica* isolates, *N. musculi* released much lower levels of PG-derived peptides compared to PG monomers (Figure 1F). Similar analyses with *N. mucosa* and quantitative fragment release comparisons with *N. gonorrhoeae* showed that *N. mucosa* released more PG-derived peptides but lower levels of PG monomer compared to the pathogenic *N. gonorrhoeae* (Figure 2).

Analyses of PG recycling by animal-associated *N. musculi* and macaque isolate AP312 using mutation of *ampG*. AmpG is an inner membrane permease that transports PG monomers and anhydro-disaccharide from the periplasm to the cytoplasm for recycling in Gram-negative bacteria (32–34). Both *N. gonorrhoeae* and *N. meningitidis* recycle PG fragments in an AmpG-dependent manner, and deletion of *ampG* in either species results in a large increase in PG monomer and anhydro-disaccharide release (21, 28). By comparing the amount of PG released by *ampG* mutants compared to the amount released by WT strains, the normal amounts of PG recycled and released can be calculated. We previously demonstrated that the human-associated species *N. sicca* and *N. mucosa* encode a functional AmpG permease and recycles 95% of PG monomers liberated during growth ((31), Chapter 2).

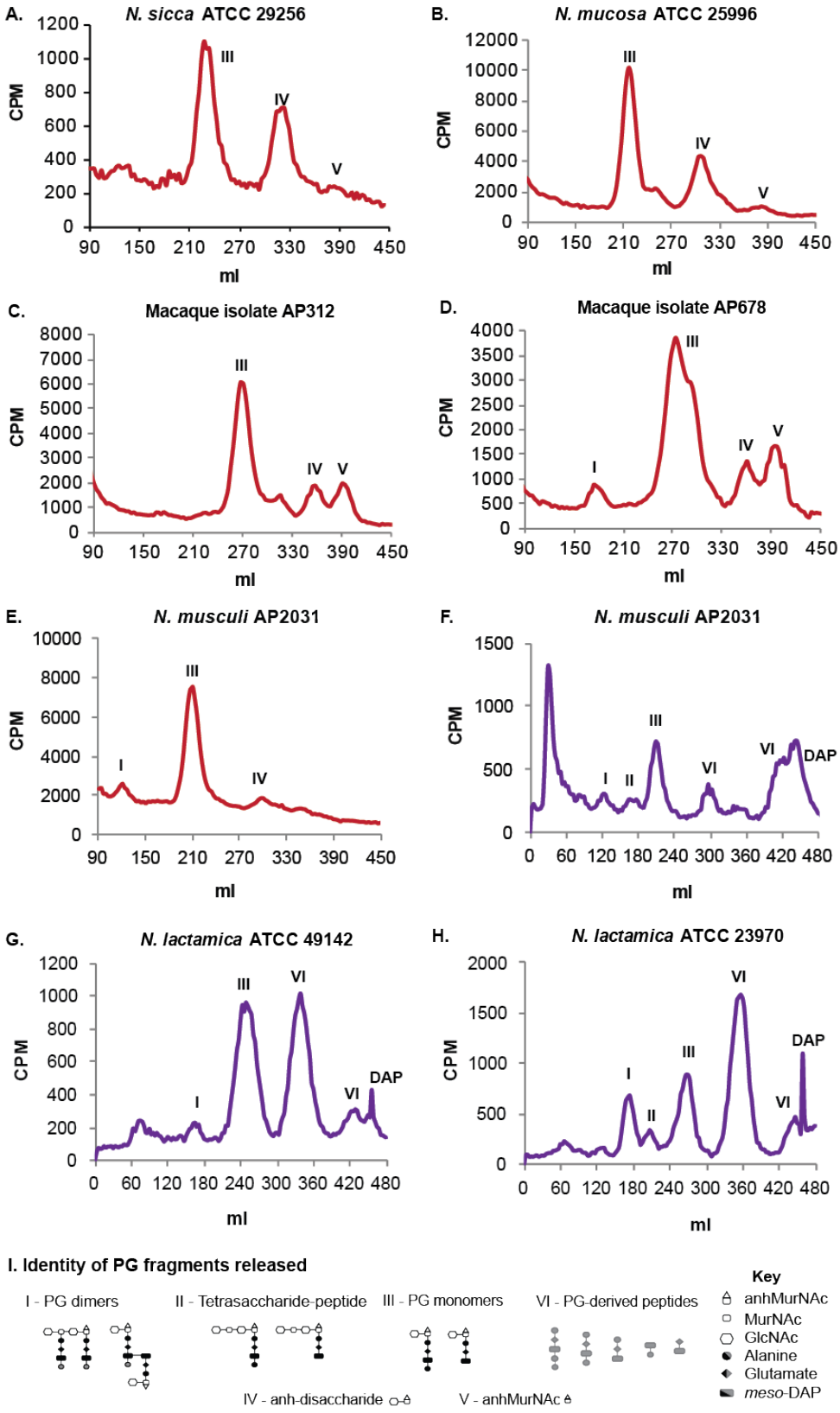
A.
N. sicca ATCC 29256
CPM
ml
III
IV
V
B.
N. mucosa ATCC 25996
C.
Macaque isolate AP312
D.
Macaque isolate AP678
I
E.
N. musculi AP2031
F.
N. musculi AP2031
II
VI
DAP
G.
N. lactamica ATCC 49142
H.
N. lactamica ATCC 23970
I. Identity of PG fragments released
I - PG dimers
II - Tetrasaccharide-peptide
III - PG monomers
VI - PG-derived peptides
IV - anh-disaccharide
V - anhMurNAc
Key
anhMurNAc
MurNAc
GlcNAc
Alanine
Glutamate
meso-DAP

Figure 1. Nonpathogenic human-associated and animal-associated *Neisseria* release PG fragments. Metabolic labeling of peptidoglycan with [^{3}H] glucosamine (A-E; red) and [^{3}H] DAP (F-H; purple) was performed with *N. sicca* ATCC 29256 (A), *N. mucosa* ATCC 25996 (B), macaque isolates AP312 (C) and AP678 (D), *N. musculi* AP2031 (E, F), *N. lactamica* ATCC 49142 (G) and ATCC 23970 (H). (I) Cartoon depictions of the PG fragments found in each peak, using symbols from Jacobs *et al.* (33) Structures in black has been determined by HPLC and mass spectrometry while structures in grey are predicted based on size and known activities of PG degrading enzymes. All strains tested released PG monomers (III). *N. lactamica, N. musculi* and macaque symbiont AP678 released PG dimers (I). However, *N. sicca*, *N. mucosa*, and macaque isolate AP312 released little to no PG dimers.

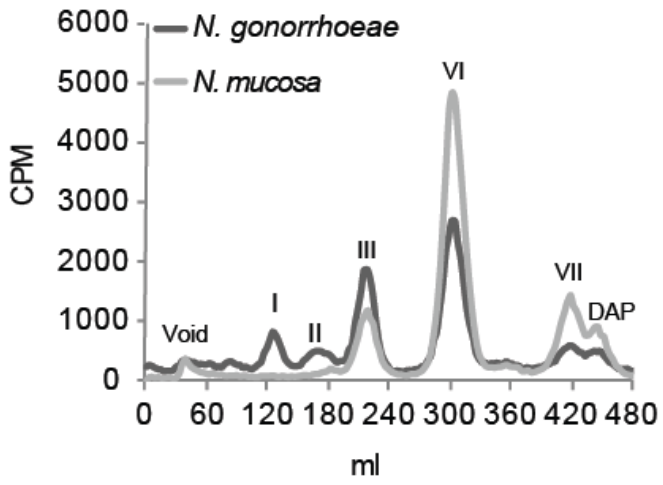

Figure 2. *Neisseria mucosa* released lower levels of PG monomers but higher levels of PG peptides compared to the pathogenic *Neisseria gonorrhoeae*. *N. mucosa* and *N. gonorrhoeae* were metabolically labeled with [^{3}H] DAP and quantitative fragment release analysis was performed. The nonpathogenic *N. mucosa* released less PG monomer (III), but more PG-derived peptides (VI, VII) compared to *N. gonorrhoeae*.

We mutated *ampG* in *N. musculi* and macaque isolate AP312 by insertional inactivation with an antibiotic resistance marker and determined the PG fragment release profile of the *ampG* mutants. Mutation of *ampG* in both *N. musculi* and macaque isolate AP312 resulted in a 8.7-fold and 10.8-fold increase in PG monomer release, respectively, with modest changes to anhydro-disaccharide release (Figure 3A-B). *N. musculi* releases around 12% and recycles around 88% of PG monomer generated during growth, while macaque isolate AP312 releases 10% and recycles approximately 90% of PG monomers. *N. musculi* released very little PG dimers, while AP312 did not release observable amounts of PG dimers (Figure 1C, 1E, 1F). Like other *Neisseria* species, mutation of *ampG* did not alter PG dimer release in *N. musculi* or in macaque isolate AP312. (Figure 3A-B) This observation is consistent with the reported inability of *E. coli* AmpG to transport PG dimers (34).

The difference in PG monomer release by *N. lactamica* ATCC 23970 and *N. lactamica* ATCC 49142 is partially due to a single nucleotide polymorphism in AmpG. We were unable to genetically manipulate either *N. lactamica* isolate to study PG recycling in *N. lactamica*. As an alternative strategy, we expressed *N. lactamica* ATCC 23970 *ampG* (*ampG*$_{NL23970}$) or *N. lactamica* ATCC 49142 *ampG* (*ampG*$_{NL49142}$) in *N. gonorrhoeae* in lieu of the native gonococcal *ampG* (*ampG*$_{GC}$). Expression of *N. lactamica ampG* in this background is driven by the native *ampG*$_{GC}$ promoter. Determination of the amount of PG monomers released by the allelic replacement mutants relative to the amount released by WT *N. gonorrhoeae* will allow us to determine if *N. lactamica* AmpG is more, less, or equally efficient as AmpG$_{GC}$. Curiously, expression of *ampG*$_{NL23970}$, but not of *ampG*$_{NL49142}$ in *N. gonorrhoeae* resulted in lower levels of PG monomer release compared to WT *N. gonorrhoeae* (Figure 4).

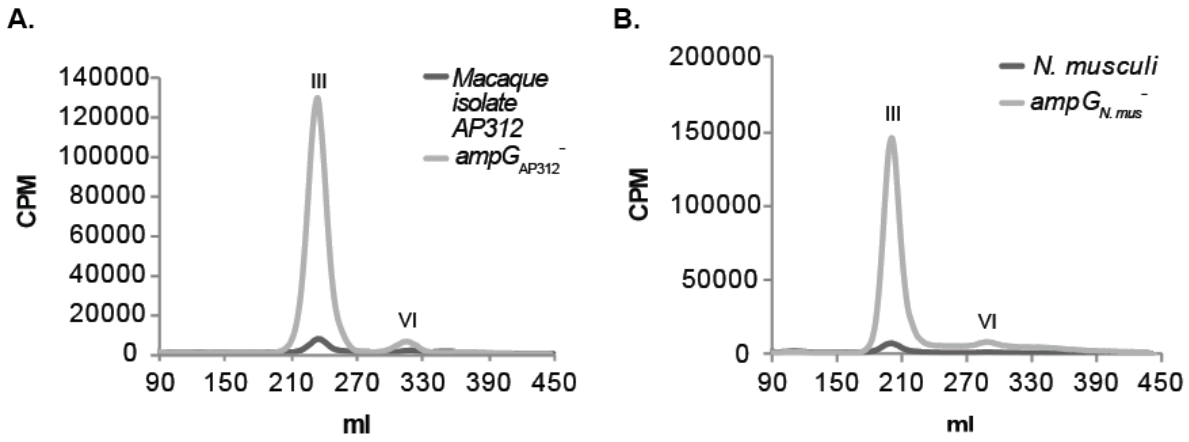

Figure 3. Mutation of *ampG* impaired PG fragment recycling in *N. musculi* and macaque symbiont AP312. Mutation of *ampG* in *N. musculi* (A) and the macaque isolate AP312 (B) resulted in a large increase in the amount of PG monomer (III) and disaccharide (IV) release, without affecting PG dimer release.

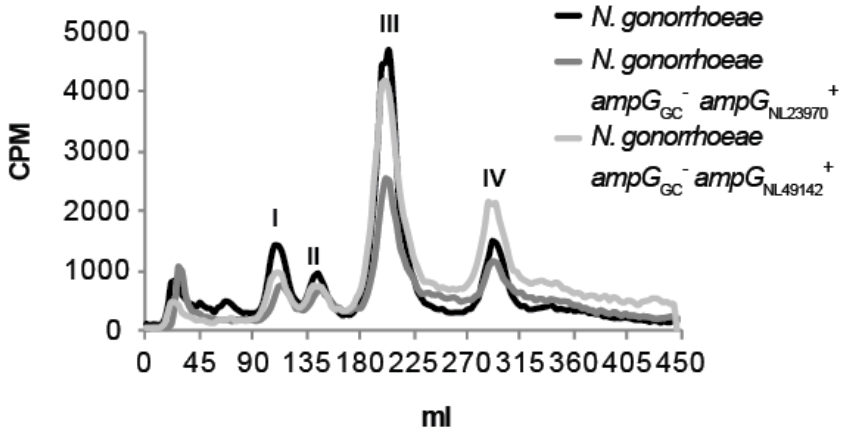

Figure 4. Gonococcal *ampG*$^{-}$ strains expressing *ampG* from two different strains of *N. lactamica* released different amounts of PG monomer. The *ampG* gene from *N. lactamica* ATCC 49142 or *N. lactamica* ATCC 23970 were expressed in *N. gonorrhoeae* in lieu of the native gonococcal *ampG* gene. Expression of $ampG_{NL23970}$ but not $ampG_{NL49142}$ in *N. gonorrhoeae* reduced the amount of PG monomer (III) released by the mutant strain.

The gonococcal strain expressing *ampG*$_{NL49142}$ released similar levels of PG monomer as WT (Figure 3). These results suggest that AmpG$_{NL49142}$ transports similar amounts of PG monomer as AmpG$_{GC}$, while AmpG$_{NL23970}$ is the most efficient at recycling of the three.

AmpG$_{NL49142}$ and AmpG$_{NL23970}$ differ only by five residues. Previous work established that natural polymorphisms of gonococcal and meningococcal AmpG at residues 391, 398 and 402 contribute to differences in PG monomer release in these two pathogenic *Neisseria* ((31), Chapter 2). Both isolates of *N. lactamica* encode the same amino acids at AmpG positions 391, 398 and 402. We compared AmpG sequences from the two *N. lactamica* isolates, *N. gonorrhoeae* and *N. meningitidis*, and one of the five aforementioned residues is only found in AmpG$_{NL49142}$. AmpG residue 272 is a threonine in *N. lactamica* ATCC 49142, and is an alanine in the other three species. We performed site-directed mutagenesis to determine if AmpG residue 272 plays a role in modulating AmpG efficiency in *N. lactamica*.

Expression of *ampG*$_{NL49142}$T272A in *N. gonorrhoeae* lacking *ampG*$_{GC}$ resulted in lower levels of PG monomer release compared to WT *N. gonorrhoeae* (Figure 5A), mimicking the phenotype seen when *ampG*$_{NL23970}$ is expressed by *N. gonorrhoeae.* Additionally, expression of *ampG*$_{NL23970}$A272T *in N. gonorrhoeae* resulted in WT-like levels of PG monomer release, which phenocopied the gonococcal strain expressing *ampG*$_{NL49142}$ (Figure 5B). We conclude that *N. lactamica* ATCC 23970 is better at recycling PG monomers compared to *N. lactamica* ATCC 49142 due to a polymorphism at AmpG site 272, which contributes in part to differences in the amount of PG fragments released by the two *N. lactamica* isolates.

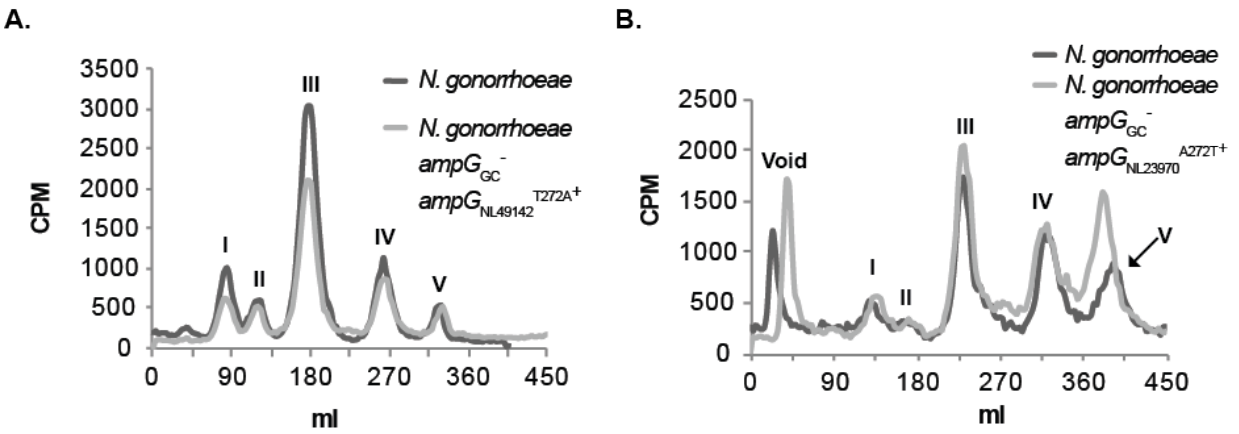

Figure 5. Polymorphism of *N. lactamica* AmpG contribute to the differences in the amounts of PG monomer released. A) *N. gonorrhoeae* expressing *ampG*$_{NL49142}$ with a single substitution at AmpG$_{NL49142}$ residue 272 from a threonine to an alanine show reduced PG monomer release by around half. B) *N. gonorrhoeae* expressing *ampG*$_{NL23970}$ with a single substitution at AmpG$_{NL23970}$ residue 272 from an alanine to a threonine released *N. gonorrhoeae* WT-like levels of PG monomer.

DISCUSSION

Due to the role of PG monomers in causing damage to mucosal epithelium by inducing death and sloughing of ciliated cells during *N. gonorrhoeae* and *Bordetella pertussis* infections, we hypothesized that nonpathogenic *Neisseria* would release very little to no inflammatory PG fragments. The first characterization of PG fragments released by *N. sicca* and *N. mucosa*, performed as quantitative fragment release in comparison to *N. gonorrhoeae*, showed that both species release lower levels of proinflammatory PG monomers compared to *N. gonorrhoeae* and no PG dimers (31). It was logical to infer that the reduced PG monomer release by *N. sicca* and *N. mucosa* means that nonpathogenic *Neisseria* are less inflammatory compared to *N. gonorrhoeae*. This inference is also supported by the observation that nonpathogenic human-associated *Neisseria* induce lower Toll-like receptor (TLR4) response compared to *N. gonorrhoeae* and *N. meningitidis* (35). TLR4 is an innate immune receptor that responds to lipopolysaccharide and lipooligosaccharide (LOS) (36). LOS from *N. cinerea*, *N. flavescens*, *N. perflava* and *N. subflava* lack lipid A modification that is seen with LOS from *N. gonorrhoeae* and *N. meningitidis* (35).

As we continue to investigate PG fragment release by more strains of human- and animal-associated *Neisseria*, it became clear that the situation is not as simple as we initially hypothesized. There are both interspecies and intraspecies variations in PG fragment release patterns. *N. sicca*, *N. mucosa* and macaque isolate AP312 did not release PG dimers (peak I), while *N. lactamica*, *N. musculi* and macaque isolate AP678 released PG dimers (Figure 1). The two strains of *N. lactamica* tested also showed differences in the relative amounts of PG monomer (peak III) and PG peptides (peaks VI) released (Figure 1). Labeling of *N. mucosa* with [^{3}H] DAP revealed that although *N. mucosa* released less PG monomer (peak III) compared to *N.*

gonorrhoeae, *N. mucosa* released more PG-derived peptides (peaks VI) that could also activate hNOD1 (Figure 2). *N. meningitidis*, which despite its ability to cause invasive disease is more commonly found as a colonizer of the nasopharyngeal space, also releases less PG monomer and more PG peptides compared to *N. gonorrhoeae* (Chapter 3). We were unable to metabolically label *N. sicca* with [^{3}H] DAP; however, given the similarities in PG fragment release between *N. sicca* and *N. mucosa* thus far, it is likely that *N. sicca* also releases more PG peptides.

The two strains of *N. lactamica* used in the study displayed differences in the relative amounts of PG monomer and PG peptides released in part due to differences in the efficiency of PG recycling. Such intraspecies variation in PG monomer release has been observed previously with two different isolates of *N. meningitidis* that have polymorphisms at AmpG residues 398 and 402 (31). We identified another AmpG residue (residue 272) capable of modulating PG recycling efficiency and indirectly controlling the amount of PG monomer released. AmpG residue 272 is a threonine in *N. lactamica* ATCC 49142 and an alanine in *N. lactamica* ATCC 23970, WT *N. gonorrhoeae* and WT *N. meningitidis*. This finding suggests that different species of *Neisseria* independently evolved strategies to fine-tune the amount of PG fragments released. According to ATCC, *N. lactamica* ATCC 49142 is a clinical isolate, while *N. lactamica* ATCC 23970 is nasopharyngeal isolate. *N. lactamica* can infrequently cause invasive disease in immunocompromised individuals (18), and it is not known if the clinical isolate *N. lactamica* ATCC 49142 was isolated from a sick or a healthy individual. It is possible that alterations to PG fragment release allowed the two strains to colonize different body sites more effectively.

The recent establishment of macaque and mice-associated *Neisseria* as model organisms provide avenues for studying aspects of *Neisseria* colonization and infection in their cognate host organisms (10, 11, 17). One caveat of using mice as a model organism for understanding PG

fragment release by humans is that the murine NOD1 detects tetrapeptide monomers instead of tripeptide monomers like the human NOD1 (37). Still, our findings indicate that both macaque isolates and *N. musculi* release PG monomers, and that macaque isolate AP312 and *N. musculi* recycle PG fragments liberated during turnover (Figure 1, 3). Preliminary results suggest that *N. musculi* and the *ampG* mutant of macaque isolate AP312 release both tripeptide and tetrapeptide monomer. Our ability to mutate genes in macaque isolate AP312 and *N. musculi* provides us with tools to vary the amounts and types of PG fragments that the host organism is exposed to, and to study the corresponding host response. We have already constructed *ampG* mutants that release approximately 8.7 times more PG monomers, and we also have other peptidoglycanase mutants in *N. musculi* that we could use in infection and colonization studies. Current work underway in our laboratory to generate complementation constructs for use in *N. musculi* would lead to more tools for studying animal-associated *Neisseria*. In conclusion, there are exciting new avenues for further research on the consequences of PG fragment release during infections.

ACKNOWLEDGEMENT

We would like to thank Nate Weyand for the gift of *N. sicca* ATCC 29256, *N. mucosa* ATCC 25996, *N. musculi* AP2031 and macaque isolates AP312 and AP678.

Table 1. Strains and plasmids used in this study.

Strain/ Plasmid	Description	Source/ Reference
Strains		
N. sicca ATCC 29256	*N. sicca* nasopharyngeal isolate	ATCC
N. mucosa ATCC 25996	*N. mucosa* pharyngeal isolate	ATCC
N. lactamica ATCC 49142	*N. lactamica* clinical isolate	ATCC
N. lactamica ATCC 23970	*N. lactamica* nasopharyngeal isolate	ATCC
N. musculi AP2031	*N. musculi* oral isolate	(11)
Macaque isolate AP312	*N. macacae*-like bite wound isolate	(10)
Macaque isolate AP678	*N. macacae*-like nasopharyngeal isolate	(10)
N. gonorrhoeae MS11	*N. gonorrhoeae* clinical isolate	(38)
DG132	Δ*ampG*$_{GC}$	(28)
EC2000	*ampG*$_{AP312}$::*cat*	This study
EC2003	*ampG*$_{Nmu}$::*kan*	(31)
EC2004	*ampG*$_{Nsi}$::*kan*	(31)
EC2005	*ampG*$_{Nmus}$::*kan*	This study
EC540	*ampG*$_{GC}^{-}$ *ampG*$_{NL23970}^{+}$	This study
EC544	*ampG*$_{GC}^{-}$ *ampG*$_{NL49142}^{+}$	This study
EC561	*ampG*$_{GC}^{-}$ *ampG*$_{NL49142}^{T272A+}$	This study
EC564	*ampG*$_{GC}^{-}$ *ampG*$_{NL23970}^{A272T+}$	This study
Plasmids		
pIDN3	Cloning vector (Erm^{R})	(39)
pKH6	Cloning vector (Cm^{R}); source of *cat*	(40)
pHSS6	Cloning vector (Kan^{R}); source of *kan*	(41)
pEC012	*ampG*$_{AP312}$::*cat* in pIDN3	This study
pEC088	P$_{ampGGC}$-*ampG*$_{NL49142}$ in pIDN3	This study
pEC089	P$_{ampGGC}$-*ampG*$_{NL23970}$ in pIDN3	This study
pEC095	*ampG*$_{Nmus}$ in pIDN3	This study
pEC096	*ampG*$_{Nmus}$::*kan* in pIDN3	This study
pEC113	P$_{ampGGC}$-*ampG*$_{NL49142}$T272A in pIDN3	This study
pEC116	P$_{ampGGC}$ -*ampG*$_{NL23970}$A272T in pIDN3	This study

Table 2. Primers used in this study. Restriction enzyme sites are underlined. Introduced missense mutations are in bold.

Primer name	Sequence
MC ampG SacI F3	ATTCAGAGCTCCATCGGCGGCATCATCAAAC
ampG 3' flank R BamHI	CTCAGGATCCGTTCTTTATATGAGCGGCAGG
AP312 ampG SacI F	GTATTGAGCTCGTCTTGTTCGGATTTCGTCTG
AP312 ampG BamHI R	GACTAGGATCCGTCCATTACTTCGGCGTATATGC
SOE-NL ampG F	GCTGTACGAACGATGACTGCATCGAAATCAGG
SOE-NL ampG R	GTTTGACGCGTTCATCTGCCTGCATCCTGAG
NL SOE-MS11 ampG 5' flank R	CCTGATTTCGATGCAGTCATCGTTCGTACAGC
NL SOE- MS11 ampG 3' flank F	GCAGGCAGATGAACGCGTCAAACTGGAGCG
NL49142 AmpG T272A F	GATTGCGAAAAAT**G**CAGGACTGTGGC
NL49142 AmpG T272A R	GCCACAGTCCTG**C**ATTTTTCGCAATC
NL23970 ampG A272T F	GATTGCGAAAAAT**A**CAGGACTGTGGC
NL23970 ampG A272T R	GCCACAGTCCTG**T**ATTTTTCGCAATC
AP2031 ampG SacI F	CGGCCGAGCTCCTTCGTTGATACAATAACC
AP2031 ampG BamHI R	CATTAGGATCCCGCAAACGGGTTTGCTGTGG

REFERENCES

1. **Knapp JS**. 1988. Historical perspectives and identification of *Neisseria* and related species. Clin Microbiol Rev **1**:415–431.
2. **Liu G**, **Tang CM**, **Exley RM**. 2015. Non-pathogenic *Neisseria*: members of an abundant, multi-habitat, diverse genus. Microbiology **161**:1297–1312.
3. **Stephens DS**, **Greenwood B**, **Brandtzaeg P**. 2007. Epidemic meningitis, meningococcaemia, and *Neisseria meningitidis*. Lancet **369**:2196–2210.
4. **Aas JA**, **Paster BJ**, **Stokes LN**, **Olsen I**, **Dewhirst FE**. 2005. Defining the normal bacterial flora of the oral cavity. J Clin Microbiol **43**:5721–5732.
5. **Keijser BJF**, **Zaura E**, **Huse SM**, **van der Vossen JMBM**, **Schuren FHJ**, **Montijn RC**, **ten Cate JM**, **Crielaard W**. 2008. Pyrosequencing analysis of the oral microflora of healthy adults. J Dent Res **87**:1016–1020.
6. **Zaura E**, **Keijser BJ**, **Huse SM**, **Crielaard W**. 2009. Defining the healthy "core microbiome" of oral microbial communities. BMC Microbiol **9**:259.
7. **Dewhirst FE**, **Chen T**, **Izard J**, **Paster BJ**, **Tanner ACR**, **Yu WH**, **Lakshmanan A**, **Wade WG**. 2010. The human oral microbiome. J Bacteriol **192**:5002–5017.
8. **Bogaert D**, **Keijser B**, **Huse S**, **Rossen J**, **Veenhoven R**, **van Gils E**, **Bruin J**, **Montijn R**, **Bonten M**, **Sanders E**. 2011. Variability and diversity of nasopharyngeal microbiota in children: A metagenomic analysis. PLoS One **6**.
9. **Gong H-L**, **Shi Y**, **Zhou L**, **Wu C-P**, **Cao P-Y**, **Tao L**, **Xu C**, **Hou D-S**, **Wang Y-Z**. 2013. The composition of microbiome in larynx and the throat biodiversity between laryngeal squamous cell carcinoma patients and control population. PLoS One **8**:e66476.
10. **Weyand NJ**, **Wertheimer AM**, **Hobbs TR**, **Sisko JL**, **Taku NA**, **Gregston LD**, **Clary S**, **Higashi DL**, **Biais N**, **Brown LM**, **Planer SL**, **Legasse AW**, **Axthelm MK**, **Wong SW**, **So M**. 2013. *Neisseria* infection of rhesus macaques as a model to study colonization, transmission, persistence, and horizontal gene transfer. Proc Natl Acad Sci U S A **110**:3059–64.
11. **Weyand NJ**, **Ma M**, **Phifer-Rixey M**, **Taku NA**, **Rendón MA**, **Hockenberry AM**, **Kim WJ**, **Agellon AB**, **Biais N**, **Suzuki TA**, **Goodyer-Sait L**, **Harrison OB**, **Bratcher HB**, **Nachman MW**, **Maiden MCJ**, **So M**. 2016. Isolation and characterization of *Neisseria musculi* sp. nov., from the wild house mouse. Int J Syst Evol Microbiol **66**:3585–3593.
12. **Gold R**, **Goldschneider I**, **Lepow ML**, **Draper TF**, **Randolph M**. 1978. Carriage of *Neisseria meningitidis* and *Neisseria lactamica* in infants and children. J Infect Dis **137**:112–121.
13. **Oliver KJ**, **Reddin KM**, **Bracegirdle P**, **Hudson MJ**, **Borrow R**, **Feavers IM**, **Robinson A**, **Cartwright K**, **Gorringe AR**. 2002. *Neisseria lactamica* protects against experimental meningococcal infection. Infect Immun **70**:3621–3626.
14. **Deasy AM**, **Guccione E**, **Dale AP**, **Andrews N**, **Evans CM**, **Bennett JS**, **Bratcher HB**, **Maiden MCJ**, **Gorringe AR**, **Read RC**. 2015. Nasal inoculation of the commensal *Neisseria lactamica* inhibits carriage of *Neisseria meningitidis* by young adults: A controlled human infection study. Clin Infect Dis **60**:1512–1520.
15. **Donati C**, **Zolfo M**, **Albanese D**, **Truong DT**, **Asnicar F**, **Iebba V**, **Cavalieri D**, **Jousson O**, **Filippo C De**, **Huttenhower C**, **Segata N**. 2016. Uncovering oral *Neisseria* tropism and persistence using metagenomic sequencing. Nat Microbiol **1**:1–9.
16. **Richards VP**, **Alvarez AJ**, **Luce AR**, **Bedenbaugh M**, **Mitchell ML**, **Burne RA**,

Nascimento M. 2017. Microbiomes of site-specific dental plaques from children with different caries status. Infect Immun **85**:e00106-17.

17. **Ma M**, **Powell DA**, **Weyand NJ**, **Rhodes KA**, **Rendón MA**, **Frelinger JA**, **So M**. 2018. A mouse model for *Neisseria* colonization. Infect Immun doi:10.1128/IAI.00839-17.
18. **Johnson AP**. 1983. The pathogenic potential of commensal species of *Neisseria*. J Clin Pathol **36**:213–23.
19. **Marri PR**, **Paniscus M**, **Weyand NJ**, **Rendon MA**, **Calton CM**, **Hernandez DR**, **Higashi DL**, **Sodergren E**, **Weinstock GM**, **Rounsley SD**, **So M**. 2010. Genome sequencing reveals widespread virulence gene exchange among human *Neisseria* species. PLoS One **5**:e11835.
20. **Melly MA**, **McGee ZA**, **Rosenthal RS**. 1984. Ability of monomeric peptidoglycan fragments from *Neisseria gonorrhoeae* to damage human Fallopian-tube. J Infect Dis **149**:378–386.
21. **Woodhams KL**, **Chan JM**, **Lenz JD**, **Hackett KT**, **Dillard JP**. 2013. Peptidoglycan fragment release from *Neisseria meningitidis*. Infect Immun **81**:3490–3498.
22. **Moreira LO**, **Zamboni DS**. 2012. NOD1 and NOD2 signaling in infection and inflammation. Front Immunol **3**:328.
23. **Morse SA**, **Bartenstein L**. 1974. Factors affecting autolysis of *Neisseria gonorrhoeae*. Proc Soc Exp Biol Med **145**:1418–1421.
24. **Kellogg DS**, **Peacock WL**, **Deacon WE**, **Brown L**, **Pirkle CI**. 1963. *Neisseria gonorrhoeae*: Virulence genetically linked to clonal variation. J Bacteriol **85**:1274–1279.
25. **Dillard JP**. 2011. Genetic manipulation of *Neisseria gonorrhoeae*. Curr Protoc Microbiol **4**:Unit4A.2.
26. **Rosenthal RS**, **Dziarski R**. 1994. Isolation of peptidoglycan and soluble peptidoglycan fragments. Methods Enzymol **235**:253–285.
27. **Cloud KA**, **Dillard JP**. 2002. A lytic transglycosylase of *Neisseria gonorrhoeae* is involved in peptidoglycan-derived cytotoxin production. Infect Immun **70**:2752–2757.
28. **Garcia DL**, **Dillard JP**. 2008. Mutations in *ampG* or *ampD* affect peptidoglycan fragment release from *Neisseria gonorrhoeae*. J Bacteriol **190**:3799–3807.
29. **Rosenthal RS**. 1979. Release of soluble peptidoglycan from growing gonococci: hexaminidase and amidase activities. Infect Immun **24**:869–878.
30. **Sinha RK**, **Rosenthal RS**. 1980. Release of soluble peptidoglycan from growing gonococci: Demonstration of anhydro-muramyl-containing fragments. Infect Immun **29**:914–925.
31. **Chan JM**, **Dillard JP**. 2016. *Neisseria gonorrhoeae* crippled its peptidoglycan fragment permease to facilitate toxic peptidoglycan monomer release. J Bacteriol **198**:3029–3040.
32. **Korfmann G**, **Sanders CC**. 1989. *ampG* is essential for high-level expression of AmpC beta-lactamase in *Enterobacter cloacae*. Antimicrob Agents Chemother **33**:1946–1951.
33. **Jacobs C**, **Huang L**, **Bartowsky E**, **Normark S**, **Park JT**. 1994. Bacterial cell wall recycling provides cytosolic muropeptides as effectors for beta-lactamase induction. EMBO J **13**:4684–4694.
34. **Cheng Q**, **Park JT**. 2002. Substrate specificity of the AmpG permease required for recycling of cell wall anhydro-muropeptides. J Bacteriol **184**:6434–6436.
35. **John CM**, **Liu M**, **Phillips NJ**, **Yang Z**, **Funk CR**, **Zimmerman LI**, **Griffiss M**, **Stein DC**, **Jarvis GA**. 2012. Lack of lipid A pyrophosphorylation and functional *lptA* reduces inflammation by *Neisseria* commensals. Infect Immun **80**:4014–4026.

36. **Shimazu R**, **Akashi S**, **Ogata H**, **Nagai Y**, **Fukudome K**, **Miyake K**, **Kimoto M**. 1999. MD-2, a molecule that confers lipopolysaccharide responsiveness on Toll-like receptor 4. J Exp Med **189**:1777–1782.
37. **Magalhaes JG**, **Philpott DJ**, **Nahori M-A**, **Jéhanno M**, **Fritz J**, **Le Bourhis L**, **Viala J**, **Hugot J-P**, **Giovannini M**, **Bertin J**, **Lepoivre M**, **Mengin-Lecreulx D**, **Sansonetti PJ**, **Girardin SE**. 2005. Murine Nod1 but not its human orthologue mediates innate immune detection of tracheal cytotoxin. EMBO Rep **6**:1201–1207.
38. **Swanson J**. 1972. Studies on gonococcus infection. II. Freeze-fracture, freeze-etch studies on gonococci. J Exp Med **136**:1258–1271.
39. **Hamilton HL**, **Schwartz KJ**, **Dillard JP**. 2001. Insertion-duplication mutagenesis of *Neisseria*: Use in characterization of DNA transfer genes in the gonococcal genetic island. J Bacteriol **183**:4718–4726.
40. **Woodhams KL**, **Benet ZL**, **Blonsky SE**, **Hackett KT**, **Dillard JP**. 2012. Prevalence and detailed mapping of the gonococcal genetic island in *Neisseria meningitidis*. J Bacteriol **194**:2275–2285.
41. **Mehr IJ**, **Long CD**, **Serkin CD**, **Seifert HS**. 2000. A homologue of the recombination-dependent growth gene, *rdgC*, is involved in gonococcal pilin antigenic variation. Genetics **154**:523–532.

CHAPTER 5

Discussion

This thesis describes research progress in studying inflammatory PG fragment release and recycling in multiple species of pathogenic and nonpathogenic *Neisseria.* Seminal work on the release of PG fragments by *Neisseria gonorrhoeae* and the toxic effects of PG monomers on ciliated Fallopian tube explants were first described almost forty years ago (1, 2). Since then, there have been great strides in identifying and understanding the mechanisms of PG degrading enzymes (peptidoglycanases) that generate these fragments. At the start of my PhD studies, it was known that the production and release of inflammatory PG monomers by *N. gonorrhoeae* is facilitated by two lytic transglycosylases, LtgA and LtgD, and that 85% of PG monomers generated in the periplasm are recycled instead of released (3, 4). In 2012, ongoing work in the Dillard laboratory looking at PG fragment release by a closely related species, *N. meningitidis*, revealed that *N. meningitidis* too released PG fragments, albeit at different amounts compared to *N. gonorrhoeae*, and this difference led to lower levels of hNOD1 activation by *N. meningitidis* compared to *N. gonorrhoeae* (Appendix 1; also published as (5)). This study, which was published in 2013, suggested that differences in PG recycling efficiency impact the release of inflammatory PG monomers (5).

The aim of my thesis work is to expand our knowledge on the recycling and release of PG fragments by *N. meningitidis* and other nonpathogenic species of *Neisseria.* Chapter 2 describes a mechanism underlying the differences in PG monomer release by the pathogens *N. gonorrhoeae* and *N. meningitidis.* Chapter 3 details the characterization of PG-derived peptides generated and released by *N. meningitidis* and the study of the effects of abolishing peptide release on the bacterium. Chapter 4 describes characterization PG fragment release by nonpathogenic species of *Neisseria* that typically colonize the nasopharyngeal and oropharyngeal space of humans, macaques and mice without causing disease.

Increased peptidoglycan monomer release by *N. gonorrhoeae* compared to *N. meningitidis* is in part controlled by differences in AmpG-dependent recycling (Chapter 2)

The amount of inflammatory PG monomers released by *N. meningitidis* is 2.8x lower than that released by *N. gonorrhoeae* (Appendix 1, (5)). The difference in PG monomer release between the two species is in part mediated by differences in AmpG-dependent recycling. AmpG is an integral inner membrane protein that functions to transport PG fragments with a minimal subunit of an anhydro-disaccharide from the periplasm to the cytoplasm for recycling (6). I showed that expression of meningococcal *ampG* in lieu of the native gonococcal *ampG* reduced PG monomer release by *N. gonorrhoeae* by ~50% (5). This observation suggests that AmpG is a major, but not the sole determinant of the amount of PG fragment released by *N. gonorrhoeae* and *N. meningitidis*.

Gonococcal and meningococcal AmpG have 97% identity and differ only by 9 residues. Through chimeric protein analysis and site-directed mutagenesis, I determined that three residues near the C-terminal end of AmpG, which are residues 391, 398 and 402, work cooperatively to modulate AmpG efficiency. Substitution of all three residues from the gonococcal to the meningococcal variants reduced PG monomer release by *N. gonorrhoeae* by 50%. I surveyed the AmpG sequences of multiple *N. gonorrhoeae* and *N. meningitidis* strains, and found that all gonococcal strains have the same amino acids at positions 391, 398 and 402 while meningococcal strains have more heterogeneity in the identity of the residues. A meningococcal clinical isolate that has gonococcal-like residues 398 and 402 released more PG monomers compared to our usual WT strain. Our results suggest that *N. gonorrhoeae* evolved and maintained specific AmpG residues to facilitate consistently higher levels of PG monomer release compared to *N. meningitidis*.

Structural modeling places AmpG residues 391, 398 and 402 near the periplasmic face of the protein. Based on the position of the residues, it is unlikely that they play a role in directly binding PG fragments. However, these residues may play a role in modulating conformational changes necessary for uptake, or may mediate protein-protein interactions with PGases such as the lytic transglycosylase LtgA. LtgA is responsible for generating for 38% of PG monomer released by *N. gonorrhoeae* (7). The other 62% of released PG fragments are generated by LtgD (8). However, mutation of both *ltgA* and *ampG* revealed that LtgA generates more PG monomers in the periplasm compared to LtgD, suggesting that most of the PG fragments liberated by LtgA action are recycled (9). Perhaps the meningococcal residues at AmpG positions 391, 398 and 402 allow for better association between AmpG and LtgA or an adaptor protein to facilitate efficient recycling. Pulldown, coimmunoprecipitation and BACTH (bacterial adenylate cyclase based two hybrid systems) assays may be useful to identify potential AmpG interaction partners and to determine if AmpG interacts with other proteins to facilitate efficient PG recycling.

My findings also suggest that the release of inflammatory PG monomer is more important for gonococcal biology than for meningococcus. Cell-free supernatant from *N. gonorrhoeae* has demonstrated toxic effects and causes death and extrusion of ciliated Fallopian tube cells, while cell-free supernatant from *N. meningitidis* does not cause similar death of ciliated nasopharyngeal cells isolated from tonsil tissue (2, 10). It is possible that the release of inflammatory PG monomers is important for the establishment of colonization in the upper female reproductive tract or other body sites such as the cervix or the urethra by *N. gonorrhoeae*. However, uncontrolled release of PG monomers and lack of PG recycling are likely to be detrimental to *N. gonorrhoeae*. Preliminary data suggest that an *ampG* mutant has a minor growth defect compared to WT when grown in low glucose media. While mutation of any one of

three different AmpG residues (A154, G273, G385) to an aspartate increased PG monomer release to similar levels as an *ampG* deletion mutant (Appendix 4), such mutations are not seen in nature. Hence, gonococcus has evolved exquisite methods to increase and potentially control the amounts of PG monomer released to induce optimal levels of inflammation while maintaining mechanisms for PG recycling. Future comparative studies of peptidoglycanases encoded by *N. gonorrhoeae* and *N. meningitidis* will inform other mechanisms employed by gonococcus to increase PG fragment release.

Release of hNOD1-activating PG-derived peptides by *N. meningitidis* (Chapter 3)

As previously established, *N. meningitidis* releases lower levels of PG monomers compared to *N. gonorrhoeae*. However, *N. meningitidis* released higher levels of PG-derived peptides compared to PG monomers. Like tripeptide monomer, free tripeptide can also be recognized by the innate immune receptor hNOD1, resulting in the induction of an inflammatory response. We determined that such peptides are generated by the periplasmic *N*-acetylmuramyl-L-alanine amidase AmiC, and deduced that WT-like AmiC activity requires the presence of the activator protein NlpD based on our data and published observations of AmiC and NlpD homologues in other organisms. *In vitro* experiments using purified gonococcal AmiC and NlpD (11, 12), as well purified *E. coli* AmiC and NlpD (13) demonstrated that AmiC's PGase activity is significantly enhanced by the presence of NlpD, and that NlpD is unlikely to be catalytically active. Additionally, crystallography and biochemical studies show that *E. coli* NlpD binds to *E. coli* AmiC, and suggests that *E. coli* NlpD displaces an autoinhibitory loop that prevents substrate access to the *E. coli* AmiC active site (14). Mutation of *amiC* or *nlpD* in *N. meningitidis* abolished peptide release, and caused cell-separation defects. *N. meningitidis* usually presents as

diplococci or monococci. When *amiC* or *nlpD* is mutated, mutant cells formed clumps of five or more cells, and frequently there are dozens of cells in one cluster.

Stochastic optical reconstruction microscopy (STORM) analysis showed that NlpD-FLAG3 localized as a band between two DNA foci, which we interpret as the septum, and can also be found distributed non-randomly with spots of enrichment around the cell. It is unclear if NlpD activates AmiC activity at sites other than the septum, or if NlpD is recruited to specific spots around the cell to sequester NlpD away from AmiC when the cell is not dividing. Use of dual-color STORM imaging to look at co-localization of proteins is a novel technique that can potentially be applied to answer this question (15, 16). If AmiC and NlpD work together to cleave peripheral PG when the cell is not actively dividing, the two proteins would co-localize at the periphery of cell when visualized by dual-color STORM imaging. If NlpD and AmiC do not co-localize except at the septum, it would provide support to the hypothesis that AmiC exclusively digests septal PG, and is only active during cell separation.

In contrast to *N. gonorrhoeae,* which primarily releases PG monomers, *N. meningitidis* predominantly releases PG-derived peptides. The nonpathogenic species *N. mucosa* also releases more peptides compared to PG monomers (Chapter 4). Abolishing PG peptide release by mutating *amiC* significantly reduced the hNOD1 activation capability of *N. meningitidis*, but not of *N. gonorrhoeae*, compared to their respective WT strains as tested with a reporter cell line (Chapter 3, (11)). The stark differences in the amount and the consequence of PG peptide release by gonococcus and meningococcus suggest that release of PG-peptides, like that of PG monomers, is a regulated process. If and how the release of PG peptides is regulated are open questions. Several hypotheses that can be tested include: (i) meningococcal AmiC acts at non-septal sites to generate PG peptides fated for release, while gonococcal AmiC only acts at the

septum, (ii) gonococcus encodes an uncharacterized inner membrane transporter/recycling protein for PG peptides that is absent or less efficient in meningococcus, (iii) meningococcus encodes an outer membrane transporter that pumps PG peptides out of the cell that is absent or less efficient in gonococcus.

Peptidoglycan fragment release by nonpathogenic *Neisseria* (Chapter 4)

Multiple species of human associated nonpathogenic *Neisseria* form the healthy core oral microbiome (17). As such, nonpathogenic *Neisseria* are commonly found associated with, and may colonize all humans. We investigated if nonpathogenic *Neisseria* release PG fragments, with the initial hypothesis that nonpathogenic *Neisseria* would release little to no inflammatory PG fragments. I characterized PG fragment release by four strains from three species of human associated *Neisseria*, *N. sicca*, *N. mucosa* and *N. lactamica*. None of the four strains examined released higher levels of PG monomers compared to *N. gonorrhoeae*, and in fact three of the four released only about half the amount released by gonococcus. However, *N. mucosa* released higher levels of PG peptides compared to *N. gonorrhoeae*, while the two strains of *N. lactamica* released similar or lower levels of PG peptides as gonococcus.

Examination of the PG fragment release profiles of two strains of *N. lactamica*, ATCC 49142 and ATCC 23970 revealed intraspecies variation in the amount of PG monomer released by these two strains. *N. lactamica* ATCC 49142 released similar levels of PG monomer but lower levels of PG peptides compared to *N. gonorrhoeae*. In contrast, *N. lactamica* ATCC 23970 released less PG monomer but similar levels of PG-derived peptides compared to gonococcus. The difference in PG monomer release between the two strains of *N. lactamica* was facilitated by differences in AmpG recycling efficiency. However, unlike in *N. gonorrhoeae* and *N.*

meningitidis, the difference in AmpG recycling efficiency was not mediated by differences in AmpG residues 391, 398 or 402. Instead, AmpG residue 272 modulated the amount of PG monomer released by *N. lactamica* ATCC 49142 and *N. lactamica* ATCC 23970. This residue is an alanine in *N. lactamica* ATCC 23970 as well as in *N. gonorrhoeae* and *N. meningitidis*, and a threonine in *N. lactamica* ATCC 49142. In fact, out of 31 strains surveyed for their AmpG protein sequence (Chapter 2), only *N. lactamica* ATCC 49142 and *N. elongata* ATCC 29315 encode a residue other than an alanine at position 272. The *N. elongata* ATCC 29315 residue at position 272 is a glycine. Residue 272 is predicted by structural modeling to be close to the substrate transporting channel. As such, residue 272 may play a role in interacting with PG fragments during PG transport. Uptake assays with purified PG monomers can help us determine if AmpG residue 272 plays a role in substrate transport. Ultimately, experimental determination of the AmpG structure, preferably with a bound substrate, would be very instructive in determining how AmpG residue 272 impacts PG recycling, as well as provide insight into the mechanism of PG fragment transport by AmpG.

Nonpathogenic *Neisseria*, despite the nomenclature, can very rarely cause invasive disease such as septicemia and endocarditis in patients predisposed to these conditions (18). *N. lactamica* ATCC 23970 was isolated from the nasopharynx, while *N. lactamica* ATCC 49142 was designated a clinical isolate. In the absence of additional information, it cannot be determined if *N. lactamica* ATCC 49142 was isolated from a healthy person, or from a person with invasive *N. lactamica* infection. However, if the latter is true, I speculate that selective pressures during infection favored increased PG monomer release. Comparative analysis of carriage and invasive disease isolates, coupled with mutation of isogenic strains for animal infection studies, would be ideal to determine the role of PG fragments in nonpathogenic and

pathogenic lifestyles of *Neisseria*. Such studies have not been carried out thus far due to the lack of a relevant animal model. This is because the species described thus far do not naturally infect mice or other common animal models, and in the case of *N. gonorrhoeae* and *N. meningitidis*, are also restricted to colonizing humans.

PG fragment release by animal-associated *Neisseria* (Chapter 4)

In the past decade, there is resurging interest in identifying *Neisseria* strains that naturally colonize animals to develop natural *Neisseria*-host organism models for studying colonization, persistence and transmission. From such efforts, strains of *Neisseria* that naturally colonize macaques and wild mice were identified, characterized and developed as models (19, 20). Such models provide us with the opportunity to examine the role of released PG fragments in colonization and infection in a relevant host organism. As a first step in adopting such models, I characterized the PG fragment release profiles of two macaque isolates, AP312 and AP678, as well as a mouse colonizer, *N. musculi* AP2031. Like human-associated strains, all three animal-associated isolates released PG monomers and disaccharide. Release of PG dimers *N. musculi* AP2031 were quite low and were close to the limit of detection using our assays. Macaque isolate AP312 did not release observable amounts of PG dimers. In conclusion, we established that these three isolates release PG fragments, including inflammatory PG monomers, with variations in PG dimer release.

The ability to genetically manipulate a model organism, allowing for studies of specific mutations in otherwise isogenic strains, is a powerful tool to dissect the cellular and molecular mechanisms of bacterial physiology and pathogenesis. As such, I designed insertional inactivation constructs to mutate *ampG* in these animal-associated strains. *N. gonorrhoeae*, *N.*

meningitidis, *N. sicca* and *N. mucosa* are naturally competent, and piliated cells are able to take up and perform homologous recombination to integrate exogenously supplied DNA into the chromosome. One requirement for DNA uptake is the presence of a DNA uptake sequence (DUS), the exact sequence of which varies slightly between species (21, 22). Using plasmids designed for genetic manipulation of *N. gonorrhoeae* and *N. meningitidis*, I was able to generate *ampG* mutants in the macaque isolate AP312 and *N. musculi* AP2031. The *ampG* mutants of AP312 and AP2031 released 10.8 and 8.7 times more PG monomers compared to the respective WT strains. Through this analysis, we established that AP312 and AP2031 recycle PG monomers through AmpG, and produced mutant strains that release high levels of inflammatory PG monomer for colonization and infection studies.

Constructing cloning plasmids for use with nonpathogenic *Neisseria* (Appendix 2)

Although both *N. sicca* and *N. mucosa* are naturally competent, transformation of *N. sicca* and *N. mucosa* using existing plasmids for *N. gonorrhoeae* were largely unsuccessful because the DUS recognized by *N. sicca* and *N. mucosa* (AG-DUS) differ from the DUS recognized by gonococcus (AT-DUS) (22). Using site-directed mutagenesis, I modified the existing AT-DUS sequence on the plasmid backbone of pIDN3 to the AG-DUS sequence. The resulting plasmid, pEC026, was used successfully to generate insertional inactivation *ampG* mutants in both *N. sicca* and *N. mucosa* (Chapter 2). Additionally, due to chromosomal rearrangements, the two genes that form the ectopic complementation loci for gonococcus and meningococcus are not found next to each other in *N. sicca* and *N. mucosa*. As such, my undergraduate student, Emma Rehnelt, and I designed and constructed new complementation

plasmids for use with *N. sicca* and *N. mucosa*. This effort increased the number of tools that we have to study the biology of nonpathogenic *Neisseria.*

Concluding remarks and future directions

A significant portion of my thesis work utilized comparative analysis of different species of *Neisseria*, revealing interesting similarities and differences in the PG fragment release profiles of various *Neisseria* isolates. For instance, all *Neisseria* species tested, whether pathogenic or nonpathogenic, human- or animal-associated, released inflammatory PG monomers during normal growth. However, the amount of PG monomer released and the extent of PG recycling showed interspecies and sometimes intraspecies variations. From such comparative studies, I found that two types of AmpG polymorphisms govern recycling efficiency and alter the amount of PG monomers released. The molecular mechanism(s) through which these polymorphisms modulate recycling efficiency is currently unknown. Based on the modeled positions of these polymorphic sites, we propose that AmpG residues 391, 398 and 402 facilitate protein-protein interactions between AmpG and other PGases, while AmpG residue 272 is involved in stabilization of the PG substrate during transport. AmpG is a major facilitator superfamily (MFS) transporter. MFS proteins are found in all kingdoms of life, and share little sequence identity but significant structural conservation (23). Further investigation on how the different residues identified modulate AmpG function, especially if the residues play a role in conformational changes required for substrate transport, would hopefully also inform the biology of MFS transporters.

The observation that all *Neisseria* species tested released proinflammatory PG monomers is particularly interesting. Few other species of Gram-negative bacteria are known to release

significant amounts of PG monomers during normal growth. Release of tetrapeptide PG monomers by *Bordetella pertussis* and *Vibrio fisheri* induces damage of ciliated epithelia, resulting in symptomatic disease or establishment of symbiosis, respectively (24, 25). The damage to ciliated tracheal cells during pertussis infections results in inefficient clearance of mucus and debris from the throat, and may first provide a safe, nutrient rich reservoir for *B. pertussis* to replicate in. One symptom of pertussis infections is severe and persistent coughing, which physically displaces the accumulated mucus and respiratory droplets. Thus, PG monomer release by *B. pertussis* is likely to facilitate dispersal and transmission of the bacterium.

It is not known if PG fragments play a role in facilitating transmission of *N. gonorrhoeae*. It is also unclear if gonococcal cells that have ascended to Fallopian tubes can be transmitted to an uninfected person, or if only gonococcal cells at the primary sites of infection (ie, cervix or urethra) are transmitted. Studies on the immunological consequences of PG fragment release by gonococcus have primarily focused on the Fallopian tube model because of the severity of the damage caused to the epithelium, as well as the long lasting health problems arising from complicated gonococcal infections. Unlike the Fallopian tube, which is a largely sterile site, the primary infection site in women is the cervix; the ectocervix encounters many different microbes and is likely less sensitive to bacterial products (26). It is possible that PG fragments contribute to the inflammatory environment during cervicitis, leading to vaginal discharge, which *N. gonorrhoeae* can theoretically use as a vehicle to infect another host, without large-scale tissue damage seen in Fallopian tube infections. Release of PG fragments may also be advantageous for colonization of a new body site. Recent outbreaks of meningococcal urethritis reminded us that *N. meningitidis* can also infect the urogenital tract (27, 28). It would be interesting to determine if meningococcal urethritis strains naturally release more PG monomers compared to

nasopharyngeal isolates, and if the urethritis strains are more likely to have gonococcal-like residues at AmpG residues 391, 398 and 402 that lead to increased PG monomer release. It may be worth investigating if increased PG monomer release help facilitate colonization of multiple body sites by pathogenic and nonpathogenic *Neisseria*.

Additionally, one hallmark of gonococcal urethritis is the discharge of purulent exudate from symptomatic men; these purulent exudates contain neutrophils that are filled with gonococcal cells. Treatment of Fallopian tube explants with PG fragments in filtered supernatant induces production of the chemoattractant IL-8, and IL-8 is known to recruit neutrophils to the site of infection (5). Gonococcus is able to replicate intracellularly in neutrophils, and neutrophils do not express hNOD1 and do not respond to hNOD1 agonists (29, 30). As such, the release of PG fragments may play a role in facilitating transmission of *N. gonorrhoeae* from an infected man to a naïve host. Expanding the range of tissues studied with various gonococcal PG mutants to include primary cervical or urethral tissue may be very informative in understanding the role(s) of PG fragment release during uncomplicated gonorrhea in both men and women.

Equally intriguing is the observation that *N. meningitidis* and *N. mucosa* released lower levels of PG monomers but higher levels of PG-derived peptides compared to *N. gonorrhoeae*. Both tripeptide PG monomer and free tripeptide induce hNOD1 activation (31, 32). However, tripeptide PG monomer, if internalized and processed by phagosomes to liberate the *N*-acetylglucosamine monosaccharide, may also activate the NLRP3 inflammasome (33). Unlike Fallopian tube explants, which are sensitive to treatment with hNOD1 agonists, treatment of gingival tissue and oral epithelial cell lines with iE-DAP, a synthetic hNOD1 agonist, altered gene expression without a concomitant inflammatory response that leads to tissue damage (2, 34–36). It is tempting to speculate that low levels of hNOD1 activation induced by the release of

PG peptides facilitate colonization of the nasal and oral spaces by *N. meningitidis* and other species of nonpathogenic *Neisseria*. By limiting PG monomer release, *N. meningitidis* and nonpathogenic *Neisseria* may avoid stimulating a large inflammatory response that may lead to immune clearance during asymptomatic colonization.

The animal-associated *Neisseria* that we have examined so far are nonpathogenic strains that are isolated from generally healthy animals. While macaque isolate AP312 was isolated from a bite wound, there was no report of a festering infection of the wound (19). As such, we do not know yet if a pathogenic animal-associated *Neisseria* would release similar levels of PG fragments as a nonpathogenic animal-associated strain, or if like *N. gonorrhoeae*, a pathogenic species would show increased release of inflammatory PG monomers. Nonetheless, with new animal models, especially the *N. musculi*-mouse model, we will be able to investigate the role of PG fragment release on colonization and infection during host-microbe interactions in the near future. The knowledge acquired from such studies would hopefully help the design of therapeutic agents for neisserial infections, perhaps to ameliorate symptoms and limit damage to tissues, or in the case of meningococcus, bias the bacterium to a nonpathogenic lifestyle.

References

1. **Rosenthal RS**. 1979. Release of soluble peptidoglycan from growing gonococci: hexaminidase and amidase activities. Infect Immun **24**:869–878.
2. **Melly MA**, **McGee ZA**, **Rosenthal RS**. 1984. Ability of monomeric peptidoglycan fragments from *Neisseria gonorrhoeae* to damage human Fallopian-tube. J Infect Dis **149**:378–386.
3. **Garcia DL**, **Dillard JP**. 2008. Mutations in *ampG* or *ampD* affect peptidoglycan fragment release from *Neisseria gonorrhoeae*. J Bacteriol **190**:3799–3807.
4. **Chan YA**, **Hackett KT**, **Dillard JP**. 2012. The lytic transglycosylases of *Neisseria gonorrhoeae*. Microb Drug Resist **18**:271–279.
5. **Woodhams KL**, **Chan JM**, **Lenz JD**, **Hackett KT**, **Dillard JP**. 2013. Peptidoglycan fragment release from *Neisseria meningitidis*. Infect Immun **81**:3490–3498.
6. **Cheng Q**, **Park JT**. 2002. Substrate specificity of the AmpG permease required for recycling of cell wall anhydro-muropeptides. J Bacteriol **184**:6434–6436.
7. **Cloud KA**, **Dillard JP**. 2002. A lytic transglycosylase of *Neisseria gonorrhoeae* is involved in peptidoglycan-derived cytotoxin production. Infect Immun **70**:2752–2757.
8. **Cloud-Hansen KA**, **Hackett KT**, **Garcia DL**, **Dillard JP**. 2008. *Neisseria gonorrhoeae* uses two lytic transglycosylases to produce cytotoxic peptidoglycan monomers. J Bacteriol **190**:5989–5994.
9. **Schaub RE**, **Chan YA**, **Lee M**, **Hesek D**, **Mobashery S**, **Dillard JP**. 2016. Lytic transglycosylases LtgA and LtgD perform distinct roles in remodeling, recycling, and releasing peptidoglycan in *Neisseria gonorrhoeae*. Mol Microbiol **102**:865–881.
10. **Stephens DS**, **Whitney AM**, **Melly MA**, **Hoffman LH**, **Farley MM**, **Frasch CE**. 1986. Analysis of damage to human ciliated nasopharyngeal epithelium by *Neisseria meningitidis*. Infect Immun **51**:579–585.
11. **Lenz JD**, **Stohl EA**, **Robertson R**, **Hackett KT**, **Fisher K**, **Xiong K**, **Lee M**, **Hesek D**, **Mobashery S**, **Seifert HS**, **Davies C**, **Dillard JP**. 2016. Amidase activity of AmiC controls cell separation and stem-peptide release and is enhanced by NlpD in *Neisseria gonorrhoeae*. J Biol Chem **291**:10916–10933.
12. **Stohl EA**, **Lenz JD**, **Dillard JP**, **Seifert HS**. 2016. The gonococcal NlpD protein facilitates cell separation by activating peptidoglycan cleavage by AmiC. J Bacteriol **198**:615–622.
13. **Uehara T**, **Parzych KR**, **Dinh T**, **Bernhardt TG**. 2010. Daughter cell separation is controlled by cytokinetic ring-activated cell wall hydrolysis. EMBO J **29**:1412–22.
14. **Rocaboy M**, **Herman R**, **Sauvage E**, **Remaut H**, **Moonens K**, **Terrak M**, **Charlier P**, **Kerff F**. 2013. The crystal structure of the cell division amidase AmiC reveals the fold of the AMIN domain, a new peptidoglycan binding domain. Mol Microbiol **90**:267–277.
15. **Rust MJ**, **Bates M**, **Zhuang X**. 2006. Sub-diffraction-limit imaging by stochastic optical reconstruction microscopy (STORM). Nat Methods **3**:793–795.
16. **Bates M**, **Huang B**, **Dempsey GT**, **Zhuang X**. 2007. Multicolor super-resolution imaging with photo-switchable fluorescent probes. Science **317**:1749–1754.
17. **Zaura E**, **Keijser BJ**, **Huse SM**, **Crielaard W**. 2009. Defining the healthy "core microbiome" of oral microbial communities. BMC Microbiol **9**:259.
18. **Johnson AP**. 1983. The pathogenic potential of commensal species of *Neisseria*. J Clin Pathol **36**:213–23.

19. **Weyand NJ**, **Wertheimer AM**, **Hobbs TR**, **Sisko JL**, **Taku NA**, **Gregston LD**, **Clary S**, **Higashi DL**, **Biais N**, **Brown LM**, **Planer SL**, **Legasse AW**, **Axthelm MK**, **Wong SW**, **So M**. 2013. *Neisseria* infection of rhesus macaques as a model to study colonization, transmission, persistence, and horizontal gene transfer. Proc Natl Acad Sci U S A **110**:3059–64.
20. **Ma M**, **Powell DA**, **Weyand NJ**, **Rhodes KA**, **Rendón MA**, **Frelinger JA**, **So M**. 2018. A mouse model for *Neisseria* colonization. Infect Immun doi:10.1128/IAI.00839-17.
21. **Elkins C**, **Thomas CE**, **Seifert HS**, **Sparling PF**. 1991. Species-specific uptake of DNA by gonococci is mediated by a 10-base-pair sequence. J Bacteriol **173**:3911–3913.
22. **Frye SA**, **Nilsen M**, **Tonjum T**, **Ambur OH**. 2013. Dialects of the DNA Uptake Sequence in *Neisseriaceae*. PLoS Genet **9**:e1003458.
23. **Yan N**. 2015. Structural biology of the major facilitator superfamily transporters. Annu Rev Biophys **44**:257–283.
24. **Goldman WE**, **Klapper DG**, **Baseman JB**. 1982. Detection, isolation, and analysis of a released *Bordetella pertussis* product toxic to cultured tracheal cells. Infect Immun **36**:782–794.
25. **Koropatnick TA**, **Engle JT**, **Apicella MA**, **Stabb EV**, **Goldman WE**, **McFall-Ngai MJ**. 2004. Microbial factor-mediated development in a host-bacterial mutualism. Science **306**:1186–1188.
26. **Ghosh M**, **Shen Z**, **Fahey J V.**, **Crist SG**, **Patel M**, **Smith JM**, **Wira CR**. 2013. Pathogen recognition in the human female reproductive tract: expression of intracellular cytosolic sensors NOD1, NOD2, RIG-1, and MDA5 and response to HIV-1 and *Neisseria gonorrhea*. Am J Reprod Immunol **69**:41–51.
27. **Bazan JA**, **Peterson AS**, **Kirkcaldy RD**, **Briere EC**, **Maierhofer C**, **Turner AN**, **Licon DB**, **Parker N**, **Dennison A**, **Ervin M**, **Johnson L**, **Weberman B**, **Hackert P**, **Wang X**, **Kretz CB**, **Abrams AJ**, **Trees DL**, **Del Rio C**, **Stephens DS**, **Tzeng Y-L**, **DiOrio M**, **Roberts MW**. 2016. Notes from the field. Increase in *Neisseria meningitidis*-associated urethritis among men at two sentinel clinics - Columbus, Ohio, and Oakland County, Michigan, 2015. Morb Mortal Wkly Rep **65**:550–552.
28. **Bazan JA**, **Turner AN**, **Kirkcaldy RD**, **Retchless AC**, **Kretz CB**, **Briere E**, **Tzeng Y-L**, **Stephens DS**, **Maierhofer C**, **Del Rio C**, **Abrams AJ**, **Trees DL**, **Ervin M**, **Licon DB**, **Fields KS**, **Roberts MW**, **Dennison A**, **Wang X**. 2017. Large Cluster of *Neisseria meningitidis* urethritis in Columbus, Ohio, 2015. Clin Infect Dis **65**:92–99.
29. **Ekman A-K**, **Cardell LO**. 2009. The expression and function of Nod-like receptors in neutrophils. Immunology **130**:55–63.
30. **Criss AK**, **Seifert HS**. 2012. A bacterial siren song: intimate interactions between *Neisseria* and neutrophils. Nat Rev Microbiol **10**:178–90.
31. **Girardin SE**, **Boneca IG**, **Carneiro LAM**, **Antignac A**, **Jehanno M**, **Viala J**, **Tedin K**, **Taha M-K**, **Labigne A**, **Zahringer U**, **Coyle AJ**, **DiStefano PS**, **Bertin J**, **Sansonetti PJ**, **Philpott DJ**. 2003. Nod1 detects a unique muropeptide from Gram-negative bacterial peptidoglycan. Science **300**:1584–1587.
32. **Chamaillard M**, **Hashimoto M**, **Horie Y**, **Masumoto J**, **Qiu S**, **Saab L**, **Ogura Y**, **Kawasaki A**, **Fukase K**, **Kusumoto S**, **Valvano MA**, **Foster SJ**, **Mak TW**, **Nuñez G**, **Inohara N**. 2003. An essential role for NOD1 in host recognition of bacterial peptidoglycan containing diaminopimelic acid. Nat Immunol **4**:702–707.
33. **Wolf AJ**, **Reyes CN**, **Liang W**, **Becker C**, **Shimada K**, **Wheeler ML**, **Cho HC**, **Popescu**

NI, **Coggeshall KM**, **Arditi M**, **Underhill DM**. 2016. Hexokinase is an innate immune receptor for the detection of bacterial peptidoglycan. Cell **166**:624–636.

34. **Uehara A**, **Sugawara S**, **Tamai R**, **Takada H**. 2001. Contrasting responses of human gingival and colonic epithelial cells to lipopolysaccharides, lipoteichoic acids and peptidoglycans in the presence of soluble CD14. Med Microbiol Immunol **189**:185–192.
35. **Uehara A**, **Sugawara Y**, **Kurata S**, **Fujimoto Y**, **Fukase K**, **Kusumoto S**, **Satta Y**, **Sasano T**, **Sugawara S**, **Takada H**. 2005. Chemically synthesized pathogen-associated molecular patterns increase the expression of peptidoglycan recognition proteins via toll-like receptors, NOD1 and NOD2 in human oral epithelial cells. Cell Microbiol **7**:675–686.
36. **Lenz JD**, **Hackett KT**, **Dillard JP**. 2017. A single dual-function enzyme controls the production of inflammatory NOD agonist peptidoglycan fragments by *Neisseria gonorrhoeae*. MBio **8**:e01464-17.

APPENDIX 1

Peptidoglycan fragment release from *Neisseria meningitidis*

Katelynn L. Woodhams, Jia Mun Chan, Jonathan D. Lenz, Kathleen T. Hackett,

and Joseph P. Dillard

KL Woodhams and JP Dillard designed the experiments and wrote the manuscript.

KL Woodhams, JM Chan, JD Lenz and KT Hackett performed the experiments.

JM Chan's specific contribution is Figure 5.

Originally published as

Woodhams KL, Chan JM, Lenz JD, Hackett KT, Dillard JP. 2013. Peptidoglycan fragment release from *Neisseria meningitidis*. Infect Immun. **81**: 3490-3498.

ABSTRACT

Neisseria meningitidis (meningococcus) is a symbiont of the human nasopharynx. On occasion, meningococci disseminate from the nasopharynx to cause invasive disease. Previous work showed that purified meningococcal peptidoglycan (PG) stimulates human Nod1, which leads to activation of NF-κB and production of inflammatory cytokines. No studies have determined if meningococci release PG or activate Nod1 during infection. The closely related pathogen *N. gonorrhoeae* releases PG fragments during normal growth. These fragments induce inflammatory cytokine production and ciliated cell death in human fallopian tubes. We determined that meningococci also release PG fragments during growth, including fragments known to induce inflammation. We found that *N. meningitidis* recycles PG fragments via the selective permease AmpG, and that meningococcal PG recycling is more efficient than gonococcal PG recycling. Comparison of PG fragment release from *N. meningitidis* and *N. gonorrhoeae* showed that meningococci release less of the proinflammatory PG monomers than gonococci and degrade PG to smaller fragments. Released PG fragments in meningococcal supernatants induced significantly less Nod1-dependent NF-κB activity than released fragments in gonococcal supernatants and tended to induce less IL-8 secretion in primary Fallopian tube explants. These results support a model in which efficient PG recycling and extensive degradation of PG fragments lessens inflammatory responses, and may be advantageous for maintaining meningococcal carriage in the nasopharynx.

INTRODUCTION

Neisseria meningitidis (meningococcus, Mc) colonizes the nasopharynx of up to 40% of the healthy human adult population (1). In approximately 1000 cases annually in the United States, *N. meningitidis* disseminates from the nasopharynx to cause a highly inflammatory meningitis and septicemia. Even with treatment there is a high rate of morbidity and mortality associated with meningococcal disease. Giardin et al. (2003) showed that purified meningococcal peptidoglycan (PG) stimulates NF-κB activation via the intracellular pattern recognition receptor Nod1, which could contribute to the inflammatory state observed during invasive disease (2). That study demonstrated that *N. meningitidis* peptidoglycan is inflammatory, although it remains unclear if meningococci release PG during infection. Even though meningococcal disease is highly inflammatory, meningococci are usually carried asymptomatically, implying that the bacteria are able to control release of inflammatory compounds and/or have differential interactions with host cells.

N. gonorrhoeae (gonococcus, Gc) is the etiologic agent of the sexually transmitted disease gonorrhea and is closely related to *N. meningitidis*. During normal growth gonococci release fragments of cell wall-derived PG (3). Nearly 50% of gonococcal PG is broken down per generation, but in the recycling process most PG fragments are brought back into the cytoplasm, and a much lower percentage of PG fragments is released (4). Gonococci release 15% of their PG per generation (5). AmpG, a permease selective for 1,6-anhydro-muramyl residues, is required for PG recycling in gonococci and other gram-negative bacteria such as *E. coli* (5-7). An *ampG* deletion in gonococci leads to a large increase in PG monomer release (5).

Released PG fragments stimulate inflammation and cell damage in multiple bacterial infections. In *Bordetella pertussis* infection, release of the 1,6-anhydro-disaccharide tetrapeptide PG monomer (also known as tracheal cytotoxin, TCT) causes the death and sloughing of ciliated cells of the trachea (8-10). The mechanism involved in this cell damage, determined using the hamster tracheal ring model, demonstrated that the damage is immune mediated. Non-ciliated cells sense TCT and respond with IL-1 production (10). Ciliated cells respond to IL-1 with increased expression of iNOS, and the amount of nitric oxide produced is sufficient to kill the ciliated cells (10, 11). Similar pathology is seen in gonococcal infection of human fallopian tubes, and ciliated cells die and slough from the epithelium (12). The addition of gonococcal PG monomers (a mixture of 1,6-anhydro-disaccharide tetrapeptide and 1,6-anhydro-disaccharide tripeptide) was shown to recapitulate the cell damage (13). During *Shigella flexneri* infections, release of tripeptide monomer leads to Nod1 stimulation and inflammatory cytokine production (14). Human Nod1 specifically recognizes PG fragments containing DAP as the C-terminal amino acid, including tripeptide monomer (15). It is unclear if it is the tetrapeptide PG monomer (TCT), tripeptide PG monomer, or a combination of both that causes the ciliated cell damage in the fallopian tube.

N. gonorrhoeae typically causes an acute disease involving a large inflammatory reaction in the host, while *N. meningitidis* is most often an asymptomatic colonizer (1, 16). We hypothesized that differences between meningococci and gonococci in amounts or types of PG fragments released could contribute to the ability of meningococci to exist as a member of the nasopharyngeal microbiota rather than causing the inflammatory responses typical of gonococcal infections. We determined the identity and amounts of PG fragments released by meningococci. We also examined PG recycling in *N. meningitidis* and found that meningococci are very

efficient in uptake of liberated PG fragments, recycling 96% of PG monomers. Quantitative comparison with *N. gonorrhoeae* revealed that meningococci release less proinflammatory monomer than gonococci and differ in the ratio of tripeptide monomer and tetrapeptide monomer. In a direct test of inflammatory potential, supernatants from *N. meningitidis* were found to stimulate less NF-κB activation via Nod1 than supernatants from *N. gonorrhoeae*, suggesting that differences in the release and breakdown of PG fragments contribute to differences in the inflammatory response to the pathogenic *Neisseria*.

MATERIALS AND METHODS

Bacterial strains and growth conditions

All strains used for this study are listed in Table 1. Meningococci and non-piliated gonococci were both grown in gonococcal base liquid medium (GCBL) with Kellogg's supplements and 0.042% $NaHCO_3$ (cGCBL) with aeration or on GCB agar plates (Difco) in the presence of 5% CO_2 (17). *E. coli* were grown in LB broth or on LB agar plates (Difco). Chloramphenicol was used for selection at concentrations of either 25 μg/ml (*E. coli*) or 5 μg/ml (Mc). Kanamycin was used at 40 μg/ml (*E. coli*) and 80 μg/ml (Mc). Erythromycin was used for selection of meningococci at 10 μg/ml and for *E. coli* at a concentration of 500 μg/ml. IPTG was used at a concentration of 1mM to induce expression of the *ampG* complement.

Plasmid and strain construction

All plasmids used in this study are listed in Table 1. A strain with a mutation in *ampG* was constructed to examine meningococcal PG recycling. The fragment containing an in-frame deletion of *ampG* and flanking DNA was excised from pDG132 with restriction enzymes HindIII and SpeI and sub-cloned into the cloning vector pKH6 at the same restriction sites to generate plasmid pKL26. The kanamycin resistance marker was cut from pKH99 with EcoRV and EcoICRI. Plasmid pKL26 was cut with BglII and blunted with T4 DNA polymerase. The kanamycin resistance marker was inserted into the blunted BglII site in the same orientation as *ampG* to generate pKL37. Strain ATCC 13102 Str was transformed with pHC10 in order to generate a capsule null variant, ATCC 13102 *cap*. To generate an *ampG* deletion in *N. meningitidis*, ATCC 13102 *cap* was transformed with pKL37 linearized with NheI. Deletion of

ampG was confirmed by PCR. An *ampG* complementation was generated by amplifying the *ampG* coding region from ATCC 13102 chromosomal DNA with primers SacI *ampG* F (CGGGAGCTCGCGATATTTGCTACAATAGGC) and XbaI *ampG* R (GCCCTCTAGACACAATATCAGGTAAACGCTCC). Both the PCR product and plasmid pMR33 were digested with SacI and XbaI and then ligated together to create pKL47. Strain KL1074 was transformed with pKL47 linearized with NcoI to make the *ampG* complement strain KL1090.

The fragment containing the *ampG*-coding region with 50 bp of flanking DNA was amplified from ATCC 13102 chromosomal DNA using primers *ampG*-F2 (GGCGATATTTGCTACAATAGGCT) and *ampG*-1325R (CAATATCAGGTAAACGCTCCAGTTTGA). A fragment containing 600 bp of *ampG* upstream DNA sequence was amplified from MS11 chromosomal DNA using primers Mc-*ampG*-SacI-F3 (ATTCAGAGCTCCATCGGCGGCATCATCAAAC) and *ampG*-5'-flank-R (AGCCTATTGTAGCAAATATCGCC), while the fragment containing around 400 bp of *ampG* downstream DNA sequence was amplified similarly using primers *ampG*-3'-flank-F (TCAAACTGGAGCGTTTACCTGATATTG) and *ampG*-3'flank-R-BamHI (CTCAGGATCCGTTCTTTATATGAGCGGCAGG). The full length DNA fragment containing *N. meningitidis* ATCC 13102 derived *ampG* coding sequence flanked by *N. gonorrhoeae* MS11 derived *ampG* upstream and downstream DNA sequence was generated using a PCR-based method of extension overlap using aforementioned DNA fragments and primers Mc-*ampG*-SacI-F3 and *ampG*-3'flank-R-BamHI. The full-length DNA fragment and plasmid pIDN3 were digested with SacI and BamHI and ligated together to generate pEC006. To generate a gonococcal strain expressing meningococcal *ampG*, strain DG130 (*N. gonorrhoeae*

ampG::ermC) was transformed with plasmid pEC006. The resulting strain, EC505, was screened for loss of erythromycin resistance and confirmed by PCR and sequencing.

Characterization of released PG fragments

Labeling and characterization of released fragments were performed according to the methods described by Rosenthal and Dziarski and modified by Cloud and Dillard (18, 19). Quantitative fragment release analysis was performed as described by Garcia and Dillard (5). Meningococci and gonococci were pulse labeled with 10 μCi/ml [6-^{3}H]glucosamine in GCBL without glucose but containing pyruvate as the carbon source. A two-hour chase period in cGCBL followed. For quantitative release, radioactive counts per minute (CPM) in cell pellets after labeling was determined by liquid scintillation counting. The chase period started with equal numbers of CPM in each strain. After the chase, the cells were removed by centrifugation and supernatants passed through a 0.22 μm filter. PG fragments in the supernatants were separated by size-exclusion chromatography and detected by liquid scintillation counting. Relative amounts of PG fragments were determined by calculating the area under the curve. The monomer fractions were pooled, concentrated, and desalted.

High-performance liquid chromatography (HPLC) analysis was carried out as described by Kohler et al. (20). Desalted PG monomers were separated by reversed-phase HPLC over a 4.6 x 250 mm C18 column using a 4-13% acetonitrile gradient over 30 minutes. PG monomers were detected by liquid scintillation counting.

PG monomers were analyzed by LC-MS at the University of Wisconsin-Madison Biotechnology Center Mass Spectrometry facility. Liquid chromatography separation was performed on an Agilent 1200 HPLC using a Agilent Zorbax SB-C18 2.1 mm x 50 mm column

with 1.8 μm particles. Solvents were A: 0.1% formic acid in water, B: 0.1% formic acid in acetonitrile. The flow rate was 250 □L/min and the gradient was as follows: 2% B, hold for 1 min; ramp to 40% B at 48 min; ramp to 60% B at 55 min; ramp to 95% B at 60min; return to 2% B at 62 min; hold for 18 min. The column was held at 35 °C. The mass spectrometer was an Agilent LC/MSD TOF model G1969A operated in positive ion mode. Data were collected over the m/z range 100 to 3200 with 10,000 transients collected per scan and 0.89 scans acquired per second. The source was held at 35 °C with electrospray voltage of 3600V. Drying gas was 8 L/min, nebulizer gas was at 40 psig, fragmentor was at 160 V. Spectra were internally calibrated using a dual-ESI source in which the second electrospray delivered calibrant solution at a flow rate of 20 □L/min.

Peptidoglycan turnover

Meningococcal PG was metabolically labeled with 10 μCi/ml [6-^{3}H]glucosamine as described above. During a two-hour chase period, 500 μl samples were taken every 30 minutes. Whole sacculi were purified from each sample as described by Cloud and Dillard (2002). Cell pellets were resuspended in 165 μl 50 mM sodium phosphate buffer, pH 5.0. An equivalent amount of boiling 8% SDS was added to the sample. After 30 min. of boiling, whole sacculi were collected by centrifugation at 41,000 rcf for 30 min. at 15 °C. The supernatant was removed and the pellet resuspended in 100 l sterile water. Radiation in the entire sample was detected by liquid scintillation. Data shown is the average of three independent experiments, with error bars representing the standard deviation. Significance was determined using the Student's T-test.

NF-κB activation in epithelial cells

HEK293-Blue hNod1 cells (InvivoGen) were grown in DMEM with 4.5 g/l glucose, 2 mM L-glutamine, 10% FBS, 100 μg/ml Normocin, 30 μg/ml Blasticidin, and 100 μg/ml Zeocin at 37 °C with 5% CO_2. These cells overexpress human Nod1 and express a soluble alkaline phosphatase NF-κB reporter. Gonococci and meningococci were grown into log phase in liquid culture. Cultures were centrifuged to remove bacteria and supernatants filtered with a 0.22 □m filter. Total protein in the cell pellet was determined by BCA assay (Pierce) and supernatants were normalized based on total protein. HEK293-Blue cells were resuspended at a density of $2.8x10^5$ cells/ml in DMEM with 4.5 g/l glucose, 2 mM L-glutamine, and 10% heat-inactivated FBS. 180 μl of cells were plated in a 96-well plate along with 20 μl of bacterial supernatant, 10 μg/ml Tri-DAP positive control (InvivoGen), 10 μg/ml Tri-Lys negative control (InvivoGen), or media only control and incubated at 37 °C with 5% CO_2 for 24 hr. After incubation, 20 μl of supernatant was added to 200 μl of QUANTI-Blue reagent (InvivoGen). The reaction was incubated at 37°C for two hours. Absorbance was read at 650 nm in a plate reader to determine alkaline phosphatase activity. Values reported are the mean fold increase over media only from three independent biological replicates performed in duplicate. Significance was determined using the Student's T-test.

Fallopian tube organ cultures (FTOC) and cytokine analysis.

Samples of human fallopian tube (FT) were obtained from consenting donors via the National Human Tissue Resource Center at the National Disease Research Interchange in accordance with the University of Wisconsin-Madison Human Studies protocol. Upon arrival, FT samples were placed in Eagles Minimal Essential Medium (MEM) (Cellgro) with HEPES pH

7.4 and penicillin/streptomycin, where they were trimmed to remove muscle tissue and cut to expose epithelia prior to dissection with a 3 mm biopsy punch. Segments were removed to individual wells of a 24-well plate containing 1 mL of the above media and cultured overnight at 37°C with 5% CO_2. Following overnight incubation, segments were evaluated microscopically to confirm the presence of peripheral ciliated cell activity. Prior to treatment, each punch was washed with sterile phosphate-buffered saline (PBS) and removed to a new 24-well plate containing 900 μL of the above media without antibiotics. A minimum number of three segments per condition were then treated with either 100 μL of GCBL (mock), or supernatant from strains MS11, DG132, ATCC 13102, or KL1074 grown into log phase in liquid culture as described above. At 24 hours post-infection, 250 μL of FTOC media was removed, filtered by centrifugation through a 0.22 μm filter (Costar) and stored at -80°C. Filtered FTOC supernatants were assayed for the presence of IL-8 by sandwich ELISA using the Ready-Set-Go human IL-8 ELISA kit (eBioscience), according to the manufacturer's standard protocol. Significance was determined by the Mann-Whitney test.

RESULTS

Peptidoglycan fragment release by *N. meningitidis*

Purified *N. meningitidis* peptidoglycan (PG) induces an inflammatory response and inflammatory cytokine production (2), but it has not been determined if Mc release PG fragments or how PG affects meningococcal disease and carriage. We hypothesized that meningococci could be limiting proinflammatory PG fragment release, which may facilitate carriage in the human nasopharynx. To examine PG fragment release from *N. meningitidis*, we used a pulse-chase, metabolic labeling method that has been used to characterize PG fragment release from *N. gonorrhoeae* and other bacteria. Growth of *N. meningitidis* strain ATCC 13102 in the presence of [6-^{3}H]-glucosamine with pyruvate as the carbon source was successful in incorporating label into the SDS-insoluble cell wall PG. However, a substantial amount of label was incorporated into other molecules, likely the polysaccharide capsule. Therefore, we constructed an isogenic capsule-null strain of ATCC 13102 by introduction of a *siaD* mutation. The unencapsulated strain exhibited 1.9 fold increased labeling efficiency for introduction of [6-^{3}H]-glucosamine into the cell wall PG (data not shown). All subsequent labeling with [6-^{3}H]-glucosamine was performed on capsule null strains.

We metabolically labeled ATCC 13102 *cap* with [6-^{3}H]glucosamine, and after a two-hour chase period, the supernatant was collected for evaluation of released PG fragments. PG fragments in the medium were separated by size-exclusion chromatography, and by comparison with known standards, we were able to identify most of the PG fragments released by *N. meningitidis*. The release profile for strain ATCC 13102 *cap* shows the presence of PG dimers,

PG monomers, free disaccharide, and a monosaccharide fraction containing anhydro-MurNAc and possibly other molecules (Figure 1).

As is seen in the release of PG fragments by *N. gonorrhoeae*, the major PG fragments released by *N. meningitidis* include PG monomers and free disaccharide. PG monomers are generated by the action of lytic transglycosylases that breakdown PG strands into 1,6-anhydro-disaccharide tripeptide and 1,6-anhydro-disaccharide tetrapeptide monomers (9, 22, 21 23), and these PG fragments cause ciliated cell death and proinflammatory cytokine production in various bacterial infections (10, 13). Free disaccharides are generated by the *N*-acetylmuramyl-L-alanine amidase AmiC, which cleaves peptides from the glycan chains (24, 25). The PG fragment that elutes after free disaccharide in the *N. meningitidis* profile has only barely been detected in *N. gonorrhoeae* profiles and has not been previously analyzed. The peak elutes earlier than *N*-acetylglucosamine (data not shown). Mass spectrometry of an unlabeled sample demonstrated the presence of anhyro-MurNAc at this elution time in the meningococcal profile. The less abundant PG fragments released by *N. meningitidis* include PG dimers: peptide-crosslinked PG dimer, glycosidically-linked PG dimer, and a tetrasaccharide with a single peptide chain. We also noted that *N. meningitidis* has an additional PG monomer peak not found in the release profile of *N. gonorrhoeae*, representing a molecule smaller than tripeptide monomer. The presence of this smaller monomer suggests that meningococci degrade liberated PG monomers, possibly removing more of the peptide side chain or removing the glucosamine from the PG monomers.

Since PG monomers induce an inflammatory response in multiple bacterial infections (10, 13, 26) and purified *N. meningitidis* peptidoglycan stimulates Nod1, we examined what types of PG monomers are released by *N. meningitidis*. PG monomers released by unencapsulated ATCC 13102 were purified by size-exclusion chromatography and analyzed by

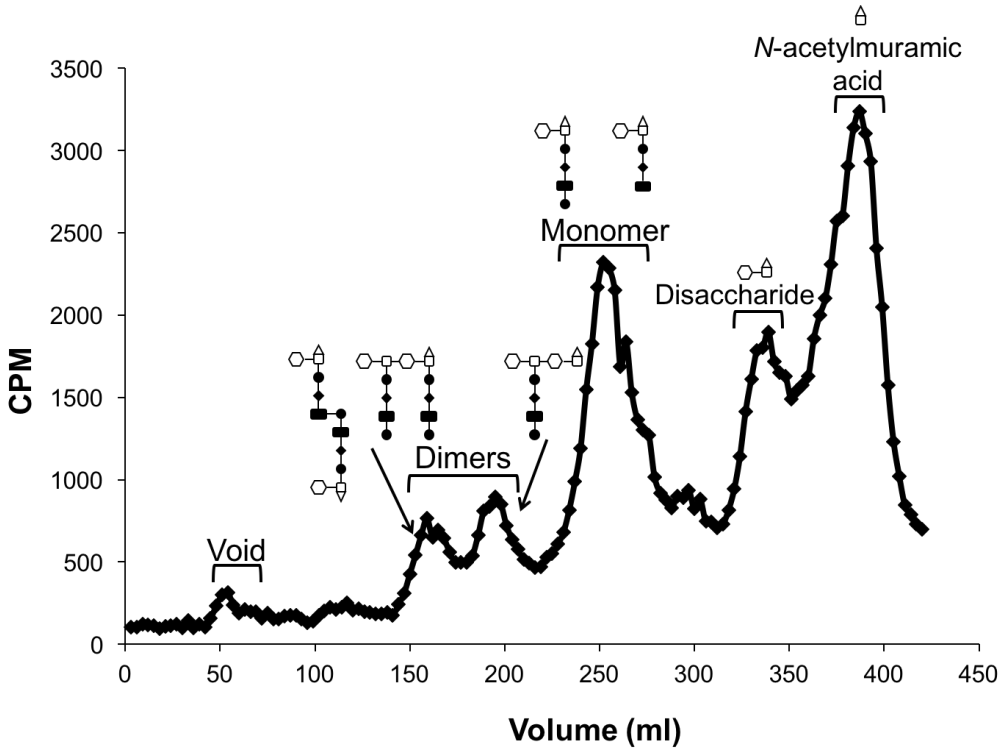

Figure 1. Meningococci release peptidoglycan fragments during normal growth. Meningococci were metabolically labeled with [6-^{3}H]glucosamine. After a chase period, supernatants were collected. Radiolabeled fragments were separated by size-exclusion chromatography and detected by liquid scintillation counting. During logarithmic growth meningococci release PG dimers, monomers, free disaccharide, and anhydro-*N*-acetylmuramic acid. GlcNAc: *N*-acetylglucosamine; MurNAc: *N*-acetylmuramic acid; anhMurNAc: anhydro-*N*-acetylmuramic acid. Although only one structure is shown, the location of the peptide on the tetrasaccharide-peptide is not known.

LC/MS (Figure 2). The mass spectrometry analysis identified mass-to-charge ratios consistent with 1,6-anhydro-disaccharide tetrapeptide monomer (Figure 2A), 1,6-anhydro-disaccharide tripeptide monomer (Figure 2B), reducing disaccharide tetrapeptide monomer, and reducing disaccharide tripeptide monomer (data not shown). Together, the size-exclusion analysis and the LC/MS data show that meningococci release known proinflammatory PG fragments into the extracellular milieu.

Meningococci efficiently recycle peptidoglycan

Examination of the *N. meningitidis* genome sequences shows that meningococci have a homolog of the anhydromuramyl specific permease, AmpG, which is involved in uptake of PG fragments for recycling in *N. gonorrhoeae*, *Citrobacter freundii*, and other gram-negative bacterial species (5, 6, 27). In order to characterize meningococcal PG recycling, we made a deletion of *ampG* and an *ampG* complement in *N. meningitidis* and examined PG turnover during growth. We metabolically labeled capsule null *N. meningitidis* strain ATCC 13102, and the isogenic *ampG* deletion mutant, and the complemented strain and measured radioactivity remaining in purified sacculi over a two-hour chase period. We found that the *ampG* mutant released significantly more PG throughout the chase period than both the wild-type and complemented strains (Figure 3), suggesting that meningococci recycle significant amounts of PG fragments generated during cell wall growth and use AmpG in this process.

To determine the effects of an *ampG* deletion on fragment release, the wild-type and *ampG* mutant strains were radiolabeled as described above; however, at the beginning of the chase period the cultures were diluted to give equal amounts of radioactivity in the wild-type and *ampG* cultures to allow for a quantitative comparison of PG fragment release. The *ampG*

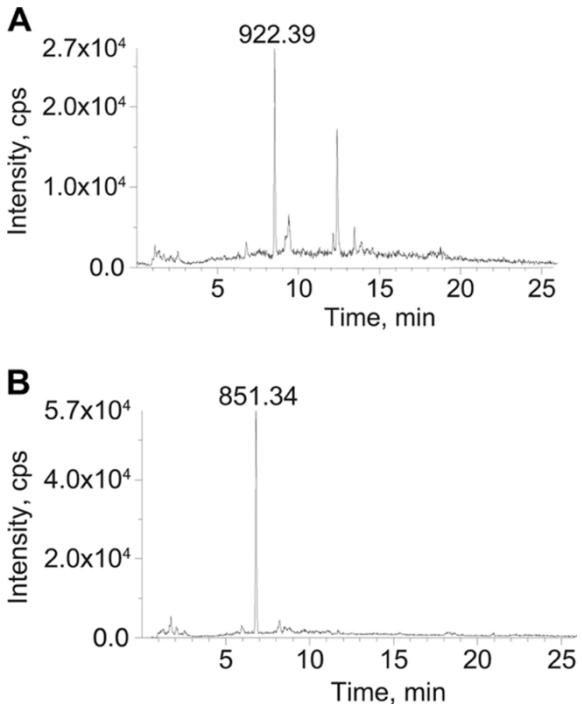

Figure 2. Meningococci release anhydro-disaccharide tripeptide monomer and anhydro-disaccharide tetrapeptide monomer. PG fragments in supernatant from unlabeled ATCC 13102 were separated by size-exclusion chromatography. The monomer fractions were pooled, desalted, and concentrated. LC/MS analysis showed species with mass-to-charge ratios consistent with 1,6-anhydro-disaccharide tetrapeptide monomer (A) and 1,6-anhydro-disaccharide tripeptide monomer (B).

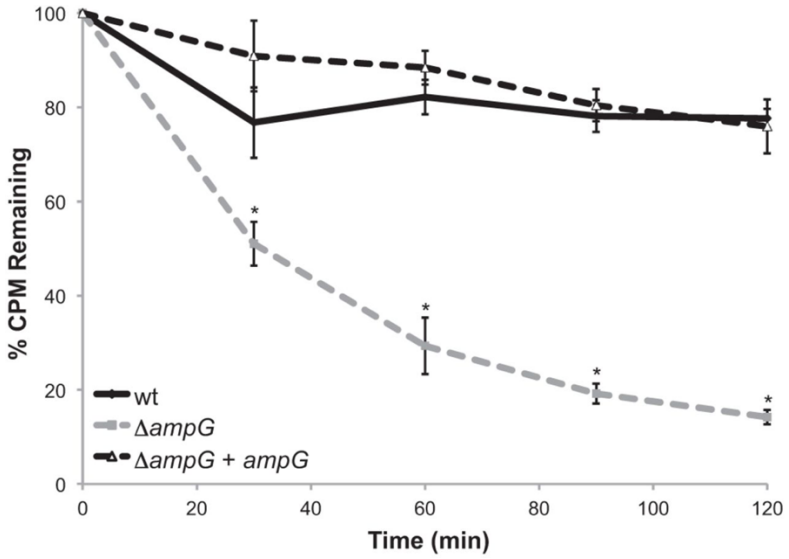

Figure 3. Turnover of peptidoglycan is significantly increased in an *ampG* mutant over wild-type. Meningococcal strains were labeled with [6-^{3}H]glucosamine. During the 120-minute chase period, samples were taken every 30 minutes. Whole sacculi were purified and total CPM determined by liquid scintillation counting. The *ampG* deletion mutant KL1074 showed significantly more PG turnover than its parent, ATCC 13102 *cap*, and the complemented strain KL1090. *$p<0.05$ by ANOVA, error bars represent the standard deviation, n=3.

deletion strain showed increased release of PG monomers and free disaccharide relative to wild-type (Figure 4). The amount of monomer released by the *ampG* mutant was 29 times greater than that released by wild-type, indicating that wild-type meningococci recycle 96% of monomers. Similarly, meningococci were found to recycle 90% of disaccharide fragments. Previous work with *N. gonorrhoeae* showed that gonococci recycle 85% of peptidoglycan monomer (5). Our results indicate that *N. meningitidis* recycles PG fragments via AmpG more efficiently than does *N. gonorrhoeae*.

Alignment of AmpG from meningococci and gonococci showed that AmpG is 97% identical at the amino acid level. Given the differences we observed in AmpG efficiency between *N. gonorrhoeae* and *N. meningitidis*, and given that meningococcal AmpG is also responsible for free disaccharide recycling, we wanted to determine if these differences were solely due to AmpG or the overall PG degradation and recycling systems in the two organisms. We constructed a gonococcal strain EC505 that expresses meningococcal *ampG* in place of the native gonococcal *ampG*. Quantitative comparison of EC505 to the parental gonococcal strain MS11 showed that EC505 releases 1.97 times less PG monomer than MS11 (Figure 5), indicating that meningococcal AmpG is more efficient at PG recycling than gonococcal AmpG.

Meningococci release less proinflammatory PG monomers than gonococci

To examine differences in PG fragment release between *N. meningitidis* and *N. gonorrhoeae*, we labeled meningococci and gonococci with [6-^{3}H]glucosamine and used a quantitative method to determine differences in PG fragment release between the two species (Figure 5). We also determined that meningococci and gonococci incorporate [6-^{3}H]glucosamine into PG at nearly identical labeling frequencies, 56.06% and 56.58%, respectively. We found that

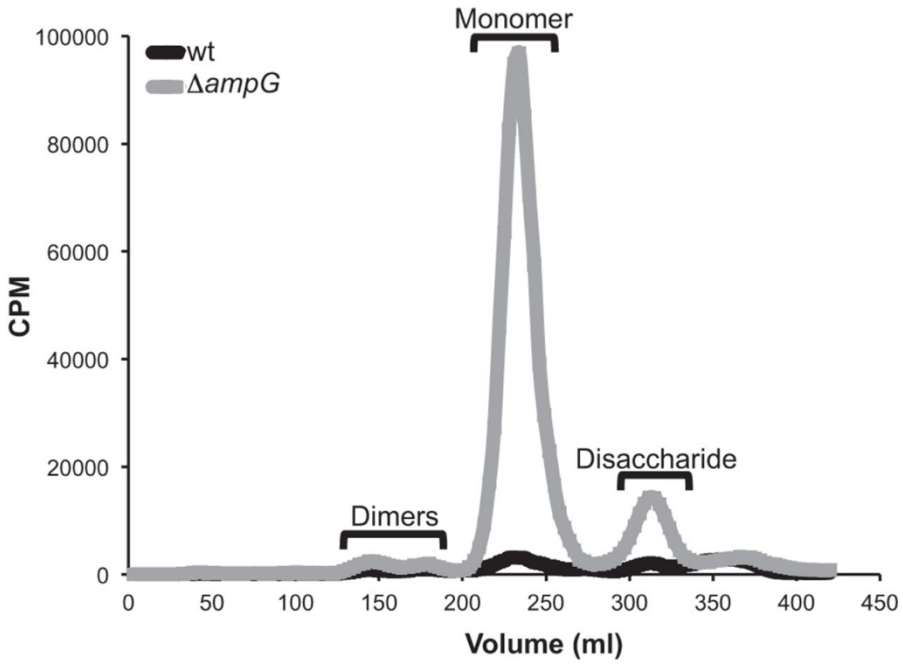

Figure 4. Deletion of *ampG* results in increased monomer and free disaccharide release over wild-type. An *ampG* deletion mutant (KL1074) and its parent (ATCC 13102 *cap*) were labeled with [6-^{3}H]glucosamine. Following a two-hour chase, supernatants were collected, fragments separated by size-exclusion chromatography, and detected by liquid scintillation counting. Based on differences in monomer peak area, meningococci recycle 96% of PG monomers.

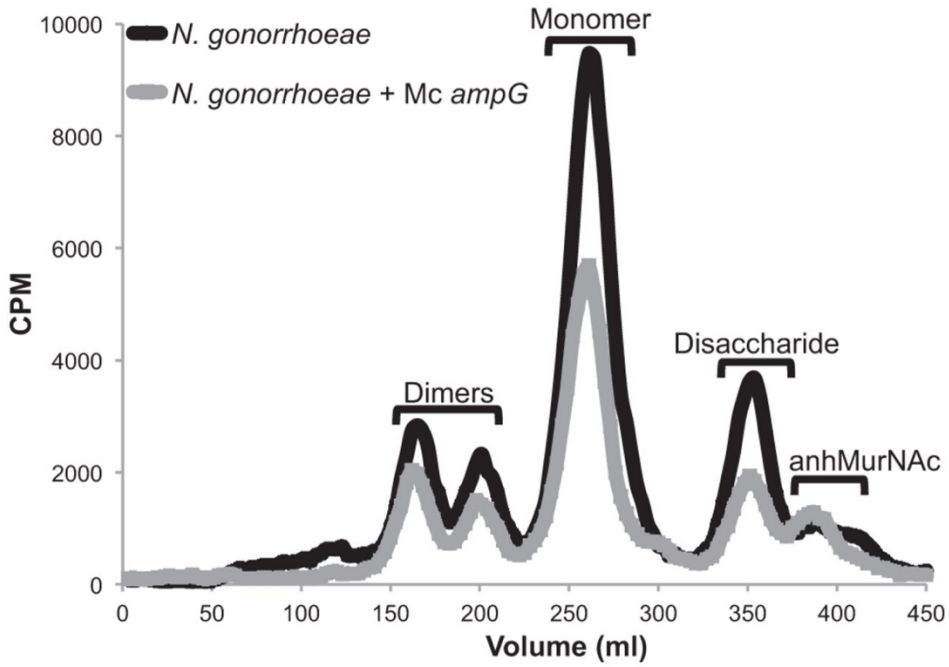

Figure 5. Expression of meningococcal *ampG* increases recycling efficiency in *N. gonorrhoeae*. Gonococcal strains expressing either gonococcal *ampG* or meningococcal *ampG* were equivalently labeled with (6-^{3}H)glucosamine and fragment release was analyzed. Gonococci expressing meningococcal *ampG* show a 1.97 fold decrease in peptidoglycan monomer release from wild-type gonococci indicating that meningococcal AmpG recycles peptidoglycan monomers more efficiently than gonococcal AmpG.

N. meningitidis releases 2.8 times less PG monomer than *N. gonorrhoeae* (Figure 6). The increased monomer recycling efficiency of meningococcal AmpG likely contributes to differences in monomer release between the pathogenic *Neisseria* (Figure 5). Free disaccharide release was very similar between meningococci and gonococci, but dimer release appeared slightly reduced in the meningococcal profile. As noted above, the meningococcal profile includes a PG monomer peak for a molecule smaller than tripeptide monomer and a large peak for anhydro-*N*-acetylmuramic acid. The latter is also seen to a smaller extent in the *N. gonorrhoeae* profile of released fragments. The appearance of these smaller PG fragments suggests that *N. meningitidis* is degrading multiple PG fragments to smaller products.

The PG monomer fractions from *N. meningitidis* and *N. gonorrhoeae* were further analyzed by reversed-phase HPLC (Figure 7). The *N. meningitidis* monomer fraction contained both tripeptide monomer (human Nod1 agonist) and tetrapeptide monomer (TCT) consistent with our LC/MS analysis described above. The amount of tripeptide monomer released by *N. meningitidis* was 1.8 fold as much as tetrapeptide monomer. In addition, we detected three peaks with shorter retention times. These are consistent with reducing monomers, i.e., monomers lacking the 1,6-anhydro bond on the *N*-acetylmuramic acid. The PG monomers released by *N. gonorrhoeae* included tripeptide monomer and tetrapeptide monomer. The gonococcal strain released 2.6 times more tripeptide monomer, than tetrapeptide monomer, consistent with previous results (20). The decrease in the ratio of tripeptide monomer to tetrapeptide monomer in *N. meningitidis* could alter PG sensing by Nod1 as human Nod1 only recognizes tripeptide monomer and not tetrapeptide monomer (15). In total, these data indicate that meningococci are breaking down PG more extensively or to different products than those found in gonococci.

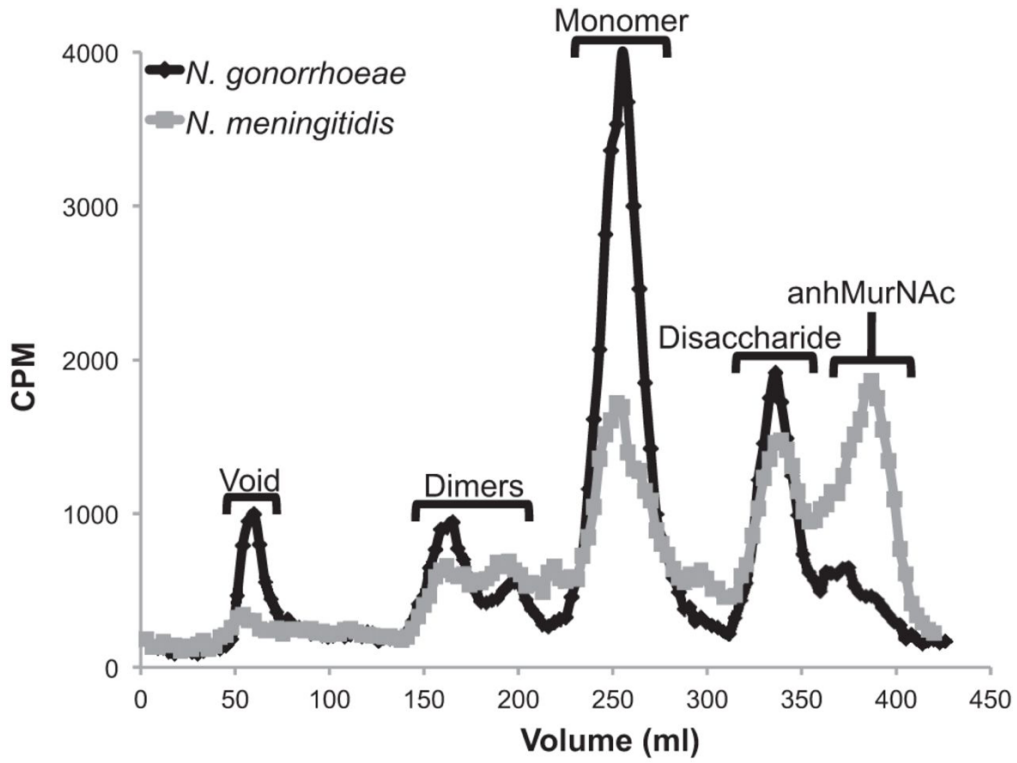

Figure 6. *N. meningitidis* releases less cytotoxic monomer than *N. gonorrhoeae*. Meningococci and gonococci were quantitatively labeled with [6-^{3}H]glucosamine. After a chase period, supernatants were collected, fragments separated by size-exclusion chromatography, and detected by liquid scintillation counting. *N. meningitidis* releases less monomer than *N. gonorrhoeae*, and has altered PG multimer release.

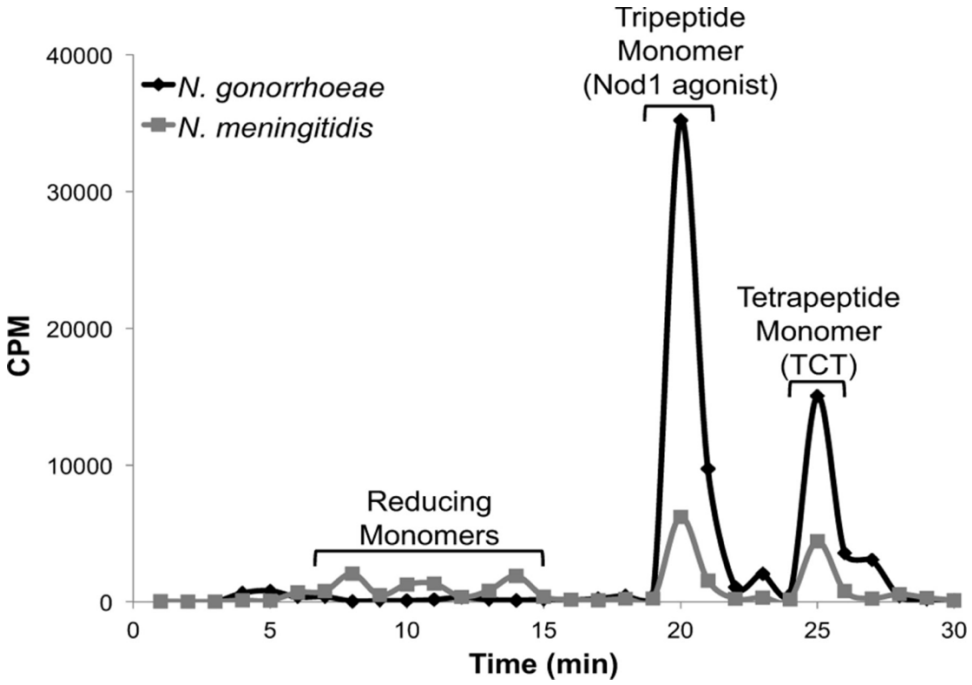

Figure 7. Meningococci release PG monomers in different proportions than gonococci. Radiolabeled PG monomer was pooled and analyzed by reversed-phase HPLC over a C18 column. Meningococci release 1.8 times more tripeptide monomer than tetrapeptide monomer. *N. gonorrhoeae* releases 2.6 times more tripeptide monomer than tetrapeptide monomer, suggesting that meningococci degrade PG fragments differently than gonococci.

Meningococci stimulate less Nod1-dependent activation of NF-κB than gonococci

To determine if differences in PG fragment release and recycling between *N. meningitidis* and *N. gonorrhoeae* may result in altered host responses, we measured Nod1-dependent NF-κB activation in response to supernatants from Mc and Gc cultures. We exposed HEK293 cells overexpressing human Nod1 (hNod1) along with an alkaline phosphatase NF-κB reporter to meningococcal or gonococcal supernatants or a medium-only control. Supernatants were from bacteria grown to log phase and were normalized based on total protein in the cell pellet. After 24 hours of exposure to bacterial supernatants, alkaline phosphatase activity in the medium was measured and compared to activity in the medium-only control (Table 2). NF-κB activity was significantly higher in cells expressing hNod1 than the parental Null line, indicating that we were detecting hNod1-dependent NF-κB activity (data not shown). As expected, HEK293 cells overexpressing hNod1 showed NF-κB activity in response to tripeptide containing DAP, but not to tripeptide containing lysine. We found that gonococcal supernatants stimulated significantly more hNod1-dependent NF-κB activity than meningococcal supernatants (Table 2).

Cytokine induction in human Fallopian tube explants

While *N. gonorrhoeae* and *N. meningitidis* are naturally human-restricted pathogens and few relevant in vivo models of human disease are available, a human fallopian tube organ culture (FTOC) model has been established to study the pathogenicity of the gonococcus (28). In this model, PG fragments from gonococci have been shown to damage fallopian tube mucosa (13) and infection with gonococci has been shown to induce the production of proinflammatory cytokines (29-31). Since activation of NF-kB in response to Nod1 activation is known to stimulate the secretion of proinflammatory cytokines and chemokines, the human FTOC model

could be used to evaluate the in vivo relevance of proportional differences in bacterial PG-fragment release. Since we have established that proinflammatory PG fragments are released in different proportions by gonococci and meningococci in an AmpG-dependent manner, we hypothesized that PG-containing supernatant from these strains would induce different levels of inflammatory cytokines in FTOC. Following 24 hours of exposure to gonococcal and meningococcal supernatants prepared as described above, tissue culture medium was removed, filtered and assayed for levels of IL-8 by sandwich ELISA. Fallopian tube explant segments treated with ATCC 13102 appear to induce less IL-8 secretion than segments treated with wild-type gonococci (MS11), with the deletion of *ampG* resulting in an increase in IL-8 secretion (Figure 8). While treatment with bacterial supernatant significantly increases IL-8 secretion over mock-treated controls, the differences between strains do not reach statistical significance due to the variation seen in these primary human samples. However, these changes are in line with the results seen in hNod1-reporter cells (Table 2).

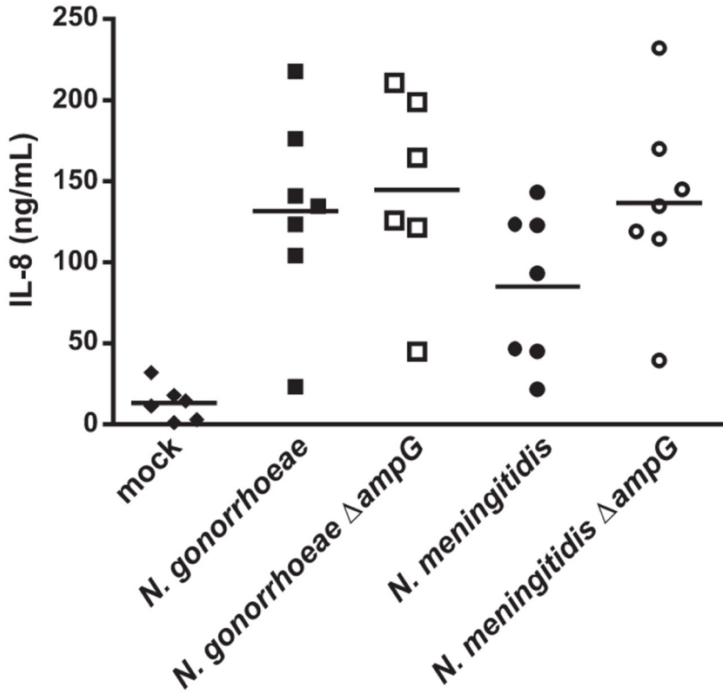

Figure 8. Fallopian tube organ culture explants secrete the proinflammatory cytokine IL-8 in response to exposure to meningococcal and gonococcal supernatants. Explants from two patients were exposed to supernatants from meningococci, gonococci, and isogenic *ampG* deletion mutants. After 24 hours of exposure IL-8 secretion was measured by ELISA. Data points are representative of IL-8 secretion from two independent experiments where n≥3 replicates per condition per experiment. Bars indicate the mean. There was no statistically significant difference between samples as determined by the Mann-Whitney test.

DISCUSSION

It appears that all bacteria that produce PG release some portion of what they produce into the environment in the course of normal growth. PG fragments are generated as the cell grows – PG strands in the cell wall are degraded to make a space for insertion of additional strands and PG is broken down in the process of septum formation and splitting (32). It is how the PG is broken down, into what form, that affects its potential to elicit an immune response. Also, the amounts of PG fragments taken back into the cytoplasm for recycling affect the amounts available for release into the environment and thus possible detection by the immune system (33). In this study, we found that *N. meningitidis* has high efficiency recycling and increased degradation of PG fragments, resulting in reduced release of proinflammatory PG fragments relative to *N. gonorrhoeae*.

By comparing the amounts of PG fragments released by the wild-type strain and an *ampG* mutant, we determined that *N. meningitidis* normally recycles 96% of the PG monomers liberated from the cell wall. This rate of recycling is very similar to that seen with *E. coli*, but is substantially higher than the rate determined for *N. gonorrhoeae* (34). Gonococci recycle 85% of PG monomers (5). The mechanism of the higher rate of recycling in *N. meningitidis* is not clear. Meningococcal and gonococcal AmpG sequences are 97% identical at the amino acid level. It is possible that these minor differences may affect AmpG stability or activity. Also, expression of *ampG* may be higher in meningococci than in gonococci. It is clear that there are differences between meningococci and gonococci in PG fragment recycling in addition to the amounts of PG monomers recycled. In *N. gonorrhoeae* an *ampG* mutant is not affected in release of free disaccharide, and an *ampD* (recycling-defective) mutant shows increased uptake of free

disaccharide (5). These data suggest that gonococci sense and respond to levels of PG in the cytoplasm. In *N. meningitidis*, mutation of *ampG* leads to an increase in free disaccharide and PG monomer release over wild-type, thus demonstrating that AmpG is responsible for free disaccharide uptake in meningococci and that meningococcal uptake of free disaccharide differs from gonococcal free disaccharide uptake.

A comparison of the PG fragments released by *N. meningitidis* and *N. gonorrhoeae* shows that *N. meningitidis* releases lower amounts of PG monomers and releases additional PG fragments not released by *N. gonorrhoeae*. These additional PG fragments include smaller PG dimers, smaller PG monomers, and 1,6 anyhdro-*N*-acetylmuramic acid. The presence of these PG fragments indicates that meningococci are breaking down the liberated PG fragments more extensively than gonococci. Furthermore, the HPLC analysis of meningococcal PG monomers shows that this fraction contains not just 1,6-anhydro-disaccharide tetrapeptide monomer and 1,6-anhydro-disaccharide tripeptide monomer but also contains reducing monomers. The net effect of the highly efficient monomer recycling and additional PG fragment degradation contributes to detoxification of released PG fragments, as evidenced by meningococcal supernatants inducing less Nod-1 dependent NF-κB activation (Table 2) and reduced IL-8 section (Figure 8) than gonococcal supernatants. *E. coli* also degrades PG fragments prior to their release. In *E. coli*, liberated PG monomers are degraded by the *N*-acetylmuramyl-L-alanine amidase AmiD (35). AmiD converts PG monomers into free peptides and free disaccharides. The free peptides could still participate in inducing inflammation through the Nod1 pathway since free tetrapeptides or free tripeptides would be Nod1 agonists in mice or humans, respectively (36). However, in the *B. pertussis* model, peptides have to be blocked at the N-terminus to have cell damaging activity (37), and thus AmiD activity would detoxify PG monomers.

This is the first characterization of PG fragments released by *N. meningitidis* during normal growth. We found that meningococci release multiple PG fragments, including proinflammatory PG monomers. Meningococcal PG monomer release is lower than that of *N. gonorrhoeae*, and meningococci also release additional PG fragments not present in the gonococcal PG fragment release profile. These data indicate that meningococci are breaking down PG further than gonococci. Reduction of proinflammatory monomer release and additional PG degradation may be advantageous for meningococci in maintaining an asymptomatic colonization of the human nasopharynx.

ACKNOWLEDGEMENTS

We thank Dr. Sanjay Ram for the generous gift of plasmid pHC10. This work was supported by NIH grants R01AI097157 and R21AI072605 to JPD.

Table 1. Bacterial strains and plasmids

Strain/Plasmid	Description	Source/ Reference
N. meningitidis		
ATCC 13102	Clinical isolate, serogroup C	ATCC
ATCC 13102 Str	ATCC 13102 *rpsL*K43R	(38)
ATCC 13102 *cap*	ATCC 13102 Str transformed with pHC10 (*rpsL*K43R *siaD::cat*)	This study
KL1074	ATCC 13102 *cap* transformed with pKL37 (*rpsL*K43R *siaD::cat* Δ*ampG::kan*)	This study
KL1090	KL1074 transformed with pKL47 (*rpsL*K43R *siaD::cat* Δ*ampG::kan* +*ampG*)	This study
N. gonorrhoeae		
MS11	Wild-type *N. gonorrhoeae*	(39)
DG130	MS11 transformed with pGC3 (*ampG::ermC*)	This study
DG132	MS11 Δ*ampG*	(5)
EC505	DG130 transformed with pEC006 (Mc *ampG*)	
Plasmids		
pKL26	pDG132 (Δ*ampG*) insert moved into pKH6 at HindIII and SpeI	This study
pKL37	*aph3* from pKH99 (EcoRV, EcoICRI) in Δ*ampG* of pKL26 at blunted BglII	This study
pKL47	*ampG* coding sequence in pMR33 complementation vector at SacI and XbaI	This study
pEC006	*ampG* coding region from ATCC 13102 with MS11 flanking DNA in pIDN3 at SacI and BamHI	This study
pIDN3	*N. gonorrhoeae* cloning plasmid	(40)
pHC10	serogroup C *siaD::cat*	(41)
pGC3	*N. gonorrhoeae ampG::ermC*	W. Goldman
pDG132	In-frame *ampG* deletion	(5)
pMR33	IPTG inducible *Neisseria* complementation vector at *iga-trpB*	(42)
pKH6	Cloning vector derived from pIDN1 and pGCC6	(38)
pKH99	*aph3* from pHSS6 into BamHI site of pIDN2	(38)

Table 2. Meningococci stimulate less hNod1-dependent NF-κB activity than gonococci

Sample	**Nod1-dependent PhoA activity (Fold change)†**
N. gonorrhoeae	6.43±0.47
N. meningitidis	3.90±0.86 *
Tri-DAP	12.03±4.13
Tri-Lys	1.01±0.04

† Represents fold increase over media-only control

* Significantly less than fold change stimulated by *N. gonorrhoeae* by T-test, p=0.011

REFERENCES

1. **Stephens DS, Greenwood B, Brandtzaeg P.** 2007. Epidemic meningitis, meningococcaemia, and *Neisseria meningitidis*. Lancet **369:**2196-2210.
2. **Girardin SE, Boneca IG, Carneiro LA, Antignac A, Jehanno M, Viala J, Tedin K, Taha MK, Labigne A, Zahringer U, Coyle AJ, DiStefano PS, Bertin J, Sansonetti PJ, Philpott DJ.** 2003. Nod1 detects a unique muropeptide from gram-negative bacterial peptidoglycan. Science **300:**1584-1587.
3. **Rosenthal RS.** 1979. Release of soluble peptidoglycan from growing gonococci: hexaminidase and amidase activities. Infect Immun **24:**869-878.
4. **Hebeler BH, Young FE.** 1976. Chemical composition and turnover of peptidoglycan in *Neisseria gonorrhoeae*. J Bacteriol **126:**1180-1185.
5. **Garcia DL, Dillard JP.** 2008. Mutations in *ampG* or *ampD* affect peptidoglycan fragment release from *Neisseria gonorrhoeae*. J Bacteriol **190:**3799-3807.
6. **Jacobs C, Huang LJ, Bartowsky E, Normark S, Park JT.** 1994. Bacterial cell wall recycling provides cytosolic muropeptides as effectors for beta-lactamase induction. EMBO J **13:**4684-4694.
7. **Lindquist S, Weston-Hafer K, Schmidt H, Pul C, Korfmann G, Erickson J, Sanders C, Martin HH, Normark S.** 1993. AmpG, a signal transducer in chromosomal beta-lactamase induction. Mol Microbiol **9:**703-715.
8. **Goldman WE, Klapper DG, Baseman JB.** 1982. Detection, isolation, and analysis of a released *Bordetella pertussis* product toxic to cultured tracheal cells. Infect Immun **36:**782-794.
9. **Rosenthal RS, Nogami W, Cookson BT, Goldman WE, Folkening WJ.** 1987. Major fragment of soluble peptidoglycan released from growing *Bordetella pertussis* is tracheal cytotoxin. Infect Immun **55:**2117-2120.
10. **Heiss LN, Moser SA, Unanue ER, Goldman WE.** 1993. Interleukin-1 is linked to the respiratory epithelial cytopathology of pertussis. Infect Immun **61:**3123-3128.
11. **Flak TA, Goldman WE.** 1999. Signalling and cellular specificity of airway nitric oxide production in pertussis. Cell Microbiol **1:**51-60.
12. **McGee ZA, Johnson AP, Taylor-Robinson D.** 1981. Pathogenic mechanisms of *Neisseria gonorrhoeae*: observations on damage to human fallopian tubes in organ culture by gonococci of colony type 1 or type 4. J Infect Dis **143:**413-422.
13. **Melly MA, McGee ZA, Rosenthal RS.** 1984. Ability of monomeric peptidoglycan fragments from *Neisseria gonorrhoeae* to damage human fallopian-tube mucosa. J Infect Dis **149:**378-386.
14. **Nigro G, Fazio LL, Martino MC, Rossi G, Tattoli I, Liparoti V, De Castro C, Molinaro A, Philpott DJ, Bernardini ML.** 2008. Muramylpeptide shedding modulates cell sensing of *Shigella flexneri*. Cell Microbiol **10:**682-695.
15. **Girardin SE, Jehanno M, Mengin-Lecreulx D, Sansonetti PJ, Alzari PM, Philpott DJ.** 2005. Identification of the critical residues involved in peptidoglycan detection by Nod1. J Biol Chem **280:**38648-38656.
16. **Hook EW, III, Handsfield HH.** 1999. Gonococcal infections in the adult, p. 451-466. *In* Holmes KK, Mardh P-A, Sparling PF, Lemon SM, Stamm WE, Piot P, Wasserheit JN (ed.), Sexually Transmitted Diseases. McGraw-Hill, New York.

17. **Kellogg DS, Jr., Peacock WL, Jr., Deacon WE, Brown L, Pirkle CL.** 1963. *Neisseria gonorrhoeae*. I. Virulence genetically linked to clonal variation. J Bacteriol **85:**1274-1279.
18. **Rosenthal RS, Dziarski R.** 1994. Isolation of peptidoglycan and soluble peptidoglycan fragments. Meth Enzymol **235:**235-285.
19. **Cloud KA, Dillard JP.** 2002. A lytic transglycosylase of *Neisseria gonorrhoeae* is involved in peptidoglycan-derived cytotoxin production. Infect Immun **70:**2752-2757.
20. **Kohler PL, Hamilton HL, Cloud-Hansen K, Dillard JP.** 2007. AtlA functions as a peptidoglycan lytic transglycosylase in the *Neisseria gonorrhoeae* type IV secretion system. J Bacteriol **189:**5421-5428.
21. **Lee M, Hesek D, Llarrull LI, Lastochkin E, Pi H, Boggess B, Mobashery S.** 2013. Reactions of all *Escherichia coli* lytic transglycosylases with bacterial cell wall. J Am Chem Soc **135:**3311-3314.
22. **Cloud-Hansen KA, Hackett KT, Garcia DL, Dillard JP.** 2008. *Neisseria gonorrhoeae* uses two lytic transglycosylases to produce cytotoxic peptidoglycan monomers. J Bacteriol **190:**5989-5994.
23. **Sinha RK, Rosenthal RS.** 1980. Release of soluble peptidoglycan from growing gonococci: demonstration of anhydro-muramyl-containing fragments. Infect Immun **29:**914-925.
24. **Heidrich C, Templin MF, Ursinus A, Merdanovic M, Berger J, Schwarz H, de Pedro MA, Höltje JV.** 2001. Involvement of *N*-acetylmuramyl-L-alanine amidases in cell separation and antibiotic-induced autolysis of *Escherichia coli*. Mol Microbiol **41:**167-178.
25. **Garcia DL, Dillard JP.** 2006. AmiC functions as an *N*-acetylmuramyl-L-alanine amidase necessary for cell separation and can promote autolysis in *Neisseria gonorrhoeae*. J Bacteriol **188:**7211-7221.
26. **Girardin SE, Tournebize R, Mavris M, Page AL, Li X, Stark GR, Bertin J, DiStefano PS, Yaniv M, Sansonetti PJ, Philpott DJ.** 2001. CARD4/Nod1 mediates NF-κB and JNK activation by invasive *Shigella flexneri*. EMBO Rep **2:**736-742.
27. **Johnson JW, Fisher JF, Mobashery S.** 2013. Bacterial cell-wall recycling. Ann N Y Acad Sci **1277:**54-75.
28. **Melly MA, Gregg CR, McGee ZA.** 1981. Studies of toxicity of *Neisseria gonorrhoeae* for human fallopian tube mucosa. J Infect Dis **143:**423-431.
29. **Maisey K, Nardocci G, Imarai M, Cardenas H, Rios M, Croxatto HB, Heckels JE, Christodoulides M, Velasquez LA.** 2003. Expression of proinflammatory cytokines and receptors by human fallopian tubes in organ culture following challenge with *Neisseria gonorrhoeae*. Infect Immun **71:**527-532.
30. **McGee ZA, Clemens CM, Jensen RL, Klein JJ, Barley LR, Gorby GL.** 1992. Local induction of tumor necrosis factor as a molecular mechanism of mucosal damage by gonococci. Microb Pathog **12:**333-341.
31. **Velasquez L, Garcia K, Morales F, Heckels JE, Orihuela P, Rodas PI, Christodoulides M, Cardenas H.** 2012. *Neisseria gonorrhoeae* pilus attenuates cytokine response of human fallopian tube explants. J Biomed Biotechnol **2012:**491298.
32. **Typas A, Banzhaf M, Gross CA, Vollmer W.** 2012. From the regulation of peptidoglycan synthesis to bacterial growth and morphology. Nat Rev Microbiol **10:**123-136.

33. **Boudreau MA, Fisher JF, Mobashery S.** 2012. Messenger functions of the bacterial cell wall-derived muropeptides. Biochemistry **51:**2974-2990.
34. **Greenway DL, Perkins HR.** 1985. Turnover of the cell wall peptidoglycan during growth of *Neisseria gonorrhoeae* and *Escherichia coli*. Relative stability of newly synthesized material. J Gen Microbiol **131:**253-263.
35. **Uehara T, Park JT.** 2007. An anhydro-*N*-acetylmuramyl-L-alanine amidase with broad specificity tethered to the outer membrane of *Escherichia coli*. J Bacteriol **189:**5634-5641.
36. **Magalhaes JG, Philpott DJ, Nahori MA, Jehanno M, Fritz J, Le Bourhis L, Viala J, Hugot JP, Giovannini M, Bertin J, Lepoivre M, Mengin-Lecreulx D, Sansonetti PJ, Girardin SE.** 2005. Murine Nod1 but not its human orthologue mediates innate immune detection of tracheal cytotoxin. EMBO Rep **6:**1201-1207.
37. **Luker K, Tyler A, Marshall G, Goldman W.** 1995. Tracheal cytotoxin structural requirements for respiratory epithelial damage in pertussis. Mol Microbiol **16:**733-743.
38. **Woodhams KL, Benet ZL, Blonsky SE, Hackett KT, Dillard JP.** 2012. Prevalence and detailed mapping of the gonococcal genetic island in *Neisseria meningitidis*. J Bacteriol **194:**2275-2285.
39. **Swanson J, Kraus SJ, Gotschlich EC.** 1971. Studies on gonococcus infection I. Pili and zones of adhesion: their relation to gonococccal growth patterns. J Exp Med **134:**886-906.
40. **Hamilton HL, Schwartz KJ, Dillard JP.** 2001. Insertion-duplication mutagenesis of *Neisseria*: Use in characterization of DNA transfer genes in the gonococcal genetic island. J Bacteriol **183:**4718-4726.
41. **Ram S, Cox AD, Wright JC, Vogel U, Getzlaff S, Boden R, Li J, Plested JS, Meri S, Gulati S, Stein DC, Richards JC, Moxon ER, Rice PA.** 2003. Neisserial lipooligosaccharide is a target for complement component C4b. Inner core phosphoethanolamine residues define C4b linkage specificity. J Biol Chem **278:**50853-50862.
42. **Ramsey ME, Hackett KT, Kotha C, Dillard JP.** 2012. New complementation constructs for inducible and constitutive gene expression in *Neisseria gonorrhoeae* and *Neisseria meningitidis*. Appl Environ Microbiol **78:**3068-3078.

APPENDIX 2

Generation of complementation constructs for use in *Neisseria sicca* and *Neisseria mucosa*

Jia Mun Chan, Emma S. Rehnelt, Joseph P. Dillard

JM Chan and JP Dillard designed the experiments;

ES Rehnelt constructed plasmids pER7-12 and strain ER2000.

JM Chan constructed all of the other plasmids and strains, and performed all other experiments.

INTRODUCTION

Genetic manipulation, in the form of mutation and complementation of a gene, is a powerful tool for dissecting the function of the encoded gene product. Multiple cloning and complementation plasmids have been developed for use with *Neisseria gonorrhoeae* and *Neisseria meningitidis* (1, 2). Despite growing interest in nonpathogenic *Nesiseria*, the toolbox for genetic manipulation in these species is limited. Cloning and complementation plasmids developed for *N. gonorrhoeae* and *N. meningitidis* do not work well with nonpathogenic *Neisseria* for two main reasons: differences in the DNA uptake sequence and lack of sequence and gene order conservation between *Neisseria* species.

First, uptake of DNA for transformation relies on the recognition of a 10-12 nucleotide sequence called the DNA uptake sequence (DUS) (3–6). The DUS varies slightly from species to species; transformation using DNA with a cognate DUS is significantly enhanced compared to using DNA with a non-cognate DUS (6–8). pIDN3 is a cloning plasmid with two copies of the gonococcal DUS 10-mer (GCCGCTGAA), which allows for efficient uptake and transformation by *N. gonorrhoeae* and *N. meningitidis* (9). A simple modification of the sequence of the DUS to match that of *N. mucosa* (GTCGCTGAA) was done to construct pEC026, the pIDN3 derivative used for gene knockouts in *N. sicca* and *N. mucosa*. Details of pEC026 construction were described in Chapter 2 (10).

The second challenge in adapting existing tools for use in nonpathogenic *Neisseria* is chromosomal rearrangements. Two loci used for ectopic site complementation in *N. gonorrhoeae* and *N. meningitidis*, the *lctP-aspC* locus and *trpB-igA* locus, are not found in the same genetic context in *N. sicca*, *N. mucosa* and *N. lactamica* (data not shown) (2, 11). As such, we identified a new locus, and designed and generated new complementation plasmids for use

with nonpathogenic species using similar techniques employed by Ramsey and colleagues (2). We then used these plasmids to complement gene interruptions in *N. mucosa*, and attempted to do the same with *N. sicca*.

MATERIALS AND METHODS

Bacterial strains and growth conditions. Table 1 contains a full list of all bacterial strains used in this study. *N. sicca* and *N. mucosa* were grown on gonococcal base medium (GCB) agar plates (Difco) at 37°C with 5% CO_2, or grown in gonococcal base liquid medium supplemented with 0.042% $NaHCO_3$ and Kellogg's supplements (12) (cGCBL) at 37°C with aeration. *Escherichia coli* was grown either in LB broth (Difco) with aeration or on LB agar plates (Difco) at 37°C. When necessary, antibiotics were added into the media. Chloramphenicol was used at concentrations of 2 μg/ml and 5 μg/ml (*N. sicca* and *N. mucosa*) or 25 μg/ml (*E. coli*), while kanamycin was used at concentrations of 60 μg/ml and 80 μg/ml (*N. sicca* and *N. mucosa*) or 40 μg/ml (*E. coli*). Erythromycin was used at a concentration of 500 μg/ml (*E. coli*). 1 mM isopropyl β-D-1-thiogalactopyranoside (IPTG) was added to the growth medium when appropriate.

Construction of strains. Spot transformation of *N. sicca* and *N. mucosa* was performed as described previously (1, 10) using 20 μg of linearized plasmid DNA. To select for antibiotic resistant transformants of *N. sicca* and *N. mucosa*, the relevant isolates are first grown on plates containing the lower concentration of antibiotic and subsequently restreaked onto plates containing higher levels of antibiotic. This two-step selection process increases the chances of obtaining successful transformants and reduces instances of false-positive results.

Construction of plasmids. All plasmids used in this study are listed in Table 1. Most plasmids were constructed by ligation of restriction enzyme digested insert and vector backbone. The insert is generated by one of three methods: (i) PCR, (ii) overlap-PCR of two or more pieces of DNA, or (iii) excision from an existing plasmid (subcloning). 10 µl ligation reaction was transformed into *E. coli* TAM1 RapidTrans™ chemically competent cells (Active Motif). Successful transformants were selected for by growth on media supplemented with relevant antibiotics, and checked with PCR and sequencing.

The complementation plasmids for *N. sicca* and *N. mucosa*, pER11 and pER12 respectively, were generated in a step-wise approach, yielding a total of six plasmids. To make pER7 (*N. sicca* RS03325-RS13485 region in pHSS6), a 2.3 kb region was amplified from *N. sicca* ATCC 29256 chromosomal DNA using primers NotI ATPase F3 and Not1 hyp R2. The PCR product, as well as the cloning vector pHSS6 were digested with NotI, ligated and transformed into *E. coli.* pER8 (*N. mucosa* RS05105-RS05110 in pHSS6) was constructed similarly, however, *N. mucosa* ATCC 25996 chromosomal DNA was used as the template for PCR instead. To generate pER9, pEC7 was amplified using primers BsaI KpnI pER1 F and BsaI pER1 R, digested with BsaI and self-ligated. Sequences to introduce second termination loop (*ermC* terminator), a BsaI site and a KpnI site into the pER7 base were included in the primers. pER10 was generated similarly using pER8 as a template instead. A region containing IPTG inducible *lac* promoter, *lac* repressor, multiple cloning site and a chloramphenicol acetyltransferase (*cat*) gene was amplified from pKH37 using primers pKH37F and pKH37 KpnI R, and subsequently digested with KpnI. The KpnI digested product was ligated with a KpnI digested pER9 to generate pER11, and ligated with a KpnI digested pER10 to generate pER12. The orientation of the inserts was determined by PCR.

The insert for pEC059 ($P_{ampG\text{GC}}$-$ampG_{\text{Nsi}}$ cloned into pIDN3) was generated by overlap-PCR. First, the upstream and downstream regions of gonococcal *ampG* were amplified from *N. gonorrhoeae* MS11 chromosomal DNA using primer pairs Mc ampG SacI F3 and NSi SOE ampG 5' flank R, and NSi SOE 3' flank F and ampG 3' flank R BamHI respectively. Then, $ampG_{\text{Nsi}}$ was amplified from *N. sicca* ATCC 29256 chromosomal DNA using primers SOE-NSi ampG F and SOE-NSi ampG R. The three PCR products were then used as templates in overlap-PCR using primers Mc ampG SacI F3 and ampG 3' flank R BamHI. The cloning plasmid pIDN3 and the subsequent overlap-PCR product was digested with SacI and BamHI, and used in a ligation reaction to generate pEC059.

pEC060 ($P_{ampG\text{GC}}$-$ampG_{\text{Nmu}}$ cloned into pIDN3) was generated in the same way as pEC059 with two exceptions. Firstly, $ampG_{\text{Nmu}}$ was amplified from *N. mucosa* ATCC 25996 chromosomal DNA using primers SOE-NMu ampG F and SOE-NMu ampG R instead. Secondly, the upstream region of the upstream and downstream regions of gonococcal *ampG* were amplified from *N. gonorrhoeae* MS11 chromosomal DNA using primer pairs Mc ampG SacI F3 and Nmu SOE ampG 5' flank R, and Nmu SOE 3' flank F and ampG 3' flank R BamHI respectively.

The coding sequence of $ampG_{\text{Nsi}}$ was excised from pEC063 using enzymes SacI and XhoI, and subcloned into pKH37 digested similarly to make pEC068 ($ampG_{\text{Nsi}}$ cloned into pKH37), or subcloned into pER11 to generate pEC144 ($ampG_{\text{Nsi}}$ cloned into pER11).

The coding sequence of $ampG_{\text{Nmu}}$ was excised from pEC064 using enzymes SacI and XhoI, and ligated with pKH37 digested similarly to generate pEC071 ($ampG_{\text{Nmu}}$ cloned into pKH37), or subcloned into pER12 to construct pEC145 ($ampG_{\text{Nmu}}$ cloned into pER12).

Analyses of aligned genomes and individual genes. The partially and fully annotated genome assemblies of *N. sicca* ATCC 29256 (assembly accession number GCA_000174655.1), *N. mucosa* ATCC 25996 (assembly accession number GCA_000173875.1), *N. gonorrhoeae* FA1090 (accession number AE004969.1), *N. meningitidis* MC58 (accession number AE002098.2) and *N. lactamica* ATCC 23970 (assembly accession number GCA_000741965.1) were downloaded from GenBank in July 2015 (13). Since then, annotated gene information for some of the species have been discontinued. The downloaded genomes were aligned using the genome alignment software MAUVE and manually surveyed to identify possible complementation loci (14). Locus and allele designations listed in Table 3 were obtained from the BIGSdb database for *Neisseria* and from NCBI (15, 16). Predicted gene product function, localization and presence of conserved domain(s) were obtained from GenBank and checked using NCBI Conserved Domain Database (CDD) or with SignalP as needed (17, 18). Comparison of alleles and determination of percent identity was done using MAFFT (19).

Characterization of released peptidoglycan (PG) fragments. Metabolic labeling of peptidoglycan and quantitative fragment release was performed as described by Rosenthal and Dziarski (20) with modifications by Cloud and Dillard (21) and Garcia and Dillard (22). Briefly, strains were grown in cGCBL to mid-log phase, back diluted to OD_{540} of 0.2, and grown in GCBL supplemented with 0.042% $NaHCO_3$, a modified Kellogg's supplement containing pyruvate instead of glucose and 10 μCi/ml [6-^{3}H] glucosamine for 45 minutes. Unincorporated [6-^{3}H] glucosamine was then removed, and the amount of radioactive counts (counts per minute, CPM) in the cultures were normalized. Strains were then grown for an additional 2.5 hours in cGCBL. Released PG fragments in the cell-free supernatant, harvested by centrifugation at 3000

x *g* for 10 mins and filtration of the supernatant using a 0.22 μm pore filter, were analyzed using tandem size-exclusion chromatography and high performance liquid chromatography (HPLC) where relevant. Tandem size-exclusion chromatography was carried out using Bio-Gel P6 and P30 polyacrylamide beads (Bio-Rad) as the stationary phase and 0.1 M LiCl as the mobile phase. CPM values were determined using liquid scintillation counting.

RESULTS

Selection of *NEIS1146-NEIS1147* locus as a complementation locus. We examined the aligned genomes of *N. sicca* ATCC 29256, *N. mucosa* ATCC 25996, *N. gonorrhoeae* FA1090, *N. meningitidis* MC58 and *N. lactamica* ATCC 23970 to identify potential complementation loci, using the following criteria: 1) the presence of two adjacent genes in opposite orientations of each other, 2) found in the same genetic context in *N. sicca* and *N. mucosa*, 3) preferably with one or more transcriptional terminators separating the two genes. The *NEIS1146-NEIS1147* locus fulfills all three criteria and is also found in *N. gonorrhoeae, N. meningitidis* and *N. lactamica*. The orientations of *NEIS1146*, *NEIS1147* and two adjacent genes, *NEIS1145* and *NEIS1148* are depicted in Figure 1A. Alternate names for the four genes and the predicted function of the gene products are summarized in Table 3.

NEIS1146, in *N. sicca* and *N. mucosa*, is a 429 bp gene encoding a hypothetical periplasmic protein with a predicted signal peptide. The gene product is predicted to have a conserved CpxP domain, and CpxP domain proteins are annotated as periplasmic chaperone proteins in the Conserved Domain Database (18). Alleles of *NEIS1146* in *N. sicca* and *N. mucosa*, named NEISICOT_RS03325 and NEIMUCOT_RS05110 respectively, share 94.41% identity. *NEIS1147* is an 866 bp gene encoding a predicted AAA family ATPase.

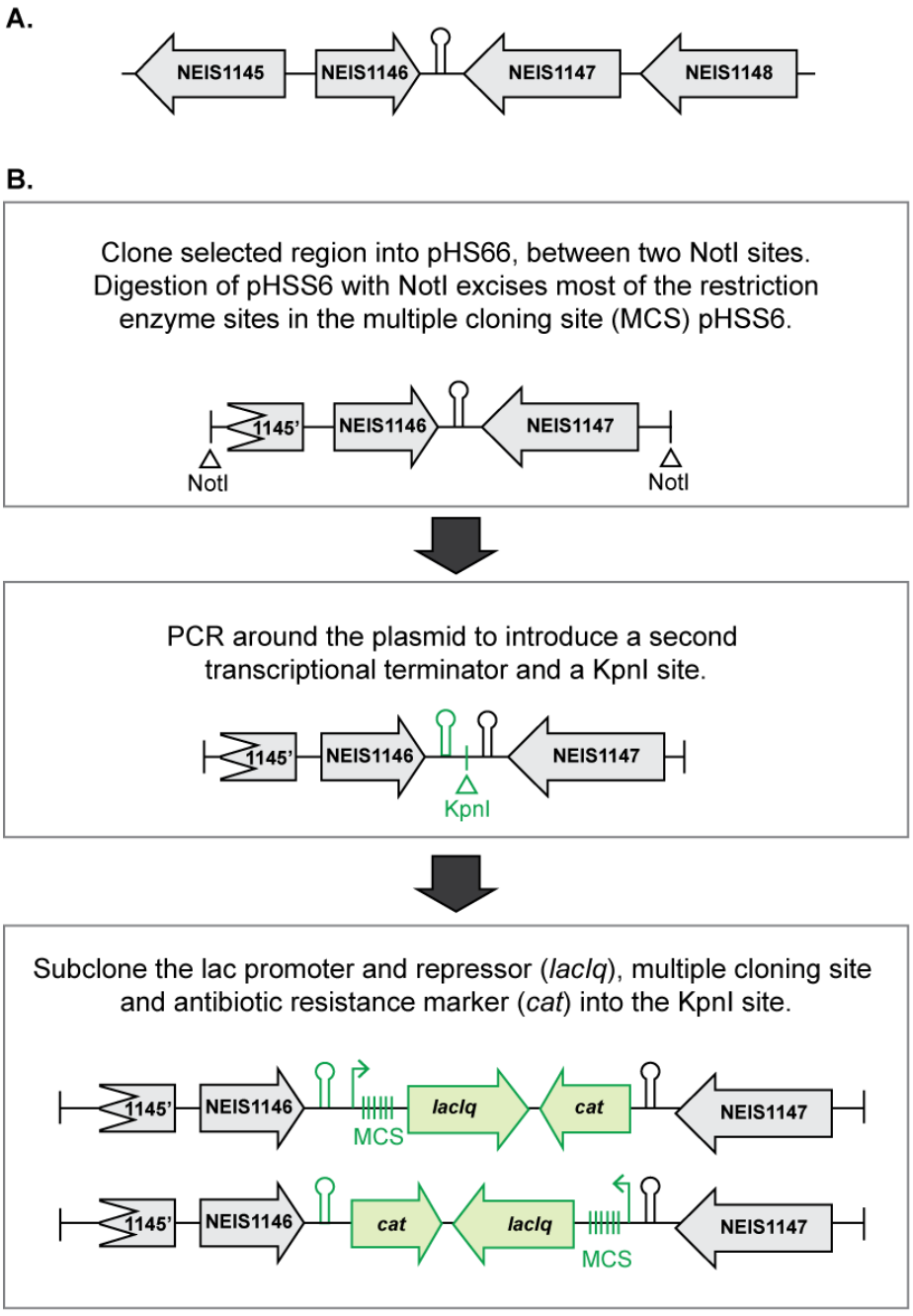

Figure 1. Design of a complementation construct at the intergenic region between *NEIS114* and *NEIS1147*. A) Genetic context of the *NEIS1146-NEIS1147* locus; not to scale. B) Flow chart depicting the stepwise construction of the complementation locus; not to scale.

The corresponding alleles in *N. sicca* and *N. mucosa*, named NEISICOT_RS13485 and NEIMUCOT_RS05105 respectively, share 91.93% identity. NEISICOT_RS13485 is annotated as a pseudogene due to a frameshift mutation; however, we sequenced this allele from our stock of *N. sicca* ATCC 29256 twice and found no evidence of a frameshift mutation (data not shown).

Design of complementation plasmids. We utilized the same stepwise strategy reported by Ramsey and colleagues (2) to generate our complementation plasmids. The general workflow is summarized in Figure 1B, and specific details of plasmid construction can be found in the methods section. Briefly, we cloned a 2.3 kb region containing the entire coding sequence of *NEIS1146* and *NEIS1147*, the first 199 bp of *NEIS1145* and the intergenic region between *NEIS1146* and *NEIS1147* containing a transcription termination loop from both *N. sicca* and *N. mucosa* into the cloning vector pHSS6. Two complementary DUS sequences based-paired to form the shared native terminator for *NEIS1146* and *NEIS1147*. Instead of making only one complementation plasmid for use with both *N. sicca* and *N. mucosa*, we chose to clone the aforementioned 2.3 kb region from both *N. sicca* and *N. mucosa* to increase the chances of having at least one functional complementation plasmid.

We introduced a second termination loop in the intergenic region between *NEIS1146* and *NEIS1147* to ensure that transcription of both *NEIS1146* and *NEIS1147* are completed correctly. We then cloned elements needed for IPTG inducible expression of target genes and for selection of successful transformants in between the two terminators. The elements were amplified from the gonococcal complementation plasmid pKH37, and they include *lac* promoter, the gene $lacI^{Q}$ encoding a Lac repressor, the gene *cat* encoding a chloramphenicol acetyltransferase that confers resistance against the antimicrobial activity of chloramphenicol, and a multiple cloning site

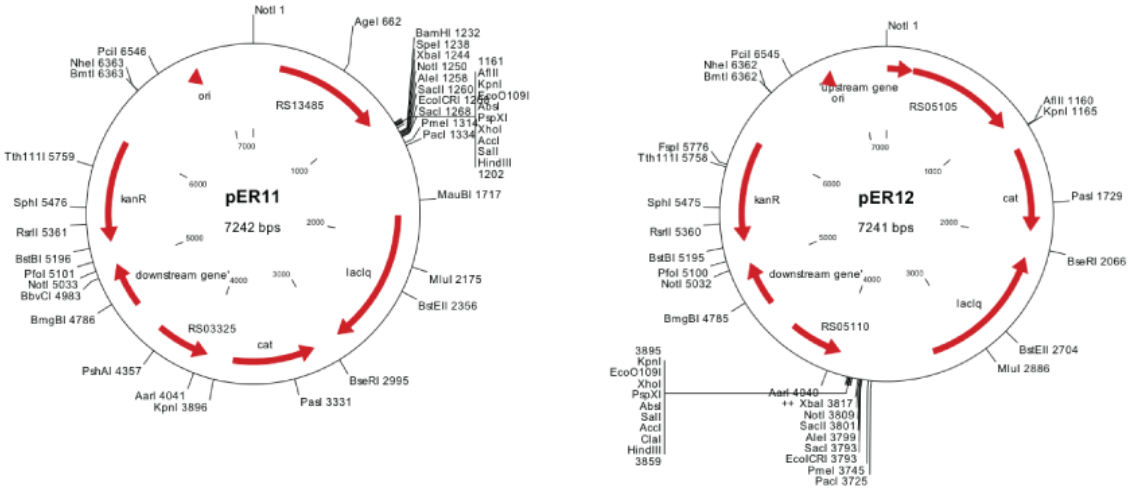

Figure 2. Plasmid maps of the final complementation plasmids for *N. sicca* (pER11) and *N. mucosa* (pER12) generated using Clone Manager (SciEd Software). Restriction enzyme sites that only cut once in the plasmid, as well as NotI and KpnI sites, are shown in the maps. Gene names correspond to the specific allele designations in the relevant species.

(MCS). Expression of target genes cloned into the MCS will be under the control of the *lac* promoter and can be induced with addition of exogenous IPTG in the growth medium. The resulting approximately 5 kb region cloned into pHSS6 is hereafter referred to as the complementation locus. The final plasmids for gene complementation in *N. sicca* and *N. mucosa* are named pER11 and pER12, respectively (Figure 2).

Transformation of *N. sicca* and *N. mucosa* with pER11 and pER12. The complementation loci in pER11, pER12 and derivative plasmids were stably integrated into the chromosome using the spot transformation technique described in the methods and elsewhere (1, 10). We selected for chloramphenicol resistant isolates, and were able to recover such isolates reliably when *N. mucosa* was transformed with 20 μg pER12. We verified the complementation locus was stably integrated into the chromosome of the chloramphenicol resistant isolates by PCR and sequencing, and saved one of the isolates as ER2000. Despite multiple attempts, we were unable to recover similar chloramphenicol resistant isolates when *N. sicca* was transformed with 20 μg pER11.

Expression of *ampG* from the complementation locus does not restore wild-type like peptidoglycan fragment release of an *N. mucosa ampG* mutant. We previously reported that disruption in the gene encoding the PG permease AmpG in *N. sicca* and *N. mucosa* impairs PG fragment recycling and results in a large increase in PG monomers released (Chapter 2, (10)). We cloned *N. mucosa ampG* (*ampG*$_{Nmu}$) into pER12, and transformed the resulting plasmid pEC145 into the *N. mucosa ampG* mutant EC2003. Unfortunately, the resulting complement strain, EC2014, released similar amounts of PG monomers as EC2003 instead of phenocopying a

wild-type strain (Figure 3). We also cloned *N. sicca ampG* (*ampG*$_{Nsi}$) into pER11 (pEC147); however, our efforts to transform *N. sicca* with pEC147 were unsuccessful.

Heterologous expression of *ampG* from *N. sicca* or *N. mucosa* in a gonococcal *ampG* mutant does not restore wild-type like peptidoglycan fragment release. Concurrent with the efforts to generate cloning vectors for *N. sicca* and *N. mucosa* were efforts to express *ampG*$_{Nmu}$ and *ampG*$_{Nsi}$ in *N. gonorrhoeae*. Expression of meningococcal *ampG* in lieu of gonococcal *ampG* (*ampG*$_{GC}$) had been instructive in understanding the differences in PG recycling between *N. gonorrhoeae* and *N. meningitidis*. We first attempted to express *ampG*$_{Nsi}$ and *ampG*$_{Nmu}$ in *N. gonorrhoeae* at the native *ampG*$_{GC}$ site under the control of the native *ampG*$_{GC}$ promoter (EC524, EC525); however, both strains released large amounts of PG fragments in a pattern reminiscent of an *ampG* mutant (Figure 4A). Expression of *ampG*$_{Nsi}$ and *ampG*$_{Nmu}$ from the gonococcal *lctP-aspC* complementation locus under the control of an IPTG inducible *lac* promoter (EC529, EC530) also failed to fully complement an *ampG*$_{GC}$ deletion, although EC530 released less PG monomer compared to EC529 (Figure 4B).

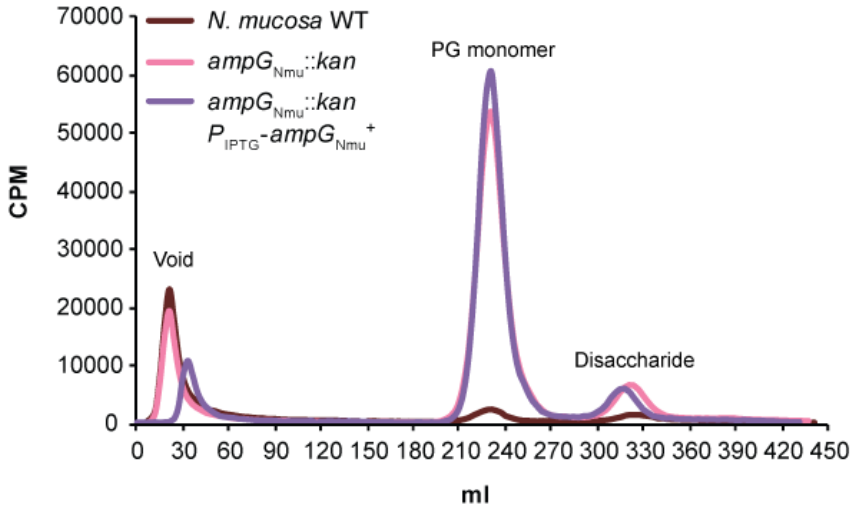

Figure 3. Expression of *ampG*$_{Nmu}$ from the complementation site under the control of an IPTG-inducible promoter does not restore wild-type like PG fragment release in *N. mucosa*.

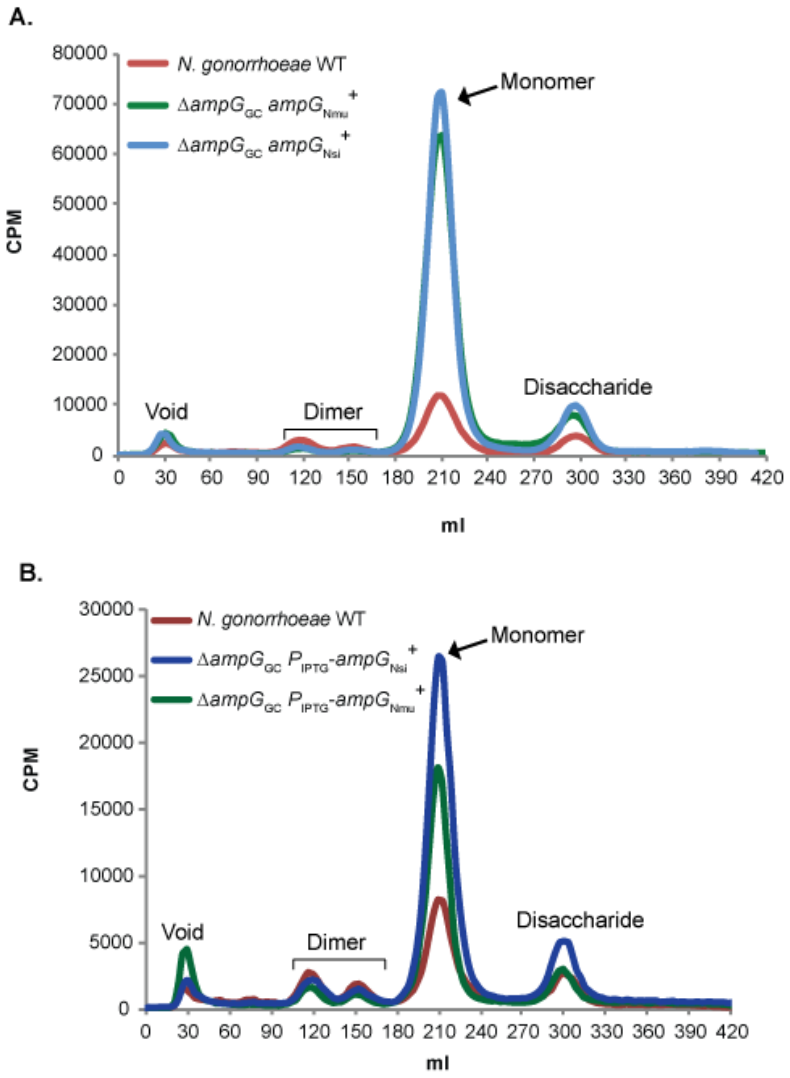

Figure 4. Heterologous expression of *ampG*$_{Nmu}$ from the native gonococcal *ampG* site (A), or from the complementation site under an IPTG-inducible promoter (B) does not restore wild-type like PG fragment release in *N. gonorrhoeae*.

Discussion and future direction

Due to a lack of tools to genetically manipulate nonpathogenic *Neisseria,* we designed and constructed complementation plasmids pER11 and pER12 for use with *N. sicca* and *N. mucosa*, respectively. Target gene(s) can be cloned into a MCS on the plasmid, which is immediately downstream of an IPTG inducible promoter. Homologous recombination of portions of the complementation plasmids into the chromosome allows for stable complementation of target gene(s) at the *NEIS1146-NEIS1147* intergenic region. We showed that pER12 and a pER12 derivative, pEC145, can be used to transform *N. mucosa*. Successful transformations of *N. sicca* with pER11 and a pER11 derivative, pEC144 have not been demonstrated. We noticed, from general observation of transformation attempts using *N. sicca* and *N. mucosa* as recipient strains, that our strain of *N. mucosa* transforms more easily compared to *N. sicca*. As such, we need to develop strategies to ensure reliable and replicable uptake and integration of the complementation locus of pER11. One possible approach is to increase uptake of pER11 by *N. sicca*, perhaps through electroporation.

Expression of $ampG_{Nmu}$ from the *NEIS1146-NEIS1147* complementation locus in an $ampG_{Nmu}$ mutant did not restore wild-type like PG fragment release profile. However, our previous attempt to express $ampG_{Nmu}$ from the established *lctP-aspC* locus in *N. gonorrhoeae* has not been successful, either. When we induced expression of a C-terminal tandem FLAG tagged version of $ampG_{Nmu}$ from the gonococcal *lctP-aspC* locus, we were able to detect the protein by immunoblotting for the FLAG epitope (data not shown). As such, it is equally possible that $AmpG_{Nmu}$ is fully functional only when a specific amount of $AmpG_{Nmu}$ is made by the cell, or that pER12 is defective as a complementation plasmid. More attempts to use pER12 to complement gene mutations in *N. mucosa* will demonstrate the functionality, or lack thereof,

of pER12 as a complementation plasmid. One such attempt is described in Appendix 1II. We have also mutated and complemented an *mltG*$_{Nmu}$ mutation, which encodes the putative PG polymerization termination protein (23). Since an *mltG*$_{Nmu}$ mutant released WT-levels of PG fragments, the fragment release analysis did not reveal if the complementation was successful (data not shown). Future work looking at other altered phenotypes of an *mltG*$_{Nmu}$ mutant may provide us with more phenotypic assays to test the functionality of the complementation construct.

Table 1. Strains and plasmids used in this study.

Strain/ Plasmid	Description	Source/ Reference
Strains		
25996	*N. mucosa* WT	ATCC
29256	*N. sicca* WT	ATCC
MS11	*N. gonorrhoeae* WT	(24)
DG132	*N. gonorrhoeae* Δ*ampG*$_{GC}$	(22)
ER2000	25996 transformed with pER12	This study
EC2003	*ampG*$_{Nmu}$::*kan*	(10)
EC2004	*ampG*$_{Nsi}$::*kan*	(10)
EC2014	EC2003 transformed with pEC145; *ampG*$_{Nmu}$::*kan* P_{IPTG}-*ampG*$_{Nmu}^{+}$	This study
EC524	MS11 transformed with pEC060; Δ*ampG*$_{GC}$ *ampG*$_{Nmu}^{+}$	This study
EC525	MS11 transformed with pEC059; Δ*ampG*$_{GC}$ *ampG*$_{Nsi}^{+}$	This study
EC529	DG132 transformed with pEC068; Δ*ampG*$_{GC}$ P_{IPTG}-*ampG*$_{Nsi}^{+}$	This study
EC530	DG132 transformed with pEC071; Δ*ampG*$_{GC}$ P_{IPTG}-*ampG*$_{Nmu}^{+}$	This study
Plasmids		
pHSS6	Cloning plasmid; vector backbone for complementation plasmid (Kan^{R})	(25)
pKH37	Complementation plasmid for *N. gonorrhoeae*/*N. meningitidis* (Cm^{R})	(11)
pEC026	Cloning plasmid for *N. mucosa* (Erm^{R})	(10)
pEC063	*ampG*$_{Nsi}$ cloned into pEC026	(10)
pEC064	*ampG*$_{Nmu}$ cloned into pIDN3	(10)
pER7	*N. sicca* RS03325-RS13485 region cloned into pHSS6	This study
pER8	*N. mucosa* RS05105-RS05110 region cloned into pHSS6	This study
pER9	*ermC* terminator cloned into pER6	This study
pER10	*ermC* terminator cloned into pER7	This study
pER11	P_{IPTG}-MCS, *lacI*^{Q} and *cat* cloned into pER9; final complementation plasmid for *N. sicca* (Cm^{R})	This study
pER12	P_{IPTG}-MCS, *lacI*^{Q} and *cat* cloned into pER10; final complementation plasmid for *N. mucosa* (Cm^{R})	This study
pEC059	$P_{ampG}$$_{GC}$-*ampG*$_{Nsi}$ cloned into pIDN3	This study
pEC060	$P_{ampG}$$_{GC}$-*ampG*$_{Nmu}$ cloned into pIDN3	This study
pEC068	*ampG*$_{Nsi}$ cloned into pKH37	This study
pEC071	*ampG*$_{Nmu}$ cloned into pKH37	This study
pEC144	*ampG*$_{Nsi}$ cloned into pER11	This study
pEC145	*ampG*$_{Nmu}$ cloned into pER12	This study

Table 2. Primers used in this study. Restriction enzyme sites are underlined

Primer name	Sequence
NotI ATPase F3	AATGCGGCCGCTTGCAGCCTGACCATAG
NotI hyp R2	GATGCGGCCGCGATTCAACACCAATCCTGC
BsaI KpnI pER1 F	GAGGTCTCTTATGCATCCCTTAAGGTACCGCATCGCTTTGAATCGC
BsaI pER1 R	CGCCAGGTCTCTCATAAACTGCATCCCTTAACCTACCCTTATCCTCCC
pKH37F	CCATCCGTTCTGCTCTATAC
pKH37R-KpnI	GGTGGTACCTTGGTCATGGCCAGCTTATC
MC ampG SacI F3	ATTCAGAGCTCCATCGGCGGCATCATCAAAC
ampG 3' flank R BamHI	CTCAGGATCCGTTCTTTATATGAGCGGCAGG
NSi SOE-ampG 3' flank F	ATATGCCACCTCAAACTGGAGCGTTTACCTG
NSi SOE-ampG 5' flank R	GATGAGCAGTACAGCCTATTGTAGCAAATATCG
NMu SOE-ampG 3' flank F	GTATCGGTAGGTCAAACTGGAGCGTTTACCTG
NMu SOE-ampG 5' flank R	GGAGAACAACATCAGCCTATTGTAGCAAATATCG
SOE-NSi ampG F	CTACAATAGGCTGTACTGCTCATCCATTATGAC
SOE-NSi ampG R	GCTCCAGTTTGAGGTGGCATATTTAAGCAGATTG
SOE-NMu ampG F	CTACAATAGGCTGATGTTGTTCTCCCATTATGAC
SOE-NMu ampG R	GCTCCAGTTTGACCTACCGATACATTCAAACG

Table 3. Alternate names and predicted gene products for complementation loci genes.

MLST locus designation	**NEIS1145**	**NEIS1146**	**NEIS1147**	**NEIS1148**
Alias in *N. sicca* ATCC 29256	NEISICOT_ RS03330	NEISICOT_ RS03325	NEISICOT_ RS13485	NEISICOT_ RS03315
Alias in *N. mucosa* ATCC 25996	NEIMUCOT_ RS05115	NEIMUCOT_ RS05110	NEIMUCOT_ RS05105	NEIMUCOT_ RS05100
Alias in *N. gonorrhoeae* FA1090	NGO0758	NGO0757	NGO0756	NGO0755
Aliases in *N. meningitidis* MC58	*rpe*; NMB1244	NMB1245	NMB1246	*ribE*; NMB1247
Alias in *N. lactamica* ATCC 23970	RS02700	RS02705	RS02710	RS02715
Predicted gene product	Ribulose-phosphate 3-epimerase	Hypothetical periplasmic protein	AAA family ATPase protein	Riboflavin synthesis subunit alpha

REFERENCES

1. **Dillard JP**. 2011. Genetic manipulation of *Neisseria gonorrhoeae*. Curr Protoc Microbiol **4**:Unit4A.2.
2. **Ramsey ME**, **Hackett KT**, **Kotha C**, **Dillard JP**. 2012. New complementation constructs for inducible and constitutive gene expression in *Neisseria gonorrhoeae* and *Neisseria meningitidis*. Appl Environ Microbiol **78**:3068–3078.
3. **Goodman SD**, **Scocca JJ**. 1988. Identification and arrangement of the DNA sequence recognized in specific transformation of *Neisseria gonorrhoeae*. Proc Natl Acad Sci U S A **85**:6982–6986.
4. **Elkins C**, **Thomas CE**, **Seifert HS**, **Sparling PF**. 1991. Species-specific uptake of DNA by gonococci is mediated by a 10-base-pair sequence. J Bacteriol **173**:3911–3913.
5. **Ambur OH**, **Frye SA**, **Tønjum T**. 2007. New functional identity for the DNA uptake sequence in transformation and its presence in transcriptional terminators. J Bacteriol **189**:2077–2085.
6. **Duffin PM**, **Seifert HS**. 2010. DNA uptake sequence-mediated enhancement of transformation in *Neisseria gonorrhoeae* is strain dependent. J Bacteriol **192**:4436–4444.
7. **Frye SA**, **Nilsen M**, **Tonjum T**, **Ambur OH**. 2013. Dialects of the DNA Uptake Sequence in *Neisseriaceae*. PLoS Genet **9**:e1003458.
8. **Berry JL**, **Cehovin A**, **McDowell MA**, **Lea SM**, **Pelicic V**. 2013. Functional analysis of the interdependence between DNA uptake sequence and its cognate ComP receptor during natural transformation in *Neisseria* species. PLoS Genet **9**:e1004014.
9. **Hamilton HL**, **Schwartz KJ**, **Dillard JP**. 2001. Insertion-duplication mutagenesis of *Neisseria*: Use in characterization of DNA transfer genes in the gonococcal genetic island. J Bacteriol **183**:4718–4726.
10. **Chan JM**, **Dillard JP**. 2016. *Neisseria gonorrhoeae* crippled its peptidoglycan fragment permease to facilitate toxic peptidoglycan monomer release. J Bacteriol **198**:3029–3040.
11. **Kohler PL**, **Hamilton HL**, **Cloud-Hansen K**, **Dillard JP**. 2007. AtlA functions as a peptidoglycan lytic transglycosylase in the *Neisseria gonorrhoeae* type IV secretion system. J Bacteriol **189**:5421–5428.
12. **Kellogg DS**, **Peacock WL**, **Deacon WE**, **Brown L**, **Pirkle CI**. 1963. *Neisseria gonorrhoeae*: Virulence genetically linked to clonal variation. J Bacteriol **85**:1274–1279.
13. **Benson DA**, **Karsch-Mizrachi I**, **Lipman DJ**, **Ostell J**, **Sayers EW**. 2009. GenBank. Nucleic Acids Res **37**:D26–D31.
14. **Darling ACE**, **Mau B**, **Blattner FR**, **Perna NT**. 2004. Mauve: Multiple alignment of conserved genomic sequence with rearrangements. Genome Res **14**:1394–1403.
15. **Sayers EW**, **Barrett T**, **Benson DA**, **Bryant SH**, **Canese K**, **Chetvernin. V**, **Church DM**, **Dicuccio M**, **Edgar R**, **Federhen S**, **Feolo M**, **Geer LY**, **Helmberg W**, **Kapustin Y**, **Landsman D**, **Lipman DJ**, **Madden TL**, **Maglott DR**, **Miller V**, **Mizrachi I**, **Ostell J**, **Pruitt KD**, **Schuler GD**, **Sequeira E**, **Sherry ST**, **Shumway M**, **Sirotkin K**, **Souvorov A**, **Starchenko G**, **Tatusova TA**, **Wagner L**, **Yaschenko E**, **Ye J**. 2009. Database resources of the National Center for Biotechnology Information. Nucleic Acids Res **37**:5–15.
16. **Jolley KA**, **Maiden MCJ**. 2010. BIGSdb: Scalable analysis of bacterial genome variation at the population level. BMC Bioinformatics **11**:595.
17. **Petersen TN**, **Brunak S**, **von Heijne G**, **Nielsen H**. 2011. SignalP 4.0: discriminating

signal peptides from transmembrane regions. Nat Methods **8**:785–786.
18. **Machler-Bauer A**, **Bo Y**, **Han L**, **He J**, **Lanczycki C**, **Lu S**, **Chitsaz F**, **Derbyshire M**, **Geer R**, **Gonzales N**, **Gwadz M**, **Hurwitz D**, **Lu F**, **Machler G**, **Song J**, **Thanki N**, **Wang Z**, **Yamashita R**, **Zhang D**, **Zheng C**, **Geer L**, **Bryant S**. 2017. CDD/SPARCLE: functional classification of proteins via subfamily domain architectures. Nucleic Acids Res **45**:D200–D203.
19. **Katoh K**, **Rozewicki J**, **Yamada KD**. 2017. MAFFT online service: multiple sequence alignment, interactive sequence choice and visualization. Brief Bioinform **bbx108**:doi.org/10.1093/bib/bbx108.
20. **Rosenthal RS**, **Dziarski R**. 1994. Isolation of peptidoglycan and soluble peptidoglycan fragments. Methods Enzymol **235**:253–285.
21. **Cloud KA**, **Dillard JP**. 2002. A lytic transglycosylase of *Neisseria gonorrhoeae* is involved in peptidoglycan-derived cytotoxin production. Infect Immun **70**:2752–2757.
22. **Garcia DL**, **Dillard JP**. 2008. Mutations in *ampG* or *ampD* affect peptidoglycan fragment release from *Neisseria gonorrhoeae*. J Bacteriol **190**:3799–3807.
23. **Yunck R**, **Cho H**, **Bernhardt TG**. 2016. Identification of MltG as a potential terminase for peptidoglycan polymerization in bacteria. Mol Microbiol **99**:700–718.
24. **Swanson J**. 1972. Studies on gonococcus infection. II. Freeze-fracture, freeze-etch studies on gonococci. J Exp Med **136**:1258–1271.
25. **Mehr IJ**, **Long CD**, **Serkin CD**, **Seifert HS**. 2000. A homologue of the recombination-dependent growth gene, *rdgC*, is involved in gonococcal pilin antigenic variation. Genetics **154**:523–532.

APPENDIX 3

Construction of *Neisseria spp* mutants defective in H_2S production.

Jia Mun Chan, Joseph P. Dillard, Rodney E. Willoughby

RE Willoughby and JP Dillard designed the experiments,

JM Chan generated mutant strains.

Hydrogen sulfide (H_2S) is a product of sulfur metabolism in bacteria. Many species of bacteria across different phyla encode genes for H_2S producing enzymes. A 2011 study from Shatalin and coworkers showed that H_2S production by bacteria mitigates oxidative stress induced by multiple classes of antibiotics (1). Mutation of genes encoding enzymes involved in H_2S production in the Gram-negative *Escherichia coli* and *Pseudomonas aeruginosa* and the Gram-positive *Bacillus anthracis* and *Staphylococcus aureus* increases sensitivity of these bacteria to antibiotics (1). It was previously reported that *Neisseria meningitidis* and *N. lactamica*, but not *N. gonorrhoeae*, has the genetic potential to reduce sulfate to H_2S (2, 3).

A survey of multiple *Neisseria* species revealed that *N. meningitidis, N. lactamica, N. sicca, N. mucosa, N. cinerea* and *N. perflava* produce copious H_2S (personal communication). In contrast, *N. gonorrhoeae* does not produce H_2S. We decided to take a genetics approach to further study the effects of H_2S on the growth and pathogenic potential of the bacteria. The gene *metC* encodes a carbon-sulfur lyase that in *E. coli*, has been reported to degrade L-cysteine to pyruvate, ammonia and sulfide (4). We mutated *metC* and complemented the *metC* mutation in *N. meningitidis, N. mucosa* and *N. gonorrhoeae* to abolish and restore H_2S production, respectively. These species were chosen for genetic manipulation due to the availability of complementation constructs. The gonococcal strains were used as a negative control. The genetic context of native and mutated *metC* in *N. gonorrhoeae, N. meningitidis* and *N. mucosa* are shown in Figure 1. Gene nomenclature are from *N. gonorrhoaeae* FA1090. We made an in-frame markerless deletion of *metC* in *N. gonorrhoeae*, and interrupted the *metC* coding region in *N. mucosa* and *N. meningitidis* with a kanamycin resistance gene. We tried to make in-frame markerless deletion of *metC* in *N. meningitidis* and *N. mucosa* to avoid polarity on nearby genes; unfortunately, our attempts were not successful.

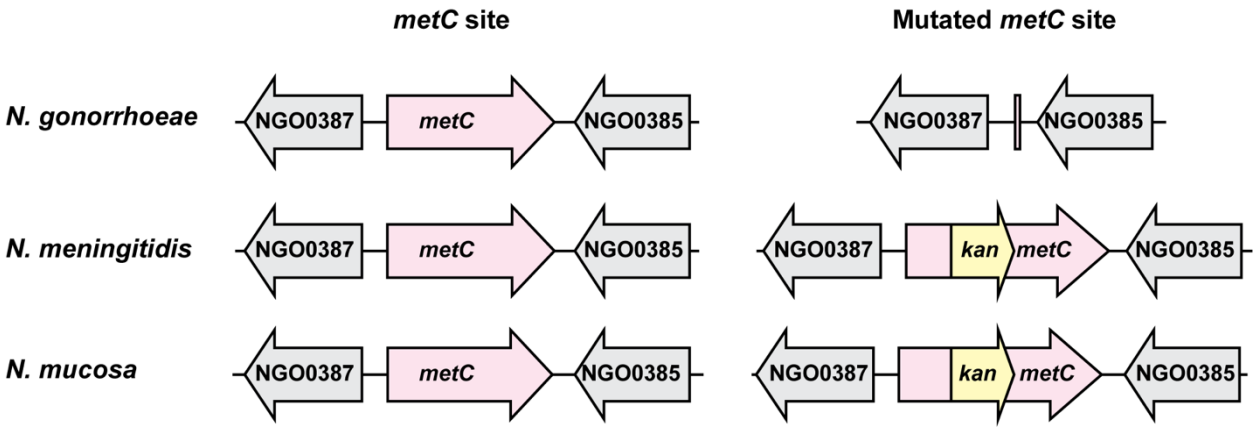

Figure 1. Cartoon depiction (not to scale) of the genetic context of *metC* (left) and the resulting *metC* mutations (right) in *N. gonorrhoeae*, *N. meningitidis* and *N. mucosa.*

MATERIALS AND METHODS

Construction of plasmids and strains. All plasmids and strains are listed in Table 1. Spot transformation was used to generate mutant or complemented strains of *N. gonorrhoeae*, *N. meningitidis* and *N. mucosa* (5). Briefly, 500 ng (for *N. gonorrhoeae* MS11), 5 μg (for *N. meningitidis* 8013) or 20 μg (for *N. meningitidis* ATCC 13102 and *N. mucosa* ATCC 25996) of linearized plasmid DNA was spotted onto GCB plates. Five to ten piliated colonies were streaked over the dried DNA spots. The plate was incubated overnight at 37°C with 5% CO_2. Antibiotics was used for selection when applicable at the following concentrations: chloramphenicol at 10 μg/ml for *N. gonorrhoeae*, and 5 μg/ml for all other species, and kanamycin at 60 μg/ml for *N. mucosa* and 80 μg/ml for *N. meningitidis*. Transformants were screened by PCR and confirmed by sequencing.

All plasmids were built either by ligation of one PCR product of a two-way ligation of two PCR products into a vector backbone, with subsequent transformation of the ligation product into

Escherichia coli RapidTrans™ (Active Motif) TAM1 chemical competent cells. Successful transformants were checked by PCR and sequencing. Primers used for PCR are listed in Table 2.

To make pEC155 (pKH37 + *metC*$_{GC}$), gonococcal *metC* was amplified using primers SacI Ngo metC F and XhoI Ngo Nme metC R using MS11 chromosomal DNA as a template. The resulting PCR product, as well as the complementation plasmid pKH37 were digested with SacI and XhoI, and used in a one-way ligation reaction to generate pEC155.

The first step in the generation of pEC156 (pIDN3 + Δ*metC*$_{GC}$; start/stop in-frame markerless deletion) is the amplification of approximately 1kb of gonococcal *metC* upstream and downstream regions using *N. gonorrhoeae* MS11 chromosomal DNA as a template. The upstream region was amplified using the primer pair SacI Ngo Nme metC up F/NheI Ngo metC up R and the resulting PCR product digested with SacI and NheI. The downstream region was amplified using the primer pair NheI Ngo Nme metC down F/BamHI Ngo Nme metC down R, and digested with NheI and XhoI. There is an internal XhoI site in the downstream region of *metC*. The cloning plasmid, pIDN3 served as a vector backbone and was digested with SacI and XhoI. A two-way ligation was performed to generate pEC156.

pEC159 (pKH37 + *metC*$_{MC}$) was generated firstly by amplification of the meningococcal *metC* coding sequence using the primers SacI Nme Nmu metC F and XhoI Ngo Nme metC R and *N. meningitidis*. The PCR product and pKH37 were digested with SacI and XhoI, and ligated to each other to generate pEC159.

pEC164 (pIDN3 + *metC*$_{MC}$*::kan*) was generated in two steps. First, pEC161 (pIDN3 + *metC*$_{MC}$) was constructed using the same strategy as pEC159, with the exception that pIDN3 was used as vector backbone instead of pKH37. Then, pEC161 was digested with AccI, and the resulting digested plasmid was blunted using T4 DNA polymerase (NEB). An antibiotic resistant cassette conferring kanamycin resistance (*kan*) was amplified from the cloning vector pHSS6 using primers kan F BamHI and kan R BamHI, and blunt ligated into the blunted, AccI-digested pEC161, to produce pEC164. The orientation of *kan* was in the same direction as *metC*$_{MC}$.

To generate pEC158 (pER12 + *metC*$_{Nmu}$), *N. mucosa metC* coding sequence was first amplified from *N. mucosa* ATCC 25996 chromosomal DNA using primers SacI Nmuc metC F and XhoI Nmuc metC R. The resulting PCR product and complementation vector pER12 were both digested with SacI and XhoI, and used in a ligation reaction to make pEC158.

pEC163 (pEC026 + *metC*$_{Nmu}$*::kan*) was made in two steps. Firstly, pEC162 (pEC026 + *metC*$_{Nmu}$) was generated essentially the same way as pEC158; the only exception was that pEC026 was used as a vector backbone instead of pER12. pEC162 was then digested with DraIII, blunted with T4 DNA polymerase, and ligated with a *kan* marker that was amplified from pHSS6 with primers kan F BamHI and kan R BamHI to make pEC163. The orientation of *kan* was in the same direction as *metC*$_{Nmu}$.

Table 1. Strains and plasmids used in this study.

Strain/ Plasmid	Description	Source/ Reference
Strains		
MS11	*N. gonorrhoeae* strain	(6)
13102	*N. meningitidis* Group C strain *rpsL*^{K43R}	(7)
8013	*N. meningitidis* Group C strain	(8)
29256	*N. mucosa* strain	ATCC
EC577	MS11 transformed with pEC156; Δ*metC*$_{GC}$	This study
EC578	EC577 transformed with pEC157; Δ*metC*$_{GC}$ *P*$_{IPTG}$-*metC*$_{GC}$	This study
EC1027	8013 transformed with pEC159; *P*$_{IPTG}$-*metC*$_{MC}$	This study
EC1028	8013 transformed with pEC164; *metC*$_{MC}$::*kan*	This study
EC1029	EC1027 transformed with pEC164; *metC*$_{MC}$::*kan P*$_{IPTG}$-*metC*$_{MC}$	This study
EC1030	13102 transformed with pEC164; *metC*$_{MC}$::*kan*	This study
EC1031	EC1030 transformed with pEC159; *metC*$_{MC}$::*kan P*$_{IPTG}$-*metC*$_{MC}$	This study
EC2015	29256 transformed with pEC158; *P*$_{IPTG}$-*metC*$_{Nmu}$	This study
EC2018	29256 transformed with pEC163; *metC*$_{Nmu}$::*kan*	This study
EC2019	EC2015 transformed with pEC163; *metC*$_{Nmu}$::*kan P*$_{IPTG}$-*metC*$_{Nmu}$	This study
Plasmids		
pIDN3	Cloning plasmid for *N. gonorrhoeae*/*N. meningitidis* (Erm^{R})	(9)
pKH37	Complementation plasmid for *N. gonorrhoeae*/*N. meningitidis* (Cm^{R})	(10)
pEC026	Cloning plasmid for *N. mucosa* (Erm^{R})	(11)
pER12	Complementation plasmid for *N. mucosa* (Cm^{R})	Appendix II
pHSS6	Cloning plasmid; source of *kan*	(12)
pEC155	*metC*$_{GC}$ cloned into pKH37	This study
pEC156	*metC*$_{GC}$ upstream and downstream regions cloned into pIDN3; final construct Δ*metC*$_{GC}$	This study
pEC158	*metC*$_{Nmu}$ cloned into pER12	This study
pEC159	*metC*$_{MC}$ cloned into pKH37	This study
pEC161	*metC*$_{MC}$ cloned into pIDN3	This study
pEC162	*metC*$_{Nmu}$ cloned into pEC026	This study
pEC163	*kan* subcloned into pEC162; final construct *metC*$_{Nmu}$::*kan* in pEC026	This study
pEC164	*kan* subcloned into pEC161; final construct *metC*$_{MC}$::*kan* in pIDN3	This study

Table 2. Primers used in this study. Restriction enzyme sites are underlined.

Primer name	**Sequence**
kanF-BamHI	CAGGATCCAAAGCCAGTCCGCAGAAACG
kanR-BamHI	CTGGATCCTGGGCGAAGAACTCCAGCAT
SacI Ngo Nme metC up F	GATCAGAGCTCGGCATAAGCCGAATGGTTG
NheI Ngo metC up R	GATCTGCTAGCGGTACGGGTCGGGAATTTC
NheI Ngo Nme metC down F	GATTGCTAGCGATATTTCCGCCGCACTC
BamHI Ngo Nme metC down R	GATCAGGATCCGCTCGGTATTCCGATGTTG
SacI Ngo metC F	GATGAGAGCTCGCGGCTGCATTGATTGTTTC
SacI NMe NMu metC F	GAGTAGAGCTCCCGCCTGCATTGATTGTTTC
XhoI Ngo Nme metC R	GACATCTCGAGGCTGGCATTCAAACGTG
SacI NSi metC F	AGTAGAGCTCCCGTGTCCGCATTGATTG
XhoI NSi metC R	GACTACTCGAGCGGTCAGAATGATTGCAGTC

REFERENCES

1. **Shatalin K**, **Shatalina E**, **Mironov A**, **Nudler E**. 2011. H_2S: A universal defense against antibiotics in bacteria. Science **334**:986–990.
2. **Rusniok C**, **Vallenet D**, **Floquet S**, **Ewles H**, **Mouzé-Soulama C**, **Brown D**, **Lajus A**, **Buchrieser C**, **Médigue C**, **Glaser P**, **Pelicic V**. 2009. NeMeSys: a biological resource for narrowing the gap between sequence and function in the human pathogen *Neisseria meningitidis*. Genome Biol **10**:R110.
3. **Schoen C**, **Kischkies L**, **Elias J**, **Ampattu BJ**. 2014. Metabolism and virulence in *Neisseria meningitidis*. Front Cell Infect Microbiol **4**:114.
4. **Awano N**, **Wada M**, **Kohdoh A**, **Oikawa T**, **Takagi H**, **Nakamori S**. 2003. Effect of cysteine desulfhydrase gene disruption on L-cysteine overproduction in *Escherichia coli*. Appl Microbiol Biotechnol **62**:239–243.
5. **Dillard JP**. 2011. Genetic manipulation of *Neisseria gonorrhoeae*. Curr Protoc Microbiol **4**:Unit4A.2.
6. **Swanson J**. 1972. Studies on gonococcus infection. II. Freeze-fracture, freeze-etch studies on gonococci. J Exp Med **136**:1258–1271.
7. **Woodhams KL**, **Chan JM**, **Lenz JD**, **Hackett KT**, **Dillard JP**. 2013. Peptidoglycan fragment release from *Neisseria meningitidis*. Infect Immun **81**:3490–3498.
8. **Nassif X**, **Lowy J**, **Stenberg P**, **O'Gaora P**, **Ganji A**, **So M**. 1993. Antigenic variation of pilin reguiates adhesion of *Neisseria meningitidis* to human epitheiiai ceiis. Mol Microbiol **8**:719–725.
9. **Hamilton HL**, **Schwartz KJ**, **Dillard JP**. 2001. Insertion-duplication mutagenesis of *Neisseria*: Use in characterization of DNA transfer genes in the gonococcal genetic island. J Bacteriol **183**:4718–4726.
10. **Kohler PL**, **Hamilton HL**, **Cloud-Hansen K**, **Dillard JP**. 2007. AtlA functions as a peptidoglycan lytic transglycosylase in the *Neisseria gonorrhoeae* type IV secretion system. J Bacteriol **189**:5421–5428.
11. **Chan JM**, **Dillard JP**. 2016. *Neisseria gonorrhoeae* crippled its peptidoglycan fragment permease to facilitate toxic peptidoglycan monomer release. J Bacteriol **198**:3029–3040.
12. **Mehr IJ**, **Long CD**, **Serkin CD**, **Seifert HS**. 2000. A homologue of the recombination-dependent growth gene, *rdgC*, is involved in gonococcal pilin antigenic variation. Genetics **154**:523–532.

APPENDIX 4

Mutations of three AmpG residues abolish peptidoglycan recycling in *N. gonorrhoeae.*

Jia Mun Chan, Joseph P. Dillard

JM Chan and JP Dillard designed the experiments.

JM Chan performed the experiments and analyzed the data.

.

AmpG is an integral inner membrane protein that functions to transport peptidoglycan (PG) fragments with a minimal subunit of a *N*-acetyl-glucosamine-1,6-anhydro-*N*-acetylmuramic acid disaccharide (anhydro-disaccharide) from the periplasm into the cytoplasm (1, 2). AmpG is also capable of transporting anhydro-disaccharide-peptides (PG monomers), and gonococcal AmpG ($AmpG_{GC}$) plays a major role in PG monomer recycling in *Neisseria gonorrhoeae* (2, 3). *E. coli* AmpG ($AmpG_{Ec}$) is capable of transporting anhydro-disaccharide and PG monomers with similar efficiencies, but primarily function to recycle anhydro-disaccharide during growth (2, 4).

AmpG was first discovered as an inducer of AmpC β-lactamase expression in *Enterobacter cloacae*, and mutation of *ampG* in bacterial species that encode the inducble AmpC system sensitizes the bacteria to β-lactam treatment (1, 5). Accumulation of PG-recycling intermediates in the cytoplasm and the subsequent binding of such intermediates to the response regulator AmpR during β-lactam treatment leads to AmpR-dependent induction of AmpC expression (6–8). In the course of studying β-lactam resistance, it was discovered that spontaneous mutation resulting in the substitutions of three $AmpG_{Ec}$ residues from glycine (G) to aspartate (D) prevents induction of the AmpC β-lactamase (9). The corresponding residues in $AmpG_{GC}$ are alanine 154 (A154), glycine 273 (G273) and glycine 385 (G385), and were predicted to be located close to the substrate transporting channel of AmpG by tertiary structure modeling (Figure 1) (10, 11). *N. gonorrhoeae* does not encode the AmpC-AmpR system. We ask instead if these three residues are necessary for PG recycling.

Deletion of $ampG_{GC}$ in *N. gonorrhoeae* resulted in a 7x increase in PG monomer release compared to WT (3). To determine if residues A154, G273 and G385 are required for AmpG function, I performed site-directed mutagenesis to substitute these $AmpG_{GC}$ residues with an aspartate (D). Using metabolic labeling of PG fragments with [^{3}H] glucosamine and quantitative

fragment release, I compared the amount of PG monomer released by WT *N. gonorrhoeae* and the site-directed mutants. In this iteration of the experiment we observed a 6x increase in PG monomer release compared to WT (Figure 2B). Gonococcal mutants expressing *ampG*^{A154D}, *ampG*^{G273D} and *ampG*^{G385D} released around 10x, 7x and 4x more PG monomers compared to WT (Figure 2A-B). In conclusion, substitution of AmpG residues 154, 273 and 385 to an aspartate abolished regular levels of PG recycling by *N. gonorrhoeae*, leading to a large increase in the amount of PG monomers released by the mutants.

A.

```
Ec    1 ---MSSQYLRIFQQPRSAILLILGFASGLPLALTSGTLQAWMTVENIDLKTIGFFSLVGQ
Ng    1 MTASKSGFIGQIFSRNMLVCIFTGFASGLPLYFLINLIPAWLRSEQVDLKSIGLMALIGL

Ec   58 AYVFKFLWSPLMDRYTPPFFGRRRGWLLATQILLLVAIAAMGFLEPGTQLRWMAALAVVI
Ng   61 PFTWKFLWSPLMDAVRLPVLGRRRGWMLLTQAGLLAALAAYAFLNPRNHLPLIAGLSVLV

Ec  118 AFCSASQDIVFDAWKTDVLPAEERGAGAAISVLGYRLGMLVSGGLALWLADKWLGWQGMY
Ng  121 AFFSASQDIVLDAFRREILSDEELGLGNSVHVNAYRVAALIPGSLSLVLADR-MPWSEVF

Ec  178 WLMAALLIPCIIATL-LAPEPTDTIPVPKTLEQAVVAPLRDFFGRN---NAWLILLLIVL
Ng  180 VITSLFMLPGLLMTLFLAHEPVLPPSVPKTLKQTVVEPFKEFFTRKGIASAVCVLLFIFL

Ec  234 YKLGDAFAMSLTTTFLIRGVGFDAGEVGVVNKTLGLLATIVGALYGGILMQRLSLFRALL
Ng  240 YKLGDSMATALATPFYL-DMGFSKTDIGLIAKNAGLWPAVAAGILGGVWMLKIGVNKALW

Ec  294 IFGILQGASNAGY-WLLSITDKHLYSMGAAVFFENLCG------GMGTSAFVALLMTLCN
Ng  299 LFGAVQAITVLGFVWLAGFGHFDTVGTGERLMLAAVIGAEAVGVGLGTAAFVSYMARETN

Ec  347 KSFSATQFALLSALSAVGRVYVGPVAGWFVEAHGWSTFYLFSVAAAVPGLILLLVCRQTL
Ng  359 PAFTATQLALFTSLSAVPRTVINSFAGYLIEWMGYVPFFRLCFILALPGMLLLLK-----

Ec  407 EYTRVNDNFISRTAYPAGYAFAMWTLAAGVSLLAVWLLLLTMDALDLTHFSFLPALLEVG
Ng  414 --------------------------------VAPWNGEKTQDA----------------

Ec  467 VLVALSGVVLGGLLDYLALRKTHLT
Ng  426 ----------GR-------------
```

B.

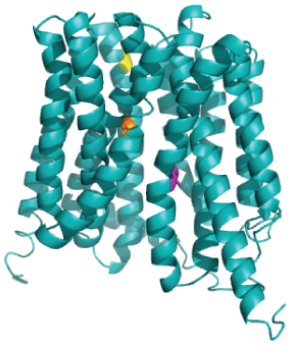

Figure 1. Partial conservation of three AmpG residues important for PG recycling. A) Alignment of *E. coli* (Ec) and *N. gonorrhoeae* (Ng) AmpG protein sequences. The two homologues show 39.71% identity. The three glycine residues that when mutated, inactivate $AmpG_{Ec}$, are found as an alanine (A154, magenta diamond), glycine (G273, orange diamond), and glycine (G385, yellow diamond) in $AmpG_{GC}$. B) Predicted structure of $AmpG_{GC}$ using I-TASSER server placed residues A154 (magenta), G273 (orange) and G385 (yellow) close to the central substrate transporting channel of the protein.

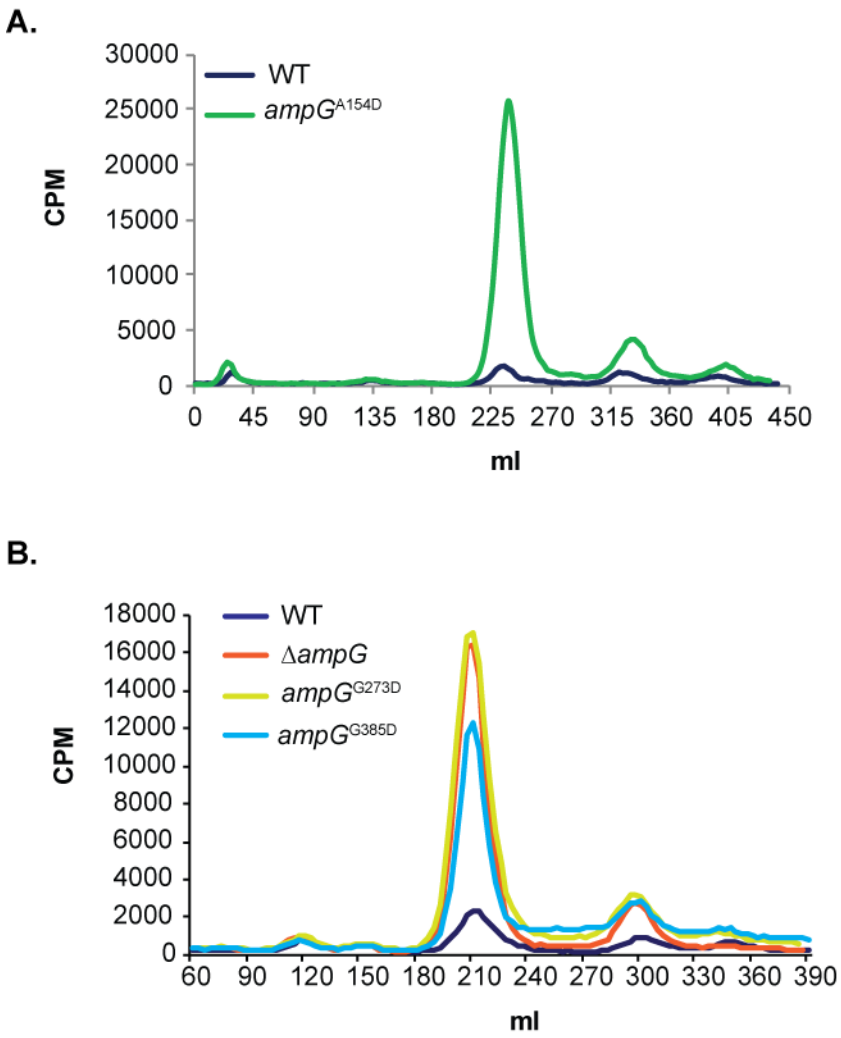

Figure 2. Non-conservative mutations of $AmpG_{GC}$ residues 154, 273 and 385 abolished PG recycling. A) Single substitution of $AmpG_{GC}$ residue A154 to aspartate led to 10x more PG monomer release by the mutant compared to WT. B) Single substitution of $AmpG_{GC}$ residue G273 to aspartate increased PG monomer release by the site-directed mutant to levels seen with an *ampG* deletion mutant. Single substitution of $AmpG_{GC}$ residue G385 also increased PG monomer release, but not to levels seen with an *ampG* deletion mutant.

MATERIALS AND METHODS

Bacterial growth. *N. gonorrhoeae* strains were grown at 37°C on gonococcal base medium (GCB) agar plates (Difco) with 5% CO_2 or in gonococcal base liquid medium (GCBL) with Kellogg's supplements (12) and 0.042% $NaHCO_3$ (13) with aeration. *E. coli* strains were grown at 37°C on LB agar plates (Difco) or in LB broth containing 500 μg/ml erythromycin.

Strain construction. All plasmids used in this study were generated using the cloning vector pIDN3 as the vector backbone (14). pIDN3 was digested with SacI and BamHI, and ligated with similarly digested PCR products (inserts). Such PCR products are generated by a two-step overlap extension PCR using primers that amplify the *ampG*$_{GC}$ coding sequence and primers that introduce the intended mutation. PCR products were amplified using pEC007 as a template (15). pEC007 carries an *ampG*$_{GC}$ coding sequence with a silent mutation conferring an NheI recognition site. The NheI site is used for screening of transformants using PCR and restriction enzyme digest.

The insert for pEC107 (pIDN3 with *ampG*$_{GC}$G273D) was constructed first by amplifying partial *ampG*$_{GC}$ sequences with primers SacI ampG F (CGGGAGCTCGCGATATTTGCTACAATAGGC) and ampG G273D R (CACTGCCGGCCACAGGTCTGCATTTTTGGC), or with primers ampG 273D F (GCCAAAAATGCAGACCTGTGGCCGGCAGTG) and XhoI ampG R (GCGGCTCGAGACACAATATCAGGTAAACG). The two PCR products are then used with

primers SacI ampG F and XhoI ampG R in overlap extension PCR to generate the final insert for pEC107.

The insert for pEC108 (pIDN3 with *ampG*$_{GC}$G385D) was similarly generated using primers ampG G385D F (CAATTCCTTTGCAGACTATCTGATCGAATGG) and ampG G385D R (CCATTCGATCAGATAGTCTGCAAAGGAATTG) instead of ampG G273D F and ampG G273D R. The insert for pEC117 (pIDN3 with *ampG*$_{GC}$A154D) was also generated with the same method using primers ampG A154D F (GTTCATGTGAACGACTACCGGGTTGCC) and ampG A154D R (GGCAACCCGGTAGTCGTTCACATGAAC).

Plasmids pEC107, pEC108 and pEC117 were transformed into *N. gonorrhoeae* MS11 using spot transformation (16) to generate EC553, EC554 and EC566. Transformants were screened by PCR, digestion with NheI and sequencing.

Metabolic labeling with [^{3}H] glucosamine and quantitative fragment release. Gonococcal strains were metabolically labeled with [^{3}H] glucosamine as described in Chapter 2. The amount of radiolabel, determined as counts per minute (CPM) by liquid scintillation counting, in each culture was normalized prior to the chase period (3). Cell-free supernatant was subjected to tandem size-exclusion chromatography to separate PG fragments by size.

REFERENCES

1. **Korfmann G**, **Sanders CC**. 1989. *ampG* is essential for high-level expression of AmpC beta-lactamase in *Enterobacter cloacae*. Antimicrob Agents Chemother **33**:1946–1951.
2. **Cheng Q**, **Park JT**. 2002. Substrate specificity of the AmpG permease required for recycling of cell wall anhydro-muropeptides. J Bacteriol **184**:6434–6436.
3. **Garcia DL**, **Dillard JP**. 2008. Mutations in *ampG* or *ampD* affect peptidoglycan fragment release from *Neisseria gonorrhoeae*. J Bacteriol **190**:3799–3807.
4. **Schaub RE**, **Lenz JD**, **Dillard JP**. 2016. Analysis of peptidoglycan fragment release. Methods Mol Biol **1440**:185–200.
5. **Tuomanen E**, **Lindquist S**, **Sande S**, **Galleni M**, **Light K**, **Gage D**, **Normark S**. 1991. Coordinate regulation of beta-lactamase induction and peptidoglycan composition by the *amp* operon. Science **251**:201–204.
6. **Jacobs C**, **Huang L**, **Bartowsky E**, **Normark S**, **Park JT**. 1994. Bacterial cell wall recycling provides cytosolic muropeptides as effectors for beta-lactamase induction. EMBO J **13**:4684–4694.
7. **Dietz H**, **Pfeifle D**, **Wiedemann B**. 1997. The signal molecule for β-lactamase induction in *Enterobacter cloacae* is the anhydromuramyl-pentapeptide. Antimicrob Agents Chemother **41**:2113–2120.
8. **Balcewich MD**, **Reeve TM**, **Orlikow EA**, **Donald LJ**, **Vocadlo DJ**, **Mark BL**. 2010. Crystal structure of the AmpR effector binding domain provides insight into the molecular regulation of inducible AmpC Beta-lactamase. J Mol Biol **400**:998–1010.
9. **Lindquist S**, **Weston-Hafer K**, **Schmidt H**, **Pul C**, **Korfmann G**, **Erickson J**, **Sanders C**, **Martin HH**, **Normark S**. 1993. AmpG, a signal transducer in chromosomal beta-lactamase induction. Mol Microbiol **9**:703–715.
10. **Zhang Y**. 2008. I-TASSER server for protein 3D structure prediction. BMC Bioinformatics **9**:40.
11. **Yang J**, **Yan R**, **Roy A**, **Xu D**, **Poisson J**, **Zhang Y**. 2015. The I-TASSER Suite: Protein structure and function prediction. Nat Methods **12**:7–8.
12. **Kellogg DS**, **Peacock WL**, **Deacon WE**, **Brown L**, **Pirkle CI**. 1963. *Neisseria gonorrhoeae*: Virulence genetically linked to clonal variation. J Bacteriol **85**:1274–1279.
13. **Morse SA**, **Bartenstein L**. 1974. Factors affecting autolysis of *Neisseria gonorrhoeae*. Proc Soc Exp Biol Med **145**:1418–1421.
14. **Hamilton HL**, **Schwartz KJ**, **Dillard JP**. 2001. Insertion-duplication mutagenesis of *Neisseria*: Use in characterization of DNA transfer genes in the gonococcal genetic island. J Bacteriol **183**:4718–4726.
15. **Chan JM**, **Dillard JP**. 2016. *Neisseria gonorrhoeae* crippled its peptidoglycan fragment permease to facilitate toxic peptidoglycan monomer release. J Bacteriol **198**:3029–3040.
16. **Dillard JP**. 2011. Genetic manipulation of *Neisseria gonorrhoeae*. Curr Protoc Microbiol **4**:Unit4A.2.

APPENDIX 5

Peptidoglycan-remodeling proteins encoded by various *Neisseria spp*.

Jia Mun Chan, Joseph P. Dillard

Peptidoglycan (PG) remodeling, characterized by synthesis and degradation of PG strands, is an important process to allow for cell separation and cell enlargement in bacteria. Small PG fragments are generated by the action of PG digesting enzymes called peptidoglycanases (PGases); most PG fragments liberated in the periplasm are recycled by Gram-negative bacteria such as *Neisseria gonorrhoeae* (1–3). Extensive work has been done to characterize PGases and PG recycling proteins in *N. gonorrhoeae*. We seek to determine if various species of human- and animal-associated *Neisseria* also encode homologues of PGases that are found in *N. gonorrhoeae.*

We utilized the whole genome sequence data of various *Neisseria spp*. available on the PubMLST and NCBI databases to determine if genes encoding specific PGases are present in the genome of a certain *Neisseria* species (4, 5). To accomplish this analysis, the nucleotide- and protein-sequences of various PGases and PG recycling proteins were compiled and used to query the databases (Table 1). We included the coding sequence of *gdh* (glucose-6-phosphate dehydrogenase; housekeeping gene in *Neisseria*), *ftsZ* (an essential cell division protein), *penA* (PG biosynthesis protein PBP2) as positive controls.

A locus is marked as present in a strain if it fulfils one of three conditions: (i) an allele designation has been defined for the locus on the PubMLST database, (ii) a sequence tag has been defined for the locus on the PubMLST database, (iii) the genome contains sequences that have >30% identity to >50% of the queried coding sequence (Table 1, pale gray). Using this definition, *N. musculi* AP2031 does not encode an *ampG* homologue (29% identity, 52% coverage). However, we have demonstrated experimentally that *N. musculi* AP2031 encodes a functional AmpG protein (Chapter 4). As such, a locus is also marked as present in a strain if it fails to meet criteria (i), (ii), (iii), but (iv) have 20-40% identity to 40-50% of the queried coding

that fulfils criteria (i)-(iv) (Table 1, gray). A locus is marked as absent if sequences that meet conditions (i) – (iv) are not found in the whole genome data (Table 1, black).

Using the above criteria as a guideline, we determined that multiple species of *Neisseria* encode homologues of characterized gonococcal PGases and PG recycling proteins. The only exception is *N. dentiae* ATCC 700276, which does not appear to have the *dacB* gene encoding PBP3. PBP3 acts as a D,D-carboxypeptidase and endopeptidase in *N. gonorrhoeae* (6). *N. dentiae* is a nonpathogenic *Neisseria* isolated from cow dental plaques (7). Our results suggest that with the exception of *N. dentiae* ATCC 700726, which requires more experimental investigation, all strains tested have the genetic potential to carry out the same PG degrading and PG recycling processes as *N. gonorrhoeae*.

Table 1. Presence or absence of homologues of known gonococcal PGases and PG recycling proteins in *Neisseria* spp.

		Lytic transglycosylases						Amidase and activator		Endopeptidase/Carboxypeptidase				Transpepti	Recycling proteins			Controls		
		LtgA	LtgB	LtgC	LtgD	LtgE	MltG	AmiC	NlpD	NGO1686	PBP3	PBP4	LdcA	YnhG	AmpG	AmpD	NagZ	Gdh	FtsZ	PenA
Strain	**PubMLST ID**	NEIS1920	NEIS1401	NEIS0010	NEIS1212	NEIS1234	NEIS0618	NEIS1694	NEIS1418	NEIS1856	NEIS0425	NEIS0703	NEIS1546	NEIS1677	NEIS1808	NEIS0617	NEIS0469	NEIS1331	NEIS1737	NEIS1753
N. gonorrhoeae FA1090	2855																			
N. gonorrhoeae FA19	46275																			
N. gonorrhoeae MS11	46278																			
N. meningitidis 8013	1038																			
N. meningitidis FAM18	698																			
N. meningitidis MC58	240																			
N. meningitidis Z2491	613																			
N. lactamica 020-09	8851																			
N. lactamica ATCC 23970	5544																			
N. polysaccharea 12030-2014	36153																			
N. polysaccharea ATCC 43768	14730																			
N. cinerea ATCC 14685	14731																			
N. flavescens NRL30031	14732																			
N. subflava NJ9703	14733																			
N. mucosa ATCC 25996	3565																			
N. sicca ATCC 29256	2863																			
N. elongata ATCC 29315	14740																			
N. macacae ATCC 33926	N/A																			
N. musculi AP2031	29520																			
N. dentiae ATCC 700276	49345																			

Key

Gene encoding homologue to gonococcal protein (>30% identity, >50% coverage) present in genome.

Gene encoding homologue to gonococcal protein (20-40% identity, 40-50% coverage) present in genome.

Gene encoding homologue to gonococcal protein absent in genome.

References

1. **Park JT**, **Uehara T**. 2008. How bacteria consume their own exoskeletons (turnover and recycling of cell wall peptidoglycan). Microbiol Mol Biol Rev **72**:211–227.
2. **Uehara T**, **Park JT**. 2008. Growth of *Escherichia coli*: Significance of peptidoglycan degradation during elongation and septation. J Bacteriol **190**:3914–3922.
3. **Garcia DL**, **Dillard JP**. 2008. Mutations in *ampG* or *ampD* affect peptidoglycan fragment release from *Neisseria gonorrhoeae*. J Bacteriol **190**:3799–3807.
4. **Sayers EW**, **Barrett T**, **Benson DA**, **Bryant SH**, **Canese K**, **Chetvernin. V**, **Church DM**, **Dicuccio M**, **Edgar R**, **Federhen S**, **Feolo M**, **Geer LY**, **Helmberg W**, **Kapustin Y**, **Landsman D**, **Lipman DJ**, **Madden TL**, **Maglott DR**, **Miller V**, **Mizrachi I**, **Ostell J**, **Pruitt KD**, **Schuler GD**, **Sequeira E**, **Sherry ST**, **Shumway M**, **Sirotkin K**, **Souvorov A**, **Starchenko G**, **Tatusova TA**, **Wagner L**, **Yaschenko E**, **Ye J**. 2009. Database resources of the National Center for Biotechnology Information. Nucleic Acids Res **37**:5–15.
5. **Jolley KA**, **Maiden MCJ**. 2010. BIGSdb: Scalable analysis of bacterial genome variation at the population level. BMC Bioinformatics **11**:595.
6. **Stefanova ME**, **Tomberg J**, **Olesky M**, **Höltje J-V**, **Gutheil WG**, **Nicholas RA**. 2003. *Neisseria gonorrhoeae* penicillin-binding protein 3 exhibits exceptionally high carboxypeptidase and β-Lactam binding activities. Biochemistry **42**:14614–14625.
7. **Sneath PHA**, **Barrett SJ**. 1996. A new species of *Neisseria* from the dental plaque of the domestic cow, *Neisseria dentiae* sp. Nov. Lett Appl Microbiol **23**:355–358.